

UC Riverside

UC Riverside Electronic Theses and Dissertations

Title

A Heck-Based Approach to the Synthesis of Anacardic Acids and an Exploration of its Derivatives as Small-Molecule Inhibitors of the SUMO E1 Enzyme and Aminoalkylation of Adamantanes Using Dual Photoredox-HAT Catalysis

Permalink

<https://escholarship.org/uc/item/4rj9j8qj>

Author

Weigel, William

Publication Date

2020

Peer reviewed|Thesis/dissertation

UNIVERSITY OF CALIFORNIA
RIVERSIDE

A Heck-Based Approach to the Synthesis of Anacardic Acids and an Exploration of its
Derivatives as Small-Molecule Inhibitors of the SUMO E1 Enzyme
and
Aminoalkylation of Adamantanes Using Dual Photoredox-HAT Catalysis

A Dissertation submitted in partial satisfaction
of the requirements for the degree of

Doctor of Philosophy

in

Chemistry

by

William Kenneth Weigel III

September 2020

Dissertation Committee:

Professor David B. C. Martin, Co-Chairperson

Professor Christopher Switzer, Co-Chairperson

Professor Michael Pirrung

Professor Timothy Su

Copyright by
William Kenneth Weigel III
2020

The Dissertation of William Kenneth Weigel III is approved:

Committee Co-Chairperson

Committee Co-Chairperson

University of California, Riverside

ACKNOWLEDGEMENTS

I would like to express my deepest gratitude to my advisor Professor Dave Martin.

It has been an amazing journey chasing after your boundless knowledge. Thank you for always encouraging me, pushing me to be a better chemist, and never letting me settle for mediocrity. You are a fantastic leader, teacher, and role model. I could not have asked for a better mentor.

I cannot begin to express enough thanks to my parents, siblings, and family for all the love and support you have given me my entire life. My success is your success, I could not be where I am today without you. A special thanks to my Grandma and Bapa who never fail to remind me I am loved. And to Grammy, who taught me the value of education and made it possible to pursue my academic aspirations.

I am also deeply indebted to my friends; you are my second family. I could not have crossed the finish line without your support. You are the reason I had enough gas in the tank to make it.

A great many thanks to my lab mates Abigail, Dana, Travis, Taylor, Hoang and Cory. Thank you for always being there at ground zero to support me on the rough days. It has been a great privilege to grow and learn alongside you.

Dedicated to my mother and my sister,
thank you for unwaveringly supporting me through the good times as well as the bad.
You continually inspire me try my best, never give up, and never stop striving to be a
better person today than I was yesterday.

ABSTRACT OF THE DISSERTATION

A Heck-Based Approach to the Synthesis of Anacardic Acids and an Exploration of its
Derivatives as Small-Molecule Inhibitors of the SUMO E1 Enzyme
and
Aminoalkylation of Adamantanes Using Dual Photoredox-HAT Catalysis

by

William Kenneth Weigel III

Doctor of Philosophy, Graduate Program in Chemistry
University of California, Riverside, September 2020
Professor David B.C. Martin, Co-Chairperson
Professor Christopher Switzer, Co-Chairperson

Anacardic acids are a family of naturally occurring phenolic lipids with well-established antibacterial and anticancer bioactivities. As such, the synthesis of these compounds has been the subject of some interest. However, previous attempts at their synthesis have often relied on inefficient protection and deprotection steps, demonstrated poor regiocontrol, and offer only narrow access to specific members of the anacardic acid family. Herein, a new Heck-based approach to the synthesis of anacardic acids that circumvents these issues is presented. The use of this strategy in conjunction with stereoselective olefination enables access to virtually any member of the anacardic acid family including unnatural isoforms. This method has been used to construct a small library of anacardic acids and were then used in an MMP-2 activity assay which revealed that inhibition is not strongly related to structural morphology.

Anacardic acid is known to possess anticancer activity through inhibition of the SUMO E1 enzyme by exploiting a so called “non-oncogene addiction.” Based on these findings, a wide range of anacardic acid derivatives have been synthesized by first using computational molecular docking studies to identify promising synthetic candidates. These derivatives were then tested using *in-situ* sumoylation assays through interdisciplinary collaborations with other research groups at UCR.

In a separate line of work, a method for aminoalkylation of adamantane using imine substrates has been developed as an extension of previous work in our lab with a dual catalyst system. This catalyst system employs the use of an iridium photocatalyst with a quinuclidine-based hydrogen atom transfer (HAT) co-catalyst. The reaction is remarkably selective for adamantyl C–H bonds, even in the presence of other, weaker alkyl C–H bonds. The aminoalkylative C–C bond formation between adamantane and a variety of imines and hydrazones is possible using this method and affords valuable amino acid building blocks that are useful in the synthesis of drug-like pharmacophores. In particular, the use of a different photocatalyst with chiral imines allows for the enantioselective synthesis of rimantadine derivatives and the saxagliptin core.

Table of Contents

ACKNOWLEDGEMENTS	IV
ABSTRACT OF THE DISSERTATION	VI
LIST OF SCHEMES	XIX
LIST OF FIGURES	XXIII
LIST OF TABLES.....	XXVI
LIST OF ACRONYMS AND ABBREVIATIONS	XXVIII
1 SYNTHESIS OF ANACARDIC ACID AND ITS DERIVATIVES	1
<i>1.1 - Introduction</i>	1
<i>1.2 - Background</i>	2
1.2.1 - Natural Sources.....	2
1.2.2 - Bioactivities	5
1.2.2.1 - Antimicrobial	5
1.2.2.2 - Reactive Oxygen Species (ROS).....	6
1.2.2.3 - Histone Acetyltransferases (HATs)	7
1.2.2.4 - Anticancer.....	8
1.2.3 - Biosynthesis	9
<i>1.3 - Previous Syntheses of Anacardic Acids</i>	16
1.3.1 - Early Biomimetic Approach (1967).....	16
1.3.2 - Tyman's Aryne Alkylation-Carboxylation (1973)	18
1.3.3 - Tyman's Alkylation of Phthalic Anhydride (1979)	19

1.3.4 - Kubo's Wittig Approach for 15:0 Anacardic Acid (1987)	21
1.3.5 - Gerlach's 4+2 Cycloaddition/Reversion Method (1995)	23
1.3.6 - Satoh's Annulation of 15:1 Ginkgolic Acid (2000)	24
<i>1.4 - References</i>	26
2 HECK REDOX-RELAY REACTIONS WITH ALKENOL SUBSTRATES	33
<i>2.1 - Introduction</i>	33
<i>2.2 - Early Palladium-Catalyzed Arylation of Allylic Alcohols</i>	36
<i>2.3 - Discovery and Development of Palladium Chain-Walking</i>	39
2.3.1 - Chain-Walking in the Formation of Palladium π -allyl Complexes	39
2.3.2 - Jeffery's Ligandless Reaction Conditions	42
2.3.3 - Stereocontrol in Alkenol Additions	44
<i>2.4 - Mechanistic Investigations of the Palladium Chain-Walking Process</i>	48
2.4.1 - Deuterium Labeling Studies	48
<i>2.5 - References</i>	52
3 A HECK-BASED APPROACH TO ANACARDIC ACIDS AND RELATED PHENOLIC LIPIDS ..	56
<i>3.1 - Introduction</i>	56
<i>3.2 - Preparation of the Aromatic Core</i>	57
<i>3.3 - Optimization and Modification of Jeffery's Conditions</i>	59
<i>3.4 - Reaction Scope</i>	62
3.4.1 - Alkenol Chain Length.....	62
3.4.2 - Variation of the Electrophile	63
3.4.3 - Aryl Substituent Effects Regioselectivity	65
<i>3.5 - Synthesis of (15:1) Ginkgolic Acid and (15:2) Anacardic Acid</i>	66

<i>3.6 - Synthesis of Unnatural (14:1) E-Anacardic Acid</i>	68
<i>3.7 - Stereochemical Analysis of Olefination Reactions</i>	70
<i>3.8 - MMP-2 Inhibition Assays with Anacardic Acids</i>	71
<i>3.9 - Conclusions</i>	74
<i>3.10 - Experimental</i>	75
3.10.1 - General Methods	75
3.10.2 - General Procedures:.....	76
3.10.2.1 - Procedure A: Heck redox-relay with modified Jeffery's conditions:	76
5-hydroxy-2,2-dimethyl-4H-benzo[d][1,3]dioxin-4-one (3.8):.....	77
2,2-dimethyl-4-oxo-4H-benzo[d][1,3]dioxin-5-yl trifluoromethanesulfonate (3.9):	77
3-(2,2-dimethyl-4-oxo-4H-benzo[d][1,3]dioxin-5-yl)propanal (3.16):	78
3-(2,2-dimethyl-4-oxo-4H-benzo[d][1,3]dioxin-5-yl)butanal (17):	79
3-(2,2-dimethyl-4-oxo-4H-benzo[d][1,3]dioxin-5-yl)pentanal (3.18):.....	80
3-(2,2-dimethyl-4-oxo-4H-benzo[d][1,3]dioxin-5-yl)hexanal (3.19):	80
3-(2,2-dimethyl-4-oxo-4H-benzo[d][1,3]dioxin-5-yl)octanal (3.20):	81
phenylpentanal (3.23):.....	82
3-Methoxyphenyl trifluoromethanesulfonate (E3.1):.....	83
5-(3-methoxyphenyl)pentanal (3.27):.....	83
5-(3-methoxyphenyl)octanal (3.28):	84
(Z)-2,2-dimethyl-5-(pentadec-8-en-1-yl)-4H-benzo[d][1,3]dioxin-4-one (E3.29):.....	85
(Z)-2-hydroxy-6-(pentadec-8-en-1-yl)benzoic acid (3.29):	86
5-(7-((2R,3S)-3-hexyloxiran-2-yl)heptyl)-2,2-dimethyl-4H-benzo[d][1,3]dioxin-4-one (\pm) (E3.29a):	87
3(Z)-hepten-1-yltriphenylphosphonium bromide (3.36):	88
2,2-dimethyl-5-((8Z,11Z)-pentadeca-8,11-dien-1-yl)-4H-benzo[d][1,3]dioxin-4-one (E3.39):	89
2-hydroxy-6-((8Z,11Z)-pentadeca-8,11-dien-1-yl)benzoic acid (3.39):.....	90
(E)-2,2-dimethyl-5-(tetradec-8-en-1-yl)-4H-benzo[d][1,3]dioxin-4-one (E3.41):	91

(*E*)-2-hydroxy-6-(tetradec-8-en-1-yl)benzoic acid (3.41):..... 92

5-(7-((2*R*,3*R*)-3-hexyloxiran-2-yl)heptyl)-2,2-dimethyl-4H-benzo[*d*][1,3]dioxin-4-one (\pm) (E3.41a): 93

3.11 - References..... 95

4 HAT-MEDIATED C–H ACTIVATION OF DIAMONDOIDS AS A TOOL FOR THE

CONSTRUCTION OF NEW C–C BONDS 99

4.1 - Introduction 99

4.2 - Acylative Additions to Adamantane 105

4.2.1 - Chlorocarbonylation..... 105

4.2.2 - Acetylations..... 106

4.2.3 - Formylation 109

4.3 - Carbonylations with CO 110

4.3.1 - NHPI Mediated Carboxylation..... 110

4.3.2 - Photocatalytic Carbonylation 112

4.3.3 - Oxidative Radical Carbonylation 114

4.3.4 - Transition Metal-Catalyzed Carbonylation 114

4.4 - Alkylation via Alkene Addition (Giese-Type Reaction) 116

4.4.1 - First Giese Addition with Adamantane..... 116

4.4.2 - Photochemically Driven Alkene Additions 117

4.4.3 - Non-Photochemical Alkene Additions..... 122

4.5 - Addition-Fragmentation 125

4.5.1 - Decarboxylative Alkenylation..... 126

4.5.2 - Allylation 127

4.5.3 - Photochemical Alkenylation..... 130

4.6 - Alkynylation 131

4.6.1 - Metal-Free Alkynylations	132
4.6.2 - Metal-Catalyzed Alkynylation.....	135
4.7 - Arylation.....	137
4.7.1 - Photooxidations Using TCB	137
4.7.2 - Minisci-Type Arylations	139
4.7.3 - Dual Catalytic Arylation	144
4.8 - Amine and Nitrile Additions	146
4.8.1 - Cyanation	146
4.8.2 - Aminoalkylation	149
4.9 - Conclusion	149
4.10 - References.....	151
5 PHOTOCATALYTIC C–H AMINOALKYLATION OF ADAMANTANES.....	162
5.1 - Introduction	162
5.2 - Reaction Optimization	167
5.3 - Proposed Catalytic Cycles	175
5.3.1 - Indirect Dual Photocatalytic-HAT System.....	177
5.3.2 - Direct HAT Cycle Using Pentacenetetraone (PT).....	180
5.4 - Substrate Scope.....	181
5.4.1 - <i>N</i> -Benzoyl Hydrazones	181
5.4.2 - <i>N</i> -Tosyl Imines.....	183
5.4.3 - Cyclic Sulfonylimine	184
5.4.4 - Chiral Sulfinyl Imines	186
5.4.5 - Non-Adamantyl Substrates	189
5.5 - Deprotections.....	190

5.6 - Conclusions	191
5.7 - Experimental	192
5.7.1 - General Methods	192
5.7.2 - General Procedures.....	192
<i>General Procedure A: Photochemical Reactions with Ir-1/Q-1</i>	192
<i>General Procedure B: Photochemical Reactions with PT</i>	193
<i>General Procedure C: Hydrazone Condensations</i>	193
<i>Synthesis of Chiral N-Sulfinyl imines</i>	194
<i>Synthesis of Iridium Photocatalysts</i>	194
<i>Synthesis of Quinuclidine HAT Catalyst</i>	194
methyl 4-adamantan-1-yl((2-benzoylhydrazinyl)methyl)benzoate (5.18a):	194
methyl 4-((3,5-dimethyladamantan-1-yl)2-benzoylhydrazinyl)methyl benzoate (5.18b):	195
methyl 4-((3-hydroxyadamantan-1-yl)2-benzoylhydrazinyl)methyl)benzoate (5.18c):	196
<i>N'</i> -adamantan-1-yl((4-(trifluoromethyl)phenyl)methyl)benzohydrazide (5.18d):	196
<i>N'</i> -(3,5-dimethyladamantan-1-yl)((4-(trifluoromethyl)phenyl))methyl benzohydrazide (5.18e):	197
<i>N'</i> -(adamantan-1-yl(2-(trifluoromethyl)phenyl)methyl)benzohydrazide (5.18f):	198
<i>N'</i> -(adamantan-1-yl(4-fluorophenyl)methyl)benzohydrazide (5.18g):	199
adamantan-1-yl(4-fluorophenyl)methanamine (5.18g'):	199
<i>N'</i> -(adamantan-1-yl(2-fluorophenyl)methyl)benzohydrazide (5.18h):	201
<i>N'</i> -(adamantan-1-yl)((4-(cyanophenyl))methyl)benzohydrazide (5.18i):	202
<i>N'</i> -(3,5-dimethyladamantan-1-yl)((4-(cyanophenyl))methyl)benzohydrazide (5.18j):	202
<i>N'</i> -(3-acetyladamantan-1-yl)((4-(cyanophenyl))methyl)benzohydrazide (5.18k):	203
<i>N'</i> -(adamantan-1-yl(phenyl)methyl)benzohydrazide (5.18l):	204
<i>N</i> -adamantan-1-yl(phenyl)methyl)-4-methylbenzenesulfonamide (5.20a)	204
<i>N</i> -(adamantan-1-yl(4-methoxyphenyl)methyl)-4-methylbenzenesulfonamide (5.20b):	205
<i>N</i> -(adamantan-1-yl(4-fluorophenyl)methyl)-4'-methylbenzenesulfonamide (5.20c):	205
<i>N</i> -(3-chloroadamantan-1-yl(4-fluorophenyl)methyl)-4'-methylbenzenesulfonamide (5.20d):	206

<i>N</i> -(3-(<i>N'</i> - <i>tert</i> -butoxycarbonyl-amino)-adamantyl(4-fluorophenyl)methyl)-4'-methyl benzenesulfonamide (5.20e):.....	207
<i>N</i> -(3-(1'-(<i>N'</i> - <i>tert</i> -butylcarbonyl)-ethyl)adamantyl(4-fluorophenyl)methyl)-4'-methyl benzenesulfonamide (5.20f):	208
<i>N</i> -(3,5-dimethyladamantan-1-yl)((4-fluorophenyl)methyl)-4' methylbenzene sulfonamide (5.20g):	209
<i>N</i> -(3-adamantan-1-yl(pyridin-3-yl)methyl)-4'-methylbenzenesulfonamide (5.20h):.....	210
<i>tert</i> -Butyl-(adamantan-1-yl(phenyl)methyl)carbamate (5.20i):	210
<i>tert</i> -Butyl-(adamantan-1-yl(4-fluorophenyl)methyl)carbamate (5.20j):.....	211
ethyl 3-(adamantan-1-yl)-2,3-dihydrobenzo[d]isothiazole-3-carboxylate 1,1-dioxide (5.21a):	212
ethyl 3-(3,5-dimethyladamantyl)-2,3-dihydrobenzo[d]isothiazole-3-carboxylate 1,1-dioxide (5.21b): ..	212
ethyl 3-(3-chloroadamantyl)-2,3-dihydrobenzo[d]isothiazole-3-carboxylate 1,1-dioxide (5.21c):	213
ethyl 3-(3-hydroxyadamantyl)-2,3-dihydrobenzo[d]isothiazole-3-carboxylate 1,1-dioxide (5.21d):	214
ethyl 3-(3-cyanoadamantyl)-2,3-dihydrobenzo[d]isothiazole-3-carboxylate 1,1-dioxide (5.21e):	214
ethyl 3-(3-acetyladamantyl)-2,3-dihydrobenzo[d]isothiazole-3-carboxylate 1,1-dioxide (5.21f):	215
(<i>S</i>)- <i>N</i> -((<i>S</i>)-(adamantan-1-yl)(phenyl)methyl)-4-methylbenzenesulfonamide (5.25a):.....	216
(<i>S</i>)- <i>N</i> -((<i>S</i>)-(adamantan-1-yl)(phenyl)methyl)-2,4,6-trimethylbenzene sulfonamide (5.25b):	216
(<i>S</i>)-ethyl 2-(adamantan-1-yl)-2-((<i>S</i>)-1,1-dimethylethylsulfonamido)acetate (5.25c):	217
(<i>S</i>)-ethyl 2-(adamantan-1-yl)-2-((<i>S</i>)-4-methylphenylsulfonamido)acetate (5.25d):	217
(<i>S</i>)-ethyl 2-(adamantan-1-yl)-2-((<i>S</i>)-2,4,6-trimethylphenylsulfonamido)acetate (5.25e):	218
(<i>S</i>)-ethyl 2-(adamantanyl)-2-aminoacetate (S-5.25e'):	219
(<i>R</i>)-ethyl 2-(adamantanyl)-2-aminoacetate (R-5.25e'):	219
(<i>S</i>)-ethyl 2-(3-hydroxyadamantan-1-yl)-2-((<i>S</i>)-2,4,6-trimethylphenylsulfonamido)acetate (5.25f):	221
<i>N</i> -(cyclohexyl(4-fluorophenyl)methyl)-4'-methylbenzenesulfonamide (5.33):.....	221
ethyl 3-(tetrahydrofuran-2-yl)-2,3-dihydrobenzo[d]isothiazole-3-carboxylate 1,1-dioxide (5.32):	222
5.8 - References.....	223

6 SYNTHESIS OF SMALL MOLECULE INHIBITORS FOR THE SUMO E1 ENZYME 229

6.1 - Introduction	229
---------------------------------	------------

6.2 - Background	230
6.2.1 - Sumoylation Cycle	230
6.2.2 - Role of SUMO E1 in Carcinogenesis	233
6.3 - Molecular Docking Studies	234
6.3.1 - Docking Results	237
6.4 - Design and Synthesis of Anacardic Acid Derivatives	240
6.4.1 - Aryl Ether Anacardic Acid Derivatives	240
6.4.1.1 - Biochemical Evaluation of Selected Aryl Ether-Linked Derivatives	248
6.4.2 - Piperazine and Piperidine-Linked Anacardic Acid Derivatives.....	251
6.4.3 - Triazole-Linked Anacardic Acid Derivatives	257
6.4.3.1 - Biochemical Evaluation of Triazole-Based Anacardic Acid Derivatives.....	260
6.5 - Conclusions	262
6.6 - Experimental	263
6.6.1 - General Procedures:.....	263
6.6.1.1 - Procedure A: Copper Click Reactions.....	263
6.6.1.2 - Procedure B: KOTMS Acetonide Deprotection	263
6.6.1.3 - Procedure C: KOH Acetonide Deprotection	264
2,2-dimethyl-5-(tetradecyloxy)-4H-benzo[d][1,3]dioxin-4-one (6.3):.....	264
2-hydroxy-6-(tetradecyloxy)benzoic acid (6.4):.....	265
5-(3-hydroxypropoxy)-2,2-dimethyl-4H-benzo[d][1,3]dioxin-4-one (6.7):	265
5-(3-hydroxybutoxy)-2,2-dimethyl-4H-benzo[d][1,3]dioxin-4-one (6.8):	266
<i>N,N</i> -Bis Boc Adenine (6.11):	267
5-(3-(<i>N,N</i> -bisBoc-adenyl)butoxy)-2,2-dimethyl-4H-benzo[d][1,3]dioxin-4-one (6.14):	267
2-(4-(6-amino-9H-purin-9-yl)butoxy)-6-hydroxybenzoic acid (6.16):	268
4-(naphthalen-1-yl)butanal (6.19):.....	269
4-(naphthalen-1-yl)butanol (6.21):	270

2,2-dimethyl-5-(4-(naphthalen-1-yl)butoxy)-4H-benzo[d][1,3]dioxin-4-one (6.22):	270
2-hydroxy-6-(4-(naphthalen-1-yl)butoxy)benzoic acid (6.23)	271
4-(naphthalen-1-yloxy)but-2-yn-1-ol (6.26)	272
2,2-dimethyl-5-((4-(naphthalen-1-yloxy)but-2-yn-1-yl)oxy)-4H-benzo[d][1,3]dioxin-4-one (6.27):	272
2-hydroxy-6-((4-(naphthalen-1-yloxy)but-2-yn-1-yl)oxy)benzoic acid (6.28):	273
4-((2,2-dimethyl-4-oxo-4H-benzo[d][1,3]dioxin-5-yl)oxy)but-2-yn-1-yl 4-methylbenzenesulfonate (6.30):	274
2,2-dimethyl-5-((4-(naphthalen-2-yloxy)but-2-yn-1-yl)oxy)-4H-benzo[d][1,3] dioxin-4-one (6.31a):	275
2,2-dimethyl-5-((4-(phenylamino)but-2-yn-1-yl)oxy)-4H-benzo[d][1,3] dioxin-4-one (6.31c):	275
2,2-dimethyl-5-((4-(4-chlorophenoxy)but-2-yn-1-yl)oxy)-4H-benzo[d][1,3]dioxin-4-one (6.31d):	276
2,2-dimethyl-5-((4-(4-(trifluoromethyl)phenoxy)but-2-yn-1-yl)oxy)-4H-benzo[d][1,3] dioxin-4-one (6.31e):	277
2,2-dimethyl-5-((4-(piperidin-1-yl)but-2-yn-1-yl)oxy)-4H-benzo[d][1,3]dioxin-4-one (6.31f):	278
2,2-dimethyl-5-((4-phenoxybut-2-yn-1-yl)oxy)-4H-benzo[d][1,3]dioxin-4-one (6.31g):	278
2,2-dimethyl-5-((4-([1,1'-biphenyl]-2-yloxy)but-2-yn-1-yl)oxy)-4H-benzo[d][1,3] dioxin-4-one (6.31h):	279
2,2,5-trimethyl-4H-benzo[d][1,3]dioxin-4-one (6.32):	280
5-(bromomethyl)-2,2-dimethyl-4H-benzo[d][1,3]dioxin-4-one (6.33):	280
<i>tert</i> -butyl 4-((2,2-dimethyl-4-oxo-4H-benzo[d][1,3]dioxin-5-yl)methyl)piperazine-1-carboxylate (6.34a):	281
5-((4-benzylpiperidin-1-yl)methyl)-2,2-dimethyl-4H-benzo[d][1,3]dioxin-4-one (6.34b):	281
5-([1,4'-bipiperidin]-1'-ylmethyl)-2,2-dimethyl-4H-benzo[d][1,3]dioxin-4-one (6.34c):	282
2,2-dimethyl-5-((4-(naphthalen-2-ylmethyl)piperazin-1-yl)methyl)-4H-benzo[d][1,3]dioxin-4-one (6.36a):	283
2,2-dimethyl-5-((4-(4-methylbenzyl)piperazin-1-yl)methyl)-4H-benzo[d][1,3]dioxin-4-one (6.36b):	284
2,2-dimethyl-5-((4-(4-chlorobenzyl)piperazin-1-yl)methyl)-4H-benzo[d][1,3]dioxin-4-one (6.36c):	284
benzyl 2-hydroxy-6-((4-(naphthalen-2-ylmethyl)piperazin-1-yl)methyl)benzoate (6.37a):	285
5-((3,4-dihydroisoquinolin-2(1H)-yl)methyl)-2,2-dimethyl-4H-benzo[d][1,3]dioxin-4-one (E.6.1):	286
benzyl 2-((3,4-dihydroisoquinolin-2(1H)-yl)methyl)-6-hydroxybenzoate (6.37b):	286

5-((4-(mesitylsulfonyl)piperazin-1-yl)methyl)-2,2-dimethyl-4H-benzo[d][1,3]dioxin-4-one (6.38a):	287
5-((4-((4-bromophenyl)sulfonyl)piperazin-1-yl)methyl)-2,2-dimethyl-4H-benzo[d][1,3]dioxin-4-one (6.38c):	288
5-((4-((3-bromophenyl)sulfonyl)piperazin-1-yl)methyl)-2,2-dimethyl-4H-benzo[d][1,3]dioxin-4-one (6.38b):	288
2-((4-((3-bromophenyl)sulfonyl)piperazin-1-yl)methyl)-6-hydroxybenzoic acid (6.39b):	289
2,2-dimethyl-5-((1-(quinolin-5-yl)-1H-1,2,3-triazol-4-yl)methoxy)-4H-benzo[d][1,3]dioxin-4-one (6.51a):	290
5-((1-([1,1'-biphenyl]-2-yl)-1H-1,2,3-triazol-4-yl)methoxy)-2,2-dimethyl-4H-benzo[d][1,3]dioxin-4-one (6.51b):	290
5-((1-benzyl-1H-1,2,3-triazol-4-yl)methoxy)-2,2-dimethyl-4H-benzo[d][1,3]dioxin-4-one (6.51c):	291
2,2-dimethyl-5-((1-(naphthalen-1-yl)-1H-1,2,3-triazol-4-yl)methoxy)-4H-benzo[d][1,3]dioxin-4-one (6.51d):	291
5-((1-([1,1'-biphenyl]-4-yl)-1H-1,2,3-triazol-4-yl)methoxy)-2,2-dimethyl-4H-benzo[d][1,3]dioxin-4-one (6.51e):	292
2,2-dimethyl-5-((1-(4-morpholinophenyl)-1H-1,2,3-triazol-4-yl)methoxy)-4H-benzo[d][1,3]dioxin-4-one (6.51f):	292
2,2-dimethyl-5-((1-phenyl-1H-1,2,3-triazol-4-yl)methoxy)-4H-benzo[d][1,3]dioxin-4-one (6.51g):	293
2,2-dimethyl-5-((1-(naphthalenylmethyl)-1H-1,2,3-triazol-4-yl)methoxy)-4H-benzo[d][1,3]dioxin-4-one (6.51h):	293
5-((1-(4-benzylphenyl)-1H-1,2,3-triazol-4-yl)methoxy)-2,2-dimethyl-4H-benzo[d][1,3]dioxin-4-one (6.51j):	294
2,2-dimethyl-5-((1-(2-phenoxyphenyl)-1H-1,2,3-triazol-4-yl)methoxy)-4H-benzo[d][1,3]dioxin-4-one (6.51k):	294
5-((1-(adamantan-1-ylmethyl)-1H-1,2,3-triazol-4-yl)methoxy)-2,2-dimethyl-4H-benzo[d][1,3]dioxin-4-one (6.51m):	295
2-hydroxy-6-((1-(quinolin-5-yl)-1H-1,2,3-triazol-4-yl)methoxy)benzoic acid (6.52a):	295
2-((1-([1,1'-biphenyl]-2-yl)-1H-1,2,3-triazol-4-yl)methoxy)-6-hydroxybenzoic acid (6.52b):	296

2-((1-benzyl-1H-1,2,3-triazol-4-yl)methoxy)-6-hydroxybenzoic acid (6.52c):	296
2-hydroxy-6-((1-(naphthalen-1-yl)-1H-1,2,3-triazol-4-yl)methoxy)benzoic acid (6.52d):	297
2-((1-([1,1'-biphenyl]-4-yl)-1H-1,2,3-triazol-4-yl)methoxy)-6-hydroxybenzoic acid (6.52e):	297
2-hydroxy-6-((1-(4-morpholinophenyl)-1H-1,2,3-triazol-4-yl)methoxy)benzoic acid (6.52f):	297
2-hydroxy-6-((1-phenyl-1H-1,2,3-triazol-4-yl)methoxy)benzoic acid (6.52g):	298
2-hydroxy-6-((1-(naphthalen-1-ylmethyl)-1H-1,2,3-triazol-4-yl)methoxy)benzoic acid (6.52h/i):	298
2-((1-(4-benzylphenyl)-1H-1,2,3-triazol-4-yl)methoxy)-6-hydroxybenzoic acid (6.52j):	299
2-hydroxy-6-((1-(2-phenoxyphenyl)-1H-1,2,3-triazol-4-yl)methoxy)benzoic acid (6.52k):	299
2-((1-(cyclohexylmethyl)-1H-1,2,3-triazol-4-yl)methoxy)-6-hydroxybenzoic acid (6.52l):	300
2-((1-(adamantan-1-ylmethyl)-1H-1,2,3-triazol-4-yl)methoxy)-6-hydroxybenzoic acid (6.52m):	300
6.7 - References	301

LIST OF SCHEMES

Scheme 1.1 – Cyclization of 3,5,7-triketoacids	10
Scheme 1.2 – Fatty Acid vs Polyketide Biosynthesis.....	11
Scheme 1.3 – Natural vs Unnatural Chalcone Synthase Pathways	13
Scheme 1.4 – Biosynthesis of Olivetolic Acid	14
Scheme 1.5 – Proposed Biosynthesis of Ginkgolic Acid	15
Scheme 1.6 – Biomimetic Synthesis of β -Resorcylic Acids and Acylphloroglucinols	17
Scheme 1.7 – Synthesis of Oresellinic Acids via Alkylation of 3,5-Dimethoxy-fluorobenzene.....	18
Scheme 1.8 – Alkylative Additions to Phthalic Anhydrides	20
Scheme 1.9 – Kubo’s Synthesis of Saturated and Unsaturated Anacardic Acids	22
Scheme 1.10 – Synthesis of 6-Alkylsalicylates using the Alder–Rickert Reaction	24
Scheme 1.11 – Satoh’s Synthesis of Ginkgolic Acid	25
Scheme 2.1 – Deconjugative Remote Functionalization of a Long-Chain Alkenol.....	34
Scheme 2.2 – Heck’s Early Arylation Work with Vinyl Alcohols.....	37
Scheme 2.3 – Reaction of Amines with π -Allyl Palladium Intermediates	39
Scheme 2.4 – Larock’s Early Exploration of Palladium Chain-Walking.....	41
Scheme 2.5-Asymmetric Carbopalladation of Alkenols Using a Chiral PyrOx Ligand ..	46
Scheme 2.6 – Asymmetric Control in the Formation and Retention of Two Chiral Centers	47
Scheme 2.7 – Selective Bond Cleavage in the Remote Ring-Opening of Cyclopropanes	47

Scheme 2.8 – Mechanistic Investigations of Chain-Walking Using Deuterium Labeling	49
Scheme 3.1 – Preparation of Protected Aryl Triflate From 2,6-Dihydroxybenzoic Acid	58
Scheme 3.2 – Preliminary Heck Redox-Relay Results with 3-Buten-1-ol	59
Scheme 3.3 – Wittig Olefinations Used in the Synthesis of (15:1) and (15:2) Anacardic Acids	68
Scheme 3.4 – Unnatural Anacardic Acid Synthesis via Julia–Kocienski Olefination	69
Scheme 4.1 – Chlorocarbonylation Of Adamantane	105
Scheme 4.2 – Photoacetylation of Adamantane Using Biacetyl	106
Scheme 4.3 – Formylation of Adamantane via An Aldoxime Intermediate	109
Scheme 4.4 – General Carbonylation of the Adamantyl Radical Using CO	110
Scheme 4.5 – Carbonylation and Other Oxidative Transformations of Adamantane via NHPI	111
Scheme 4.6 – Tandem Carbonylation-Addition via TBADT Photocatalysis	113
Scheme 4.7 – Oxidative Metal-Free Radical Carbonylation	114
Scheme 4.8 – Transition Metal-Catalyzed Carbonylations of Adamantane	115
Scheme 4.9 – General Giese Reaction with Adamantane	116
Scheme 4.10 – Photochemical Addition to Alkenes Using Benzophenone	118
Scheme 4.11 – Additions to Alkenyl Nitriles	119
Scheme 4.12 – Synthesis of β -Adamantylketones via Addition to Cyclic Enones	120
Scheme 4.13 – Oxyalkylation of alkenes using Adamantane and O ₂	123
Scheme 4.14 – Mechanism for Co-Catalyzed Oxyalkylation of Alkenes	124

Scheme 4.15 – Metal-free Radical Addition Cascade with an Oxiranylcarbinyll Derivative	125
Scheme 4.16 – A General Addition-Fragmentation Sequence	126
Scheme 4.17 – Decarboxylative Alkenylation of Adamantane with Cinnamic Acid.....	127
Scheme 4.18 – Photocatalytic Allylation of Adamantane with Sulfonylated Propene... 128	
Scheme 4.19 – Photochemical Allylation Using an Amidyl Radical Cascade.....	130
Scheme 4.20 – Photochemical Alkenylation of Substituted Adamantanes	131
Scheme 4.21 – General Radical Alkynylation	132
Scheme 4.22 – Alkenylation of Adamantane Using Alkynyl Triflones	133
Scheme 4.23 – Photoinduced Alkynylation Using Tosyl-(trimethylsilyl)Acetylene	134
Scheme 4.24 – Radical Alkynylation Using an Ethynyl Benziodoxole	135
Scheme 4.25 – Alkyne Addition-Cyclization Using Alkynyl Diphenylphoshine Oxides	136
Scheme 4.26 – UV Arylation of Adamantanes Using TCB	137
Scheme 4.27 – General Minisci Arylation Involving Adamantane	139
Scheme 4.28 – Early Minisci Arylations of Adamantane.....	141
Scheme 4.29 – Oxidative Azide-Assisted Minisci Reaction with Adamantane.....	141
Scheme 4.30 – Use of DTBP in Minisci Reactions with Indoles and Purines	142
Scheme 4.31 – Cobalt-Catalyzed Cross-Couplings with Oxazoles and Thiazoles.....	143
Scheme 4.32 – Arylation of Bromo-adamantanone Using Ni/TBADT Catalysis	144
Scheme 4.33 – Adamantanone Arylation via Nickel/Decatungstate Dual Catalysis.....	145
Scheme 4.34 – Photo Induced Cyanation of Adamantanes Using Tosyl Cyanide	146

Scheme 4.35 – Cyanation of Adamantane Using Cyanobenziodoxol	149
Scheme 4.36 – Aminoalkylations Using α -Amino Carbonyls.....	149
Scheme 5.1 – Synthesis of Early Test Substrates for the Ir-1/Q-1 Catalyst System	169
Scheme 5.2 – Synthesis of Chiral Mesitylsulfinamide	188
Scheme 5.3 – Deprotection to Free Amine Products Using SmI ₂ and TFA	190
Scheme 6.1 – Mitsunobu Synthesis of an Aryl Ether Anacardic Acid Derivative	240
Scheme 6.2 – Mitsunobu Reactions with 1,3-Propanediol and 1,4-Butanediol	242
Scheme 6.3 – Synthesis of an Adenylated Anacardic Acid Derivative	244
Scheme 6.4 – Synthesis of a Naphthylated Anacardic Acid Derivative.....	245
Scheme 6.5 – Synthesis of a Butyne-Linked Naphthylated Anacardic Acid Derivative..	246
Scheme 6.6 – Synthesis of a Divergent Propargyl Tosylate Intermediate.....	247
Scheme 6.7 – Benzyl Substitution of Aryl Acetonide With Piperidines and N-Boc Piperazine.....	253
Scheme 6.8 – Piperazine-Linked Derivatives Using Reductive Amination	254
Scheme 6.9 – Alternative Acetonide Deprotection Strategy Using Hydrogenolysis	255
Scheme 6.10 –Piperazine Sulfonamide-Linked Anacardic Acid Derivatives	256
Scheme 6.11 – Synthesis of Azides For Use in Click-Reactions	257

LIST OF FIGURES

Figure 1.1–Naturally-Occurring Anacardic Acids and Related Phenolic Lipids	1
Figure 1.2 – Phytochemical Sources of Phenolic Lipids	2
Figure 1.3 – Global 2018 Cashew Production	3
Figure 2.1 – Depiction of a General Non-Dissociative Chain-Walking Process.....	33
Figure 2.2 – Catalytic Cycle of a Heck Redox-Relay Involving Chain-walking	35
Figure 2.3 – Simplified Reaction Profile Based of DFT Calculations by Sigman at al. ..	36
Figure 2.4 – Design and Optimization of Sigman’s Chiral PyrOx Ligand.....	45
Figure 3.1 – Considerations and Strategy for A Heck-Based Anacardic Acid Synthesis	57
Figure 3.2 – ¹ H NMR Spectrum of Linear and Branched Heck-Relay Products	60
Figure 3.3 – Side Product Formation in Reactions Using DMF Solvent.....	61
Figure 3.4 – Retrosynthesis for (15:1) Ginkgolic Acid	67
Figure 3.5 – ¹ H NMR Chemical Shifts for <i>cis/trans</i> 2,3-Dibutyloxiranes.....	71
Figure 3.6 – ¹ H NMR Comparison of <i>E/Z</i> Alkenes and Corresponding Epoxides.....	71
Figure 3.7 – Extent of MMP-2 Inhibition by Anacardic Acids at Different Concentrations	72
Figure 3.8 – Matrix Metalloproteinase-2 with a β-APP Derived Inhibitor.....	74
Figure 4.1 – The Structure of Adamantane.....	99
Figure 4.2 – Historical Developments in Adamantane Synthesis.....	100
Figure 4.3 – Adamantane Containing Pharmaceutical Agents	102
Figure 4.4 – Uses of Adamantanes in Non-Pharmaceutical Applications	103
Figure 4.5 –A General HAT Reaction with Adamantane and Known Reactive Species	104

Figure 4.6 – Acetylation of Higher Order Diamondoids	108
Figure 4.7 – Mechanism and Scope for TCB Arylation of Adamantane.....	138
Figure 4.8 – TCB Arylation of Higher Order Diamondoids.....	139
Figure 5.1 – Classical and Radical-Based Approaches to Aminoalkylation	162
Figure 5.2 – BDE Comparison of Activated and Unactivated C–H Bonds with Adamantane	163
Figure 5.3 –Excitation of an Ir Photocatalyst and SET From a Tertiary Amine	164
Figure 5.4 – Photocatalytic Alkylation and Aminoalkylation of Adamantane.....	166
Figure 5.5 –Adamantane Aminoalkylation using Reductive Amination.....	167
Figure 5.6 – Initial Survey of Imine Substrates and Photocatalysts	168
Figure 5.7 – Direct vs. Indirect Photocatalytic HAT Processes	175
Figure 5.8 – Examples of Direct and Indirect HAT Catalysts.....	176
Figure 5.9 – Proposed Catalytic Cycle for Indirect Aminoalkylation of Adamantane...	177
Figure 5.10 – Polar Effects During Charge Transfer in the HAT Transition State	180
Figure 5.11 – Proposed Catalytic Cycle for Direct Aminoalkylation of Adamantane ...	180
Figure 5.12 – Amino adamantanes of Medicinal Relevance	186
Figure 5.13 – ¹ H NMR of a Diastereomeric Mixture of Aminoalkyl Tolylsulfinimines	189
Figure 5.14 – Examples of Non-Adamantyl Aminoalkylated Products	190
Figure 6.1 – The Sumoylation Cycle	231
Figure 6.2 – Poly-Sumoylation of Protein Target.....	232
Figure 6.3 – Virtual Screening of Potential Inhibitors.....	235
Figure 6.4 – ATP Docking Study With SUMO E1	236

Figure 6.5 – Clustering Analysis Examples.....	237
Figure 6.6 – Ligand Docking Studies With SUMO E1	239
Figure 6.7 – Mitsunobu-based Assembly of Anacardic Acid Derivatives	242
Figure 6.8 – Sumo Inhibition Studies Using Aryl Ether Anacardic Acid Derivatives...	249
Figure 6.9 – Space Occupation of The ATP Binding Pocket by Anacardic Acid and a Butyne-Linked Derivative	251
Figure 6.10 – FRET Analysis of Triazole-Linked Anacardic Acid Derivatives	261
Figure 6.11 –Successful SUMO E1 Inhibitors Based on In-Situ FRET Assays	262

LIST OF TABLES

Table 1.1 – Naturally Sourced Anacardic Acids	4
Table 1.2 – HPLC Analysis of Solvent-Extracted CNSL.....	5
Table 2.1 – Use of Jeffery’s Conditions with Pd-Catalyzed Reactions of Allyl Alcohols	43
Table 2.2-Reaction of Arylhalides with Alkenols of Varying Length.....	44
Table 3.1 – Heck Relay Coupling with Alkenols of Varying Length	63
Table 3.2 – Comparison of Results Using Phenyl Bromide, Iodide, and Triflate	64
Table 3.3 – Comparison of Results with Various Aryl Substituted Triflates	66
Table 4.1 – Substituent Effects For Adamantane Chlorocarbonylation vs. Halogenation	106
Table 4.2 – Biacetyl Quenching Studies.....	107
Table 4.3 – Early Alkylation of Adamantane Using Electron Withdrawn Alkenes	117
Table 4.4 – Additions to α,β -Unsaturated Ketones and Other Radical Trap Reagents .	121
Table 4.5 – Scope of Photocatalytic Allylation With Substituted Adamantanes	128
Table 4.6 – Arylation of Adamantane with Heteroaromatic Bases Using BPO.....	143
Table 4.7 – NHPI-Mediated Cyanation of Adamantanes Using Tosyl Cyanide	148
Table 5.1 – Previous Work: Adamantane Alkylations with Electron Deficient Alkenes	165
Table 5.2 – Variation of Catalytic Systems with <i>N</i> -Benzoyl-Hydrazone.....	170
Table 5.3 – Variation of Catalytic Systems with a Chiral Sulfinimine	171
Table 5.4 – Effect of Water Additive in Reaction with <i>N</i> -Benzoyl-Hydrazone.....	172
Table 5.5 – Solvent Studies with Substituted Adamantanes and Cyclic Sulfonylimine ..	173

Table 5.6 – Effect of Reaction Concentration for <i>N</i> -Benzoyl-Hydrazone.....	174
Table 5.7 – Competition Experiments with Non-Adamantyl Substrates.....	178
Table 5.8 – Scope of <i>N</i> -Benzoyl-Hydrazones with Various Adamantanes	182
Table 5.9 – Scope of <i>N</i> -Tosyl Imines with Various Adamantanes.....	184
Table 5.10 – Scope of a Cyclic Sulfonylimine with Various Adamantanes.....	185
Table 5.11 – Aminoalkylation Using Chiral Sulfonylimines	187
Table 6.1 – Acetonide Deprotection Using Different Bases and Solvents	241
Table 6.2 – Scope of Butyne-Linked Derivatives from a Common Propargyl Tosylate	248
Table 6.3 –Benzylic Radical Bromination Optimization.....	252
Table 6.4 – Synthesis of 1,2,3-Triazole-Linked Anacardic Acid Derivatives.....	259

LIST OF ACRONYMS AND ABBREVIATIONS

Ac –acetyl	CIAQ –chloroanthroquinone
Acac –acetylacetone	CNSL –Cashew nutshell liquid
Acr –acridinium	CoA –Coenzyme A
AIBN –azobisisobutyronitrile	CSA –camphorsulfonic acid
AML – Acute Myeloid Leukemia	CuAAC –copper alkyne-azide cycloaddition
AMP –adenosine monophosphate	dba –dibenzylideneacetone
Ar –aryl	DCE –1,2-dichloroethane
ATP –adenosine triphosphate	DCM –dichloromethane
AURA –Aurora Kinase A	DDIT –DNA damage induced transcription factor
BDE –bond-dissociation energy	DEAD –diethyl azodicarboxylate
BHT –butylated hydroxytoluene	DMA –dimethylacetamide
Bn –benzyl	DMAP –4-Dimethylaminopyridine
Boc – <i>tert</i> -butyloxycarbonyl	DMF –dimethylformamide
BODIPY –4,4-difluoro-4-bora-3a,4a- diazas-indacene	DMSO –dimethylsulfoxide
BOX –bisoxazoline	DNA –Deoxyribonucleic acid
BPO –benzoyl peroxide	Dtbbpy –4,4'-di- <i>tert</i> -butyl-2,2'-
Bpy –2,2'-bipyridine	DTBP –di- <i>tert</i> -butyl peroxide
BzPy –4-benzoylpyridine	EC₅₀ –half maximal effective concentration
CAN –Ceric ammonium nitrate	
Cat –catalyst	

Equiv –equivalent	LUMO –lowest unoccupied molecular orbital
ESI –electrospray ionization	mCPBA – <i>meta</i> -chloroperoxybenzoic acid
et. al. – <i>et alli</i> (latin)	MIC –minimum inhibitory concentration
EY –eosin Y	MLCT –metal-to-ligand charge transfer
FDA –U.S. food and drug administration	MMP-2 –matrix metalloproteinase-2
FRET –Förster resonance energy transfer	MOF –metal-organic framework
GC –gas chromatography	MRSA –methicillin resistant <i>staph. aureus</i>
HAT –Hydrogen Atom Transfer	MS –molecular sieves
HATs –Histone Acyl Transferases	NBS – <i>N</i> -bromosuccinimide
HOMO –highest occupied molecular orbital	NHC – <i>N</i> -heterocyclic carbene
HRMS –high-resolution mass spectrometry	NHPI – <i>N</i> -hydroxyphthalimide
hν –light	NMM – <i>N</i> -methylmaleimide
IR –infrared (spectroscopy)	NMR –nuclear magnetic resonance spectroscopy
ISC –intersystem crossing	PDB –Protein Databank
KIE –kinetic isotope effect	PG –protecting group
LDA –lithium diisopropylamide	PIFA –[bis(trifluoroacetoxy)iodo]benzene
LED –light-emitting diode	PINO –phthalimide- <i>N</i> -oxyl
LG –leaving group	PT –5,7,12,14-pentacenetetraone

PyrOx–pyridine oxazoline

RNA–Ribonucleic acid

ROS–Reactive oxygen species

RT–room temperature

SAR–structure-activity relationship

SET–single electron transfer

STAB–sodium triacetoxyborohydride

SUMO–Small Ubiquitin-like Modifier

TBACl–tetrabutylammonium chloride

TBADT–tetrabutylammonium
decatungstate

TBHN–di-*tert*-butyl hyponitrite

TCB–1,2,4,5-benzenetetracarbonitrile

TCFH–
tetramethylchloroformamidinium
hexafluorophosphate

TEMPO–2,2,6,6-tetramethylpiperidine
N-oxide

TFA–trifluoroacetic acid

THF–tetrahydrofuran

THP–tetrahydropyran

TLC–thin layer chromatography

TsOH–*p*-toluenesulfonic acid

Ub–ubiquitin

UV–ultraviolet

1 Synthesis of Anacardic Acid and Its Derivatives

1.1 - Introduction

The anacardic acids (**1.1-1.4**) are phenolic lipids comprised of an aromatic salicylic acid core and a long aliphatic tail. The tail portion can vary in length and exists in both saturated and unsaturated forms. Anacardic acids and other non-isoprenoid phenolic lipids such as cardanols and cardols (**1.5** and **1.6**) are phytochemical in origin and have long been used in traditional medicine^[1] for the treatment of many ailments while urushiols (**1.7**) act as haptens responsible for the contact dermatitis associated with poison oaks, ivies, and sumacs.

Today, anacardic acids are known to possess broad bioactivities such as antioxidant, anti-inflammatory, anticancer, antibacterial, and as insect antifeedants.^[2] In

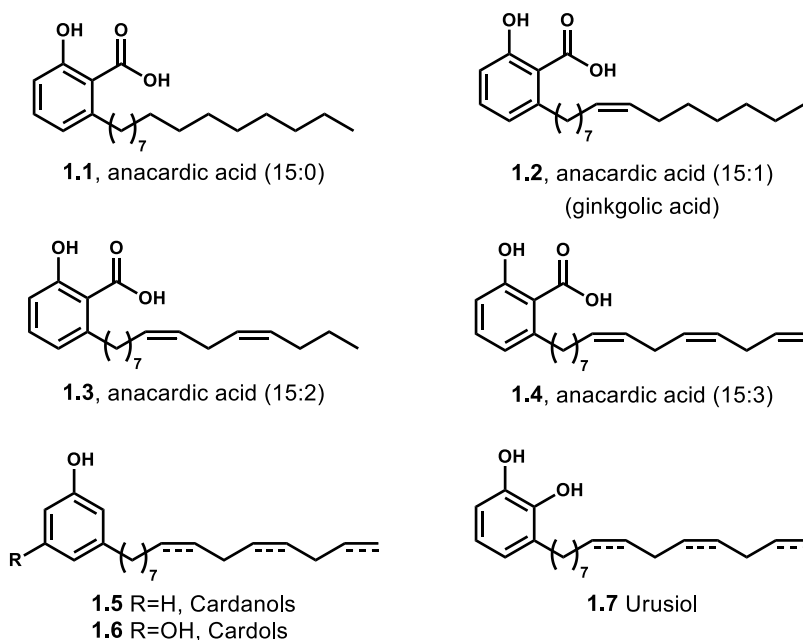


Figure 1.1–Naturally-Occurring Anacardic Acids and Related Phenolic Lipids
addition, anacardic acid itself has been found to act as an inhibitor for numerous enzyme

targets. Many of these targets have potential medicinal application due to their anticancer, antibacterial, and anti-inflammatory properties. However, isolation and study of anacardic acids from natural sources is challenging due to the presence of other similar phenolic lipids often produced in tandem. The resulting phytochemical extracts are complex and can be challenging and costly to isolate in pure form. Therefore, the use of synthetic approaches provides a useful means of accessing specific anacardic acids directly.

1.2 - Background

1.2.1 - Natural Sources

Anacardic acids are found primarily in plants (**Figure 1.2**), although some have been isolated from bacteria and brown algae.^[3] Many anacardic acids are found in high concentrations in the nutshell oils of various seeds where their antimicrobial properties may help protect the seed prior to and during germination. Nutshell oils known to contain anacardic acids and other phenolic lipids have been isolated from the cashew (*Anacardium occidentale*)^[4,5], pistachio (*Pistachia vera*)^[6], Australian daisy (*Helipterum sp.*)^[7], nutmeg

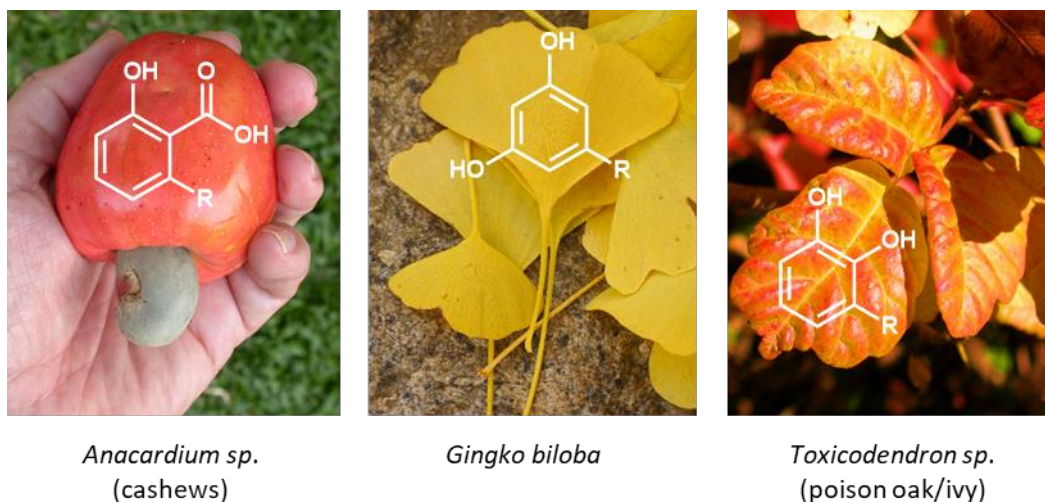


Figure 1.2 – Phytochemical Sources of Phenolic Lipids

Phenolic lipids can be isolated from a variety of plants. (R=alkyl chain)

(*Myristica sp.*)^[8], and olive drupe (*Oleaceae sp.*)^[9] Other plants from which anacardic acids have been isolated in appreciable amounts include the maidenhair tree (*Ginkgo biloba*)^[10], liverwort (*Schistochila appendiculata*)^[11], and garden geranium (*Pelargonium × hortorum*[¶]).^[12,13] The structures of the most prevalent natural anacardic acids are summarized in **Table 1.1** and where they can be naturally sourced.

Industrially, the largest natural source of anacardic acids **1.1-1.4 (Figure 1.1)** comes from cashew nutshell liquid (CNSL). This dark oily substance constitutes between 15-30% of the nutshell by mass and is produced in large quantities as a byproduct of the cashew industry which harvested over 789,000 metric tons globally in 2018 (**Figure 1.3**).^[14] CNSL is finding increasing use in the automotive, coatings, and leather industries as laminating resins, epoxy resins, cements, foundry chemicals, and rubber compounding resins.^[15] A number of methods exist for the extraction of CNSL from the rest of the shell.

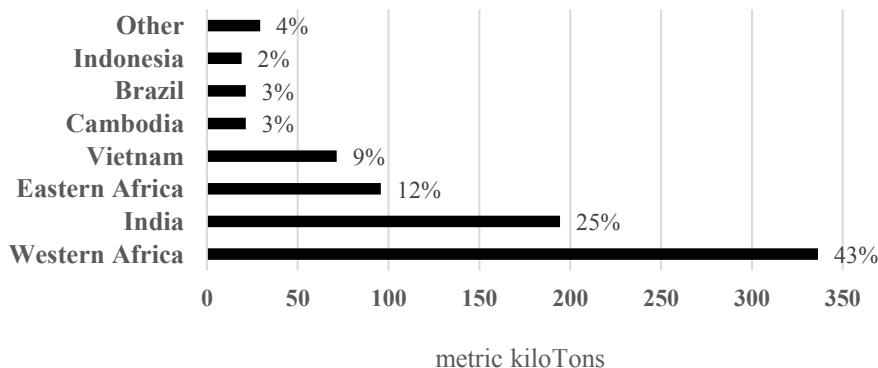


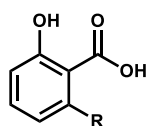
Figure 1.3 – Global 2018 Cashew Production

The cashew grows well in tropical areas and has become important economic export for many countries.

[¶] Note regarding terminology: In botanical nomenclature, interspecies hybrids are named using an “x” between the genera and the new nothospecies name resulting from the cross speciation. Here, the nothospecies name *hortorum*, from the latin hortus meaning “garden,” is cross between *Pelargonium zonale* and *Pelargonium inquinans*. This nothospecies is the most common geranium sold at garden centers.

These can include mechanical,^[16] thermal,^[17] solvent,^[18] and pyrolysis^[19] based techniques. The composition of the CNSL varies with the method of extraction used. Anacardic acids make up approximately 63% of the liquid when solvent extraction

Table 1.1 – Naturally Sourced Anacardic Acids



C:D*	Structure	Name	Natural Sources
11:0		Anagigantic Acid	nutmeg, liverwort, cashew
13:0		Anacardic Acid (13:0)	nutmeg, pistachio
15:0		Cyclogallipharic Acid	<i>Ginkgo biloba</i> , cashew, nutmeg, pistachio
15:1		Ginkgolic Acid (15:1)	<i>Ginkgo biloba</i> , cashew, daisy, nutmeg, geranium
15:2		Anacardic Acid (15:2)	<i>Ginkgo biloba</i> , cashew, pistachio
15:3		Anacardic Acid (15:3)	<i>Ginkgo biloba</i> , cashew, pistachio
17:1		Merulinic Acid C	cashew, geranium
17:2		Pelandjauic Acid	cashew
n/a		salaceyin A	<i>Streptomyces laceyi</i> (castor bean endophyte)

*Lipid numbering from fatty acid nomenclature where C is the number of carbons and D is the number of double bonds.

methods are used (**Table 1.2**). The relative proportions for the anacardic acids are 3:1:1 for the triene, diene, and monoene respectively. However, when higher temperature extraction methods are used, decarboxylation of the anacardic acids occurs and makes cardanols the major component (~65%).^[20] The cardanols isolated in this way find their use in the

chemical industry and have been shown to possess little medicinal value. The anacardic acids on the other hand offer many medicinally useful bioactivities.

Many parts of the *Anacardium occidentale* (cashew) tree have seen use in various folk remedies. The nutshell oil has been used for ulcers, warts, and cracks on the feet while old leaves can be applied to the dressings for rashes and burns. On the African Gold Coast, the bark and leaves are used to combat gingivitis and toothaches or can be used to create decoctions taken for diarrhea.^[21] In India, the bark is used in herbal tea concoctions for asthma, cold and congestion, and as an antidote for snake bites.^[22] The varied applications of this single plant have resulted in numerous studies probing the specific bioactivities of anacardic acids.

Table 1.2 – HPLC Analysis of Solvent-Extracted CNSL

Constituent	Retention Time (min)	Yield (%)
Cardol triene	4.41	15.36
Cardol diene	5.75	6.96
Anacardic acid triene	7.48	28.00
Cardol monoene	8.43	1.66
Cardanol triene	8.83	2.96
Anacardic acid diene	10.35	17.77
Cardanol diene	12.53	2.29
Anacardic acid monoene	15.93	17.13
Cardanol monoene	20.03	1.74

A reverse phase column was used. Cardol triene was the most polar, which eluted first, while cardanol monoene, being the last to elute, is the least polar component.

1.2.2 - Bioactivities

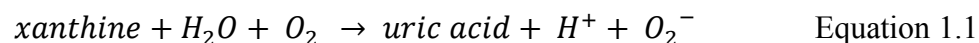
1.2.2.1 - Antimicrobial

Anacardic acids possess antimicrobial properties in many species of gram-negative bacteria. Kubo et al. found that anacardic acids were effective at inhibiting *Helicobacter pylori*, the gut flora responsible for ulcers and acute gastritis.^[23] The degree of unsaturation in the anacardic acid side chain was shown to influence the amount of inhibition observed

in *H. pylori* cell cultures. MIC values of 200 µg/mL were observed for anacardic acid (15:3) and (15:2), 400 µg/mL for (15:1), and > 800 µg/mL for (15:0). No inhibition was observed at up to 1600 µg/mL with salicylic acid indicating that presence of the alkenyl side chain and its degree of unsaturation were critical features for the improved inhibition seen with the anacardic acids. The amount of inhibition by anacardic acid for *Streptococcus mutans* is also dependent on the number of double bonds in the alkyl tail (MIC = 1.56 µg/mL for (15:3), 3.13 µg/mL for (15:2), 6.25 µg/mL for (15:1), and >800 µg/mL for (15:0)).^[24] Several gram-positive bacteria are also inhibited by anacardic acids. Minimal inhibitory concentrations (MIC) have been measured against *Propionibacterium acnes* (1.56 µg/mL), *Corynebacterium xerosis* (6.25 µg/mL), and various strains of *Staphylococcus aureus*^[25] including MRSA (3.1-6.2 µg/mL).^[26] *Aphanomyces cochlioides* and *Bacillus subtilis* have also been shown to be inhibited using anacardic acids extracted from ripe *Ginkgo biloba* fruits.^[27]

1.2.2.2 - Reactive Oxygen Species (ROS)

Anacardic acids are known to act as antioxidants and lower the concentration of ROS although they themselves possess low radical scavenging ability and possess poor affinity towards superoxides.^[28] This suggests that their antioxidant capability comes from inhibiting the production of ROS or by enhancing enzymatic antioxidant activity. Masuoka and Kubo showed that anacardic acid acts as a non-competitive inhibitor of xanthine oxidase,^[29] which produces uric acid and radical anion (**Equation 1.1**) as it aids in the degradation of purines.^[30] Anacardic acid inhibited the production of superoxide with an



EC₅₀ value of 53.6 μM. Interestingly, inhibition of uric acid formation required the use of 20 μM more than what was required for the inhibition of superoxide anion generation suggesting that anacardic acid inhibits superoxide anion formation more strongly than uric acid formation. Salicylic acid was also tested and was found to be a much less potent inhibitor (EC₅₀ = 580 μM) which indicated a beneficial hydrophobic interaction with anacardic acids alkenyl tail.

1.2.2.3 - Histone Acetyltransferases (HATs)

Histone acetyltransferases are a group of enzymes involved with regulating gene expression by covalently modifying the *N*-terminal lysine residues found on histones with acetyl groups using acetyl-CoA. These modifications result in a remodeling of chromatin's tightly packed architecture by allowing histones to wrap DNA less tightly and makes interaction with transcription proteins possible. The dysfunction of these enzymes can cause a myriad of problems and are often associated with the manifestation of cancer. Many transcriptional co-activation proteins are now known to possess HAT activity including the p300/CBP-associated factor (PCAF). Anacardic acid acts an inhibitor for PCAF (IC₅₀= 5 μM)^[31] where the salicylate moiety is thought to mimic the pyrophosphate group of CoA based on molecular docking studies by Dekker and Ghizzoni.^[32] Anacardic acid is also an inhibitor of another HAT member, Tip60. By sensitizing HeLa cells to ionizing radiation by blocking essential Tip60-dependant protein kinases, tumor cells were up to 3.6 times more sensitive to radiation therapy than healthy cells after treatment with 30 μM of anacardic acid.^[33]

1.2.2.4 - Anticancer

Anacardic acid emerged as the first known activator of aurora kinase A (AURA) as a result of a small molecule virtual screening campaign.^[34] Aurora kinase A, B (AURB), and C (AURC) play crucial roles in cell division by controlling chromatid segregation and help with distributing genetic material into newly forming cells.^[35] These kinases, particularly AURA, are known to be frequently overexpressed in colorectal, breast, gastric, prostate, ovarian, colon, and cervical tumors. At 50 μM of anacardic acid, AURA activation via autophosphorylation was increased 5-fold. Being an AURA *activator*, anacardic acid is not acting as an anticancer agent in this case. However, its enhancement of autophosphorylation can be used in anticancer pursuits where dose dependent activation of AURA *in-vivo* would mimic the overexpression of AURA in tumor cells making it easier to study AURA's role in the cell cycle and oncogenesis.

The gene-regulation factor NF- κ B, a family of proteins involved with cell proliferation, are dysregulated in many types of human tumors where it protects cancerous cells from conditions that would otherwise induce apoptosis. Anacardic acid suppressed NF- κ B α after activation tests using carcinogens, growth factors, and inflammation stimuli by inhibiting the phosphorylation of I κ B kinase complex that initiates the NF- κ B pathway.^[36] In addition to induced NF- κ B activation, anacardic acid was also able to prevent consecutive NF- κ B activations via its self-reporting mechanism.

Anacardic extracts from *ginkgo biloba* were shown to display antitumor activity against Scarcoma 180 ascites in mice.^[37] Although their potency was not specifically quantified, it was noted that conversion of the anacardic acids to their methylbenzoate derivatives resulted in a complete loss of activity. Kubo *et al.* found that anacardic acids

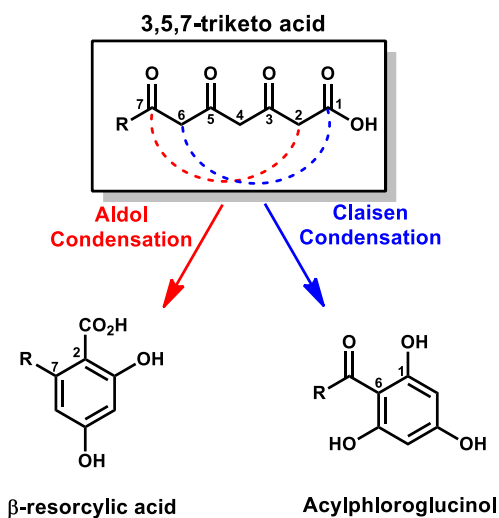
isolated from cashew apple juice were cytotoxic against BT-20 breast cells and HeLa cervix carcinoma cells with ED₅₀ values ranging from 2.69-7.42 µg/mL depending on the unsaturation of the lipid tail. [38] Less unsaturation proved to be more potent which is the opposite of what is observed in antibacterial assays.[1]

The proliferation of estrogen receptor α (ERα)-positive MCF-7 breast cancer cells and endocrine-resistant LCC9 and LY2 breast cancer cells have been inhibited by anacardic acid (24:1) isolated from the common garden geranium (*Pelargonium × hortorum*).[39] At 50 µM anacardic acid, arrest of cell cycle progression and apoptosis in cancerous cell lines was observed but was not seen in the corresponding non-cancerous cell lines.

Anacardic acid has also been shown to be an inhibitor of the SUMO E1 enzyme and the post-translational process known as “sumoylation” and is dysregulated in many cancers such as acute myeloid leukemia (AML).[40] Inhibition of SUMO E1 is the focus of Chapter 6 and therefore is only mentioned briefly here.

1.2.3 - Biosynthesis

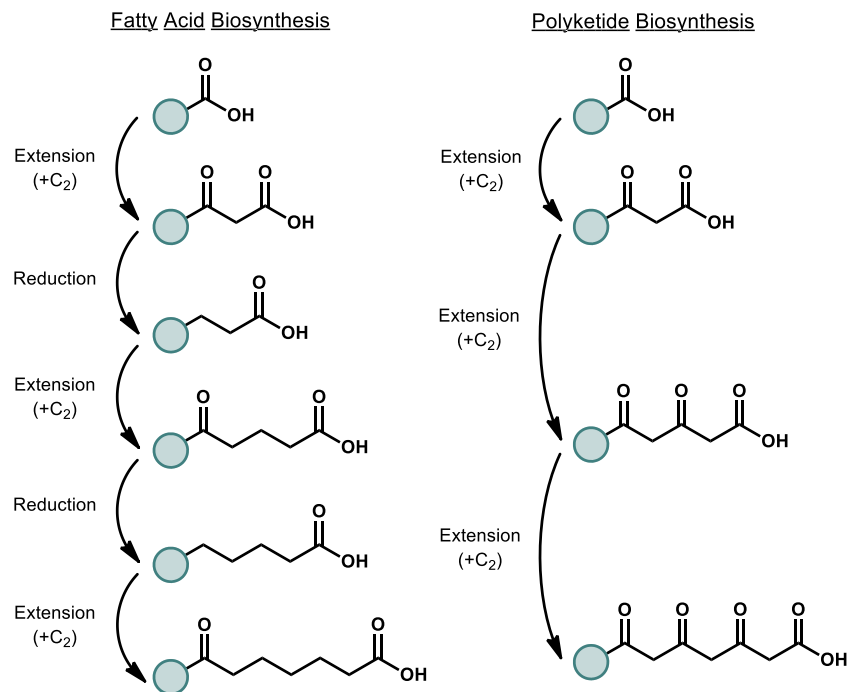
Unlike isoprenoids which can be easily mapped to a series of repeating isoprene units, the molecular building blocks for fatty compounds such as the anacardic acids are



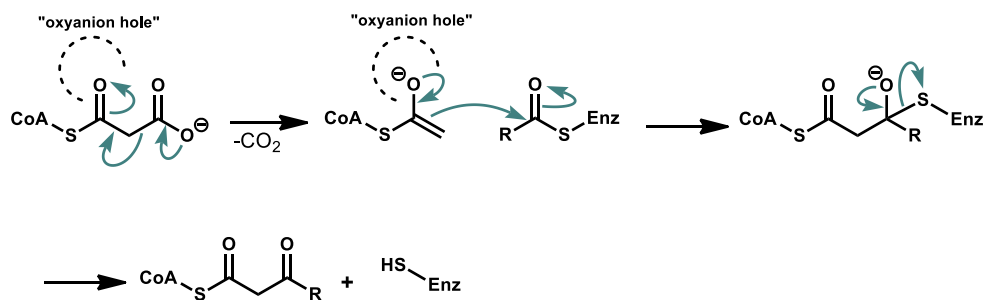
Scheme 1.1 – Cyclization of 3,5,7-triketoacids

less obvious. Pioneering work by Brady, Bloch et al. in the early 1950's used ^{14}C and deuterium labeled acetic acid to show that both acetate carbons were incorporated into cholesterol and fatty acids during *in-vitro* biosynthesis using liver cells.^[41,42] This paved the way for Birch and Donovan to consider the possibility that 3,5,7-triketo acid precursors comprised of head-to-tail acetate linkages were the precursors of phenolic compounds such as β -resorcylic acids and acylphloroglucinols in 1953 (**Scheme 1.1**).^[43] The mechanism for the biosynthesis of these polyketoacids is similar to the chain extensions used in fatty acid biosynthesis minus the reductive intermediary steps (**Scheme 1.2**).

Later, Gellerman and coworkers would go on to focus specifically on the biosynthesis of anacardic acids in plants using acetate incorporation studies in the young plantlets and maturing seeds of the *ginkgo biloba*.^[44,45] These studies showed considerably



General Extension Mechanism



Scheme 1.2 – Fatty Acid vs Polyketide Biosynthesis

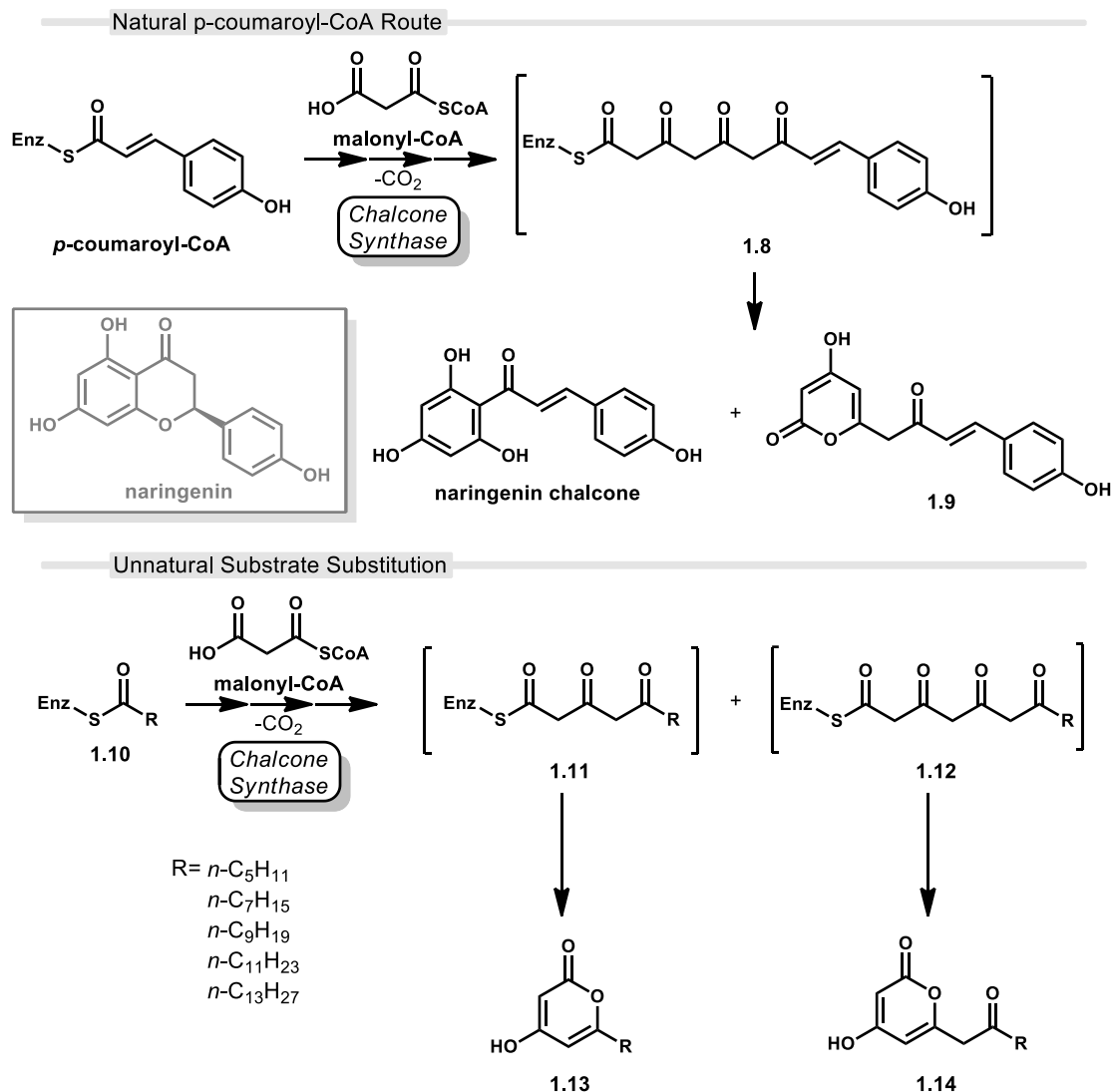
The general mechanism for chain extension in both fatty acid and polyketide biosynthesis are very similar. However, in fatty acid biosynthesis, additional reductive steps occur between condensations.

more ¹⁴C incorporation into the ring and carboxyl group of anacardic acid as opposed to the alkyl tail section. These results suggest that anacardic acid is not made from a single long acyclic precursor produced by one enzymatic system but rather two separate systems that incorporate carbon differently. This led Gellerman and her group to conclude that a

fatty acyl chain (from a lipid pathway) would act as a primer substrate for further extension and cyclization using a polyketide type system.

Even today, a complete picture for the biogenesis of anacardic acids that includes all the key enzymatic players involved has not yet been determined. However, the process is thought to proceed via a type-III polyketide synthase (PKS) that performs successive decarboxylative condensations of malonyl-CoA resembling fatty acid synthesis onto palmitoleoyl-CoA.^[46] Evidence suggests that a chalcone synthase (CHS), a subtype of type-III PKS, may be involved with the production of a host of plant phenylpropanoids including anacardic acids and other phenolic lipids.^[47] The functional promiscuity and broad substrate diversity exhibited by the CHS family is vast^[48] and based on work by Abe et al., recombinant CHS' were not only capable of accepting long-chain CoA esters as substrates, but in many cases the C₆, C₈, and C₁₀ esters were kinetically favored over the natural aromatic substrate, p-coumaroyl-CoA. C₆₋₁₄ CoA esters underwent sequential polyketide elongation with recombinant *S. baicalensis* CHS.

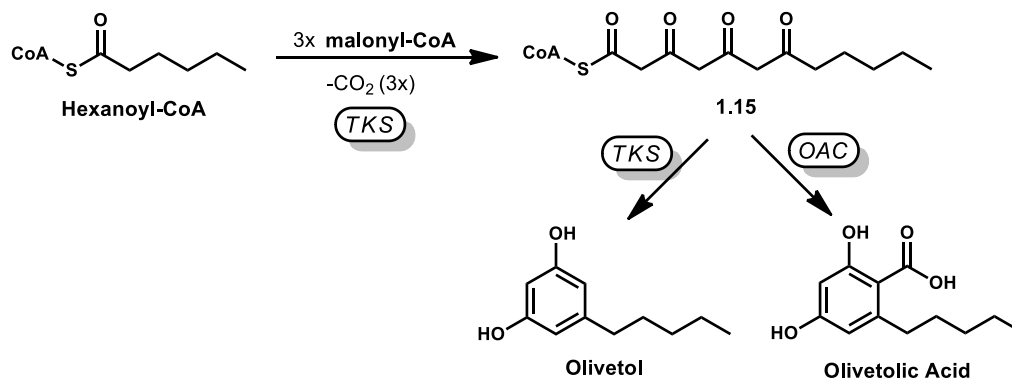
When acting on the natural p-coumaroyl-CoA substrate, naringenin chalcone is predominantly produced along with a minor amount of the α -pyrone **1.9** (**Scheme 1.3**).



Scheme 1.3 – Natural vs Unnatural Chalcone Synthase Pathways

The chalcone synthase (CHS) naturally binds aromatic substrates like *p*-coumaroyl-CoA but it is more than capable of accepting various alkyl-CoA substrates. However, its ability to aromatize polyketide intermediates is lacking and only cyclizes these intermediates into α -pyrone products

However, terminal aromatization was not observed for unnatural *n*-alkyl CoA esters **1.10**. Instead, only α -pyrone products **1.13** and **1.14** were detected; formed from the corresponding tri- and tetraketides **1.11** and **1.12**. The exact enzymes responsible for aromatization of the key tetraketide intermediates leading to the long-chain alkyl phenols observed in the Anacardiaceae and Ginkgoaceae families have yet to be identified.



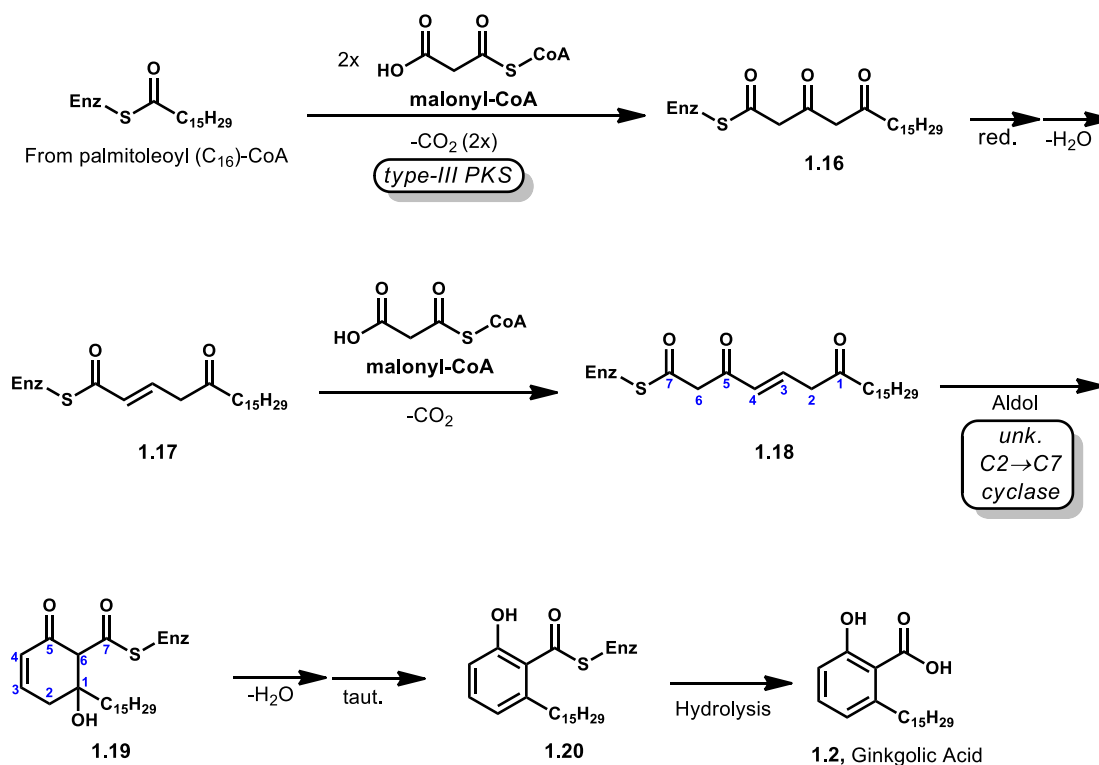
Scheme 1.4 – Biosynthesis of Olivetolic Acid

The synthesis of olivetolic acid requires the olivetolic acid cyclase (OAC) accessory protein.

On the other hand, the tetraketide synthase (TKS) responsible for formation of olivetolic acid from hexanoyl-CoA (the first step in cannabinoid biosynthesis, see **Scheme 1.4**) has been determined to require an accessory protein named olivetolic acid cyclase (OAC).^[49] After chain extension to the tetraketide intermediate **1.15**, without the OAC acting as an accessory protein, TKS alone only catalyzes the formation of resorcinolic olivetol. Similar to Abe's previous report, minor amounts of the pyrone product were detected; however, no olivetolic acid was observed. Therefore, it is likely that a similar yet to be identified accessory protein is involved with the biosynthesis of longer chain phenolic acids such as anacardic and ginkgolic acid.

A reasonable proposal for the biosynthesis of ginkgolic acid is shown in **Scheme 1.5**. Starting with palmitoleoyl-CoA, a type-III PKS (a tetraketide synthase) performs two ketide extensions using malonyl-CoA to form triketide intermediate **1.16**. A reduction-elimination of the central ketyl group to **1.17** followed by another ketide extension generates the final acyclic precursor **1.18**. Based on the known olivetolic acid pathway, an unknown cyclase is then believed to catalyze this precursor's cyclization via an

intramolecular aldol to cyclic β -hydroxyketone intermediate **1.19**. Such a cyclization would also be assisted by an *E* to *Z* isomerization of enone intermediate **1.18**. It is unclear if this would be accomplished by the cyclase itself or if a separate isomerase would be involved altogether. Completion of the condensation with loss of water followed by tautomerization establishes aromaticity and completes the phenolic core in intermediate **1.20**. Hydrolysis then releases ginkgolic acid (**1.2**).



Scheme 1.5 – Proposed Biosynthesis of Ginkgolic Acid

This proposed biosynthesis is supported by Abe's work with recombinant chalcone synthases which demonstrated the capability of these PKS enzymes to act on long-chain

aliphatic substrates. Additional evidence that hexanoyl-CoA undergoes polyketide extension followed by aromatization to the alkyl salicylic acid uses a dedicated cyclase further supports this is a likely route to the synthesis of anacardic acids. However, due the similarity between fatty acid and polyketide pathways, older prevailing theories in the 1950's and up to the early 90's assumed that modified fatty acid synthases were involved in anacardic acid biosynthesis.^[12,46,50,51]

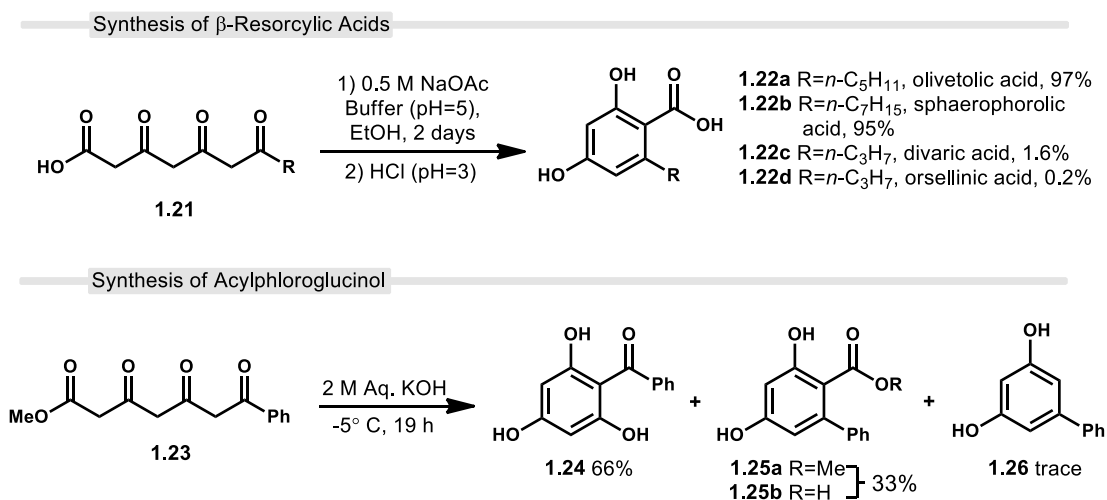
1.3 - Previous Syntheses of Anacardic Acids

The strategies for the synthesis of anacardic acids are similar to those used for other phenolic lipids. The history of phenolic lipid synthesis goes back to 1942 with the attempted synthesis of urushiol, the alkyl catechol in poison oaks and ivies.^[52] However in this section, only an overview of methods used to reach anacardic acid products will be discussed. From a synthetic standpoint, anacardic acids and related phenolic lipids are simplistic compounds, consisting of only two logical components: the aromatic core and the lipid tail. They only possess stereogenic alkene centers alleviating the need for considerations of stereocontrol past geometric isomerism. Additionally, their narrow range of functional groups eliminates complications arising from chemoselectivity issues. Despite this simplicity, a number of strategies have been developed for their synthesis. They have been broadly differentiated here based on the methods used to connect the aromatic core and the lipid tail.

1.3.1 - Early Biomimetic Approach (1967)

The earliest attempts at the synthesis of long-chain alkyl phenols were biomimetic in nature and attempted to replicate the intramolecular condensations of polyketoacids that

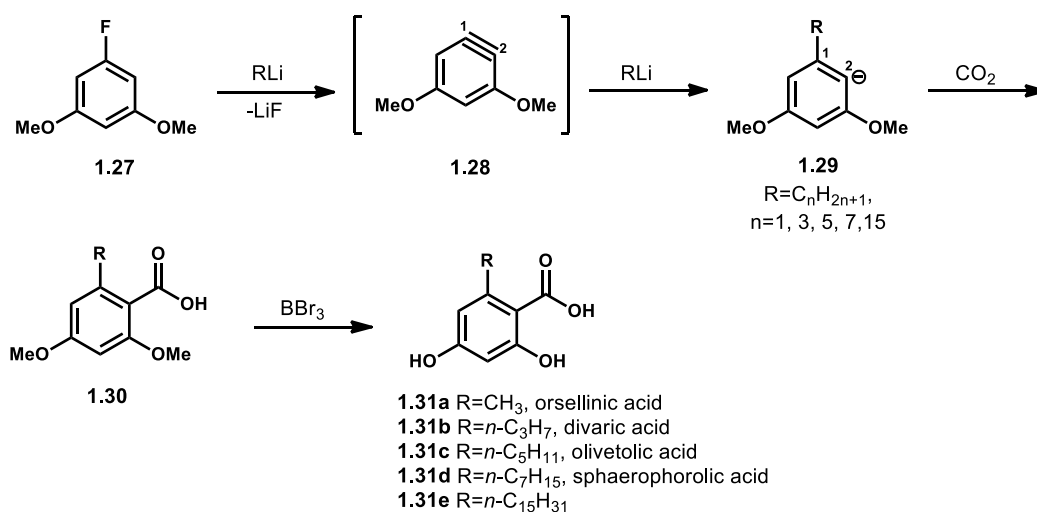
were believed to be biochemically catalyzed (see **Scheme 1.1**). Despite these polyketoacid precursors being proposed in the early 1950s, it was not until 1967 that they could be tested due to their synthetic inaccessibility at the time. It was then that Harris and Carney showed that β -resorcylic acids **1.22a-d** could be made via intramolecular aldol condensation under acidic conditions from 3,5,7-triketo acids (**1.21**, **Scheme 1.6**).^[53] These cyclizations were found to be pH sensitive, with the keto acids remaining stable at low pH in the range of 3-4 and concomitant decarboxylation occurring near pH 7. Optimal cyclizations occurred for phenylpolyketo acids with longer alkyl substituents (products **1.22a**, **1.22b**) but were significantly less efficient for shorter alkyl substituents (products **1.22c**, **1.22d**). Acylphloroglucinol was also formed under basic conditions through Claisen condensation



Scheme 1.6 – Biomimetic Synthesis of β -Resorcylic Acids and Acylphloroglucinols of the corresponding polyketo methylester **1.23**. The acylphloroglucinol product **1.24** was also accompanied by competing acylresorcinol aldol products **1.25a** and **1.25b** and trace amounts of the decarboxylated product **1.26**.

1.3.2 - Tyman's Aryne Alkylation-Carboxylation (1973)

One of the earliest reports of a synthesis beginning with a cyclic aromatic precursor is Tyman and Durrani's synthesis of orsellinic acid and related compounds using 3,5-dimethoxyfluorobenzene (**Scheme 1.7, 1.27**).^[54,55] Treatment with an alkyl lithium proceeded to give the reactive aryne intermediate **1.28** via vicinal elimination of lithium fluoride. Subsequent aryne alkylation to **1.29** favored addition at the 1-position using a second equivalent of the corresponding alkyl lithium. The resulting aryl anion was then carboxylated using solid carbon dioxide to produce the dimethoxybenzoic acids (**1.30**).



Scheme 1.7 – Synthesis of Oresellinic Acids via Alkylation of 3,5-Dimethoxyfluorobenzene

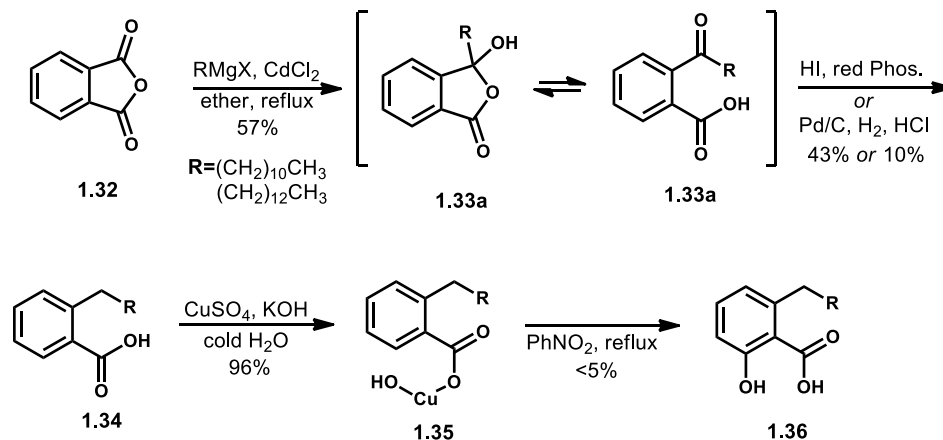
Only trace amounts of the opposite regioisomer were observed using this method. It was found that attempting demethylation using boron trichloride afforded only the

monomethoxy-deprotected products. Boron tribromide however gave the desired fully deprotected alkyl resorcinol products (**1.31a-e**).

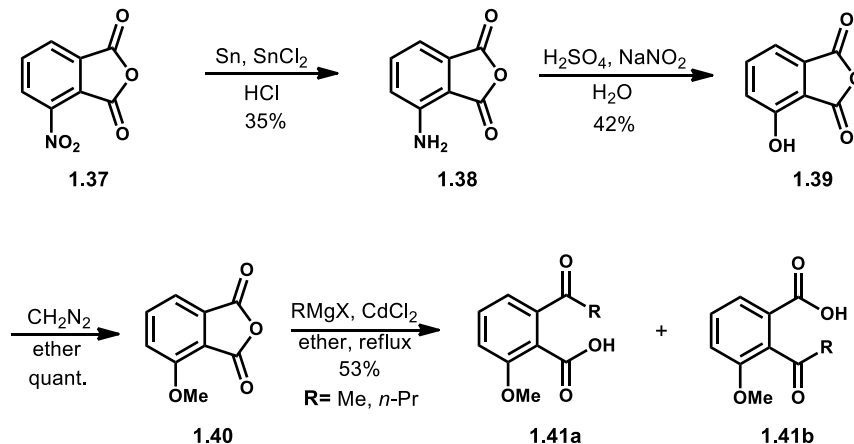
1.3.3 - Tyman's Alkylation of Phthalic Anhydride (1979)

Following his aryne lithiation method, Tyman later went on to develop two similar methods for the synthesis of 6-alkylsalicylic acids starting from phthalic anhydride.^[55] While creative, both methods suffer from issues arising from either low overall yield or isolation difficulties. The first approach (Method A, **Scheme 1.8**) uses dialkylcadmium generated *in-situ* from the corresponding Grignard for the alkylation of phthalic anhydride (**1.32**). The resulting 3-alkyl-3-hydroxyphthalide **1.33a** and its open chain benzoic acid tautomer **1.33b** proved to be difficult to reduce to the alkyl benzoic acid **1.34**. Ultimately, Tyman found success with an antiquated reduction procedure using prolonged treatment with hydroiodic acid and red phosphorus which gave reduced product in 43% yield. Acidic hydrogenolysis was also found to afford the desired reduced product albeit in much lower yield (10%). Next the reduced benzoic acid was converted into the basic copper salt **1.35** which was then heated in nitrobenzene to induce a thermal rearrangement into the desired 6-alkylsalicylic acid **1.36**. Unfortunately, the yield following the heating procedure was extremely low with a large majority of the product undergoing decarboxylation to the 3-alkylphenol.

Method A



Method B



Scheme 1.8 – Alkylative Additions to Phthalic Anhydrides

In an attempt to improve the overall yield, Tyman tried to install the hydroxyl group of the salicylic acid moiety first followed by alkylation (Method B, **Scheme 1.8**). In this approach, 3-nitrophthalic anhydride (**1.37**) was reduced to the amine **1.38** in preparation for a Sandmeyer reaction which afforded 3-hydroxyphthalic anhydride (**1.39**). Following protection using diazomethane to the aryl methoxide **1.40**, alkylation using the same dialkylcadmium method employed in method A was attempted. This reaction however

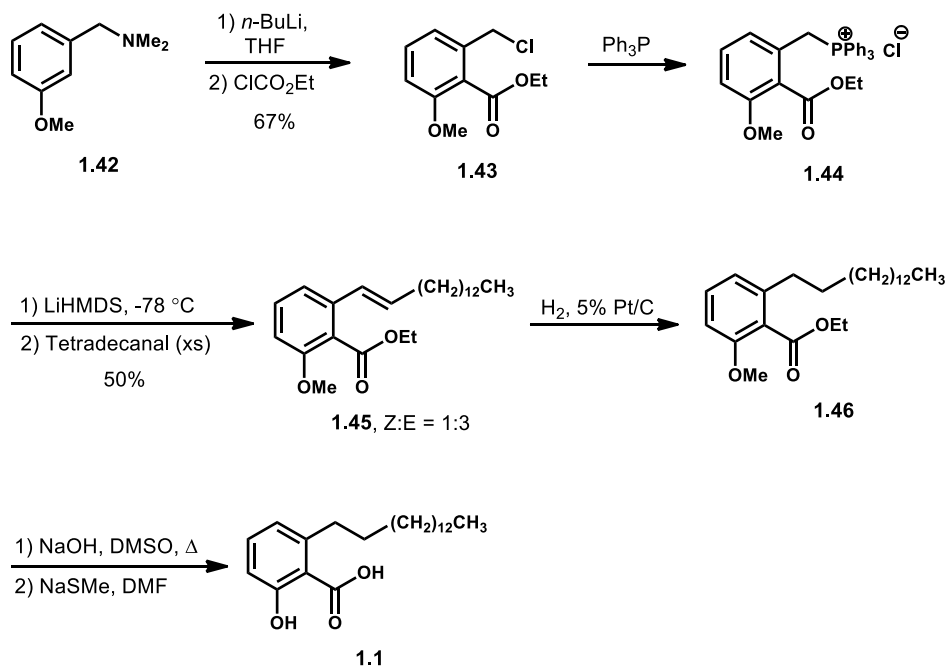
resulted in an inseparable mixture of 1,2-acylbenzoic acids (**1.41a** and **1.41b**) and this avenue too was abandoned.

1.3.4 - Kubo's Wittig Approach for 15:0 Anacardic Acid (1987)

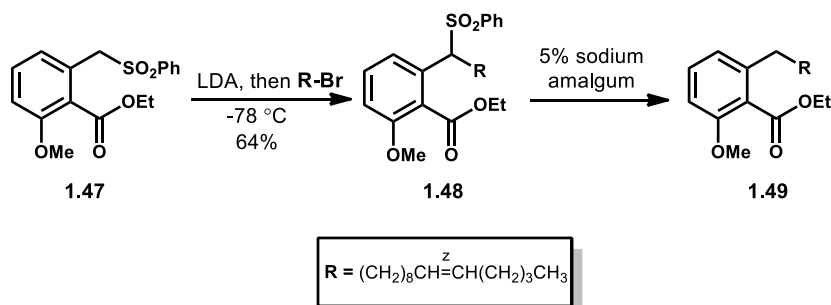
Kubo et al. (**Scheme 1.9**) devised a means to synthesize 15:0 anacardic acid in order to confirm the structures of compounds found in *Ozoroa mucronate* (Anicardiaceae) isolates that inhibited prostaglandin synthetase activity.^[56] To prepare the aromatic core, their approach utilized an ortho-metalation strategy inspired by Dean and Rapoport^[57] starting with lithiation of 3-methoxy-*N,N*-dimethylbenzylamine (**1.42**). The aryl lithium was then quenched with excess ethyl chloroformate to give chlorinated salicylate **1.43** and converted into the corresponding phosphonium salt **1.44** using triphenylphosphine. This phosphonium was then used in a Wittig reaction with tetradecanal to attach the tail as styrenyl intermediate **1.45**, followed by reductive hydrogenation to the protected anacardic acid precursor **1.46**. Deprotection carried out under basic conditions afforded anacardic acid (15:0). This strategy works for the fully saturated anacardic acid, however due to the late stage reductive conditions used, this approach is not viable for the construction of unsaturated anacardic acids.

To address this, Kubo used an alternative method to avoid the use of nondiscriminate catalytic hydrogenation. Benzyl chloride **1.43** used in the previous synthesis was converted to sulfone **1.47** using benzene sodium sulfinate. The sulfone was then treated with LDA and alkylated to form **1.48** using an unsaturated alkyl bromide.

Synthesis of Unsaturated Anacardic Acid (15:0)



Synthesis of Saturated Anacardic Acid (15:1)



Scheme 1.9 – Kubo's Synthesis of Saturated and Unsaturated Anacardic Acids

Reductive cleavage of the sulfone gave an anacardic acid (15:1) precursor leaving the olefin intact.

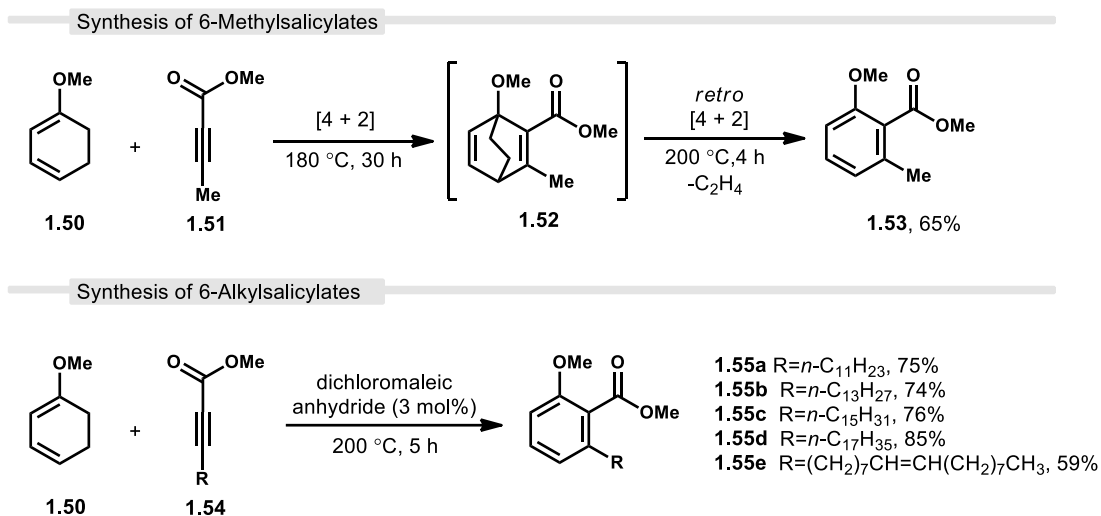
Later, Hird and Milner reported that Kubo's procedure could be improved by substituting lithium bis(trimethylsilyl)amide (LiHMDS) for sodium methoxide which

provided cleaner reactions and higher yields.^[58] They used this modification for the synthesis of anacardic acid itself in addition to several branched anacardic acid analogues.

1.3.5 - Gerlach's 4+2 Cycloaddition/Reversion Method (1995)

In 1989, Rao and coworkers reported a method for the synthesis of 6-alkylsalicylates and alkylresorcinols that utilizes a unique cycloreversion strategy (**Scheme 1.10**).^[59] This process begins with a Diels–Alder reaction between 1-methoxycyclohexa-1,3-diene (**1.50**) and acetylenic dienophile **1.51** to form an intermediate bicyclo[2.2.2]octadiene, **1.52**. Cycloreversion of this intermediate via the Alder–Rickert reaction^[60] with loss of ethylene then affords the aromatized salicylate **1.53**. Only the 6-methylsalicylate product was synthesized in this initial report.

Later, Gerlach and Zehnter would go on to demonstrate this method as a viable strategy for the construction of alkylsalicylates that possessed the characteristically long-lipid tails found in the anacardic acid family.^[61] Rao's procedure was slightly modified to include a catalytic amount of dichloromaleic anhydride which increased the reaction efficiency and cut down on reaction time. Dieneophiles with *n*-alkyl substituents of varying length underwent the reaction to form product as a single regioisomer in good yield (**1.55a-e**, 74-85%). An olefin-containing alkyl substituent was also tolerated with marginally lower yield to give **1.55e** with an unsaturated side chain similar to ginkgolic acid.

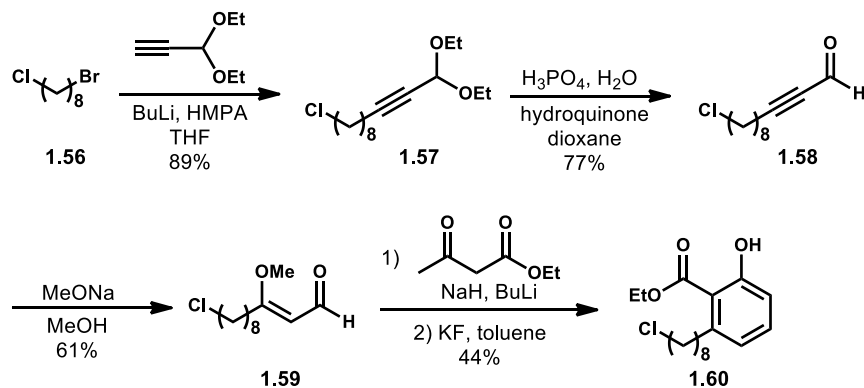


Scheme 1.10 – Synthesis of 6-Alkylsalicylates using the Alder–Rickert Reaction

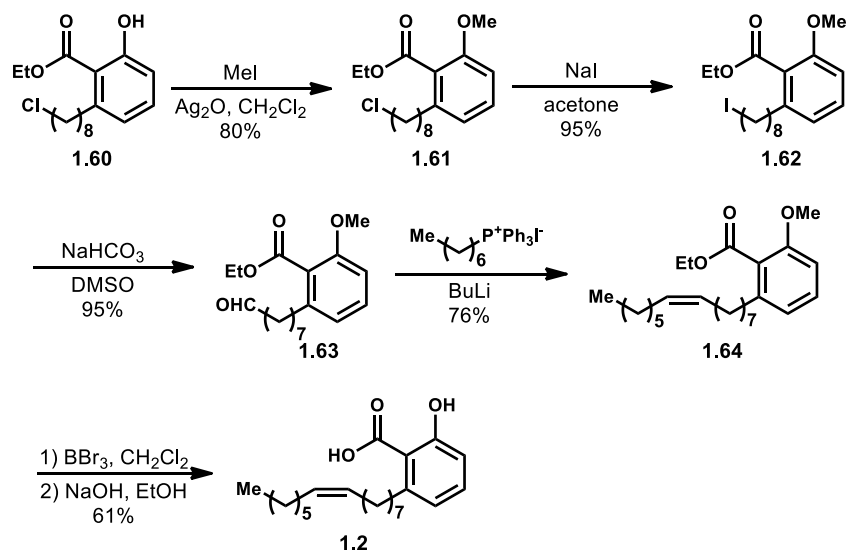
1.3.6 - Satoh's Annulation of 15:1 Ginkgolic Acid (2000)

Satoh's strategy to reach ginkgolic acid consisted of two main parts.^[62] The first was an annulation reaction closing the aromatic core using an acyclic precursor with the alkyl tail already attached (**Scheme 1.11**, part A). This eliminated the need for direct alkylation of the aryl ring as seen with previous methods. The second was to install ginkgolic acid's single *cis*-double bond by elongating the lipid tail using a Wittig reaction to give the desired internal olefin (**Scheme 1.11**, part B). To start, alkynyl acetal **1.57** was made from 1-bromo-8-chlorooctane (**1.56**) and ethynyl ethyl acetal. Conversion of acetal **1.57** to the aldehyde **1.58** was then followed by methoxide addition to the alkyne to give key acyclic intermediate **1.59**. The annulation was then performed together with ethyl acetoacetate to form the aromatic core of phenol **1.60**. Next, this phenol was protected using methyl iodide as a methyl aryl ether **1.61** and followed by a Finklestein reaction to transform the alkyl chloride to alkyl iodide **1.62**. Kornblum oxidation of this iodide into

Part A: Annulation Of The Aromatic Core



Part B: Tail Olefination



Scheme 1.11 – Satoh's Synthesis of Ginkgolic Acid

aldehyde **1.63** was performed in preparation for a Wittig reaction with heptyltriphenylphosphonium iodide. This Wittig resulted in the protected ginkgolic acid precursor **1.64**. Deprotection with sequential use of boron tribromide and sodium hydroxide yielded ginkgolic acid **1.2**.

1.4 - References

- (1) Gellerman, J. L.; Walsh, N. J.; Werner, N. K.; Schlenk, H. Antimicrobial Effects of Anacardic Acids. *Can. J. Microbiol.* **1969**, *15*, 1219–1223.
- (2) Hamad, F. B.; Mubofu, E. B. Potential Biological Applications of Bio-Based Anacardic Acids and Their Derivatives. *Int. J. Mol. Sci.* **2015**, *16*, 8569–8590.
- (3) Park, C. N.; Lee, D.; Kim, W.; Hong, Y.; Ahn, J. S.; Kim, B. S. Antifungal Activity of Salaceyin A against *Colletotrichum Orbiculare* and *Phytophthora Capsici*. *J. Basic Microbiol.* **2007**, *47*, 332–339.
- (4) Himejima, M.; Kubo, I. Antibacterial Agents from the Cashew *Anacardium Occidentale* (Anacardiaceae) Nut Shell Oil. *J. Agric. Food Chem.* **1991**, *39*, 418–422.
- (5) Sankara Subramanian, S.; Joseph, K. J.; Nair, A. G. R. Polyphenols of *Anacardium Occidentale*. *Phytochemistry* **1969**, *8*, 673.
- (6) Yalpani, M.; H.P. Tyman, J. The Phenolic Acids of *Pistachia Vera*. *Phytochemistry* **1983**, *22*, 2263–2266.
- (7) Zdero, C.; Bohlmann, F.; King, R. M.; Robinson, H. Sesquiterpene Lactones and Other Constituents from Australian *Helipterum* Species. *Phytochemistry* **1989**, *28*, 517–526.
- (8) Spencer, G. F.; Tjarks, L. W.; Kleiman, R. Alkyl and Phenylalkyl Anacardic Acids From *Knema Elegans* Seed Oil. *J. Nat. Prod.* **1980**, *43*, 724–730.
- (9) Owen, R. W.; Haubner, R.; Mier, W.; Giacosa, A.; Hull, W. E.; Spiegelhalder, B.; Bartsch, H. Isolation, Structure Elucidation and Antioxidant Potential of the Major Phenolic and Flavonoid Compounds in Brined Olive Drupes. *Food Chem. Toxicol.* **2003**, *41*, 703–717.
- (10) Hecker, H.; Johannisson, R.; Koch, E.; Siegers, C.-P. In Vitro Evaluation of the Cytotoxic Potential of Alkylphenols from *Ginkgo Biloba* L. *Toxicology* **2002**, *177*, 167–177.

- (11) Asakawa, Y.; Masuya, T.; Tori, M.; Campbell, E. O. Long Chain Alkyl Phenols from the Liverwort *Schistochila Appendiculata*. *Phytochemistry* **1987**, *26*, 735–738.
- (12) Gerhold, D. L.; Craig, R.; Mumma, R. O. Analysis of Trichome Exudate from Mite-Resistant Geraniums. *J. Chem. Ecol.* **1984**, *10*, 713–722.
- (13) Walters, D. S.; Minard, R.; Craig, R.; Mumma, R. O. Geranium Defensive Agents. III. Structural Determination and Biosynthetic Considerations of Anacardic Acids of Geranium. *J. Chem. Ecol.* **1988**, *14*, 743–751.
- (14) Nuts and Dried Fruits Statistical Yearbook 2018/19.
- (15) Taiwo, E. A. Cashew Nut Shell Oil — A Renewable and Reliable Petrochemical Feedstock. *Adv. Petrochem.* **2015**.
- (16) Aina, E. O.; Adisa, A. F.; Olayanju, T. M. A.; Ismaila, S. O. Performance Evaluation of a Developed Cashew Nut Shell Liquid Expeller. *Agric. Eng.* **2018**, *Vol. 22, No. 2*.
- (17) Gedam, P. H.; Sampathkumaran, P. S. Cashew Nut Shell Liquid: Extraction, Chemistry and Applications. *Prog. Org. Coat.* **1986**, *14*, 115–157.
- (18) Tyman, J. H. P.; Johnson, R. A.; Muir, M.; Rokhgar, R. The Extraction of Natural Cashew Nut-Shell Liquid from the Cashew Nut (*Anacardium Occidentale*). *J. Am. Oil Chem. Soc.* **1989**, *66*, 553–557.
- (19) Das, P.; Ganesh, A. Bio-Oil from Pyrolysis of Cashew Nut Shell—a near Fuel. *Biomass Bioenergy* **2003**, *25*, 113–117.
- (20) Paramashivappa, R.; Kumar, P. P.; Vithayathil, P. J.; Rao, A. S. Novel Method for Isolation of Major Phenolic Constituents from Cashew (*Anacardium Occidentale* L.) Nut Shell Liquid. *J. Agric. Food Chem.* **2001**, *49*, 2548–2551.
- (21) Green, I. R.; Tocoli, F. E.; Lee, S. H.; Nihei, K.; Kubo, I. Design and Evaluation of Anacardic Acid Derivatives as Anticavity Agents. *Eur. J. Med. Chem.* **2008**, *43*, 1315–1320.

- (22) Hemshekhar, M.; Sebastin Santhosh, M.; Kemparaju, K.; Girish, K. S. Emerging Roles of Anacardic Acid and Its Derivatives: A Pharmacological Overview. *Basic Clin. Pharmacol. Toxicol.* **2012**, *110*, 122–132.
- (23) Kubo, J.; Lee, J. R.; Kubo, I. Anti-Helicobacter Pylori Agents from the Cashew Apple. *J. Agric. Food Chem.* **1999**, *47*, 533–537.
- (24) Muroi, Hisae.; Kubo, Isao. Bactericidal Activity of Anacardic Acids against Streptococcus Mutans and Their Potentiation. *J. Agric. Food Chem.* **1993**, *41*, 1780–1783.
- (25) Green, I. R.; Tocoli, F. E.; Lee, S. H.; Nihei, K.; Kubo, I. Molecular Design of Anti-MRSA Agents Based on the Anacardic Acid Scaffold. *Bioorg. Med. Chem.* **2007**, *15*, 6236–6241.
- (26) Bouttier, S.; Fourniat, J.; Garofalo, C.; Gleye, C.; Laurens, A.; Hocquemiller, R. SS-Lactamase Inhibitors from Anacardium Occidentale. *Pharm. Biol.* **2002**, *40*, 231–234.
- (27) Begum, P.; Hashidoko, Y.; Tofazzal, I. Md.; Ogawa, Y.; Tahara, S. Zoosporicidal Activities of Anacardic Acids against Aphanomyces Cochlioides. *Z. Für Naturforschung C* **2014**, *57*, 874–882.
- (28) Arora, A.; Nair, M. G.; Strasburg, G. M. Structure–Activity Relationships for Antioxidant Activities of a Series of Flavonoids in a Liposomal System. *Free Radic. Biol. Med.* **1998**, *24*, 1355–1363.
- (29) Masuoka, N.; Kubo, I. Characterization of Xanthine Oxidase Inhibition by Anacardic Acids. *Biochim. Biophys. Acta BBA - Mol. Basis Dis.* **2004**, *1688*, 245–249.
- (30) Narahara, M.; Hamada-Kanazawa, M.; Kouda, M.; Odani, A.; Miyake, M. Superoxide Scavenging and Xanthine Oxidase Inhibiting Activities of Copper- β -Citryl-L-Glutamate Complex. *Biol. Pharm. Bull.* **2010**, *33*, 1938–1943.
- (31) Balasubramanyam, K.; Swaminathan, V.; Ranganathan, A.; Kundu, T. K. Small Molecule Modulators of Histone Acetyltransferase P300. *J. Biol. Chem.* **2003**, *278*, 19134–19140.

- (32) Ghizzoni, M.; Boltjes, A.; Graaf, C. de; Haisma, H. J.; Dekker, F. J. Improved Inhibition of the Histone Acetyltransferase PCAF by an Anacardic Acid Derivative. *Bioorg. Med. Chem.* **2010**, *18*, 5826–5834.
- (33) Sun, Y.; Jiang, X.; Chen, S.; Price, B. D. Inhibition of Histone Acetyltransferase Activity by Anacardic Acid Sensitizes Tumor Cells to Ionizing Radiation. *FEBS Lett.* **2006**, *580*, 4353–4356.
- (34) Kishore, A. H.; Vedamurthy, B. M.; Mantelingu, K.; Agrawal, S.; Reddy, B. A. A.; Roy, S.; Rangappa, K. S.; Kundu, T. K. Specific Small-Molecule Activator of Aurora Kinase A Induces Autophosphorylation in a Cell-Free System. *J. Med. Chem.* **2008**, *51*, 792–797.
- (35) Bolanos-Garcia, V. M. Aurora Kinases. *Int. J. Biochem. Cell Biol.* **2005**, *37*, 1572–1577.
- (36) Sung, B.; Pandey, M. K.; Ahn, K. S.; Yi, T.; Chaturvedi, M. M.; Liu, M.; Aggarwal, B. B. Anacardic Acid (6-Nonadecyl Salicylic Acid), an Inhibitor of Histone Acetyltransferase, Suppresses Expression of Nuclear Factor-KB–Regulated Gene Products Involved in Cell Survival, Proliferation, Invasion, and Inflammation through Inhibition of the Inhibitory Subunit of Nuclear Factor-KB α Kinase, Leading to Potentiation of Apoptosis. *Blood* **2008**, *111*, 4880–4891.
- (37) Itokawa, H.; Totsuka, N.; Nakahara, K.; Takeya, K.; Lepoittevin, J.-P.; Asakawa, Y. Antitumor Principles from Ginkgo Biloba L. *Chem. Pharm. Bull. (Tokyo)* **1987**, *35*, 3016–3020.
- (38) Kubo, Isao.; Ochi, Masamitsu.; Vieira, P. C.; Komatsu, Sakae. Antitumor Agents from the Cashew (*Anacardium Occidentale*) Apple Juice. *J. Agric. Food Chem.* **1993**, *41*, 1012–1015.
- (39) Schultz, D. J.; Wickramasinghe, N. S.; Ivanova, M. M.; Isaacs, S. M.; Dougherty, S. M.; Imbert-Fernandez, Y.; Cunningham, A. R.; Chen, C.; Klinge, C. M. Anacardic Acid Inhibits Estrogen Receptor α -DNA Binding and Reduces Target Gene Transcription and Breast Cancer Cell Proliferation. *Mol. Cancer Ther.* **2010**, *9*, 594–605.

- (40) Bettermann, K.; Benesch, M.; Weis, S.; Haybaeck, J. SUMOylation in Carcinogenesis. *Cancer Lett.* **2012**, *316*, 113–125.
- (41) Little, H. N.; Bloch, K. Studies on the Utilization of Acetic Acid for the Biological Synthesis of Cholesterol. *J. Biol. Chem.* **1950**, *183*, 33–46.
- (42) Brady, R. O.; Gurin, S. The Synthesis of Radioactive Cholesterol and Fatty Acids in Vitro. *J. Biol. Chem.* **1951**, *189*, 371–377.
- (43) Birch, A. J.; Donovan, F. W. Studies in Relation to Biosynthesis. I. Some Possible Routes to Derivatives of Orcinol and Phloroglucinol. *Aust. J. Chem.* **1953**, *6*, 360–368.
- (44) Gellerman, J. L.; Anderson, W. H.; Schlenk, H. Biosynthesis of Anacardic Acids from Acetate InGinkgo Biloba. *Lipids* **1974**, *9*, 722–725.
- (45) Gellerman, J. L.; Anderson, W. H.; Schlenk, H. Synthesis of Anacardic Acids in Seeds of Ginkgo Biloba. *Biochim. Biophys. Acta BBA - Lipids Lipid Metab.* **1976**, *431*, 16–21.
- (46) Walters, D. S.; Craig, R.; Mumma, R. O. Fatty Acid Incorporation in the Biosynthesis of Anacardic Acids of Geraniums. *Phytochemistry* **1990**, *29*, 1815–1822.
- (47) Ferrer, J.-L.; Jez, J. M.; Bowman, M. E.; Dixon, R. A.; Noel, J. P. Structure of Chalcone Synthase and the Molecular Basis of Plant Polyketide Biosynthesis. *Nat. Struct. Biol.* **1999**, *6*, 775–784.
- (48) Jez, J. M.; Noel, J. P. Mechanism of Chalcone Synthase PK a OF THE Catalytic Cystine and the Role of the Conserved Histidine in a Plant Polyketide Synthase. *J. Biol. Chem.* **2000**, *275*, 39640–39646.
- (49) Gagne, S. J.; Stout, J. M.; Liu, E.; Boubakir, Z.; Clark, S. M.; Page, J. E. Identification of Olivetolic Acid Cyclase from Cannabis Sativa Reveals a Unique Catalytic Route to Plant Polyketides. *Proc. Natl. Acad. Sci. U. S. A.* **2012**, *109*, 12811–12816.

- (50) Geissman, T. A. CHAPTER 12 - THE BIOSYNTHESIS OF PHENOLIC PLANT PRODUCTS. In *Biogenesis of Natural Compounds (Second Edition)*; Bernfeld, P., Ed.; Pergamon, 1963; pp 743–799.
- (51) Vogel, G.; Lynen, F. [38] 6-Methylsalicylic Acid Synthetase. In *Methods in Enzymology*; Antibiotics; Academic Press, 1975; Vol. 43, pp 520–530.
- (52) Wasserman, D.; Dawson, C. R. The Synthesis of Cis- and Trans-3-(Pentadecenyl-8')-Veratrole, A Dihydro Derivative of Urushiol Dimethyl Ether. *J. Org. Chem.* **1943**, *08*, 73–82.
- (53) Harris, T. Munson.; Carney, R. L. Synthesis of 3,5,7-Triketo Acids and Esters and Their Cyclizations to Resorcinol and Phloroglucinol Derivatives. Models of Biosynthesis of Phenolic Compounds. *J. Am. Chem. Soc.* **1967**, *89*, 6734–6741.
- (54) Tyman, J. H. P.; Durrani, A. A. A Novel Synthesis of Homologous Orsellinic Acids and 5-Alkylresorcinols. *Tetrahedron Lett.* **1973**, *14*, 4839–4840.
- (55) Durrani, A. A.; Tyman, J. H. P. Long Chain Phenols. Part 15. Synthesis of 6-n-Alkylsalicylic Acids (and Isomeric Acids) from Fluoroanisoles with Alkyl-Lithium. *J. Chem. Soc. Perkin 1* **1979**, No. 0, 2079–2087.
- (56) Kubo, I.; Kim, M.; Naya, K.; Komatsu, S.; Yamagiwa, Y.; Ohashi, K.; Sakamoto, Y.; Hirakawa, S.; Kamikawa, T. Prostaglandin Synthetase Inhibitors from the African Medicinal Plant *Ozoroa mucronata*. *Chem. Lett.* **1987**, *16*, 1101–1104.
- (57) Dean, R. T.; Rapoport, H. Iminium Salts from α -Amino Acid Decarbonylation. Application to the Synthesis of Berbines. *J. Org. Chem.* **1978**, *43*, 2115–2122.
- (58) Hird, N. W.; Milner, P. H. Synthesis and β -Lactamase Inhibition of Anacardic Acids and Their Analogues. *Bioorg. Med. Chem. Lett.* **1994**, *4*, 1423–1428.
- (59) Kanakam, C. C.; Mani, N. S.; Ramanathan, H.; Rao, G. S. R. S. Syntheses Based on Cyclohexadienes. Part 2. Convenient Synthesis of 6-Alkylsalicylates, 6-Alkyl-2,4-Dihydroxybenzoate, and 2,5-Dialkylresorcinols. *J. Chem. Soc. Perkin 1* **1989**, No. 11, 1907–1913.

- (60) Alder, K.; Rickert, H. F. Zur Kenntnis Der Dien-Synthese. I. Über Eine Methode Der Direkten Unterscheidung Cyclischer Penta- Und Hexa-Diene. *Justus Liebigs Ann. Chem.* **1936**, *524*, 180–189.
- (61) Zehnter, R; Gerlach, H. Synthesis of Anacardic Acids. *Liebigs Ann.* **1995**, *1995*, 2209–2220.
- (62) Satoh, M.; Takeuchi, N.; Nishimura, T.; Ohta, T.; Tobinaga, S. Synthesis of Anacardic Acids, 6-[8(Z), 11(Z)-Pentadecadienyl]Salicylic Acid and 6-[8(Z), 11(Z), 14-Pentadecatrienyl]Salicylic Acid. *Chem. Pharm. Bull. (Tokyo)* **2001**, *49*, 18–22.

2 Heck Redox-Relay Reactions with Alkenol Substrates

2.1 - Introduction

The Heck reaction (also referred to as the Mizoroki–Heck reaction) is a well-known, versatile, and highly developed method for the construction of substituted alkenes from alkenyl/aryl halides (or triflates) and alkene coupling partners in the presence of base and a palladium catalyst.^[1–4] Due to the versatility of this reaction, a vast array of variations and applications for this reaction have been developed since its discovery.^[3] One particularly fascinating subset of these is the Heck redox-relay reaction which involves the ability of palladium to migrate long distances from the site of initial carbopalladation. This migration process can be described as non-dissociative “chain-walking” that is accomplished with repeating sequences of β -hydride elimination followed by immediate reinsertion of the ensuing double bond that is formed (**Figure 2.1**). This process results in the movement of the metal center of along a chain from one carbon to next without disengagement of the organic substrate.

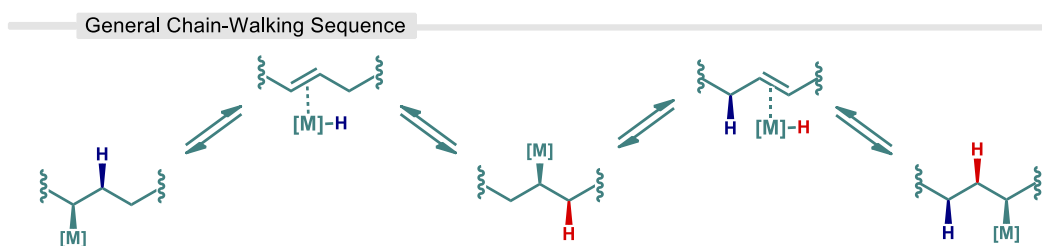
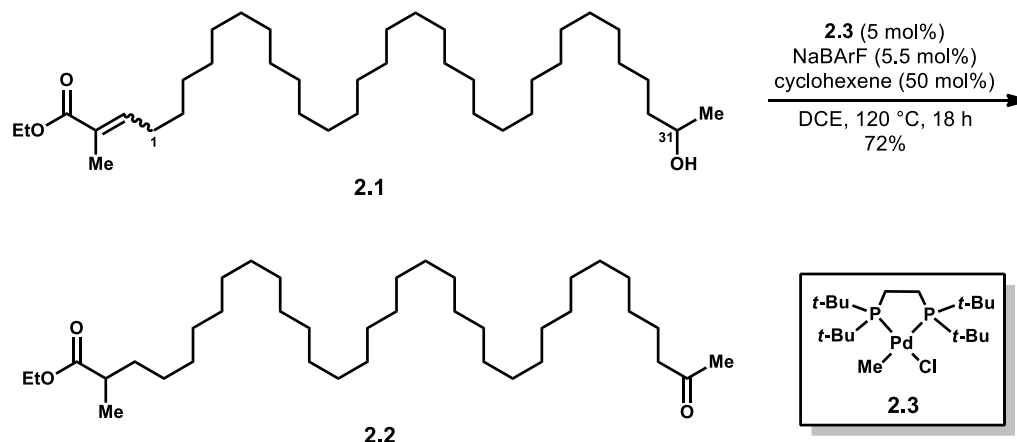


Figure 2.1 – Depiction of a General Non-Dissociative Chain-Walking Process

Palladium is the most commonly used metal for these reactions owing to the wide array of known complexes, the relative ease and user-friendliness associated with handling most of them, and the strong propensity for alkylpalladiums to undergo β -hydride elimination.^[5] While this chapter’s focus will be on palladium mediated reactions, it is



Scheme 2.1 – Deconjugative Remote Functionalization of a Long-Chain Alkenol worth noting that other metals are also capable of chain-walking as well; for example, zirconium,^[6] rhodium,^[7] nickel,^[8] and cobalt.^[9] The bifunctional ruthenium-based catalytic machinery used in an “alkene-zipper” reaction is particularly notable for its ability to isomerize olefins to ketones (**2.1** to **2.2**) over 30 bonds away.^[10] As with the alkene zipper reaction, a common substrate for these redox-relay sequences are alkenols which proceed through an initial migratory insertion of the alkene, chain-walking to the carbinol carbon, and then oxidative deprotonation to an aldehyde or ketone product (see example in **Scheme 2.1**). This particular example using a palladium hydride generated *in-situ* from a dialkylphosphinoethane catalyst **2.3** and cyclohexene showcases the remarkable ability of palladium to migrate long distances.^[11,12] Such reactions can be thought of as carbonyl terminated, with disengagement of the palladium occurring after carbonyl formation although other means of termination of the chain-walking process are possible and include tandem migration-nucleophilic addition with amines or enolates^[13] and tandem migration-cyclizations.^[14,15]

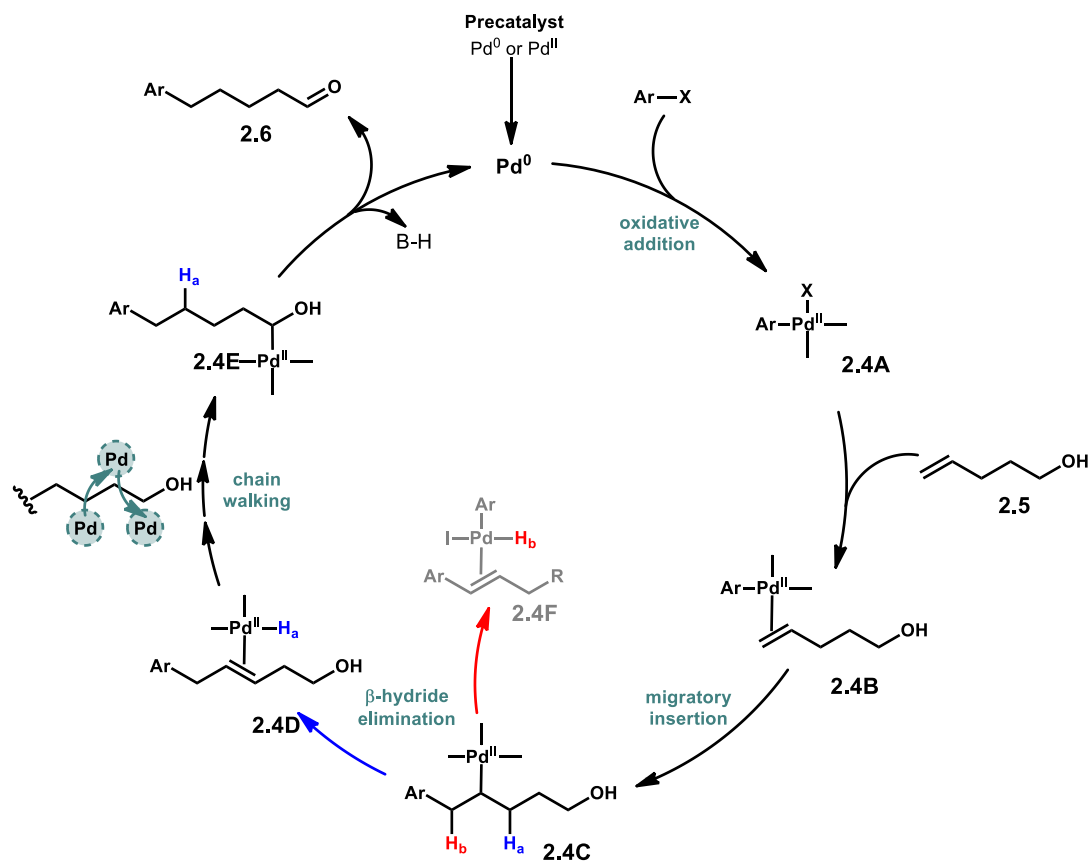


Figure 2.2 – Catalytic Cycle of a Heck Redox-Relay Involving Chain-walking

A general catalytic cycle for a Heck redox-relay process is shown in (**Figure 2.2**). Much of the process is similar to that of a “regular” Heck reaction. Beginning from Pd(0), oxidative addition into an electrophile such as an aryl halide forms arylpalladium intermediate **2.4A**. Loss of a ligand and coordination to the alkenol (**2.5**) gives intermediate **2.4B** followed by carbopalladation to the arylated alkylpalladium **2.4C**. β -hydride elimination of adjacent H_b (red) results in the styrenyl intermediate **2.4F** and would lead to the traditional Heck olefin product. Through the use of appropriate conditions however, the elimination of H_a (blue) can be favored and leads to **2.4D** which begins the chain-walking process ultimately leading to carbinol palladium intermediate

2.4E. DFT calculations conducted by Sigman and coworkers for the chain-walking process itself suggest a rather shallow energy surface profile for the alternating β -hydride elimination and migratory insertion steps.^[16] Base (or solvent) assisted oxidative deprotonation of the alcohol yields aldehyde product **2.6** and reduces palladium to turn over the catalytic cycle. Alternative theories involving solvent deprotonation of the palladium hydride in intermediate **E** have also been considered,^[17] however Sigman's work showed this pathway is nearly 15 kcal/mol less favorable than the alcohol deprotonation by DFT. The initial development of these redox relay reactions involving the arylation of alkenols using palladium actually predates the Heck reaction itself, and the next section will describe the developmental milestones of this reaction.

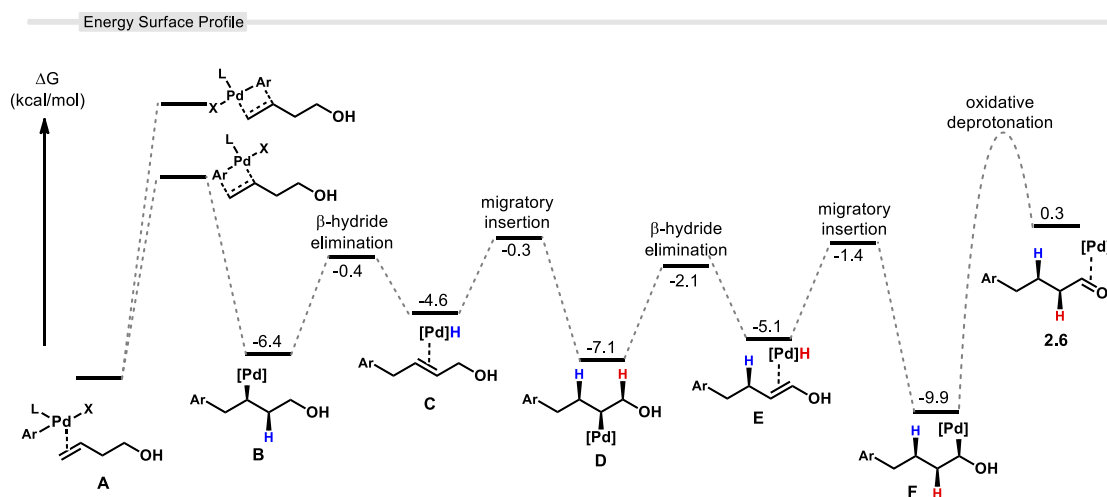


Figure 2.3 – Simplified Reaction Profile Based of DFT Calculations by Sigman at al.

2.2 - Early Palladium-Catalyzed Arylation of Allylic Alcohols

Richard Heck first reported the palladium-catalyzed arylation of allylic alcohols in 1968,^[18] a year prior to his landmark work^[19] that would later earn him a Nobel prize and an eponymous named reaction. Heck found that allylic alcohols undergo an addition-elimination reaction with arylpalladium chlorides to afford alkyl aldehyde products. In this

In these early studies with allylic alcohols, the reaction of the endogenously generated phenylpalladium chloride with propen-1-ol (**2.8**) gave 3-phenylpropionaldehyde and allylbenzene (**2.9** and **2.10**) products. Heck reasoned that after carbopalladation of the alkenol by phenylpalladium, the resulting alkylpalladium intermediate **2.16** could proceed either by β -hydride elimination to enol **2.17** and eventually the aldehyde (see **Scheme 2.2**, bottom) or by β -hydroxy elimination to allylbenzene. A major finding made early on with the use of other allylic alcohols such as crotyl alcohol (**2.11**) was that this class of reaction often exhibits a regiochemical preference during the carbopalladation step for one arylated aldehyde product over another. In the case of crotyl alcohol, the 3-aryl aldehyde **2.12** was favored over the 2-aryl aldehyde **2.13** in a 3:1 ratio. The regiochemical aspect of these reactions would garner significantly more investigation in the years to come and shall be discussed later in the chapter.

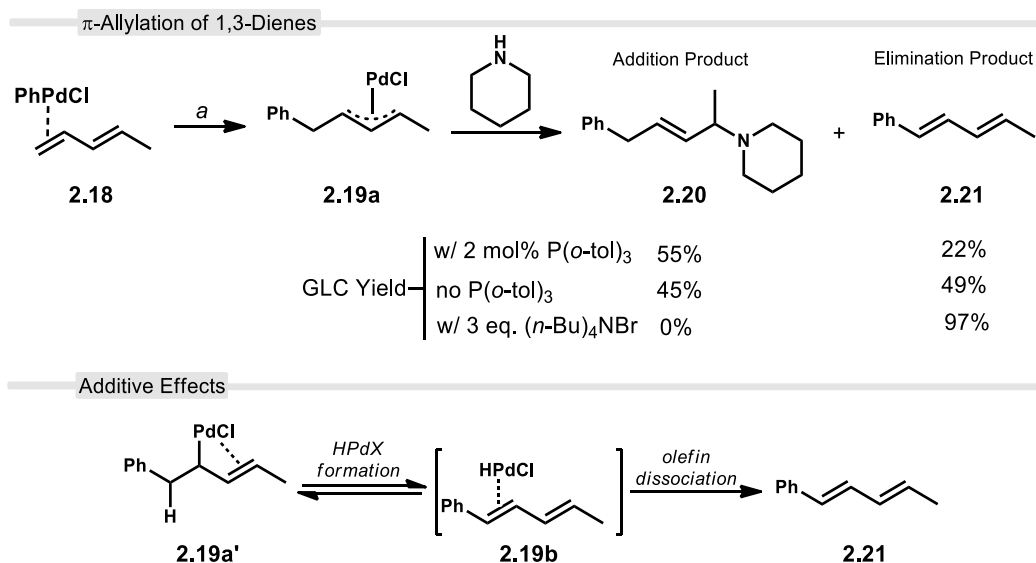
Years later in 1976, Heck would again return to the arylation of allyl alcohols, this time beginning with phenyl iodide rather than the phenylmercurial chloride he used initially (**Scheme 2.2**, middle). His earlier investigations on palladium-catalyzed alkene arylations revealed that aryl halides in the presence of palladium acetate and triethylamine were capable of directly engaging alkenes in organometallic reactions.^[1,20] Heck was the first to report the coupling of aryl halides with allyl alcohols under these conditions^[21] with similar work by Chalk and Magennis following less than a month later.^[22] Heck's application of these conditions to allyl alcohols resulted in a significant improvement in both yield and regioselectivity compared to the initial method using organomercurials used prior. The reaction of 2-propen-1-ol proceeded to give a 71% yield of 3- and 2-

phenylpropionaldehydes (**2.9** and **2.14**) in an 84:16 ratio. The reaction with crotyl alcohol also improved appreciably giving the products **2.12** and **2.15** in 84% yield (76:24 r.r., respectively).

2.3 - Discovery and Development of Palladium Chain-Walking

2.3.1 - Chain-Walking in the Formation of Palladium π -allyl Complexes

The commonly envisioned Heck reaction typically assumes that the fate of palladium following the β -hydride elimination step is dissociation from the cross-coupled olefin product, although this is not always the case. For instance, Heck demonstrated that the carbopalladation of 1,3-dienes forms a palladium π -allyl complex **2.19a** that is capable of undergoing further reaction with amines (**Scheme 2.3**).^[23] The π -allyl intermediate that forms is subject to two reaction pathways. The first is addition of a secondary amine such



Scheme 2.3 – Reaction of Amines with π -Allyl Palladium Intermediates

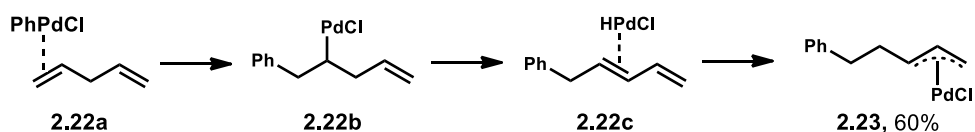
a) PhBr (1 equiv), diene (1.25 equiv), Pd(OAc)₂ (1 mol%), amine (2.5 equiv); 100 °C, 18 h. From the π -allyl complex, the presence of aryl phosphine or ammonium salts were shown to influence the ratio of the addition and elimination products.

as piperidine or morpholine into the palladium π -allyl complex to form allyl amine **2.20**. Alternatively, β -hydride elimination of a benzylic hydrogen from **2.19a'** illustrated in the bottom of **Scheme 2.3** results the palladium hydride intermediate **2.19b**. Dissociation of this metal hydride results in the conjugated diene **2.21**.

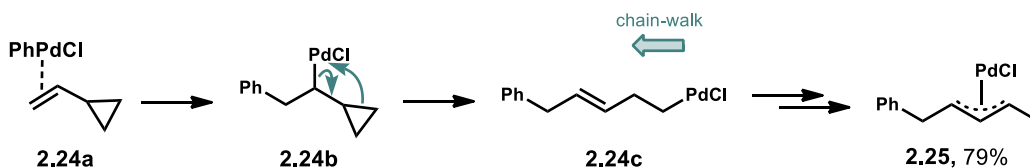
The ratio of the amine and diene products was roughly 1:1; however, it was found that the ratio of products could be modified with the introduction of additives. The addition of an aryl phosphine ligand preferentially formed the amine addition product by a 2:1 ratio. This finding suggested that the phosphine likely decreases the rate of dissociation of the palladium hydride intermediate formed after elimination and/or increases the tendency for reinsertion. The extent of this effect with phosphine additives was unpredictable and varied with the other dienes that were tested. Inclusion of tetrabutylammonium bromide on the other hand, resulted exclusively in the elimination product. This ability to influence the behavior of alkylpalladium intermediates with changes to the reaction conditions and inclusion of additives would later become a key point in allowing for the development of optimal palladium chain-walking conditions.

Richard Larock also played an important role in the development of Heck-chain-walking reactions. His initial investigations also eventually led to an examination of π -allylpalladium intermediates. To interrogate the ability of these complexes to form from nonconjugated alkene substrates, Larock tested phenylpalladium with 1,4-pentadiene (**2.22a**, **Scheme 2.4**, top).^[24] The migratory insertion of the arylpalladium into a 1,4-diene does not immediately form the π -allyl complex (compare to **Scheme 2.3**) and instead forms the alkylpalladium intermediate **2.22b**. Nevertheless, the π -allylpalladium product was still

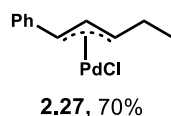
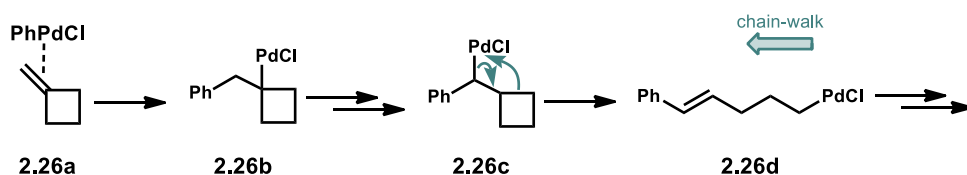
1,4-Dienes



Vinylcyclopropanes



Methylenecyclobutanes



"In this extraordinary reaction, palladium at one time or another is bonded to every carbon of the original olefin. The ability of palladium to migrate considerable distances by β hydride elimination-readdition without formation of the corresponding olefin is quite remarkable."

-Richard Larock, 1984

Scheme 2.4 – Larock's Early Exploration of Palladium Chain-Walking

In the above examples, chain-walking explains the formation of π -allyl complexes by allowing palladium to migrate to a remote double-bond. β -Hydride elimination of **2.22b** (top) and reinsertion into HPd complex **2.22c** "walks" the Pd over one carbon. These steps are not shown explicitly with vinylcyclopropanes (middle) or methylenecyclobutanes (bottom).

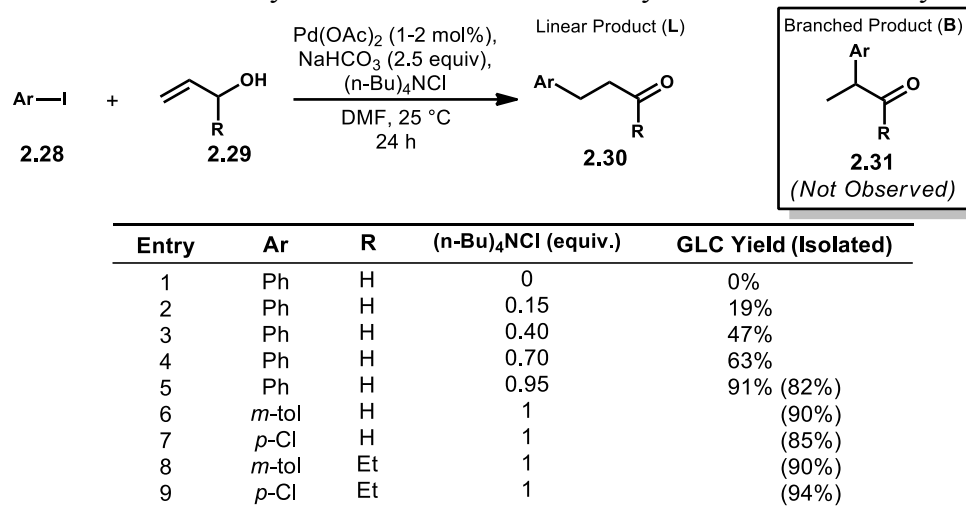
observed in 60% yield suggesting that after the initial carbopalladation, a β -hydride elimination to **2.22c** followed by a reinsertion to reach the π -allylpalladium product **2.22d** were occurring. 1,5-Hexadiene was also tested and found to form the π -allyl product (not shown) in 24% yield which added further evidence that a chain-walking process was occurring. In this case, product formation occurs after two cycles of elimination-insertion following the initial arylation. Chain-walking was also observed in the strain-promoted ring opening of cyclopropanes and cyclobutanes following organopalladium additions to form π -allylpalladium products.^[25] Following the addition of phenylpalladium to

vinylcyclopropane (**2.24a**, **Scheme 2.4**, middle), the (cyclopropylcarbinyl) palladium intermediate **2.24b** then undergoes ring opening to the acyclic alkylpalladium intermediate **2.24c**. Palladium migration via chain-walking yielded the π -allyl product **2.25** in 79% yield. A similar process occurs with methylenecyclobutane **2.26a**. However, Larock surmised that the cyclobutylpalladium **2.26b** which forms after migratory insertion must first rearrange to the cyclobutylcarbinyl position, **2.26c**, before ring opening to the linear alkylpalladium **2.26d**. Chain-walking then repositions the palladium into place for formation of the π -allyl complex **2.27** in 70% yield.

2.3.2 - Jeffery's Ligandless Reaction Conditions

Another development came when Jeffery discovered that Heck reactions could be run at lower temperatures than usually required by using a combination of sodium bicarbonate and tetrabutylammonium chloride (TBACl) with catalytic amounts of palladium acetate.^[26,27] These reaction conditions have become known as “Jeffery’s conditions” and Heck reactions carried out in this manner are sometimes referred to as “ligandless” due the absence of a specific phosphine or amine ligand.^[28] Jeffery found these conditions not only work well for traditional Heck reactions, but also for the arylation of allyl alcohols to give the corresponding aldehyde or ketone products (**Table 2.1**). No conversion of the allyl alcohol (**2.29**, entry 1) was seen when only palladium acetate and sodium bicarbonate were used. Formation of the arylated products was only seen with the inclusion of TBACl and depended on the amount used reaching a maximum of 82% yield with 0.95 equivalents (entries 2-5). Similar success was seen with other substituted aryl iodides (entries 6 and 7). The reaction of pent-1-en-3-ol to give the respective ketone

Table 2.1 – Use of Jeffery’s Conditions with Pd-Catalyzed Reactions of Allyl Alcohols



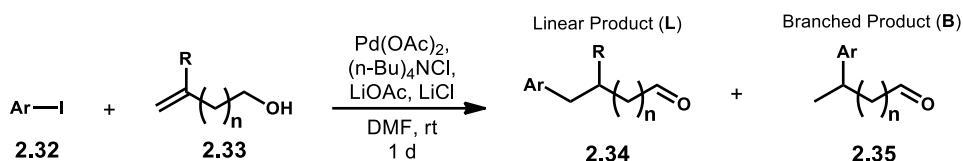
products (entries 8 and 9) also worked well. Branched regioisomers in this case were not observed.

Larock would later find that the use of these conditions with homoallylic alcohols gave yields of only ~50% with further decreases in yield observed as the number of carbons between the olefin and alcohol increased.^[29] By modifying Jeffery’s conditions, Larock discovered that the efficiency of chain-walking could be significantly improved. These modified Jeffery conditions use acetate instead of bicarbonate as base. The choice of the acetate counter-ion is also significant with yields increasing as follows: Li > Na > K > Cs. The inclusion of additional lithium and chloride ion in the form of LiCl also proved to be beneficial.

Under these conditions, olefins up to 8 carbons away were converted into their respective arylated aldehyde products in good yields (**Table 2.2**, entries 1-4). The initial carbopalladation of the alkene favors the arylation of the least substituted position to

primarily form the linear aldehyde product **2.34**. Insertion in the opposite orientation leads to the branched regioisomer **2.35**, which is still able to undergo migration to form product. The regioselectivity of these reactions typically affords a linear to branched ratio (L:B) of approximately 85:15. In the case of a trisubstituted terminal alkene (entry 5), the L:B ratio observed was 100:0 likely due to the increased steric demand for the carbopalladation leading to the branched regioisomer and certainly the lack of any available β -hydrogens on the resulting alkylpalladium to begin the chain-walking process. Other aryl iodides were well tolerated with electron rich and deficient rings proceeding with only slight variations in yield and the L:B (entries 6-9).

Table 2.2-Reaction of Arylhalides with Alkenols of Varying Length



Entry	Ar	n	R	Isolated Yield (%)	L:B
1	Ph	1	H	77	84:16
2	Ph	2	H	85	83:17
3	Ph	3	H	82	82:18
4	Ph	8	H	91*	88:12
5	Ph	1	Me	69	100:0
6	p-tol	2	H	82	82:18
7	PMP	2	H	77	76:24
8	p-EtO ₂ CPh	2	H	81	84:16
9	2-naphthyl	2	H	77	80:20

*Run at 50 °C for 3 d

2.3.3 - Stereocontrol in Alkenol Additions

Sigman et al. have developed a chiral pyridine oxazoline (PyrOx) ligand **2.37** (**Figure 2.4**) that can enantioselectively add to alkenols and then subsequently chain-walk to give aldehyde and ketone products.^[30] In the development of the ligand, certain design

considerations had to be made based on the known mechanistic features of this reaction. These considerations can be seen in **Figure 2.4**: i) The initial migratory insertion should be regioselective. ii) The β -hydride elimination should proceed toward the alcohol rather than back toward the aryl group. iii) The metal-ligand complex would have to favor reinsertion over dissociation of the metal center from the alkene in order to enable migration along the chain.

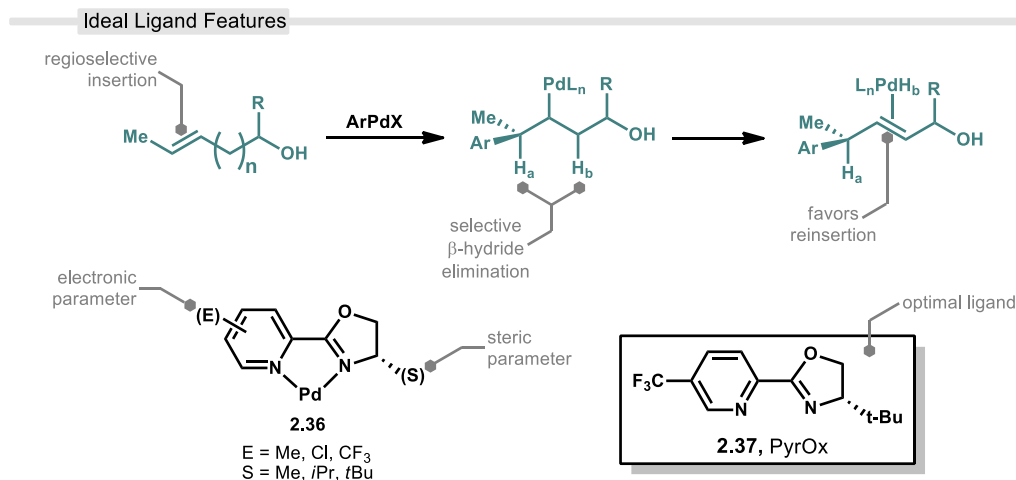
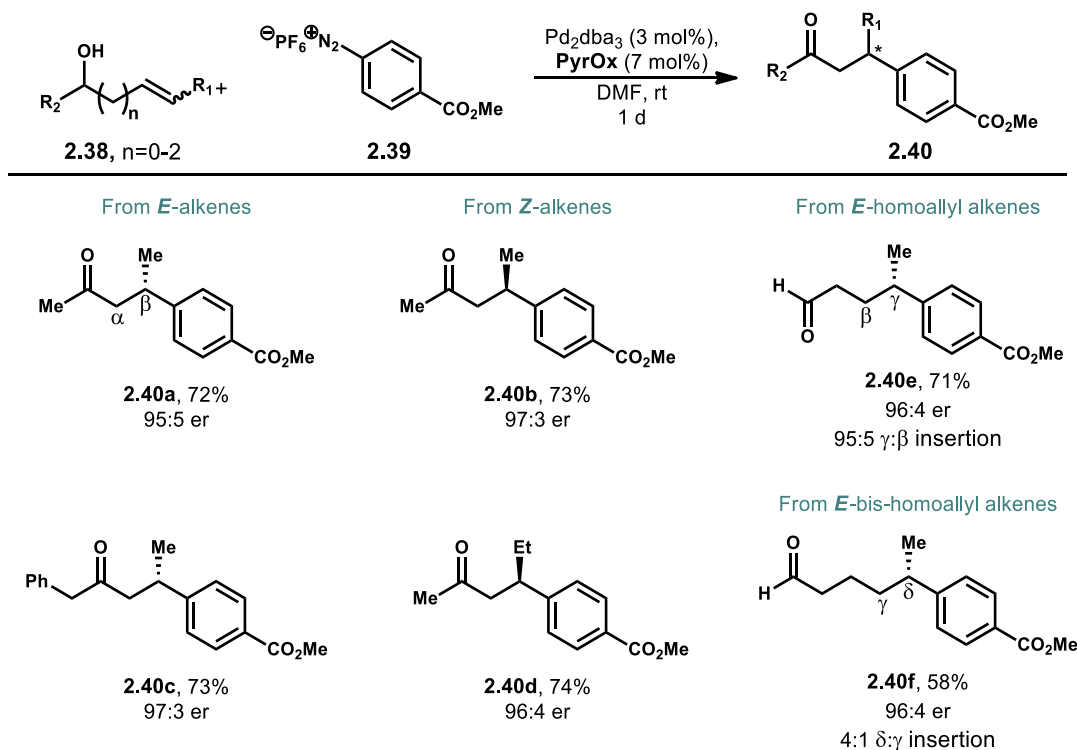


Figure 2.4 – Design and Optimization of Sigman’s Chiral PyrOx Ligand

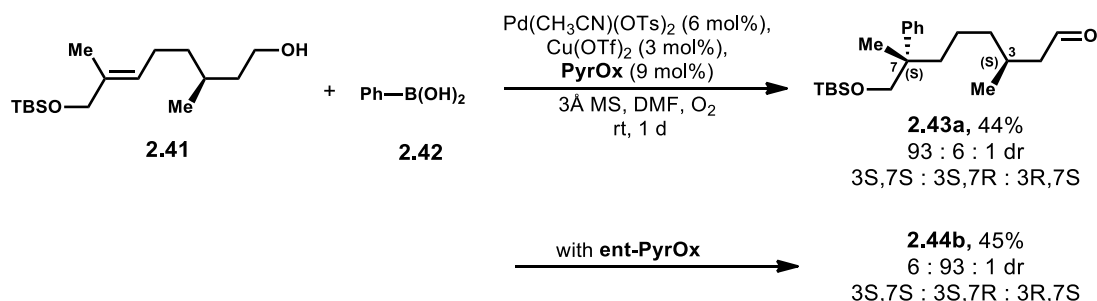
Unlike other the more symmetrical bipyridal (bpy) or bisoxazoline (BOX) ligand frameworks, the PyrOx scaffold **2.36** was chosen due to each ring having a distinct donor group. Therefore, the steric and electronic properties of each ring on the PyrOx scaffold could be individually tuned to meet the unique demands of this reaction as discussed previously. Sigman tried different combinations of ring substituents until a ligand that gave optimal performance, **2.37**, was determined. This ligand was used in conjunction with Pd₂(dba)₃ with alkenols of varying length (**2.38**, n=0-2) and an aryldiazonium electrophile (**2.39**) shown in **Scheme 2.5**. The reaction generally afforded aldehyde and ketone products



Scheme 2.5-Asymmetric Carbopalladation of Alkenols Using a Chiral PyrOx Ligand

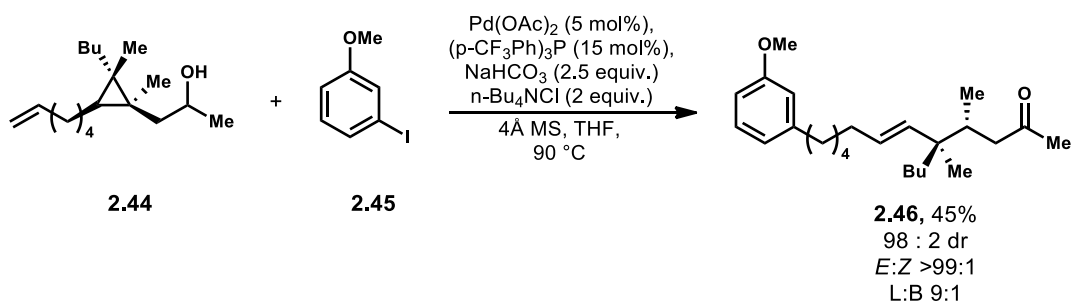
with good yield and high e r. Both enantiomeric pairs (**2.40a/b** and **2.40c/d**) are accessible with no large variations in yield or stereoselectivity between the *E* or *Z* alkenols. Migratory insertion of allylic alcohols was highly regioselective and only resulted in the β -arylated regioisomer. Minor drops in regioselectivity were observed with homoallylic alcohols (**2.40e**) while bis-homoallyl alcohols (**2.40f**) experienced more significant losses in terms of both yield and regioselectivity.

This PyrOx ligand was also used in an oxidative Heck redox-relay process using phenylboronic acid (**2.42**, **Scheme 2.6**) and an alkenol substrate (**2.41**) with an existing chiral center between the point of initial insertion and the alcohol.^[31] Surprisingly, Sigman et al. observed virtually no erosion in the stereochemical integrity of the existing chiral



Scheme 2.6 – Asymmetric Control in the Formation and Retention of Two Chiral Centers

center through the chain-walking process leading to the aldehyde product **2.43a**. This retention of stereochemical information is preserved despite being ablated during the chain-walking process. Also interesting was that the use of the ent-PyrOx ligand only affected the newly formed chiral center in **2.43b**, with the existing chiral center being unaffected by the steric alterations to the ligand. The retention of existing chiral centers throughout the chain-walking process was also observed by Singh *et al.* where palladium migration triggered the ring opening of remote, sterically congested cyclopropanes (**2.44**, **Scheme 2.7**).^[32] These findings would later be investigated by the Sigman group in a detailed mechanistic analysis of the chain-walking process with their PyrOx ligand.



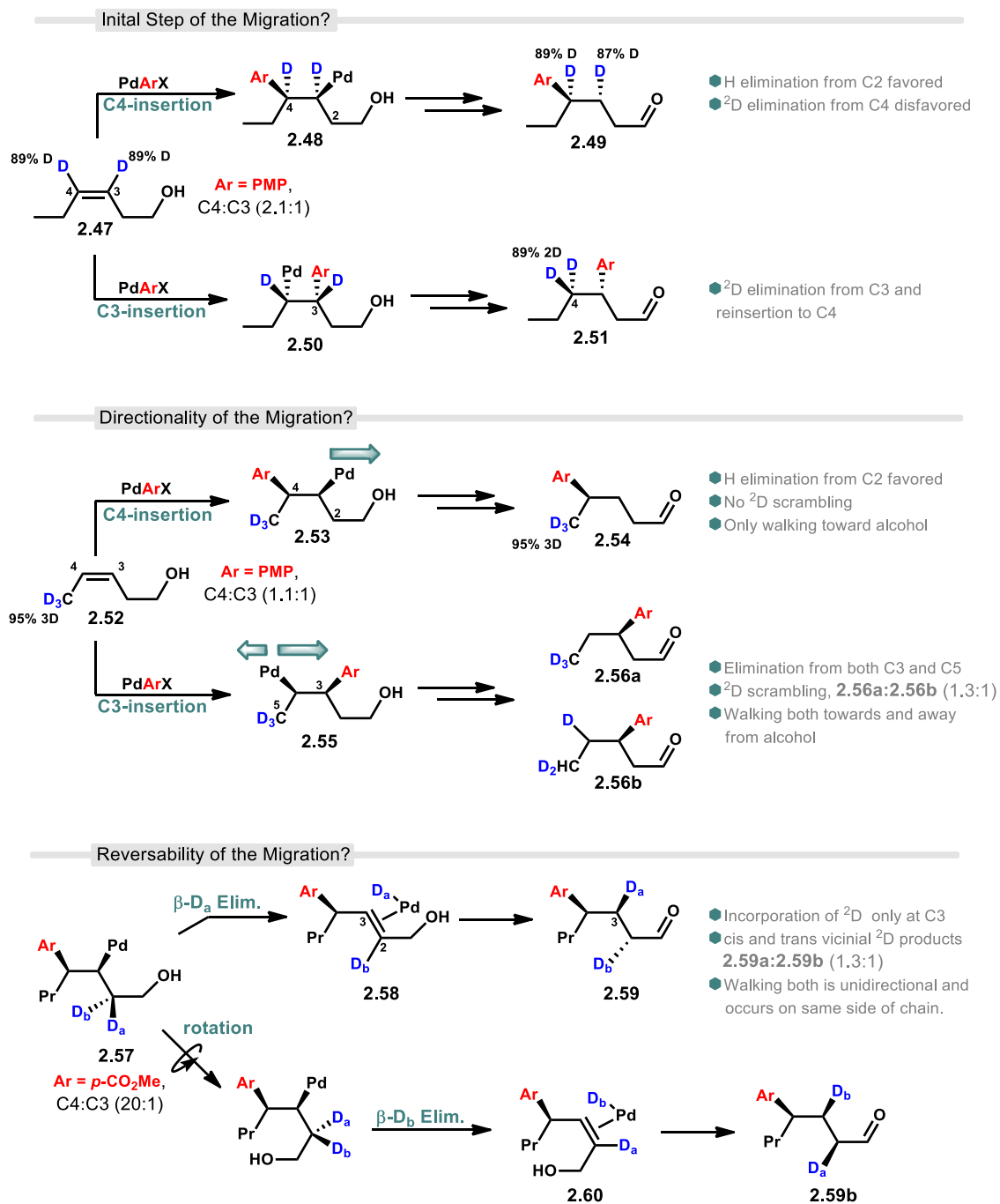
Scheme 2.7 – Selective Bond Cleavage in the Remote Ring-Opening of Cyclopropanes

2.4 - Mechanistic Investigations of the Palladium Chain-Walking Process

In the development of his PyrOx ligand, Sigman et al. performed an in-depth investigation into the mechanistic aspects of the palladium chain-walking process. The use of DFT calculations and deuterium labeling experiments led to a clearer picture for how these redox relay reactions proceed. These studies were done specifically for reactions using Sigman's chiral PyrOx ligand and therefore due to the inherent sensitivity of these reactions to variations of the ligand or inclusion of other additives, it is possible that the outcomes of these mechanistic experiments will differ under other conditions. Nevertheless, the thorough nature of these mechanistic studies are extremely helpful in understanding many aspects of the Heck redox-relay process that were previously unexplored.

2.4.1 - Deuterium Labeling Studies

Because the chain-walking process proceeds through palladium hydride intermediates, the use of deuterium labeling studies was extremely useful in establishing a better understanding of these reactions. Usually, the migratory insertion of the arylpalladium exhibits a high regiochemical preference for one regioisomer. However, to gain a better understanding of the behavior of both regioisomers arising from the initial arylpalladium insertion, *p*-methoxyphenylboronic acid was used since electron-rich aryl groups typically exhibit much lower regioselectivity allowing observation of both alkylpalladium intermediates in appreciable amounts. The initial β -hydride elimination following the arylation step was studied using the bis deuterated *Z*-alkene **2.47** (Scheme 2.8, top). In the case of arylation at C4 leading to alkylpalladium intermediate **2.48**, no



Scheme 2.8 – Mechanistic Investigations of Chain-Walking Using Deuterium Labeling

scrambling of the deuterium labels was observed in aldehyde product **2.49** which indicates that elimination of a C2 hydrogen was preferred over the deuterium at C4. Presumably, this preference arises due the bond rotation required to position the deuterium for elimination. The necessary syn-periplanar hydrogen already exists at C2 immediately following insertion and therefore the C2 elimination occurs more rapidly. Palladium insertion at the C3 position gives intermediate **2.50** that proceeds to chain walk to give aldehyde **2.51**. In this case the movement of a deuterium from C3 to C4 was observed in the migration process.

The tri-deuterated alkenol **2.52** was used to study the directionality of the palladium migration along the chain. Again, no deuterium rearrangements were observed with the C4 arylation product **2.54** (Scheme 2.8, middle). Scrambling was however seen in C3 arylated product **2.56a** and **2.56b** in a 1.3:1 ratio, indicating a fairly even chance of palladium eliminating the deuterium at C5 or a hydrogen at C3 to initiate movement in either direction. The fact that approximately half of the C3 arylated product underwent both a deuterium shift and conversion to the aldehyde on opposite ends of the chain implies that the palladium migration must be able to change directions to facilitate these transformations. This observation also opened the possibility that the palladium migration may be able to reverse direction before reaching the alcohol at any time; a phenomenon sometimes referred to as “random walk.”

To test this, the allylically deuterated methylene **2.57** (Scheme 2.8, bottom) was tested using an electron deficient arylpalladium which favors the C4 arylated product. As expected, deuterium was only incorporated into the final aldehyde **2.59a/2.59b** at the C3

position. The lack of additional deuterated aldehyde products suggests that the chain-walking process towards the alcohol is unidirectional and does not reverse. Additionally, the deuterium was observed to undergo elimination and reinsertion from the same side of the chain. β -Deuteride elimination of D_a can occur immediately following arylation and results in *E*-palladium deuteride complex **2.58** that gives the *trans*-deuterated aldehyde product **2.59a**. For elimination of D_b to occur, bond rotation leads to the *Z*-palladium deuteride complex **2.60** and ultimately the *cis*-deuterated product **2.59b**. In either case, the alkylpalladium eliminates and reinserts from the same face of the chain which is determined by the initial carbopalladation.

2.5 - References

- (1) Heck, R. F.; Nolley, J. P. Palladium-Catalyzed Vinylic Hydrogen Substitution Reactions with Aryl, Benzyl, and Styryl Halides. *J. Org. Chem.* **1972**, *37*, 2320–2322.
- (2) Mizoroki, T.; Mori, K.; Ozaki, A. Arylation of Olefin with Aryl Iodide Catalyzed by Palladium. *Bull. Chem. Soc. Jpn.* **1971**, *44*, 581–581.
- (3) Beletskaya, I. P.; Cheprakov, A. V. The Heck Reaction as a Sharpening Stone of Palladium Catalysis. *Chem. Rev.* **2000**, *100*, 3009–3066.
- (4) Crisp, G. T. Variations on a Theme—Recent Developments on the Mechanism of the Heck Reaction and Their Implications for Synthesis. *Chem. Soc. Rev.* **1998**, *27*, 427–436.
- (5) Sommer, H.; Juliá-Hernández, F.; Martin, R.; Marek, I. Walking Metals for Remote Functionalization. *ACS Cent. Sci.* **2018**, *4*, 153–165.
- (6) Marek, I.; Chinkov, N.; Levin, A. A Zirconium Promenade - An Efficient Tool in Organic Synthesis. *Synlett* **2006**, *2006*, 501–514.
- (7) Ohlmann, D. M.; Goßen, L. J.; Dierker, M. Regioselective Synthesis of β -Aryl- and β -Amino-Substituted Aliphatic Esters by Rhodium-Catalyzed Tandem Double-Bond Migration/Conjugate Addition. *Chem. – Eur. J.* **2011**, *17*, 9508–9519.
- (8) Bair, J. S.; Schramm, Y.; Sergeev, A. G.; Clot, E.; Eisenstein, O.; Hartwig, J. F. Linear-Selective Hydroarylation of Unactivated Terminal and Internal Olefins with Trifluoromethyl-Substituted Arenes. *J. Am. Chem. Soc.* **2014**, *136*, 13098–13101.
- (9) Obligacion, J. V.; Chirik, P. J. Bis(Imino)Pyridine Cobalt-Catalyzed Alkene Isomerization–Hydroboration: A Strategy for Remote Hydrofunctionalization with Terminal Selectivity. *J. Am. Chem. Soc.* **2013**, *135*, 19107–19110.
- (10) Grotjahn, D. B.; Larsen, C. R.; Gustafson, J. L.; Nair, R.; Sharma, A. Extensive Isomerization of Alkenes Using a Bifunctional Catalyst: An Alkene Zipper. *J. Am. Chem. Soc.* **2007**, *129*, 9592–9593.

- (11) Lin, L.; Romano, C.; Mazet, C. Palladium-Catalyzed Long-Range Deconjugative Isomerization of Highly Substituted α,β -Unsaturated Carbonyl Compounds. *J. Am. Chem. Soc.* **2016**, *138*, 10344–10350.
- (12) Larionov, E.; Lin, L.; Guénée, L.; Mazet, C. Scope and Mechanism in Palladium-Catalyzed Isomerizations of Highly Substituted Allylic, Homoallylic, and Alkenyl Alcohols. *J. Am. Chem. Soc.* **2014**, *136*, 16882–16894.
- (13) Wang, Y.; Dong, X.; Larock, R. C. Synthesis of Naturally Occurring Pyridine Alkaloids via Palladium-Catalyzed Coupling/Migration Chemistry. *J. Org. Chem.* **2003**, *68*, 3090–3098.
- (14) Kochi, T.; Hamasaki, T.; Aoyama, Y.; Kawasaki, J.; Kakiuchi, F. Chain-Walking Strategy for Organic Synthesis: Catalytic Cycloisomerization of 1,n-Dienes. *J. Am. Chem. Soc.* **2012**, *134*, 16544–16547.
- (15) Kochi, T.; Ichinose, K.; Shigekane, M.; Hamasaki, T.; Kakiuchi, F. Metal-Catalyzed Sequential Formation of Distant Bonds in Organic Molecules: Palladium-Catalyzed Hydrosilylation/Cyclization of 1,n-Dienes by Chain Walking. *Angew. Chem. Int. Ed.* **2019**, *58*, 5261–5265.
- (16) Hilton, M. J.; Cheng, B.; Buckley, B. R.; Xu, L.; Wiest, O.; Sigman, M. S. Relative Reactivity of Alkenyl Alcohols in the Palladium-Catalyzed Redox-Relay Heck Reaction. *Tetrahedron* **2015**, *71*, 6513–6518.
- (17) Dang, Y.; Qu, S.; Wang, Z.-X.; Wang, X. A Computational Mechanistic Study of an Unprecedented Heck-Type Relay Reaction: Insight into the Origins of Regio- and Enantioselectivities. *J. Am. Chem. Soc.* **2014**, *136*, 986–998.
- (18) Heck, R. F. The Arylation of Allylic Alcohols with Organopalladium Compounds. A New Synthesis of 3-Aryl Aldehydes and Ketones. *J. Am. Chem. Soc.* **1968**, *90*, 5526–5531.
- (19) Heck, R. F. Mechanism of Arylation and Carbomethoxylation of Olefins with Organopalladium Compounds. *J. Am. Chem. Soc.* **1969**, *91*, 6707–6714.
- (20) Dieck, H. A.; Heck, R. F. Organophosphinepalladium Complexes as Catalysts for Vinylic Hydrogen Substitution Reactions. *J. Am. Chem. Soc.* **1974**, *96*, 1133–1136.

- (21) Melpolder, J. B.; Heck, R. F. Palladium-Catalyzed Arylation of Allylic Alcohols with Aryl Halides. *J. Org. Chem.* **1976**, *41*, 265–272.
- (22) Chalk, A. J.; Magennis, S. A. Palladium-Catalyzed Vinyl Substitution Reactions. I. New Synthesis of 2- and 3-Phenyl-Substituted Allylic Alcohols, Aldehydes, and Ketones from Allylic Alcohols. *J. Org. Chem.* **1976**, *41*, 273–278.
- (23) Stakem, F. G.; Heck, R. F. Reactions of π -Allylic Palladium Intermediates with Amines. *J. Org. Chem.* **1980**, *45*, 3584–3593.
- (24) Larock, R. C.; Takagi, K. Mercury in Organic Chemistry. 27. π -Allylpalladium Synthesis via Organopalladium Additions to Nonconjugated Dienes. *Tetrahedron Lett.* **1983**, *24*, 3457–3460.
- (25) Larock, R. C.; Varaparth, S. Mercury in Organic Chemistry. 30. Synthesis of (π -Allyl)Palladium Compounds via Organopalladium Additions to Alkenyl- and Methylene-cyclopropanes and Alkenyl- and Methylene-cyclobutanes. *J. Org. Chem.* **1984**, *49*, 3432–3435.
- (26) Jeffery, T. Palladium-Catalysed Vinylation of Organic Halides under Solid–Liquid Phase Transfer Conditions. *J. Chem. Soc. Chem. Commun.* **1984**, No. 19, 1287–1289.
- (27) Jeffery, T. Highly Stereospecific Palladium-Catalysed Vinylation of Vinylic Halides under Solid-Liquid Phase Transfer Conditions. *Tetrahedron Lett.* **1985**, *26*, 2667–2670.
- (28) Jeffery, T. On the Efficiency of Tetraalkylammonium Salts in Heck Type Reactions. *Tetrahedron* **1996**, *52*, 10113–10130.
- (29) Larock, R. C.; Leung, W.-Y.; Stolz-Dunn, S. Synthesis of Aryl-Substituted Aldehydes and Ketones via Palladium-Catalyzed Coupling of Aryl Halides and Non-Allylic Unsaturated Alcohols. *Tetrahedron Lett.* **1989**, *30*, 6629–6632.

- (30) Werner, E. W.; Mei, T.-S.; Burckle, A. J.; Sigman, M. S. Enantioselective Heck Arylations of Acyclic Alkenyl Alcohols Using a Redox-Relay Strategy. *Science* **2012**, *338*, 1455–1458.
- (31) Mei, T.-S.; Patel, H. H.; Sigman, M. S. Enantioselective Construction of Remote Quaternary Stereocentres. *Nature* **2014**, *508*, 340.
- (32) Singh, S.; Bruffaerts, J.; Vasseur, A.; Marek, I. A Unique Pd-Catalysed Heck Arylation as a Remote Trigger for Cyclopropane Selective Ring-Opening. *Nat. Commun.* **2017**, *8*, 14200.

3 A Heck-Based Approach to Anacardic Acids and Related Phenolic Lipids

3.1 - Introduction

While anacardic acids are relatively simple molecules, we were mindful of a few considerations that needed be taken into account when developing a strategy for their synthesis (**Figure 3.1**, top). We found the idea of using a simple aromatic starting material to be an attractive starting point due to the abundance of commercially available options and the wide array of methods to synthetically manipulate them. With this in mind, we next thought about the available options for alkylation of the aromatic core as well as a method for the introduction of unsaturation characteristic of anacardic acid side chains. Past synthetic routes to anacardic acid using aromatic alkylation approaches have been beleaguered with high step counts, low overall yields, and limited scope. As seen in Chapter 1, these syntheses have often struggled with achieving the desired 6-alkylsalicylic acid substitution on the ring and with the protection/installation of the salicylic acid itself.

However, as discussed in Chapter 2, the Heck redox relay reaction allows for the arylation of alkenols with good regioselectivity to afford the corresponding aldehyde. A Heck redox-relay is therefore a potentially elegant method to both forge the alkyl-aryl connection and simultaneously functionalize the remote alcohol of the alkenol substrate **3.6** to an aldehyde **3.4**. This aldehyde can be directly used in a Wittig or similar olefination reaction (**Figure 3.1**, bottom). Straight chain alkenols such as **3.6**, with a primary alcohol on one end and a terminal olefin on the other, are commonly available fatty alcohols (for n=1-12) making this a versatile method for the preparation of the aldehyde intermediate leading to virtually any member of the anacardic acid family. Herein, this new strategy for

the construction of anacardic acids will be presented. Additionally, as a demonstration of utility, a biochemical assay was carried out for a small library of products synthesized using this methodology and will also be detailed.

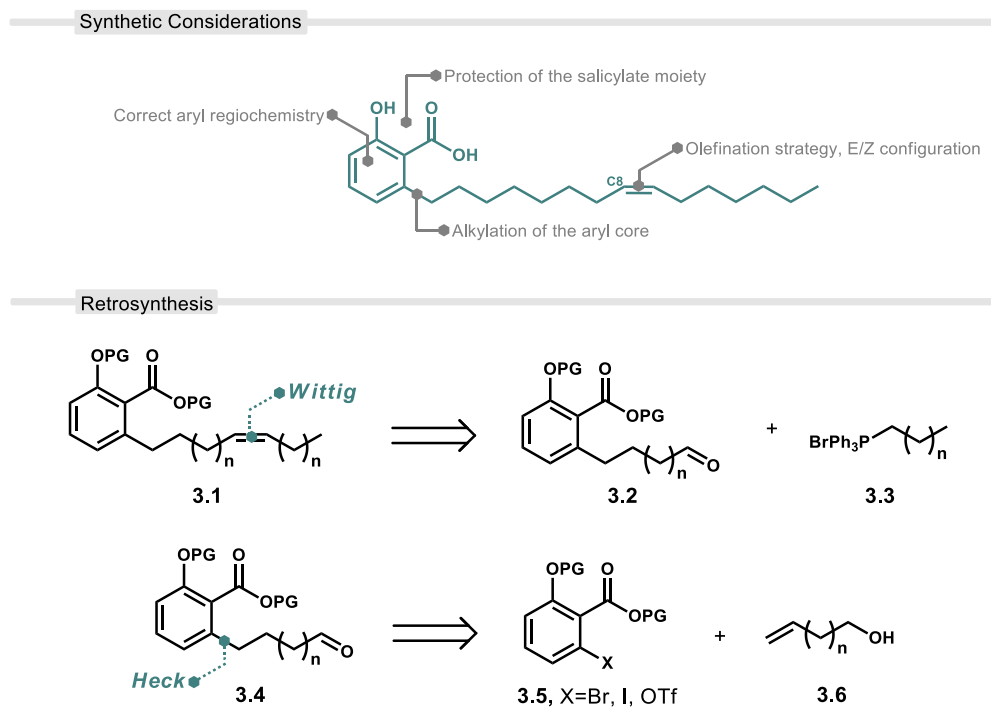
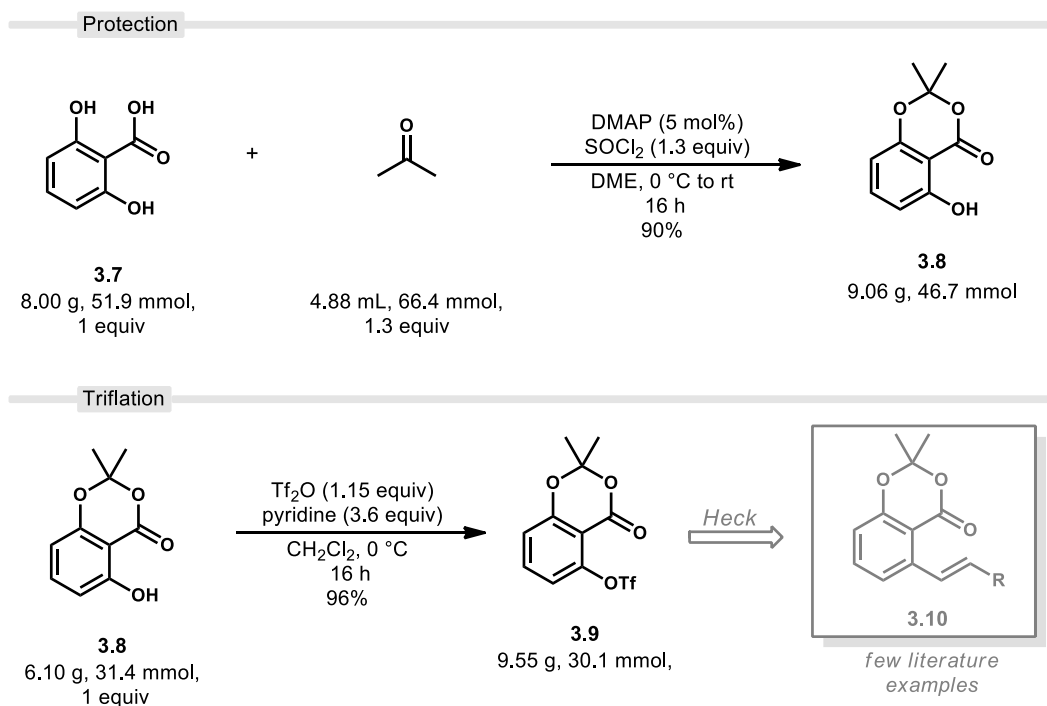


Figure 3.1 – Considerations and Strategy for A Heck-Based Anacardic Acid Synthesis

3.2 - Preparation of the Aromatic Core

Many previous anacardic acid syntheses have approached the protection of the salicylic acid moiety using two separate protecting groups (i.e. as an ether for the phenol and an ester for the carboxylate). However, this approach adds separate installation and/or removal steps which necessitates the use of caustic and volatile boron tribromide for demethylation. A much more elegant method is the simultaneous protection of both phenolic and carboxyl functionalities with acetone as an isopropylidene ketal (acetone) which can be removed with basic hydrolysis.^[1] We implemented this method starting from

2,6-dihydroxybenzoic acid (**3.7**, **Scheme 3.1**), a cheap commercially available starting material, using a small excess of acetone and thionyl chloride with catalytic 4-dimethylaminopyridine (DMAP) to form the acetonide protected product **3.8** in excellent yield. The remaining phenolic OH was then converted to aryl triflate **3.9** using triflic anhydride also in excellent yield. This aryl triflate is a competent electrophile and has been used by Molander, Fürstner, Nicolaou, and others for the synthesis of macrolide natural products using palladium-catalyzed cross-couplings such as the Suzuki, Stille, or Sonogashira.^[2-6] Significantly fewer examples involve a Heck reaction of this substrate class, leading to styrene-type products (**3.10**) that are typical of this reaction.^[7,8]

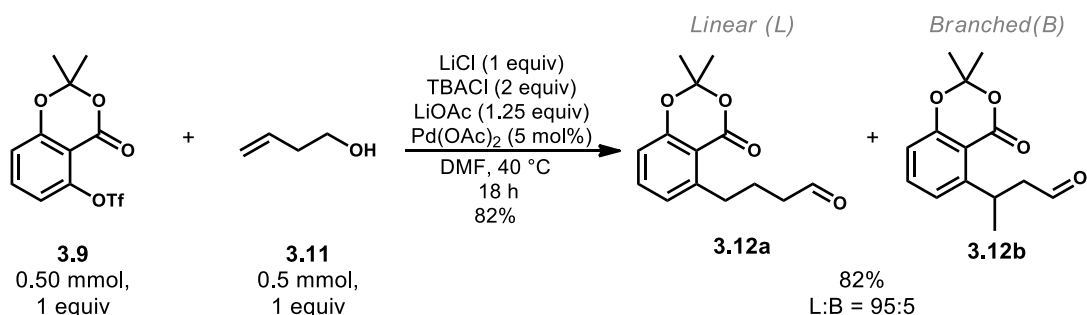


Scheme 3.1 – Preparation of Protected Aryl Triflate From 2,6-Dihydroxybenzoic Acid

3.3 - Optimization and Modification of Jeffery's Conditions

Our initial testing of the Heck redox-relay between aryl triflate **3.9**, and 3-buten-1-ol (**3.11**, **Scheme 3.2**) with the modified Jeffery's conditions reported by Larock^[9] afforded the linear (L) and branched (B) aldehyde products **3.12a** and **3.12b** in 82% yield. The regioselectivity of these reactions was consistently high (L:B 95:5) based on the integral ratios between the regioisomers by crude ¹H NMR (**Figure 3.2**), however, the overall yields for the reactions themselves were variable. While we were pleased with these initial results, the reproducibility of a high yielding result was an issue and we set out to determine the cause of the inconsistency

It was observed that the lithium salts used in the modified Jeffery's conditions were hygroscopic and underwent rapid deliquescence upon exposure to air. Heating these salts overnight under vacuum appeared to marginally improve reaction outcomes; however, the exposure to air during the process of weighing out the reagents on the balance was still of concern. Weighing out the reagents inside a glovebox under dry nitrogen atmosphere resulted in a consistently high yield.



Scheme 3.2 – Preliminary Heck Redox-Relay Results with 3-Buten-1-ol

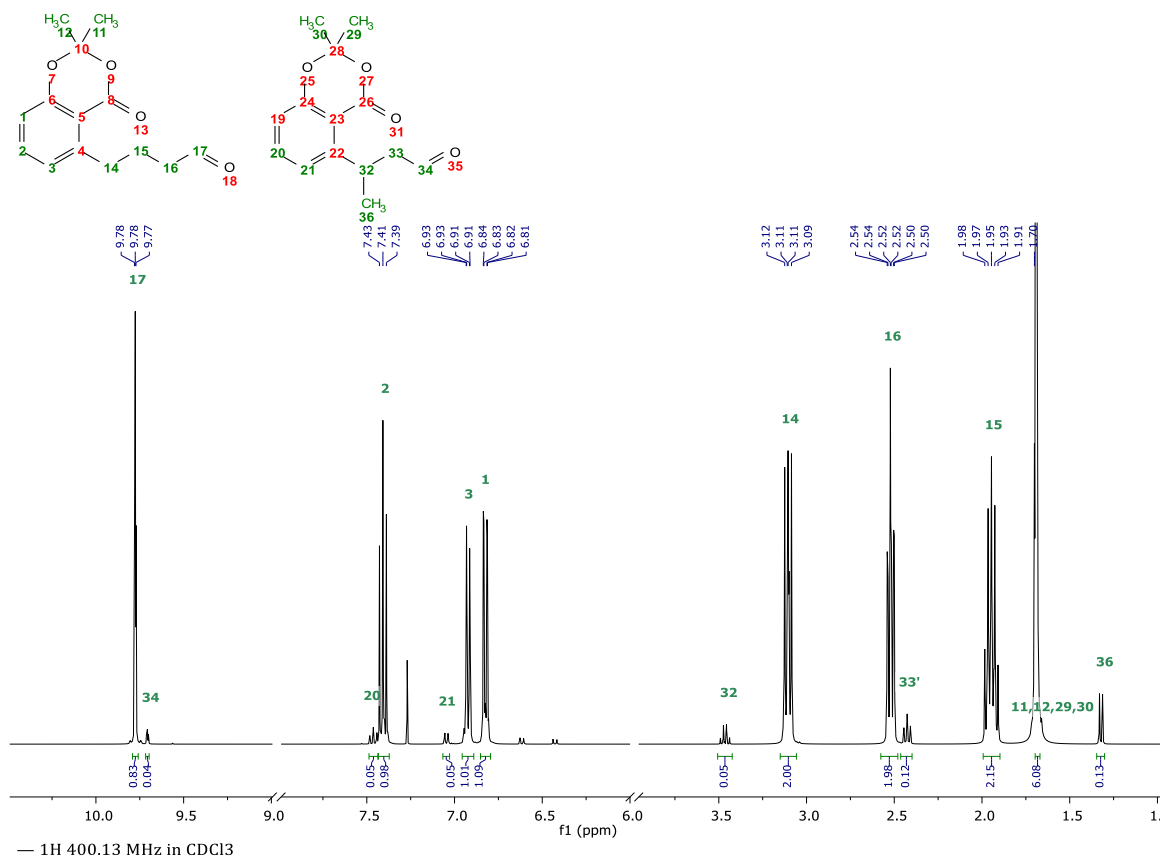


Figure 3.2 – ¹H NMR Spectrum of Linear and Branched Heck-Relay Products

Doubling the equivalents of lithium acetate (1.25 to 2.5 equiv) was also found to increase the conversion of the aryl triflate. An increase in acetate concentration led to a longer active catalyst lifetime by reducing the rate at which palladium black nanoparticles aggregate. This is qualitatively supported by the observation of the reaction mixture taking more time to develop a black coloration with higher concentrations of lithium acetate (~2 h at 0.075 M and 4-6 h at 0.15 M). This is presumably through stabilization of the metal center with a weakly bound acetate ligand.^[10] When running palladium-catalyzed reactions of any kind, the common wisdom is that nanoparticle formation should be avoided—reactions quickly forming palladium black are typically met with poor results. However,

in the case of ligandless palladium conditions, work by Reetz and coworkers have suggested that nanoparticles 2-10 nm in diameter are themselves responsible for catalysis in these Heck reactions.^[11,12] In this light, these reactions transition from being classified under homogeneous catalysis and are redesignated as heterogeneously catalyzed. The role of acetate then may instead be linked to assisting in the formation and/or stabilization of the colloidal mixture.

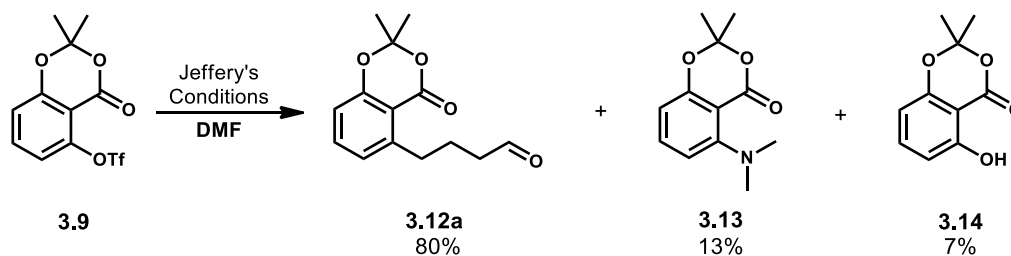


Figure 3.3 – Side Product Formation in Reactions Using DMF Solvent

While full conversion of the aryl triflate had been accomplished, the presence of two aryl side products in the crude reaction mixtures was still undesirable. These side products were identified as the protected dimethylaniline **3.13** and its phenolic counterpart (**3.14**, **Figure 3.3**) which together accounted for approximately 20% of the converted triflate. Presumably, these products are the result of reductive eliminations that form the new C(sp²)-N or C(sp²)-O bonds from the corresponding amino or hydroxy palladium complexes, although the latter could also result from hydrolysis of the triflate.^[13] These products suggested that both water and dimethylamine contaminants were likely present and coordinating with palladium. As discussed earlier, undesired hydration of the Jeffery salts or wet solvent was the likely source of water and dimethylamine is a common contaminant of dimethylformamide (DMF). Fortunately, it was found that switching

solvents to anhydrous dimethylacetamide (DMA) eliminated the formation of these side products and significantly improved yields (65% to >90%).

A final aspect of these reactions known previously from Larock's work, is the effect of temperature on the rate of the reaction. While the chain-walking process is can occur at room temperature even with longer alkenols (6+ carbons), these reactions were observed to occur much more slowly with increasing chain length. This is likely attributed to the increasing number of bond-walking operations and alkylpalladium intermediates required to isomerize longer alkenols, which slows convergence into a thermodynamic sink (product formation). The addition of mild heating to these reactions (~50-60 °C) was found to be beneficial and shortened reaction times from the order of days to hours without significantly impacting L:B selectivity.

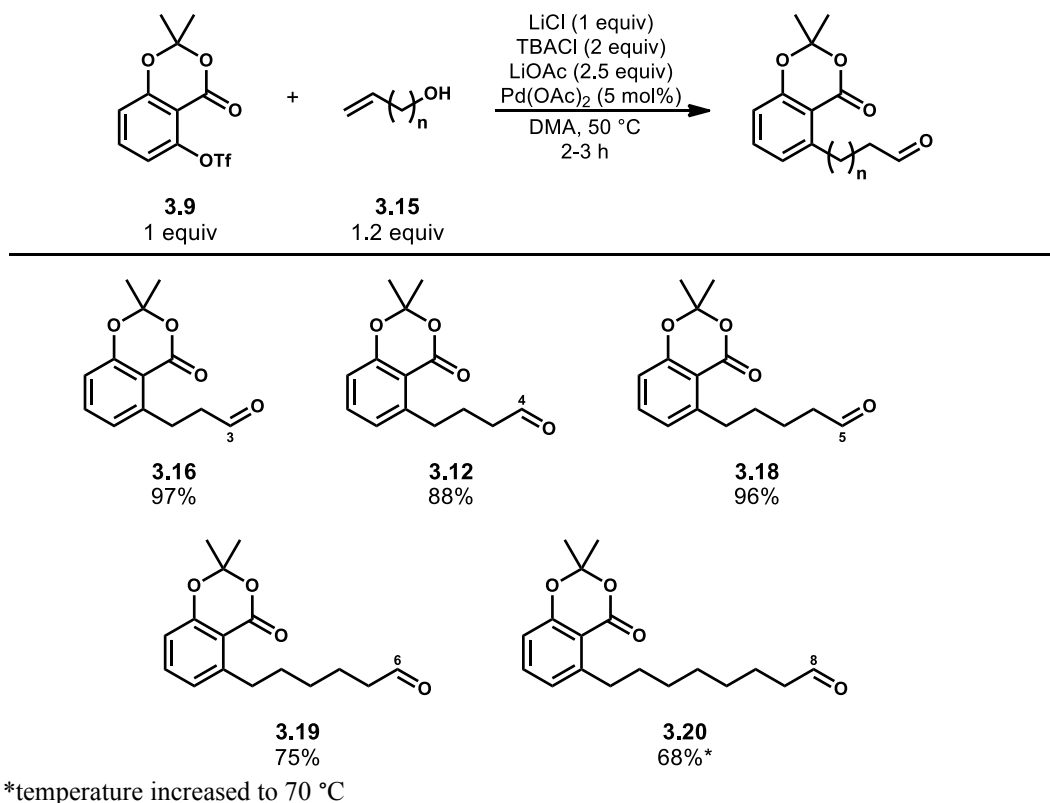
3.4 - Reaction Scope

3.4.1 - Alkenol Chain Length

Using conditions that were optimized around 3-buten-1-ol, the efficiency of the chain-walking process was investigated using a variety of alkenols of varying chain lengths (**Table 3.1**). We found that under these optimized reaction conditions, 2-propen-1-ol and 4-penten-1-ol reacted to give their linear aldehyde products **3.16** and **3.18** in both higher yield and with a shorter reaction time compared to the butenol product **3.12**. This difference in reaction performance may arise because the hydroxyl in the 4 carbon alkenol is able to chelate palladium more effectively which may reduce the efficiency of carbopalladation. The yields declined with increasing alkenol chain length as was seen for the six-carbon product (**3.19**, 75%) and the eight-carbon product (**3.20**, 68%). The eight-carbon alkenol

required an increase in temperature to achieve a reaction time similar to the shorter alkenols.

Table 3.1 – Heck Relay Coupling with Alkenols of Varying Length

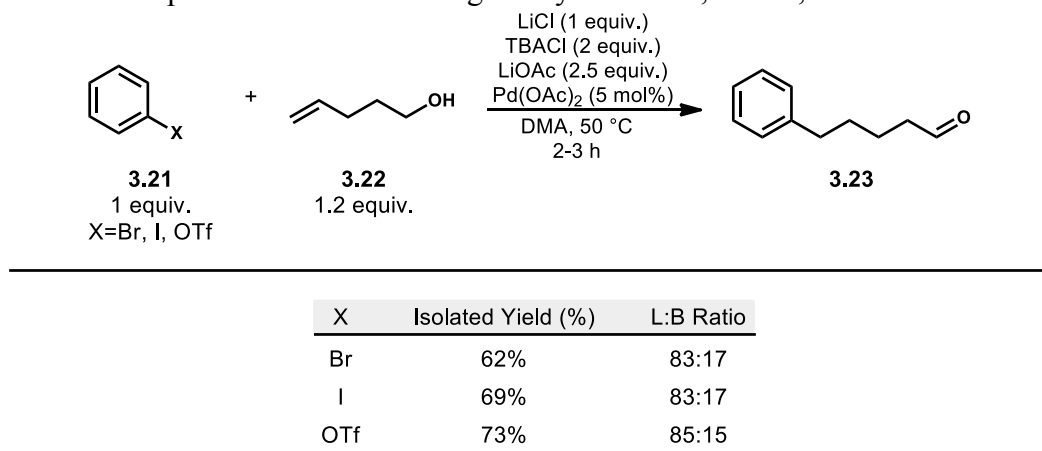


3.4.2 - Variation of the Electrophile

Interestingly, the development and application of the redox-relay Heck reaction has seldom ventured away from the use of aryl iodide electrophiles. Aryl electrophiles such as boronic acids^[14,15] and diazonium salt^[16] have been used in related oxidative Heck reactions, for example by Sigman and coworkers. By contrast, few examples exist of aryl or vinyl triflates being used for these palladium relay reactions with alkenols.^[14,17,18] We

were therefore interested to compare the efficiency and regioselectivity of these Heck relays with the more commonly used aryl halides under the optimized Jeffery's conditions.

Table 3.2 – Comparison of Results Using Phenyl Bromide, Iodide, and Triflate



We tested phenyl bromide, iodide, and triflate with 4-penten-1-ol (**3.22**, **Table 3.2**) and evaluated their performance. Some variation in the reaction yield was observed with the triflate (73%) outperforming the iodide (69%) and the bromide (63%). However, these reactions all proceeded with uniform regioselectivities of ~L:B 83:17, matching Larock's results under similar conditions (compare to entries 2-4, **Table 2.2**, pg. 42). This result could indicate that under these conditions, the identity of X in the ArPdX intermediate has little effect on migratory insertion or has undergone prior dissociation because variation in X was observed to not influence the regiochemical preference of the insertion. Instead, following oxidative addition, rapid ligand exchange of ArPdX to ArPdY (Y = OAc, Cl etc.) or dissociation of X to cationic ArPd⁺ occurs. Both ArPdY and ArPd⁺ are capable of engaging the double bond without discrimination based on the identity of X in the initial

aryl halide/triflate. Under these reaction conditions involving a polar solvent with high ionic strength due to the added salts, the cationic route is more likely.

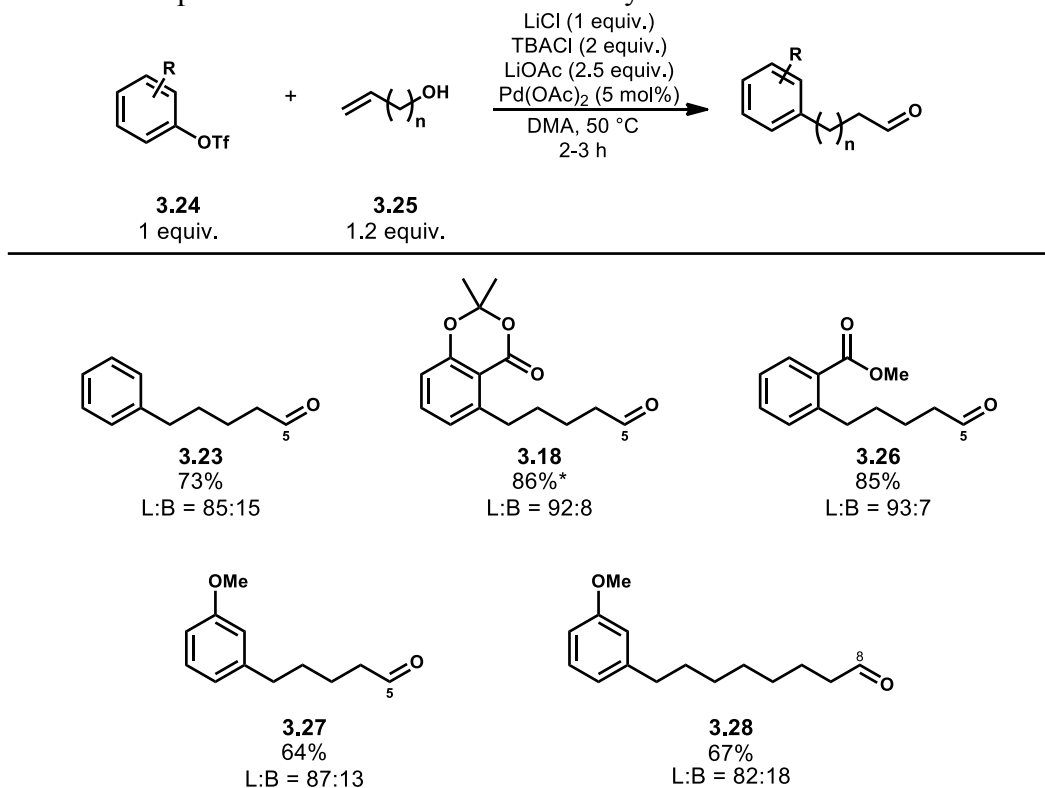
We found the regioselectivity of the reaction with triflated acetonide **3.9** to be considerably higher than those seen with phenyl triflate **3.21-OTf**. Since no change was observed with aryl halides, we concluded that the difference in this regioselectivity must be occurring due to the steric and/or electronic differences between the substituted and unsubstituted aryl substrate.

3.4.3 - Aryl Substituent Effects Regioselectivity

In order to establish whether or not the aryl substituents were exerting any steric or electronic influence over the regiochemical outcomes of the Heck reaction, we synthesized a few different aryl triflates which were then tested with a 5 or 8 carbon alkenol (**Table 3.3**). The results of these tests seem to confirm that the positioning of a carboxylate *ortho* to the triflate is responsible for the observed boost in regioselectivity. This can be concluded by considering acetonide **3.18** and methyl ester **3.26** which have higher selectivity for the linear aldehyde regioisomer compared to the *m*-methoxy derivatives (**3.27** and **3.28**) as well as the unsubstituted phenyl product **3.23**. These observations are consistent with past Hammett studies by Sigman *et al.* who also found that regioselectivity drops with more electron rich aryl boronic acids.^[19] In terms of yield, seem to also benefit more from an electron deficient ring system (**3.18** and **3.23**), an observation consistent with their role as an electrophilic reaction partner. Unfortunately, reactions using *meta*- or *para*-CO₂Me substituents were not attempted although the results of such reactions could prove

useful in evaluating the effect of the carboxylate substituent's location on yield or regioselectivity.

Table 3.3 – Comparison of Results with Various Aryl Substituted Triflates



3.5 - Synthesis of (15:1) Ginkgolic Acid and (15:2) Anacardic Acid

As seen previously in the chapter, acetone-protected triflate **3.9** can be effectively coupled with alkenols to afford predominantly linearly substituted arylated aldehyde products. For the synthesis of (15:1) ginkgolic acid[¶], the alkyl tail substituent is 15 carbons in length and features one *Z*-olefin between the C8 and C9 carbons. As the retrosynthesis

[¶] Note regarding terminology: Ginkgolic acid specifically refers to the (15:1) anacardic acid with C8 (or “ ω -7”) *Z*-monounsaturations.

in **Figure 3.4** shows, a Wittig olefination should result in the desired *Z*-alkene between C8 and C9 in the alkyl chain. Using this approach, the positioning of this olefin is determined by selecting an aldehyde/phosphonium pair each containing the proper number of carbons. In this case, an 8-carbon alkyl aldehyde (**3.31**) and a 7-carbon alkylphosphonium bromide (**3.32**) are needed. This olefination strategy enables the synthesis of a *Z*-alkene positioned at any point on a chain of any size depending on the lengths of the Wittig reagents and the point of concatenation between them. Following olefination, acetonide deprotection of **3.30** using base hydrolysis would give the final (15:1) ginkgolic acid product **3.29**.

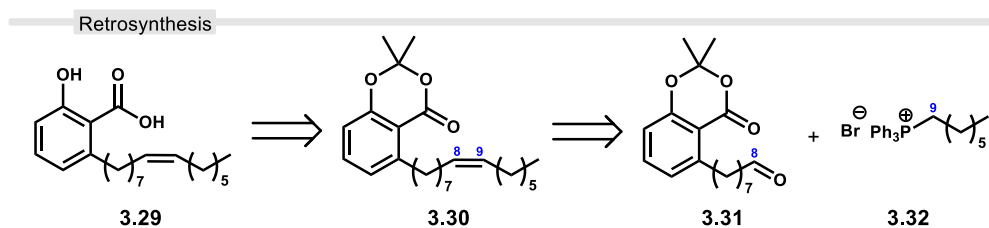
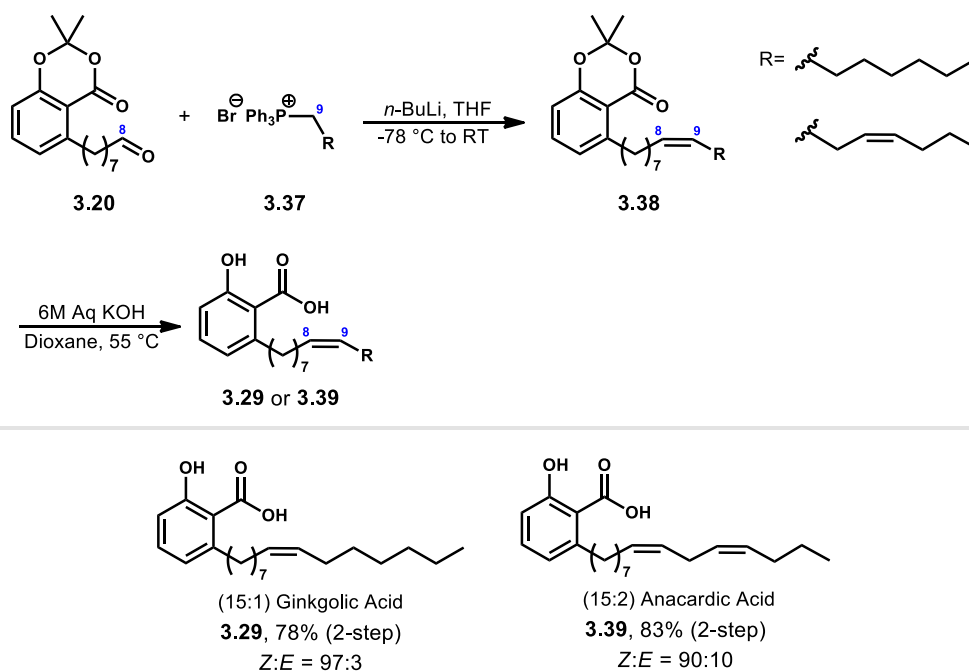


Figure 3.4 – Retrosynthesis for (15:1) Ginkgolic Acid

Synthesis of the aryl aldehyde (**3.20**, **Figure 3.4**) was conducted on gram scale using modified Jeffery's conditions at elevated temperature between triflated acetonide **3.9** and 7-octen-1-ol (**3.33**) to obtain the 8-carbon chain aldehyde **3.20** in moderate yield. The heptylphosphonium bromide used in the Wittig reaction with **3.20** is commercially available. The synthesis of the (15:2) anacardic acid requires the *Z*-hept-3-enylphosphonium salt (**3.36**) which is not commonly commercially available. This was therefore synthesized over 3 steps starting with mesylation of 3-(*Z*)-hepten-1-ol (**3.34**) followed by a Finkelstein-type displacement of the mesylate with LiBr to give the heptenyl bromide **3.35**. This was then treated with triphenylphosphine to generate the desired phosphonium bromide (**3.36**) in 65% overall yield.

Having obtained the necessary precursors, the Wittig reaction was then used on aldehyde **3.20** (Scheme 3.3) with both the saturated and unsaturated phosphonium bromide salts to obtain the acetonide-protected (15:1) and (15:2) anacardic acids **3.38**. These Wittig reactions proceeded in good yields, although lower diastereoselectivity was observed for the (15:2) anacardic acid (*Z:E* 90:10 vs 97:3). The deprotection of the acetonide was accomplished using aqueous KOH in dioxane, resulting in the final (15:1) and (15:2) anacardic acids (**3.29**, 78%; **3.39**, 83% respectively).



Scheme 3.3 – Wittig Olefinations Used in the Synthesis of (15:1) and (15:2) Anacardic Acids

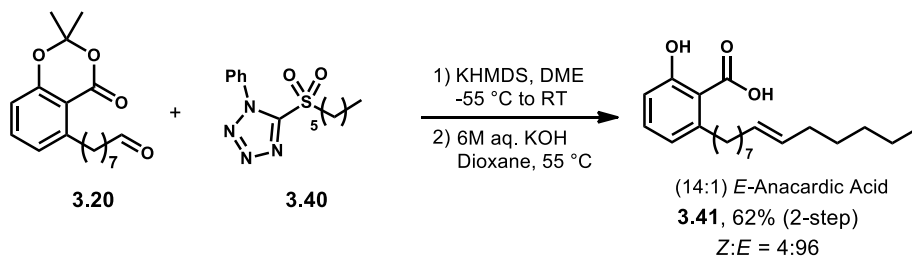
3.6 - Synthesis of Unnatural (14:1) *E*-Anacardic Acid

Natural anacardic acids are biochemically synthesized with a wide range of tail morphologies with variations in length and the extent of unsaturation. However, these variations are constrained by the limits of the catalytic machinery from which they are

made. Due to their polyketide origins, the anacardic acids are created in 2 carbon increments which places limitations on the chain lengths that are biologically accessible. Such limitations can be seen by referring back to **Table 1.1** where the list of naturally occurring chain lengths is largely limited to 13-, 15-, and 17-carbon long variants. Additionally, both the positioning of the double bonds and their *cis* geometry are enzymatically controlled and are also limiting factors.

In addition to natural anacardic acids, we also set out to demonstrate a synthesis of an unnatural variant as well. For this endeavor, we chose to synthesize an analog with a length of 14 carbons featuring a *trans* double bond. As discussed in the previous section, the length is easily controlled through proper selection of olefination precursors. The *trans* double bond can be selectively targeted using a Julia–Kocienski olefination rather than a Wittig reaction.

To this end, aldehyde **3.20** and alkyltetrazole **3.40** (**Scheme 3.4**) were reacted in the presence of KHMDS to afford the acetonide-protected *E*-alkene product with high diastereoselectivity (*Z:E* 4:96). Using the same basic hydrolysis conditions, the deprotected (14:1) *E*-anacardic acid product (**3.41**) was obtained in 62% over the two steps.



Scheme 3.4 –Unnatural Anacardic Acid Synthesis via Julia–Kocienski Olefination

3.7 - Stereochemical Analysis of Olefination Reactions

In theory, the diastereoselectivity of an olefination reaction for a disubstituted alkene can be deduced by an analysis of the coupling constants in a crude ^1H NMR spectrum of the reaction mixture. The *trans* isomer should result in a larger J -value than *cis* isomer provided the appropriate signals are distinguishable. In cases involving alkenes with a sufficient degree of polarity differential between the carbons in the double bond, the resulting chemical shifts may be different enough to allow for analysis of the individual proton signals. However, in the case of anacardic acid products, the alkene in question is located mid-way in between the alkyl chain and therefore the C–H signals overlap eliminating the ability to accurately determine coupling constants.

Epoxidation of *cis* or *trans* alkenes leads to their respective oxiranes which significantly boosts the resolution of the proton signals in mixtures containing both isomers. This difference is illustrated in **Figure 3.5** which shows the chemical shifts for both *cis* and *trans* 2,3-dibutyloxirane (**3.42** and **3.43**). We therefore reacted small aliquots of the olefination reaction mixture with *meta*-chloroperoxybenzoic acid (*mCPBA*) which effectively epoxidized the alkene product. **Figure 3.6** shows the comparison of the ^1H NMR spectra for the alkenes and their products after epoxidation. The epoxides are indeed sufficiently spaced apart after treatment with *mCPBA* and have chemical shifts consistent with those seen for the dibutyloxiranes. This method of epoxidation allowed for accurate determination of the diastereoselectivity in the Wittig and Julia–Kocienski olefinations using integral ratios and were corroborated through GC analysis.

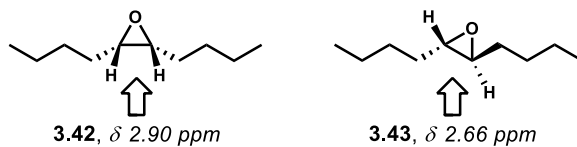


Figure 3.5 – ^1H NMR Chemical Shifts for *cis/trans* 2,3-Dibutyloxiranes

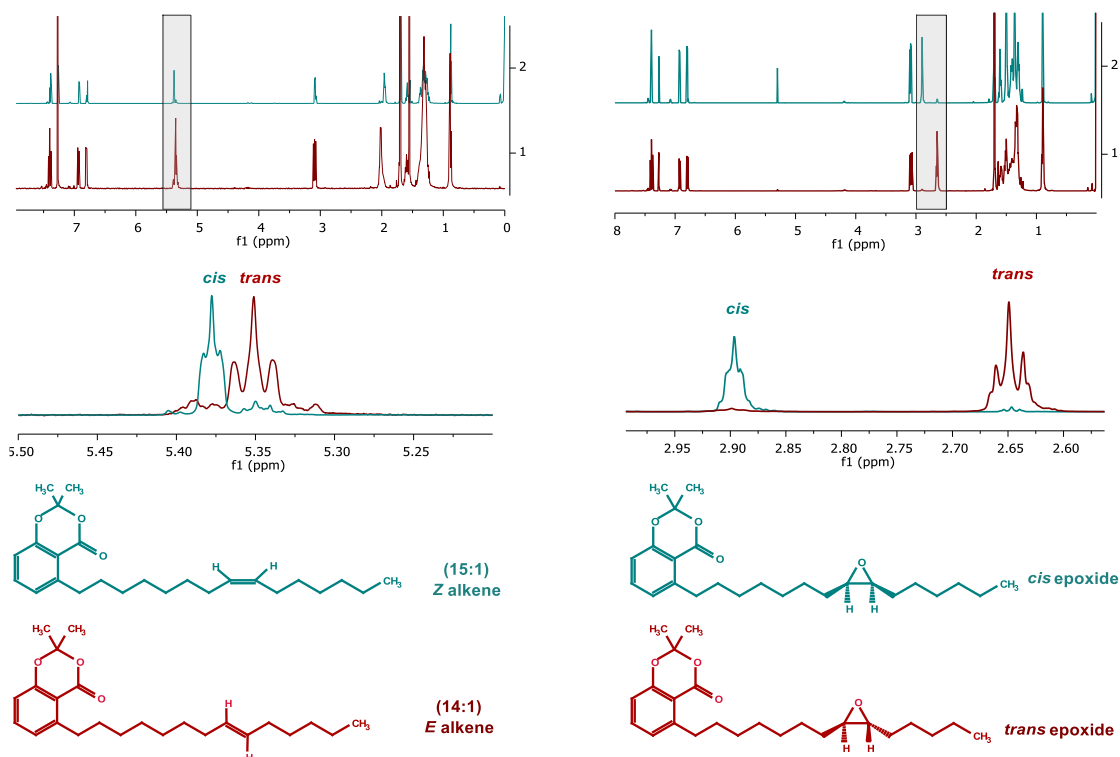


Figure 3.6 – ^1H NMR Comparison of *E/Z* Alkenes and Corresponding Epoxides

Proton signals for *E/Z* alkenes (left) have similar chemical shifts while their corresponding epoxides (right) are significantly further apart.

3.8 - MMP-2 Inhibition Assays with Anacardic Acids

Matrix metalloproteinase-2 (MMP-2) is a collagenase enzyme that is involved in the breakdown of the extracellular matrix to facilitate tissue remodeling and repair.^[20] These proteins are critical in the inflammation response, with wound healing, and the development of new blood vessels (angiogenesis).^[21] However, they have also been found

to be a significant contributor to tumorigenic tissue's ability to undergo metastasis and therefore play a role in cancer progression.^[22–24]

Anacardic acids from CNSL have been found to act as inhibitors of MMP-2^[25] and we were curious to see if a specific anacardic acid may be more potent than the others in this regard. Together in collaboration with Dr. Jeff Perry's group in the Biochemistry Department at the University of California, Riverside, we tested several natural anacardic acids and one unnatural variant.^[26] To this end, the recombinant catalytic domain of MMP-2 was preincubated with the anacardic acids at concentrations of 1, 5, 10, 25, and 50 μM . The enzymatic activity of these samples was then determined using a fluorescently

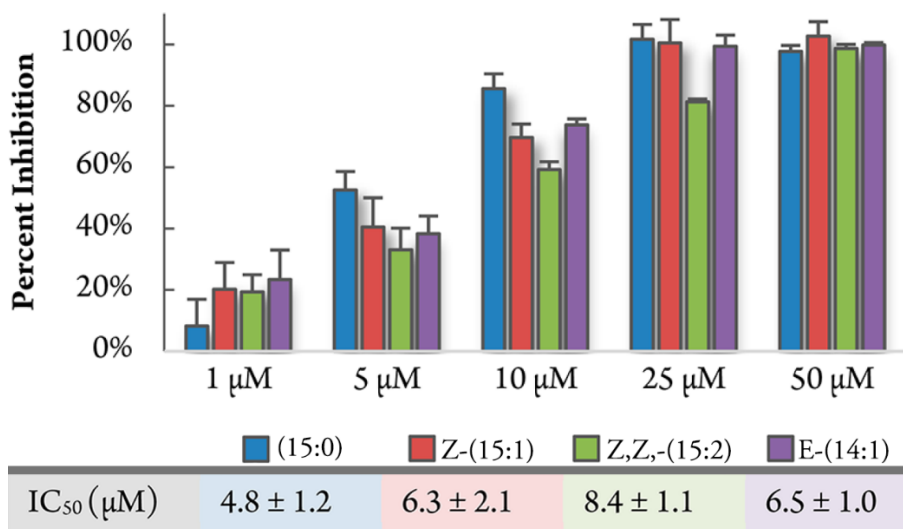


Figure 3.7 – Extent of MMP-2 Inhibition by Anacardic Acids at Different Concentrations conjugated gelatin as substrate. In this assay, fluorescence occurs based on the extent of degradation to the gelatin matrix. Thus, more active MMP-2 samples lead to greater degradation of this matrix resulting in higher levels of fluorescent response. The results of this assay with natural anacardic acids ((15:0), **3.29** Z-(15:1), **3.39** Z,Z-(15:2)) and the unnatural variant **3.41** (E-(14:1)) are shown in **Figure 3.7**.

Inhibition of MMP-2 with the anacardic acids proceeded in a dose-dependent manner, although little increase was observed after preincubation at 25 μM as inhibition was already approaching 100% at this concentration. Overall, these results indicated that tail morphology does not significantly impact the potency between specific anacardic acid isoforms. The completely saturated (15:0) anacardic acid was most potent by a small margin (calculated IC_{50} value of $4.8 \pm 1.2 \mu\text{M}$) while the least potent was the *Z,Z*-(15:2) diunsaturated variant ($8.4 \pm 1.1 \mu\text{M}$). The natural anacardic *Z*-(15:1) and unnatural *E*-(14:1) were most similar in potency ($6.3 \pm 2.1 \mu\text{M}$ and $6.5 \pm 1.0 \mu\text{M}$, respectively). Together, these data suggest there is a small dependence in the level of unsaturation within the lipid tail, with more unsaturation leading to slight decreases in potency. However, olefin geometry does not appear to play a significant role in MMP-2 binding.

Inhibition of the MMP-2 enzyme is believed to occur through coordination to the catalytic zinc by the carboxylate on the aryl core of anacardic acid. Based on previous studies by Perry *et al.*, cardanol showed minimal inhibition which implicates the role of the carboxylate in binding MMP-2.^[25] Similarly, significantly less inhibition was observed with salicylic acid alone suggesting that the alkyl tail is useful for binding. Additionally, modification of the phenol in anacardic acid to the acetylsalicylic acid resulted in loss in inhibition, presumably due to detrimental steric effects.^[25] Another known inhibitor of MMP-2 based on the β -amyloid precursor protein (APP) has been crystallized in the binding cleft and clearly shows coordination of the zinc by the carboxylate of the Asp residue in the inhibitor (**Figure 3.8**).^[27] This provides insight into how anacardic acid could interact with MMP-2.

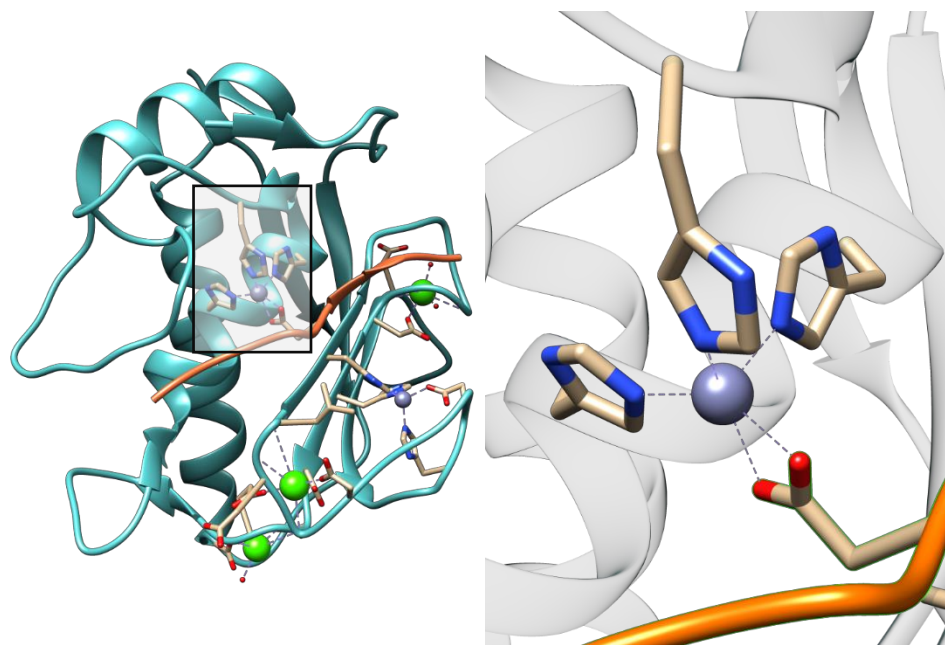


Figure 3.8 – Matrix Metalloproteinase-2 with a β -APP Derived Inhibitor

This β -amyloid precursor protein-derived inhibitory peptide (orange) forms a bidentate coordination complex with the catalytic zinc of the MPP-2 enzyme using the carboxylate of an Asp residue. A similar mode of binding is suspected for anacardic acid via its aryl carboxylate. (PDB ID: 3AYU)

3.9 - Conclusions

This Heck-based redox-relay strategy for the synthesis of anacardic acids is a significant improvement to previously used approaches. The redox-relay uses an easily prepared aryl triflate and cheap commercially available alkenols to form versatile aldehyde intermediates. This transformation is powerful, enabling the creation of a new C–C bond and the simultaneous transformation of a remote primary alcohol into an aldehyde with high yield and regioselectivity. Olefination of the resulting aldehyde using a Wittig or Julia–Kocienski reaction proceed selectively to give the *E* or *Z* alkene. The modularity of this approach easily enables the synthesis of both natural and unnatural anacardic acids and could be easily extended to include other phenolic lipids. Direct synthesis of specific

anacardic acids circumvents the need for their laborious separation from natural phytochemical mixtures and enables the biochemical study them individually. To demonstrate the applicability of this strategy in biochemical analysis, a number of these lipids were synthesized and tested in an MMP-2 assay.

3.10 - Experimental

3.10.1 - General Methods

All reactions were carried using oven dried or flame dried glassware charged with a magnetic stir bar, and conducted under an inert nitrogen atmosphere using typical Schlenk techniques. Solvents were dried by passage through columns of activated alumina or distilled and stored under nitrogen over 5 Å sieves. All starting materials were prepared according to known literature procedures or used as obtained from commercial sources, unless otherwise indicated. Reactions were monitored by thin-layer chromatography (TLC) and carried out on 0.25 mm coated commercial silica gel plates (Analtech TLC Uniplates, F254 precoated glass plates) using UV light as visualizing agent. Unless otherwise indicated, silica gel chromatography was performed using a Yamazen Smart Flash AI-580S system in conjunction with Yamazen Universal Premium 40g columns with the specified gradient elution mode.

¹H and ¹³C NMR spectra were recorded on a Varian Inova 300 MHz, Bruker Avance NEO 400, or Bruker Avance III 700 MHz spectrometer and were internally referenced to residual protio solvent signal (note: CDCl₃ referenced at δ 7.27 ppm for ¹H NMR and δ 77.16 ppm for ¹³C NMR, respectively. Data for ¹H NMR are reported as follows: chemical shift (δ ppm), multiplicity (s = singlet, d = doublet, t = triplet, q = quartet,

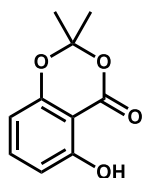
m = multiplet, app=apparent), coupling constant (Hz), and integration. Data for ^{13}C NMR are reported in terms of chemical shift and no special nomenclature is used for equivalent carbons. IR spectra were recorded on a Bruker Alpha FT-IR Spectrometer. High-resolution mass spectrometry data were recorded on an Agilent LCTOF instrument using direct injection of samples in dichloromethane into the electrospray source (ESI) with positive ionization. Gas Chromatography was carried out using a Shimadzu GC-2010 Plus instrument equipped with a Shimadzu SH-Rxi-5ms column. Column Specifications: 15 m (L), 0.25 mm (ID), 0.25 μm (df), (diphenyl/dimethyl polysiloxane) stationary phase.

3.10.2 - General Procedures:

3.10.2.1 - Procedure A: Heck redox-relay with modified Jeffery's conditions:

Tetrabutylammonium chloride (2 equiv), lithium chloride (1 equiv), lithium acetate (2.5 Equiv.), and 5 mol% palladium(II) acetate were weighed out under a dry inert nitrogen atmosphere inside a glovebox into a Schlenk vessel and capped with a septum. Outside the glovebox, to the flask was added dimethylacetamide (DMA) solvent then the alkenol (1.25 equiv) followed by the aryl triflate (1 equiv) via syringe under a positive nitrogen pressure. In cases involving a solid aryl triflate, a minimal amount of DMA was first used to dissolve the triflate. The flask was then sealed and the reaction was carried out at the indicated temperature and time. The resulting dark reaction mixture was quenched with DI water, extracted with diethyl ether (3x times), washed with brine and dried over Na_2SO_4 and concentrated *in-vacuo* to give the crude mixture

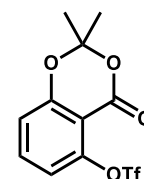
5-hydroxy-2,2-dimethyl-4H-benzo[d][1,3]dioxin-4-one (3.8):



3.8

To a round bottom flask containing 2,6-dihydroxybenzoic acid, **3.7** (8.00 g, 51.9 mmol, 1 equiv) and 4-dimethylaminopyridine (0.317 g, 2.56 mmol, 0.05 equiv) was added 35 mL of DME. The resulting solution was cooled to 0 °C before the addition of acetone (4.88 mL, 66.4 mmol, 1.28 equiv) followed by thionyl chloride (4.84 mL, 66.44, 1.28 equiv). The reaction mixture was stirred at 0°C for 1 hour and then at RT for 15 hours. The resulting red solution was neutralized using 25 mL aq. sodium bicarbonate and extracted using three 30 mL portions of diethyl ether. The combined organic layers were washed with brine, dried over MgSO₄, and volatiles removed under reduced pressure to afford a crude orange solid. Purification using silica gel chromatography with 1:4 ethyl acetate:hexanes resulted in an off-white solid (9.06 g, 46.7 mmol, 90%) consistent with previously reported spectra.^[28] **IR** (film) 3210, 3001, 1687, 1199, 1073 cm⁻¹; **¹H NMR** (300 MHz, CDCl₃) δ 10.35 (s, 1H), 7.42 (t, *J* = 8.3 Hz, 1H), 6.65 (dd, *J* = 8.5, 0.8 Hz, 1H), 6.45 (dd, *J* = 8.2, 0.8 Hz, 1H), 1.76 (s, 6H); **¹³C NMR** (176 MHz, CDCl₃) δ 165.5, 161.5, 155.7, 138.0, 110.9, 107.3, 107.2, 25.7; **HRMS** (ESI) *m/z* calcd for C₁₀H₁₁O₄ (M+H)⁺ 195.0652, found 195.0646.

2,2-dimethyl-4-oxo-4H-benzo[d][1,3]dioxin-5-yl trifluoromethanesulfonate (3.9):

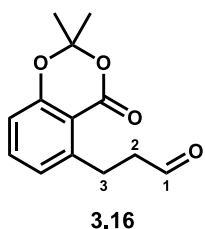


3.9

To a round bottom flask containing 5-hydroxy-2,2-dimethyl-4H-benzo[d][1,3]dioxin-4-one, **3.8** (6.10 g, 31.4 mmol, 1 equiv) was added 25 mL of dry dichloromethane. The resulting solution was cooled to 0°C before the addition of pyridine (9.12 mL, 113.2 mmol, 3.6 equiv) followed by trifluoromethanesulfonic anhydride (6.19 mL, 36.8 mmol, 1.16 equiv). The reaction mixture was stirred at 0 °C for 1 hour. The dark-orange reaction mixture was then washed

by adding 20 mL DI water and then extracted with five 15 mL portions of ethyl acetate. The combined organic layers were then washed with brine and dried over Na₂SO₄ and the solvent removed under reduced pressure affording a crude orange solid. The crude product was purified using silica gel chromatography with 300 mL of P60 silica on a 1 inch diameter column with 1:5 ethyl acetate:hexanes as eluent to yield the pure aryl triflate as a crystalline white solid (9.66 g, 30.1 mmol, 96%) consistent with previously reported spectra.^[3] **IR** (film) 3093, 2996, 2923, 2853, 1745 cm⁻¹; **¹H NMR** (400 MHz, CDCl₃) δ 7.61 (t, *J* = 8.4 Hz, 1H), 7.06 (d, *J* = 8.5 Hz, 1H), 7.00 (d, *J* = 8.3 Hz, 1H), 1.75 (s, 1H); **¹³C NMR** (175 MHz, CDCl₃) δ 157.6, 157.2, 148.7, 136.4, 118.9 (q, *J* = 321.1 Hz), 118.1, 116.7, 108.4, 107.0, 25.6; **HRMS** (ESI) *m/z* calcd for C₁₁H₉F₃O₆SNH₄ (M+NH₄)⁺ 344.0410, found 344.0413.

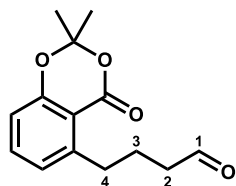
3-(2,2-dimethyl-4-oxo-4H-benzo[d][1,3]dioxin-5-yl)propanal (3.16):



Following Procedure A, aryl triflate **3.9** (0.400 g, 1.23 mmol, 1 equiv), allyl alcohol (0.101 mL, 1.47 mmol, 1.2 equiv), palladium(II) diacetate (0.013 g, 0.061 mmol, 0.05 equiv), lithium acetate (0.202 g, 3.07 mmol, 2.5 equiv), lithium chloride (0.052 g, 1.23 mmol, 1 equiv), and tetrabutylammonium chloride (0.618 g, 2.45 mmol, 2 equiv) were reacted in 15 mL DMA. The reaction was stirred for 3 hours at 50 °C and afforded a crude golden oil after workup. Purified via silica gel chromatography using a gradient elution of 15% to 30% EtOAc in hexanes. Removal of volatiles under reduced pressure gave a white solid (0.237 g, 1.19 mmol, 97%). **IR** (film) 2997, 2942, 2900, 2828, 2723, 1776, 1720 cm⁻¹; **¹H NMR** (400 MHz, CDCl₃) δ 9.81 (t, *J* = 1.4 Hz, 1H), 7.42 (t, *J* = 7.6 Hz, 1H), 6.97 (d, *J* = 7.6 Hz, 1H),

6.85 (dd, $J = 7.6, 0.9$ Hz, 1H), 3.38 (t, $J = 7.4$ Hz, 2H), 2.80 (td, $J = 7.4, 1.4$ Hz, 2H), 1.70 (s, 6H); ^{13}C NMR (100 MHz, CDCl_3) δ 201.6, 160.4, 157.4, 145.6, 135.6, 125.5, 116.1, 112.1, 105.4, 44.8, 27.3, 25.7; HRMS (ESI) m/z calcd for $\text{C}_{13}\text{H}_{15}\text{O}_4$ ($\text{M}+\text{H}$) $^+$ 235.0961, found 235.0954.

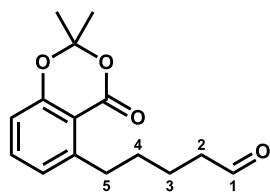
3-(2,2-dimethyl-4-oxo-4H-benzo[d][1,3]dioxin-5-yl)butanal (17):



3.12

Following Procedure A, aryl triflate **3.9** (0.300 g, 0.920 mmol, 1 equiv), 3-buten-1-ol (0.127 mL, 1.47 mmol, 1.6 equiv), palladium(II) diacetate (0.010 g, 0.046 mmol, 0.05 equiv), lithium acetate (0.157 g, 2.29 mmol, 2.5 equiv), lithium chloride (0.039 g, 0.920 mmol, 1 equiv), and tetrabutylammonium chloride (0.511 g, 1.84 mmol, 2 equiv) were reacted in 12 mL DMA. The reaction was stirred for 3 hours at 50 °C and afforded a crude pale yellow oil after workup. Purified via silica gel chromatography using a gradient elution of 10% to 30% EtOAc in hexanes Removal of volatiles under reduced pressure gave a clear oil (0.202 g, 0.801 mmol, 88%). IR (film) 2997, 2943, 2867, 2822, 2725, 1721 cm^{-1} ; ^1H NMR (400 MHz, CDCl_3) δ 9.78 (t, $J = 1.7$ Hz, 1H), 7.41 (t, $J = 8.0$ Hz, 1H), 6.92 (dd, $J = 7.6, 0.8$ Hz, 1H), 6.82 (dd, $J = 8.2, 1.2$ Hz, 1H), 3.11 (t, $J = 7.8$ Hz, 2H), 2.52 (td, $J = 7.3, 1.7$ Hz, 2H), 1.95 (p, $J = 7.6$ Hz, 2H), 1.69 (s, 6H); ^{13}C NMR (100 MHz, CDCl_3) δ 202.6, 160.34, 157.3, 146.8, 135.5, 125.3, 115.8, 112.1, 105.3, 77.5, 77.1, 76.8, 43.7, 33.7, 25.7, 23.6. HRMS (ESI) m/z calcd for $\text{C}_{14}\text{H}_{16}\text{O}_4\text{Na}$ ($\text{M}+\text{Na}$) $^+$ 271.0941, found 271.0946.

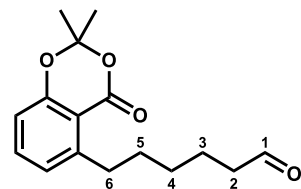
3-(2,2-dimethyl-4-oxo-4H-benzo[d][1,3]dioxin-5-yl)pentanal (3.18):



3.18

Following Procedure A, aryl triflate **3.9** (0.489 g, 1.50 mmol, 1 equiv), 4-penten-1-ol (0.170 mL, 1.65 mmol, 1.2 equiv), palladium(II) diacetate (0.016 g, 0.075 mmol, 0.05 equiv), lithium acetate (0.247 g, 3.75 mmol, 2.5 equiv), lithium chloride (0.064 g, 1.50 mmol, 1 equiv), and tetrabutylammonium chloride (0.834 g, 3.00 mmol, 2 equiv) were reacted in 16 mL DMA. The reaction was stirred for 3 hours at 50 °C and afforded a crude pale yellow oil after workup. Purified via silica gel chromatography using a gradient elution of 10% to 35% EtOAc in hexanes. Removal of volatiles under reduced pressure gave a clear oil (0.384 g, 1.46 mmol, 97%). **IR** (film) 2997, 2938, 2859, 1731, 1706 cm^{-1} ; **$^1\text{H NMR}$** (400 MHz, CDCl_3) δ 9.76 (t, $J = 1.6$ Hz, 1H), 7.39 (t, $J = 8.0$ Hz, 1H), 6.91 (d, $J = 7.6$ Hz, 1H), 6.80 (d, $J = 8.0$ Hz, 1H), 3.08 (app t, $J = 7.6$ Hz, 2H), 2.48 (td, $J = 7.2$, 1.6 Hz, 2H), 1.77 – 1.58 (m, 10H); **$^{13}\text{C NMR}$** (101 MHz, CDCl_3) δ 202.8, 160.4, 157.3, 147.6, 135.3, 125.2, 115.5, 112.1, 105.2, 77.5, 77.2, 76.8, 43.7, 34.2, 30.6, 22.0; **HRMS** (ESI) m/z calcd for $\text{C}_{15}\text{H}_{18}\text{O}_4$ (M)⁺ 262.1205, found 262.1214;

3-(2,2-dimethyl-4-oxo-4H-benzo[d][1,3]dioxin-5-yl)hexanal (3.19):

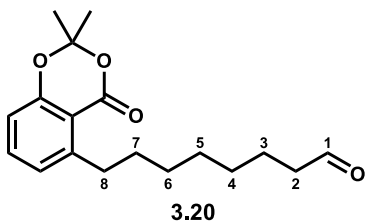


3.19

Following Procedure A, aryl triflate **3.9** (0.200 g, 0.613 mmol, 1 equiv), 5-hexen-1-ol (0.092 mL, 0.766 mmol, 1.2 equiv), palladium(II) diacetate (0.007 g, 0.031 mmol, 0.05 equiv), 0.101 g lithium acetate (1.53 mmol, 2.5 equiv), 0.026 g lithium chloride (0.613 mmol, 1 equiv), and tetrabutylammonium chloride (0.341 g, 1.23 mmol, 2 equiv) were reacted in 8 mL DMA. The reaction was stirred for 3 hours at 50 °C and afforded a crude clear oil after workup. Purified via silica gel chromatography using a gradient elution

of 10% to 35% EtOAc in hexanes. Removal of volatiles under reduced pressure gave a clear oil (0.384 g, 1.46 mmol, 97%). **IR** (film) 2998, 2934, 2858, 2719, 1730 cm^{-1} ; **^1H NMR** (400 MHz, CDCl_3) δ 9.77 (t, $J = 1.8$ Hz, 1H), 7.41 (t, $J = 8.0$ Hz, 1H), 6.92 (dd, $J = 8.0, 1.0$ Hz, 1H), 6.82 (dd, $J = 8.2, 1.2$ Hz, 1H), 3.09 (app t, $J = 7.8$ Hz, 2H), 2.45 (td, $J = 7.4, 1.8$ Hz, 2H), 1.71 (s, 6H), 1.69 – 1.58 (m, 4H), 1.50 – 1.40 (m, 2H); **^{13}C NMR** (100 MHz, CDCl_3) δ 203.0, 160.4, 157.3, 148.1, 135.3, 125.25, 115.4, 112.16, 105.16, 43.9, 34.3, 30.9, 29.2, 25.8, 21.9.; **HRMS** (ESI) m/z calcd for $\text{C}_{16}\text{H}_{20}\text{O}_4\text{Na}$ ($\text{M}+\text{Na}$) $^+$ 299.1254, found 299.1258.

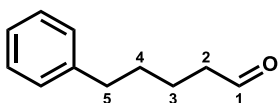
3-(2,2-dimethyl-4-oxo-4H-benzo[d][1,3]dioxin-5-yl)octanal (3.20):



Following Procedure A, aryl triflate **3.9** (0.050 g, 0.153 mmol, 1 equiv), 7-octen-1-ol (0.029 mL, 0.192 mmol, 1.2 equiv), palladium(II) diacetate (0.002 g, 0.008 mmol, 0.05 equiv), lithium acetate (0.025 g, 0.383 mmol, 2.5 equiv), lithium chloride (0.007 g, 0.153 mmol, 1 equiv), and tetrabutylammonium chloride (0.085 g, 0.307 mmol, 2 equiv) were reacted in 3 mL DMA. The reaction was stirred for 3 hours at 70 °C and afforded a crude clear oil after workup. Purified via silica gel chromatography using a gradient elution of 15% to 25% EtOAc in hexanes. Removal of volatiles under reduced pressure gave a clear oil (0.029 g, 0.104 mmol, 68%). **IR** (film) 2995, 2937, 2862, 2825, 1720 cm^{-1} ; **^1H NMR** (400 MHz, CDCl_3) δ 9.77 (t, $J = 1.8$ Hz, 1H), 7.40 (t, $J = 7.9$ Hz, 1H), 6.93 (d, $J = 7.6$ Hz, 1H), 6.81 (dd, $J = 8.2, 0.8$ Hz, 1H), 3.11 – 3.06 (m, 2H), 2.42 (td, $J = 7.4, 1.9$ Hz, 2H), 1.70 (s, 6H), 1.68 – 1.57 (m, 4H), 1.45 – 1.29 (m, 6H); **^{13}C NMR** (100 MHz, CDCl_3) δ 203.0, 160.3, 157.1, 148.4, 135.1, 125.1, 115.1, 112.1, 105.0, 43.9,

34.3, 31.1, 29.4, 29.1, 29.1, 25.7, 22.1; **HRMS** (ESI) m/z calcd for $C_{18}H_{25}O_4$ ($M+H$)⁺ 305.1747, found 305.1748.

phenylpentanal (3.23):

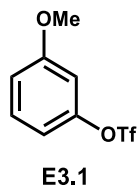


Following Procedure A, aryl triflate (**E.3.2**) (0.222 g, 0.98 mmol, 1 equiv), 4-penten-1-ol (0.177 mL, 1.72 mmol, 1.75 equiv), palladium(II) diacetate (0.022 g, 0.098 mmol, 0.1 equiv), lithium acetate (0.162 g, 2.45 mmol, 2.5 equiv), lithium chloride (0.416 g, 0.98 mmol, 1 equiv), and tetrabutylammonium chloride (0.544 g, 1.96 mmol, 2 equiv) were reacted in 8 mL DMA. The reaction was stirred for 3 hours at 70 °C and afforded a crude clear oil after workup. Purified via silica gel chromatography using a gradient elution of 15% to 35% EtOAc in hexanes. Removal of volatiles under reduced pressure gave a mixture of linear and branched isomers (L:B=87:13 determined by ¹HNMR) as a clear oil (0.116 g, 0.68 mmol, 73%) consistent with previously reported spectra.^[29] **HRMS** (ESI) m/z calcd for $C_{11}H_{14}O$ (M^+) 162.1039, found 162.1025.

As above, using phenyl iodide (0.200 g, 0.98 mmol, 1 equiv.) gave linear and branched isomers (L:B=83:17 determined by ¹HNMR) as a clear oil (0.098 g, 0.61 mmol, 62%).

As above, using bromobenzene (0.154 g, 0.98 mmol, 1 equiv.) gave linear and branched isomers (L:B=83:17 determined by ¹HNMR) as a clear oil (0.110 g, 0.68 mmol, 69%).

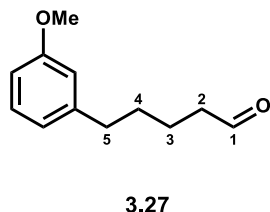
3-Methoxyphenyl trifluoromethanesulfonate (**E3.1**):



To a round bottom flask containing 3-methoxyphenol, (3.00 g, 24.17mmol, 1 equiv) was added 20 mL of dry dichloromethane. The resulting solution was cooled to 0°C before the addition of pyridine (7.01mL, 87.02 mmol, 3.6 equiv) followed by trifluoromethanesulfonic anhydride (6.19 mL, 28.31 mmol, 1.16 equiv). The reaction mixture was stirred at 0 °C for 1 hour. The dark-yellow reaction mixture was then washed by adding 20 mL DI water and then extracted with ethyl acetate (5x 15 mL). The combined organic layers were then washed with brine and dried over Na₂SO₄ and the solvent removed under reduced pressure affording a crude yellow liquid. The crude product was purified using silica gel chromatography using a gradient elution of 30% to 50% EtOAc in hexanes. Removal of volatiles under reduced pressure gave a pale-yellow liquid (4.13 g, 15.96 mmol, 66%). NMR spectra are consistent with those previously reported.^[30]

¹H NMR (400 MHz, CDCl₃) δ 7.35 (t, *J* = 8.3 Hz, 1H), 6.94 (dd, *J* = 8.4, 2.3 Hz, 1H), 6.88 (dd, *J* = 8.2, 2.2 Hz, 1H), 6.81 (t, *J* = 2.3 Hz, 1H), 3.84 (s, 3H). **¹³C NMR** (100 MHz, CDCl₃) δ 161.0, 150.4, 130.7, 168.8 (q, *J*=319.0 Hz), 114.3, 113.4, 107.6, 55.8.

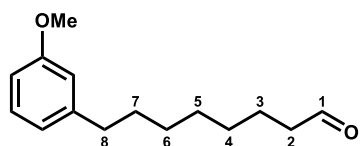
5-(3-methoxyphenyl)pentanal (**3.27**):



Following Procedure A, aryl triflate **E3.1** (0.200 g, 0.781 mmol, 1 equiv), 4-penten-1-ol (0.118 mL, 1.37 mmol, 1.75 equiv), palladium(II) diacetate (0.018 g, 0.078 mmol, 0.1 equiv), lithium acetate (0.129 g, 1.95 mmol, 2.5 equiv), lithium chloride (0.033 g, 0.781 mmol, 1 equiv), and tetrabutylammonium chloride (0.433 g, 1.56 mmol, 2 equiv) were reacted in 8 mL DMA. The reaction was stirred for 3 hours at 70 °C and afforded a crude clear oil after workup. Purified via silica gel chromatography using a gradient elution of 15% to 35%

EtOAc in hexanes. Removal of volatiles under reduced pressure gave a mixture of linear and branched isomers (L:B=87:13 determined by HNMR) as clear oil (0.094 g, 0.500 mmol, 64%). **IR** (film) 2999, 2936, 2859, 2835, 2723, 1720 cm^{-1} ; **$^1\text{H NMR}$** (400 MHz, CDCl_3) δ 9.78 (t, $J = 1.8$ Hz, 1H), 7.22 (td, $J = 7.5, 1.0$ Hz, 1H), 6.81 – 6.73 (m, 3H), 3.82 (s, 3H), 2.67 – 2.61 (m, 2H), 2.50 – 2.44 (m, 2H), 1.74 – 1.65 (m, 4H); **$^{13}\text{C NMR}$** (100 MHz, CDCl_3) δ 202.6, 159.66, 143.6, 129.3, 120.8, 114.2, 111.1, 55.2, 43.7, 35.7, 30.7, 21.7. **HRMS** (ESI) m/z calcd for $\text{C}_{12}\text{H}_{17}\text{O}_2$ ($\text{M}+\text{H}$) $^+$ 193.1223, found 193.1221.

5-(3-methoxyphenyl)octanal (3.28):

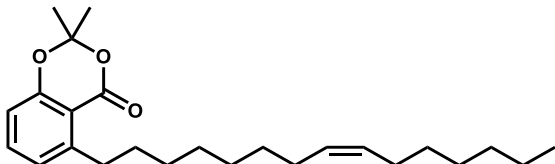


3.28

Following Procedure A, aryl triflate e3.1 (0.200 g, 0.781 mmol, 1 equiv), 4-octen-1-ol (0.206 mL, 1.37 mmol, 1.75 equiv), palladium(II) diacetate (0.018 g, 0.078 mmol, 0.1 equiv), lithium acetate (0.129 g, 1.95 mmol, 2.5 equiv), lithium chloride (0.033 g, 0.781 mmol, 1 equiv), and tetrabutylammonium chloride (0.433 g, 1.56 mmol, 2 equiv) were reacted in 8 mL DMA. The reaction was stirred for 3 hours at 70 °C and afforded a crude clear oil after workup. Purified via silica gel chromatography using a gradient elution of 15% to 35% EtOAc in hexanes. Removal of volatiles under reduced pressure gave a mixture of linear and branched isomers (L:B=82:18 determined by HNMR) as a clear oil (0.094 g, 0.500 mmol, 64%). **IR** (film) 2998, 2928, 2854, 2721, 1722 cm^{-1} ; **$^1\text{H NMR}$** (400 MHz, CDCl_3) δ 9.77 (t, $J = 1.9$ Hz, 1H), 7.22 – 7.17 (m, 1H), 6.81 – 6.71 (m, 3H), 3.81 (s, 3H), 2.62 – 2.56 (m, 2H), 2.42 (td, $J = 7.4, 1.9$ Hz, 2H), 1.68 – 1.57 (m, 4H), 1.39 – 1.30 (m, 6H); **$^{13}\text{C NMR}$** (100 MHz, CDCl_3) δ 203.0, 159.7, 144.6 129.3, 121.0, 114.3, 111.0,

77.5, 77.2, 76.8, 55.3, 44.0, 36.1, 31.4, 29.3, 29.2, 22.2. **HRMS** (ESI) m/z calcd for $C_{15}H_{23}O_2$ (M+H)⁺ 235.1698, found 235.1699.

(Z)-2,2-dimethyl-5-(pentadec-8-en-1-yl)-4H-benzo[d][1,3]dioxin-4-one (E3.29):



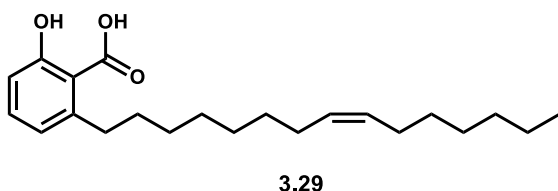
E3.29

To a round bottom flask containing heptylphosphonium bromide (1.16 g, 2.62 mmol, 4 equiv) was added 15 mL of THF and cooled to 0 °C. A 1.6 M solution of n-butyl

lithium in hexanes (1.54 mL, 2.62 mmol, 3.1 equiv) was then added dropwise. The reaction mixture was allowed to stir for 1 hour at 0 °C before being cooled to -78 °C. Aldehyde **(3.20)** (0.200 g, 0.657 mmol, 1 equiv) was cooled to -78 °C in 5 mL of THF and added to reaction mixture over 2 minutes. The reaction was then allowed to warm to RT and was allowed to stir for 1 hour. The reaction was quenched using 3 M HCl until acidic by pH paper (pH≈2). The reaction mixture was then extracted with ethyl acetate (3x), washed with brine, and dried over magnesium sulfate. The volatiles were removed under reduced pressure to give a crude pale yellow oil. The crude was purified via silica gel chromatography using a gradient elution of 10% to 20% EtOAc in hexanes. Removal of solvent under reduced pressure afforded a clear oil (0.240 g, 0.616 mmol, 94%) as an unresolvable mixture of *E:Z* isomers (*E:Z* = 4:96 based on GC analysis and comparison of the corresponding *cis* and *trans* epoxide products by ¹HNMR). **IR** (film) 3001, 2923, 2853, 1737 cm⁻¹; **¹H NMR** (400 MHz, CDCl₃) δ 7.40 (t, *J* = 7.9 Hz, 1H), 6.93 (d, *J* = 7.7 Hz, 1H), 6.80 (d, *J* = 7.4 Hz, 1H), 5.40 – 5.31 (m, 2H), 3.09 (dt, 2H), 2.06 – 1.96 (m, 4H), 1.70 (s, 6H), 1.64 – 1.57 (m, 2H), 1.43 – 1.24 (m, 19H), 0.89 (t, *J* = 6.8 Hz, 3H). **¹³C NMR** (100

MHz, CDCl₃) δ 160.4, 157.3, 148.6, 135.2, 130.0, 125.2, 115.2, 112.2, 105.1, 34.5, 31.9, 31.3, 29.9, 29.7, 29.4, 29.5, 29.1, 27.4, 25.9, 22.8, 14.2.; **HRMS** (ESI) m/z calcd for C₂₅H₃₉O₃ (M+H)⁺ 387.2894, found 387.2903.

(Z)-2-hydroxy-6-(pentadec-8-en-1-yl)benzoic acid (3.29):

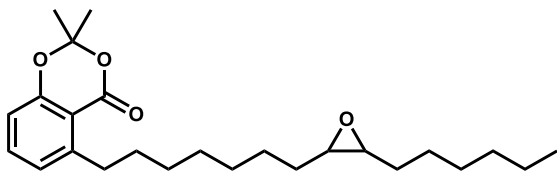


(Z)-2,2-dimethyl-5-(pentadec-8-en-1-yl)-
4H-benzo[d][1,3]dioxin-4-one (**E3.29**)

(0.078 g, 0.201 mmol) was dissolved in 2

mL of 1,4-Dioxane. To this mixture was added 2 mL 6 M Aq KOH. The resulting heterogeneous mixture was then stirred rapidly at 55 °C for 24 hours until TLC of the organic layer showed complete acetonide deprotection. The reaction mixture was then acidified (pH ~2.00) using 3 M HCl and extracted using EtOAc. The combined organic layers were washed with brine and dried over sodium sulfate. The volatiles were removed under vacuum resulting in a crude yellow oil. The crude was purified via silica gel chromatography using an isocratic elution of 2% MeOH and 0.2% AcOH in DCM to afford a waxy off white solid (0.052 g, 0.150 mmol, 75%) as an unresolvable mixture of *E:Z* isomers (*E:Z* = 4:96 based on the initial starting material). **IR** (film) 3003,2922, 2852, 1645, 1606 cm⁻¹; **¹H NMR** (400 MHz, CDCl₃) δ 11.06 (s, 1H), 7.36 (t, J = 7.9 Hz, 1H), 6.87 (d, J = 8.3 Hz, 1H), 6.78 (d, J = 7.5 Hz, 1H), 5.42 – 5.31 (m, 2H), 3.01 – 2.93 (m, 2H), 2.07 – 1.95 (m, 4H), 1.59 (d, J = 7.4 Hz, 2H), 1.30 (dd, J = 9.2, 7.6 Hz, 16H), 0.89 (t, J = 6.9 Hz, 3H); **¹³C NMR** (100 MHz, CDCl₃) δ 175.6, 163.7, 147.7, 135.4, 130.0, 129.9, 122.8, 115.9, 110.4, 36.5, 32.6, 32.0, 31.8, 29.8, 29.4, 29.3, 29.0, 27.2, 27.2, 22.7, 14.1; **HRMS** (ESI) m/z calcd for C₂₂H₃₅O₃ (M+H)⁺ 347.2581, found 347.2591.

5-(7-((2R,3S)-3-hexyloxiran-2-yl)heptyl)-2,2-dimethyl-4H-benzo[d][1,3]dioxin-4-one
(±) (**E3.29a**):

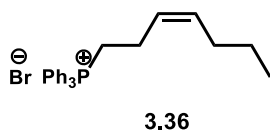


E3.29a

To a round bottom flask containing (Z)
2,2dimethyl-5-(pentadec-8-en-1-yl)-4H-
benzo[d][1,3]dioxin-4-one (**3.29**) (0.112 g,
0.292 mmol, 1 equiv) was added 4 mL DCM

and then cooled the reaction to 0 °C. An additional 2 mL was then used to dissolve of commercial 3-Chloroperoxybenzoic acid (77% by wt., 0.295 g, 1.31 mmol, 4.5 equiv) before adding to the cooled reaction mixture. The reaction was allowed warm to room temperature and was then stirred overnight. The reaction was quenched with a solution of saturated sodium thiosulfate and then extracted with DCM. The organic layers were then washed with brine and dried over magnesium sulfate. The solvent was removed under vacuum leaving a crude white solid. The crude solid was purified via silica gel chromatography using a gradient elution of 10% to 30% EtOAc in hexanes to afford a clear oil (0.089 g, 0.221 mmol, 76%, *trans:cis* = 4:96). **IR** (film) 2925, 2855, 1736 cm^{-1} ; **^1H NMR** (700 MHz, CDCl_3) Both Isomers: δ 7.39 (t, $J = 7.9$ Hz, 1H), 6.93 (d, $J = 7.6$ Hz, 1H), 6.80 (d, $J = 8.1$ Hz, 1H), 3.12 – 3.05 (m, 2H), 1.70 (s, $J = 9.2$ Hz, 6H), 1.63 – 1.57 (m, 2H), 1.51 – 1.48 (m, 4H), 1.45 – 1.26 (m, 16H), 0.89 (t, $J = 7.0$ Hz, 3H); *cis*-isomer: 2.92 – 2.87 (m, 2H); *trans*-isomer: 2.65 (t, $J = 5.0$ Hz, 2H); **^{13}C NMR** (175 MHz, CDCl_3) δ 160.4, 157.3, 148.6, 135.2, 125.2, 115.2, 112.2, 105.1, 57.4, 34.5, 31.9, 31.3, 29.7, 29.6, 29.5, 29.4, 28.0, 26.7, 25.8, 22.7 14.2; **HRMS** (ESI) m/z calcd for $\text{C}_{25}\text{H}_{39}\text{O}_4$ ($\text{M}+\text{H}$)⁺ 403.2843, found 403.2833.

3(Z)-hepten-1-yltriphenylphosphonium bromide (3.36):



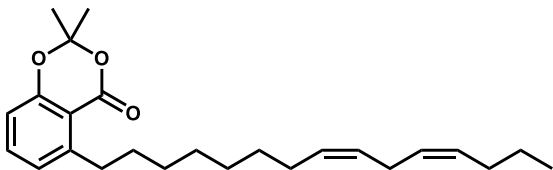
Synthesized in three steps from commercial of 3(Z)-hepten-1-ol. To a stirring solution of of 3(Z)-hepten-1-ol **3.34** , 23 (2.35 mL, 17.5 mmol, 1 equiv) and triethylamine (2.93 mL, 21.01 mmol, 1.2 equiv) in 50 mL of DCM at 0 °C, was added methanesulfonyl chloride (1.62 mL, 21.01 mmol, 1.2 equiv). The reaction was stirred at 0 °C for 3 hours and was then washed with 50 mL DI water, 20 mL 2 M HCl, saturated sodium bicarbonate, and brine. The organic layers were dried over sodium sulfate and the volatiles removed under vacuum resulting in a colorless liquid. The crude mesylate was used in the next step without further purification.

To the 3(Z)-heptenyl-1-mesylate (3.35 g, 17.5 mmol, 1 equiv) was added lithium bromide (5.30 g, 66.25 mmol, 3.7 equiv) and 35 mL of THF. The reaction mixture was stirred at 60 °C for 3 hours and overnight at RT. The reaction mixture was extracted with DCM and washed with brine. After drying with sodium sulfate the solvent was removed under reduced pressure to yield a crude yellow oil (2.62 g, 14.79 mmol). This crude bromide **3.35** was used in the subsequent step without further purification.

The above crude bromide, **3.35** (2.62 g, 14.79 mmol, 1.0 equiv) and triphenylphosphine (4.65 g, 17.75 mmol, 1.2 equiv) were stirred in 40 mL of acetonitrile at 80 °C for 36 hours. The solvent was removed under vacuum and the resulting sticky oil was triturated with ether and then hexanes to afford a crude off-white solid. Removal of the solvent gave a white solid (5.050 g, 11.39 mmol, 77%) with a 65% overall yield for the whole sequence. ¹H and ¹³C NMR are consistent with previously reported spectra.^[31] Before use, the solid

phosphonium bromide product was purified using chromatography with 10% MeOH in DCM.

2,2-dimethyl-5-((8Z,11Z)-pentadeca-8,11-dien-1-yl)-4H-benzo[d][1,3]dioxin-4-one (E3.39):



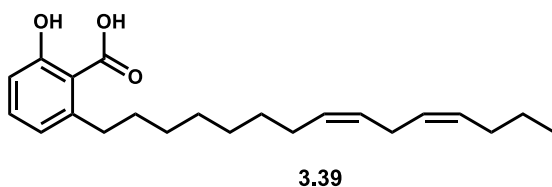
E3.39

To a flask containing Phosphonium salt (**3.36**) (0.433 g, 0.985 mmol, 4 equiv) was added 8 mL of THF and cooled to 0 °C. A 1.6 M solution of *n*-butyl lithium in hexanes (0.477

mL, 0.764 mmol, 3.1 equiv) was then added dropwise. The reaction mixture was allowed to stir for 1 hour at 0 °C before being cooled to -78 °C. Aldehyde (**3.20**) (0.075 g, 0.246 mmol, 1 equiv) was cooled to -78 °C in 2 mL of THF and added to reaction mixture over 2 minutes. The reaction was then allowed to warm to RT and was allowed to stir for 1 hour. The reaction was quenched using 3 M HCl until acidic by pH paper (pH≈2). The reaction mixture was then extracted with 3 portions of ethyl acetate, washed with brine, and dried over magnesium sulfate. The volatiles were removed under reduced pressure to give a crude pale yellow oil. The crude was purified via silica gel chromatography using a gradient elution of 10% to 20% EtOAc in hexanes. Removal of solvent under reduced pressure afforded a clear oil (0.092 g, 0.236 mmol, 96%) as an unresolvable mixture of *E* and *Z* stereoisomers (*E*:*Z* = 10:90) determined via gas chromatography. **IR** (film) 3007, 2926, 2854, 1737 cm⁻¹; **¹H NMR** (400 MHz, CDCl₃) δ 7.40 (t, *J* = 7.9 Hz, 1H), 6.93 (d, *J* = 7.6 Hz, 1H), 6.80 (dd, *J* = 8.2, 0.9 Hz, 1H), 5.42 – 5.29 (m, 4H), 3.12 – 3.05 (m, 2H), 2.78 (t, *J* = 6.2 Hz, 2H), 2.04 (dt, *J* = 6.5, 5.0 Hz, 4H), 1.70 (s, 6H), 1.64 – 1.57 (m, 2H), 1.40 – 1.26 (m, 10H), 0.92 (t, *J* = 7.4 Hz, 3H).; **¹³C NMR** (100 MHz, CDCl₃) δ 160.4,

157.3, 148.7, 135.3, 130.4, 130.1, 128.4, 128.2, 125.3, 115.3, 112.3, 105.1, 34.6, 31.4, 29.9, 29.6, 29.5, 27.4, 25.9, 23.0, 14.0; **HRMS** (ESI) m/z calcd for $C_{25}H_{37}O_3$ (M+H)⁺ 385.2737, found 385.2739.

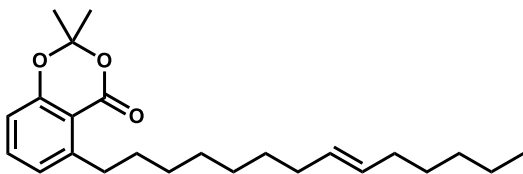
2-hydroxy-6-((8Z,11Z)-pentadeca-8,11-dien-1-yl)benzoic acid (3.39):



2,2-dimethyl-5-((8Z,11Z)-pentadeca-8,11-dien-1-yl)-4H-benzo[d][1,3]dioxin-4-one
(E3.39) (0.0917 g, 0.236 mmol) was

dissolved in 2 mL of 1,4-Dioxane. To this mixture was added 2.2 mL 6 M Aq KOH. The resulting heterogeneous mixture was then stirred rapidly at 55 °C for 18 hours until TLC of the organic layer showed complete acetonide deprotection. The reaction mixture was then acidified (pH ~2.00) using 3 M HCl and extracted using EtOAc. The combined organic layers were washed with brine and dried over sodium sulfate. The volatiles were removed under vacuum resulting in a crude yellow oil. The crude was purified via silica gel chromatography using an isocratic elution of 2% MeOH and 0.2% AcOH in DCM to afford a clear oil (0.070 g, 0.202 mmol, 86%) as an unresolvable mixture of *E:Z* isomers (*E:Z* = 10:90 based on starting material). **IR** (film) 3202, 3008, 2924, 2853, 1643, 1607 cm^{-1} ; **¹H NMR** (400 MHz, $CDCl_3$) δ 11.00 (s, 1H), 7.38 (t, J = 8.0 Hz, 1H), 6.88 (dd, J = 8.3, 0.9 Hz, 1H), 6.79 (d, J = 8.3 Hz, 1H), 5.53 – 5.20 (m, 4H), 2.99 (app t, 2H), 2.78 (t, J = 6.2 Hz, 2H), 2.12 – 1.94 (m, 4H), 1.69 – 1.56 (m, 2H), 1.45 – 1.26 (m, 10H), 0.91 (t, J = 7.4 Hz, 3H); **¹³C NMR** (100 MHz, $CDCl_3$) δ 176.1, 163.8, 147.9, 135.6, 130.3, 130.1, 128.3, 128.2, 122.9, 116.1, 110.5, 36.6, 32.1, 29.9, 29.8, 29.5, 29.4, 29.4, 27.4, 25.8, 22.9, 13.9; **HRMS** (ESI) m/z calcd for $C_{22}H_{33}O_3$ (M+H)⁺ 345.2424, found 345.2440.

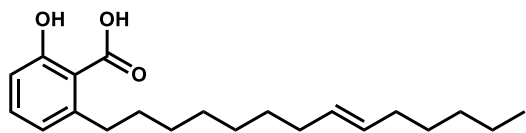
(E)-2,2-dimethyl-5-(tetradec-8-en-1-yl)-4H-benzo[d][1,3]dioxin-4-one (E3.41):



E3.41

To a round bottom flask containing hexylsulphonyl tetrazole, **3.40** (0.050 g, 0.169 mmol, 1 equiv), was added 2mL of DME and the reaction cooled to - 55 °C using a EtOH/Water/dry ice bath. To the cooled mixture was added a solution of 0.475 M potassium hexamethyldisilazide in toluene (0.447 mL, 0.212 mmol, 1.25 equiv) dropwise over three minutes and the reaction mixture was stirred for 1 hour at -55 °C. Aldehyde **3.20** (0.103 g 0.339 mmol, 2 equiv) was dissolved in 1 mL of DME and cooled to -55 °C. This cooled solution was then added dropwise to the reaction mixture. The reaction was stirred for 1 hour at -55 °C the allowed to stir at room temperature overnight. The reaction was quenched using 0.5 mL DI water followed by 20 drops of 2 M HCl. The mixture was then extracted with EtOAc (3x), washed with water then brine, and dried over MgSO₄. The volatiles were then removed to give a crude white solid. The crude solid was purified via silica gel chromatography using a gradient elution of 10% to 20% EtOAc in hexanes to afford a clear oil (0.043 g, 0.111 mmol, 66%) as a 96:4 mixture of *E/Z* isomers based on GC analysis and comparison of the corresponding epoxide products. **IR** (film) 2988, 2923, 2853, 1737 cm⁻¹; **¹H NMR** (700 MHz, CDCl₃) δ 7.38 (t, *J* = 7.9 Hz, 1H), 6.92 (d, *J* = 7.6 Hz, 1H), 6.79 (d, *J* = 8.1 Hz, 1H), 5.42 – 5.33 (m, 2H), 3.11 – 3.06 (m, 2H), 1.98 – 1.89 (m, 4H), 1.69 (s, 6H), 1.58 (qnt, *J* = 15.4, 7.6 Hz, 2H), 1.38 – 1.25 (m, 14H), 0.88 (t, *J* = 7.1 Hz, 3H); **¹³C NMR** (175 MHz, CDCl₃) δ 160.2, 157.2, 148.5, 135.0, 130.3, 130.4, 125.1, 115.1, 112.2, 104.9, 34.4, 32.6, 31.4, 31.2, 29.7 (s), 29.4, 29.1, 25.7, 22.5, 14.1.; **HRMS** (ESI) *m/z* calcd for C₂₄H₃₆O₃ (M+H)⁺ 373.2737, found 373.2727.

(E)-2-hydroxy-6-(tetradec-8-en-1-yl)benzoic acid (3.41):



3.41

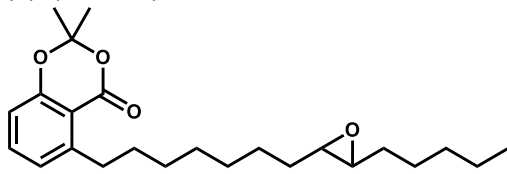
(E)-2,2-dimethyl-5-(tetradec-8-en-1-yl)-4H-

benzo[d][1,3]dioxin-4-one (**E3.41**) (0.056 g,

0.152 mmol) was dissolved in 2 mL of 1,4-

Dioxane. To this mixture was added 1.6 mL 6 M Aq KOH. The resulting heterogeneous mixture was then stirred rapidly at 55 °C for 20 hours until TLC of the organic layer showed complete acetonide deprotection. The reaction mixture was then acidified (pH ~2.00) using 3 M HCl and extracted using EtOAc. The combined organic layers were washed with brine and dried over sodium sulfate. The volatiles were removed under vacuum resulting in a crude yellow oil. The crude was purified via silica gel chromatography using an isocratic elution of 2% MeOH and 0.2% AcOH in DCM to afford a waxy white solid (0.048 g, 0.144 mmol, 95%) as a 96:4 mixture of *E/Z* isomers based on GC analysis of the starting material. **IR** (film) 3107, 29322, 2852, 1644, 1606 cm^{-1} ; **¹H NMR** (400 MHz, CDCl_3) δ 11.06 (s, 1H), 7.36 (t, $J = 7.9$ Hz, 1H), 6.87 (d, $J = 8.3$ Hz, 1H), 6.78 (d, $J = 7.1$ Hz, 1H), 5.39 (t, $J = 3.6$ Hz, 2H), 3.02 – 2.92 (m, 2H), 2.01 – 1.90 (m, 4H), 1.65 – 1.54 (m, 2H), 1.40 – 1.25 (m, 14H), 0.89 (t, $J = 6.9$ Hz, 3H); **¹³C NMR** (100 MHz, CDCl_3) δ 176.3, 163.8, 148.0, 135.6, 130.6, 130.4, 122.9, 116.0, 110.6, 53.6, 36.6, 32.7, 32.1, 31.6, 29.9, 29.8, 29.5, 29.3, 22.7, 14.2. **HRMS** (ESI) m/z calcd for $\text{C}_{21}\text{H}_{33}\text{O}_3$ (M+H)⁺ 333.2424, found 333.2416.

5-(7-((2R,3R)-3-hexyloxiran-2-yl)heptyl)-2,2-dimethyl-4H-benzo[d][1,3]dioxin-4-one
(±) (**E3.41a**):



E3.41a

To a round bottom flask containing (*E*)-2,2-dimethyl-5-(tetradec-8-en-1-yl)-4H-benzo[d][1,3]dioxin-4-one (**3.41**) (0.026 g, 0.065 mmol, 1 equiv) was added 2 mL DCM and

then cooled the reaction to 0 °C. An additional 2 mL was then used to dissolve of commercial 3-Chloroperoxybenzoic acid (77% by wt., 0.0652 g, 0.293 mmol, 4.5 equiv) before adding to the cooled reaction mixture. The reaction was allowed warm to room temperature and was then stirred overnight. The reaction was quenched with a solution of sat'd aq sodium thiosulfate and then extracted with DCM. The organic layers were then washed with brine and dried over magnesium sulfate. The solvent was removed under vacuum leaving a crude white solid. The crude solid was purified via silica gel chromatography using a gradient elution of 10% to 30% EtOAc in hexanes to afford a clear oil (0.023 g, 0.055 mmol, 86%) as a 4:96 mixture of *cis* and *trans* epoxides based GC (*cis* isomer: area=194,506 at 18.336 min; *trans* isomer: area= 3,420,802 at 21.743 min) and integration of the relevant ¹H NMR signals. **IR** (film) 2927, 2856, 1767, 1738 cm⁻¹; **¹H NMR** (400 MHz, CDCl₃) Both Isomers: δ 7.39 (t, *J* = 7.6 Hz, 1H), 6.92 (dd, *J* = 7.6, 0.8 Hz, 1H), 6.80 (dd, *J* = 8.2, 1.1 Hz, 1H), 3.08 (t, *J* = 7.6 Hz, 2H), 1.70 (s, *J* = 4.7 Hz, 6H), 1.62 – 1.24 (m, 20H), 0.92 – 0.86 (m, 3H). *cis*-isomer: 2.91 – 2.88 (m, 2H) *trans*-isomer: 2.68 – 2.61 (m, 2H); **¹³C NMR** (100 MHz, CDCl₃) δ 160.4, 157.3, 148.6, 135.2, 125.2, 115.2, 112.2, 105.1, 59.0, 34.5, 32.2, 31.8, 31.3, 29.7, 29.5, 29.5, 26.2, 25.9, 25.8, 22.7, 14.1; **HRMS** (ESI) *m/z* calcd for C₂₄H₃₆O₄ (M)⁺ 389.2686, found 389.2688.

3.11 - References

- (1) Hadfield, A.; Schweitzer, H.; Trova, M. P.; Green, K. Practical, Large-Scale Synthesis of 2,2-Dimethyl-5-Hydroxy-4-Oxo-Benzo-1,4-Dioxin. *Synth. Commun.* **1994**, *24*, 1025–1028.
- (2) Fürstner, A.; Konetzki, I. Synthesis of 2-Hydroxy-6-{{(16R)- β - δ -Mannopyransyloxy}Heptadecyl}benzoic Acid, a Fungal Metabolite with GABAA Ion Channel Receptor Inhibiting Properties. *Tetrahedron* **1996**, *52*, 15071–15078.
- (3) Fürstner, A.; Thiel, O. R.; Blanda, G. Asymmetric Synthesis of the Fully Functional Macrolide Core of Salicylihalamide: Remote Control of Olefin Geometry during RCM. *Org. Lett.* **2000**, *2*, 3731–3734.
- (4) Molander, G. A.; Dehmel, F. Formal Total Synthesis of Oximidine II via a Suzuki-Type Cross-Coupling Macrocyclization Employing Potassium Organotrifluoroborates. *J. Am. Chem. Soc.* **2004**, *126*, 10313–10318.
- (5) Nicolaou, K. C.; Kim, D. W.; Baati, R. Stereocontrolled Total Synthesis of Apicularen A and Its Δ 17,18 Z Isomer. *Angew. Chem. Int. Ed.* **2002**, *41*, 3701–3704.
- (6) Clemens, R. T.; Jennings, M. P. An Efficient Total Synthesis and Absolute Configuration Determination of Varitriol. *Chem. Commun.* **2006**, No. 25, 2720–2721.
- (7) Boivin, R.; Campagna, S. a; Du, H.; Fang, F. G.; Horstmann, T.; Lemelin, C.-A.; Li, J.; McGuinness, P.; Niu, X.; Schnaderbeck, M. J.; Wu, K. K.-M.; Zhu, X. J. Intermediates and Methods for Making Zearalenone Macrolide Analogs. WO2009075818 (A1).
- (8) Xu, J.; Ong, E. H. Q.; Hill, J.; Chen, A.; Chai, C. L. L. Design, Synthesis and Biological Evaluation of FLT3 Covalent Inhibitors with a Resorcylic Acid Core. *Bioorg. Med. Chem.* **2014**, *22*, 6625–6637.
- (9) Larock, R. C.; Leung, W.-Y.; Stolz-Dunn, S. Synthesis of Aryl-Substituted Aldehydes and Ketones via Palladium-Catalyzed Coupling of Aryl Halides and Non-Allylic Unsaturated Alcohols. *Tetrahedron Lett.* **1989**, *30*, 6629–6632.

- (10) Reetz, M. T.; Westermann, E.; Lohmer, R.; Lohmer, G. A Highly Active Phosphine-Free Catalyst System for Heck Reactions of Aryl Bromides. *Tetrahedron Lett.* **1998**, *39*, 8449–8452.
- (11) Reetz, M. T.; Westermann, E. Phosphane-Free Palladium-Catalyzed Coupling Reactions: The Decisive Role of Pd Nanoparticles. *Angew. Chem. Int. Ed.* **2000**, *39*, 165–168.
- (12) T. Reetz, M.; Lohmer, G. Propylene Carbonate Stabilized Nanostructured Palladium Clusters as Catalysts in Heck Reactions. *Chem. Commun.* **1996**, *0*, 1921–1922.
- (13) Roger, J.; Doucet, H. Aryl Triflates: Useful Coupling Partners for the Direct Arylation of Heteroaryl Derivatives via Pd-Catalyzed C–H Activation–Functionalization. *Org. Biomol. Chem.* **2007**, *6*, 169–174.
- (14) Zhang, C.; Tutkowski, B.; DeLuca, R. J.; Joyce, L. A.; Wiest, O.; Sigman, M. S. Palladium-Catalyzed Enantioselective Heck Alkenylation of Trisubstituted Allylic Alkenols: A Redox-Relay Strategy to Construct Vicinal Stereocenters. *Chem. Sci.* **2017**, *8*, 2277–2282.
- (15) Zhang, C.; Santiago, C. B.; Kou, L.; Sigman, M. S. Alkenyl Carbonyl Derivatives in Enantioselective Redox Relay Heck Reactions: Accessing α,β -Unsaturated Systems. *J. Am. Chem. Soc.* **2015**, *137*, 7290–7293.
- (16) Mei, T.-S.; Patel, H. H.; Sigman, M. S. Enantioselective Construction of Remote Quaternary Stereocentres. *Nature* **2014**, *508*, 340.
- (17) Kang, S.-K.; Lee, H.-W.; Jang, S.-B.; Kim, T.-H.; Pyun, S.-J. Complete Regioselection in Palladium-Catalyzed Arylation and Alkenylation of Allylic Alcohols with Hypervalent Iodonium Salts. *J. Org. Chem.* **1996**, *61*, 2604–2605.
- (18) Yoshizumi, T.; Takahashi, H.; Ohtake, N.; Jona, H.; Sato, Y.; Kishino, H.; Sakamoto, T.; Ozaki, S.; Takahashi, H.; Shibata, Y.; Ishii, Y.; Saito, M.; Okada, M.; Hayama, T.; Nishikibe, M. Potent and Orally Active ETA Selective Antagonists with 5,7-Diarylcyclopenteno[1,2-b]Pyridine-6-Carboxylic Acid Structures. *Bioorg. Med. Chem.* **2004**, *12*, 2139–2150.

- (19) Hilton, M. J.; Cheng, B.; Buckley, B. R.; Xu, L.; Wiest, O.; Sigman, M. S. Relative Reactivity of Alkenyl Alcohols in the Palladium-Catalyzed Redox-Relay Heck Reaction. *Tetrahedron* **2015**, *71*, 6513–6518.
- (20) Detry, B.; Erpicum, C.; Paupert, J.; Blacher, S.; Maillard, C.; Bruyère, F.; Pendeville, H.; Remacle, T.; Lambert, V.; Balsat, C.; Ormenese, S.; Lamaye, F.; Janssens, E.; Moons, L.; Cataldo, D.; Kridelka, F.; Carmeliet, P.; Thiry, M.; Foidart, J.-M.; Struman, I.; Noel, A. Matrix Metalloproteinase-2 Governs Lymphatic Vessel Formation as an Interstitial Collagenase. *Blood* **2012**, *119*, 5048–5056.
- (21) Giannelli, G.; Falk-Marzillier, J.; Schiraldi, O.; Stetler-Stevenson, W. G.; Quaranta, V. Induction of Cell Migration by Matrix Metalloprotease-2 Cleavage of Laminin-5. *Science* **1997**, *277*, 225–228.
- (22) Shimizu, A.; Hayashi, R.; Ashikari, Y.; Nokami, T.; Yoshida, J. Switching the Reaction Pathways of Electrochemically Generated β -Haloalkoxysulfonium Ions – Synthesis of Halohydrins and Epoxides. *Beilstein J. Org. Chem.* **2015**, *11*, 242–248.
- (23) Mook, O. R. F.; Frederiks, W. M.; Van Noorden, C. J. F. The Role of Gelatinases in Colorectal Cancer Progression and Metastasis. *Biochim. Biophys. Acta BBA - Rev. Cancer* **2004**, *1705*, 69–89.
- (24) Kumar, G. B.; Nair, B. G.; Perry, J. J. P.; Martin, D. B. C. Recent Insights into Natural Product Inhibitors of Matrix Metalloproteinases. *MedChemComm* **2019**, *10*, 2024–2037.
- (25) Omanakuttan, A.; Nambiar, J.; Harris, R. M.; Bose, C.; Pandurangan, N.; Varghese, R. K.; Kumar, G. B.; Tainer, J. A.; Banerji, A.; Perry, J. J. P.; Nair, B. G. Anacardic Acid Inhibits the Catalytic Activity of Matrix Metalloproteinase-2 and Matrix Metalloproteinase-9. *Mol. Pharmacol.* **2012**, *82*, 614–622.
- (26) Weigel, W. K.; Dennis, T. N.; Kang, A. S.; Perry, J. J. P.; Martin, D. B. C. A Heck-Based Strategy To Generate Anacardic Acids and Related Phenolic Lipids for Isoform-Specific Bioactivity Profiling. *Org. Lett.* **2018**, *20*, 6234–6238.
- (27) Hashimoto, H.; Takeuchi, T.; Komatsu, K.; Miyazaki, K.; Sato, M.; Higashi, S. Structural Basis for Matrix Metalloproteinase-2 (MMP-2)-Selective Inhibitory Action of β -Amyloid Precursor Protein-Derived Inhibitor. *J. Biol. Chem.* **2011**, *286*, 33236–33243.

- (28) Mallampudi, N. A.; Reddy, G. S.; Maity, S.; Mohapatra, D. K. Gold(I)-Catalyzed Cyclization for the Synthesis of 8-Hydroxy-3- Substituted Isocoumarins: Total Synthesis of Exserolide F. *Org. Lett.* **2017**, *19*, 2074–2077.
- (29) Kelly Christopher B.; Lambert Kyle M.; Mercadante Michael A.; Ovia John M.; Bailey William F.; Leadbeater Nicholas E. Access to Nitriles from Aldehydes Mediated by an Oxoammonium Salt. *Angew. Chem. Int. Ed.* **2015**, *54*, 4241–4245.
- (30) Cabri, W.; Candiani, I.; Bedeschi, A.; Penco, S.; Santi, R. ..Alpha.-Regioselectivity in Palladium-Catalyzed Arylation of Acyclic Enol Ethers. *J. Org. Chem.* **1992**, *57*, 1481–1486.
- (31) Jat, J. L.; De, S. R.; Kumar, G.; Adebessin, A. M.; Gandham, S. K.; Falck, J. R. Regio- and Enantioselective Catalytic Monoepoxidation of Conjugated Dienes: Synthesis of Chiral Allylic Cis-Epoxides. *Org. Lett.* **2015**, *17*, 1058–1061.

4 HAT-Mediated C–H Activation of Diamondoids as a Tool for the Construction of New C–C Bonds

4.1 - Introduction

Adamantane **4.1** is a rigid cage-like hydrocarbon possessing a great deal of symmetry. Because of this, despite possessing 10 carbons and 16 hydrogens, adamantane only has two distinct positions: a methine bridge head and a bridging methylene (**Figure 4.1**). Adamantane is the simplest member a family of compounds known as diamondoids, named for their ability to be superimposed onto a diamond lattice. As members of the diamondoid family grow in size, they increase in complexity as well. Diamantane **4.2**, the next largest diamondoid, possesses two differentiable methine positions referred to as “apical” and “medial”. While synthetic adamantane is commercially available at low cost today, this was not always the case.

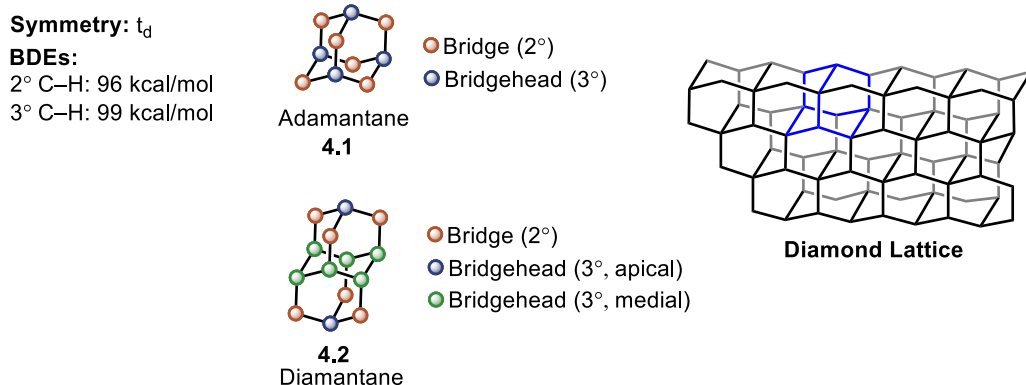


Figure 4.1 – The Structure of Adamantane

The history of the diamondoids, specifically adamantane, is an interesting tale that began as a simple proposed structure. In a series of developmental milestones, a molecule that once only existed on paper became a reality with only miniscule natural isolation potential and dismal synthetic prospects to eventually being a compound that today is

synthesized in nearly quantitative yield. The earliest attempted synthesis of an adamantane derivative was made by Meerwein in 1922 using formaldehyde and methyl malonate in the presence of piperidine but he instead obtained 1,3,5,7-tetracarboxymethoxybicyclo [3.3.1]nonane-2,6-dione (**4.3**, **Figure 4.2**). This compound would later become known as “Meerwein’s ester.”

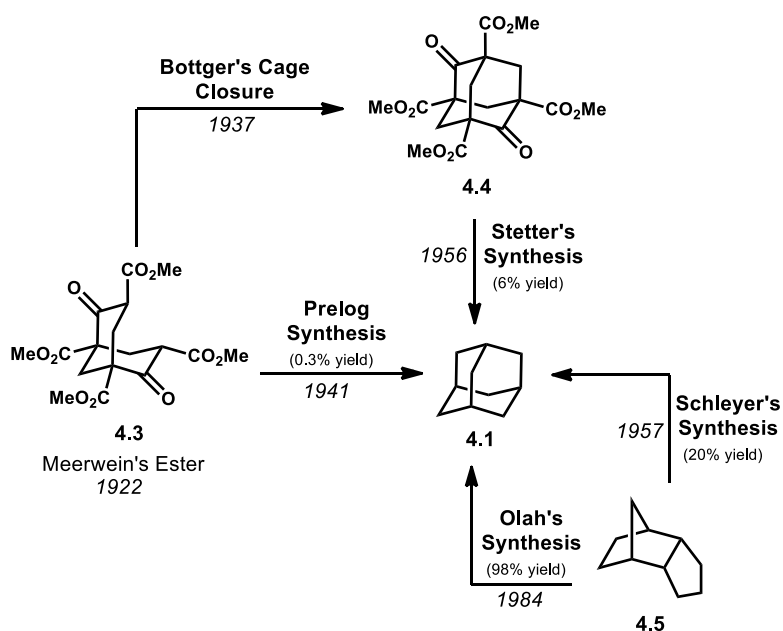


Figure 4.2 – Historical Developments in Adamantane Synthesis

Adamantane was later isolated from crude oil by Landa and Macháček in 1933 at the Hodonin oil field in Czechoslovakia.^[1] Since then, many higher-order diamondoids have been isolated from crude oil, however, these diamondoids are extremely scarce and only account for 0.0004% of petroleum content.^[2,3] As such, isolation from petroleum was extremely costly and for many years Landa and coworkers would control the world’s multi-milligram supply of adamantane until a method for its synthesis was developed.^[4]

The first synthesis of adamantane was completed by Prelog in 1941 using a methylene insertion into Meerwein's ester with 0.3% yield.^[5] A previous methylene insertion by Bottger to the cage-like adamantane precursor **4.4** was accomplished in 1937, but Bottger was unable to access adamantane itself. Later in 1956, Stetter used Bottger's intermediate to synthesize adamantane in 6% yield, the highest up to that point.^[6] A significant breakthrough was made by Paul von Ragué Schleyer a year later in 1957 by hydrogenating dicyclopentadiene to tetrahydrodicyclopentadiene **4.5** which was then used to synthesize adamantane in 20% yield using a Lewis acid catalyzed isomerization.^[7] In 1984, Olah would apply superacid catalysis and sonication to improve this isomerization method to 98% yield, reducing the cost of adamantane to less than \$1/gram.^[8,9]

Since Schleyer's synthesis, the increasing availability of adamantanes led to a great deal of new research. Soon after Schleyer's report, a number of adamantyl derivatives were synthesized *via* halogenations, amidations, carboxylations and more.^[10-12] Halogenations of adamantane became common in the late 1950's due to their ease of functionalization. In 1959, 1-bromoadamantane was successfully synthesized by Stetter et al. in 85% yield.^[13] In 1961, Haaf et al. reported the first amidation of adamantane using *tert*-butanol and sulfuric acid with hydrogen cyanide to give the adamantyl formamide in 76% yield.^[14] This could be followed by hydrolysis to give aminoadamantanes and led to the discovery of pharmaceutical drugs containing adamantane.

Amantadine (**4.6**, **Figure 4.3**) was the first pharmaceutical to contain the adamantyl scaffold after it was found to possess potent antiviral activity against influenza A in

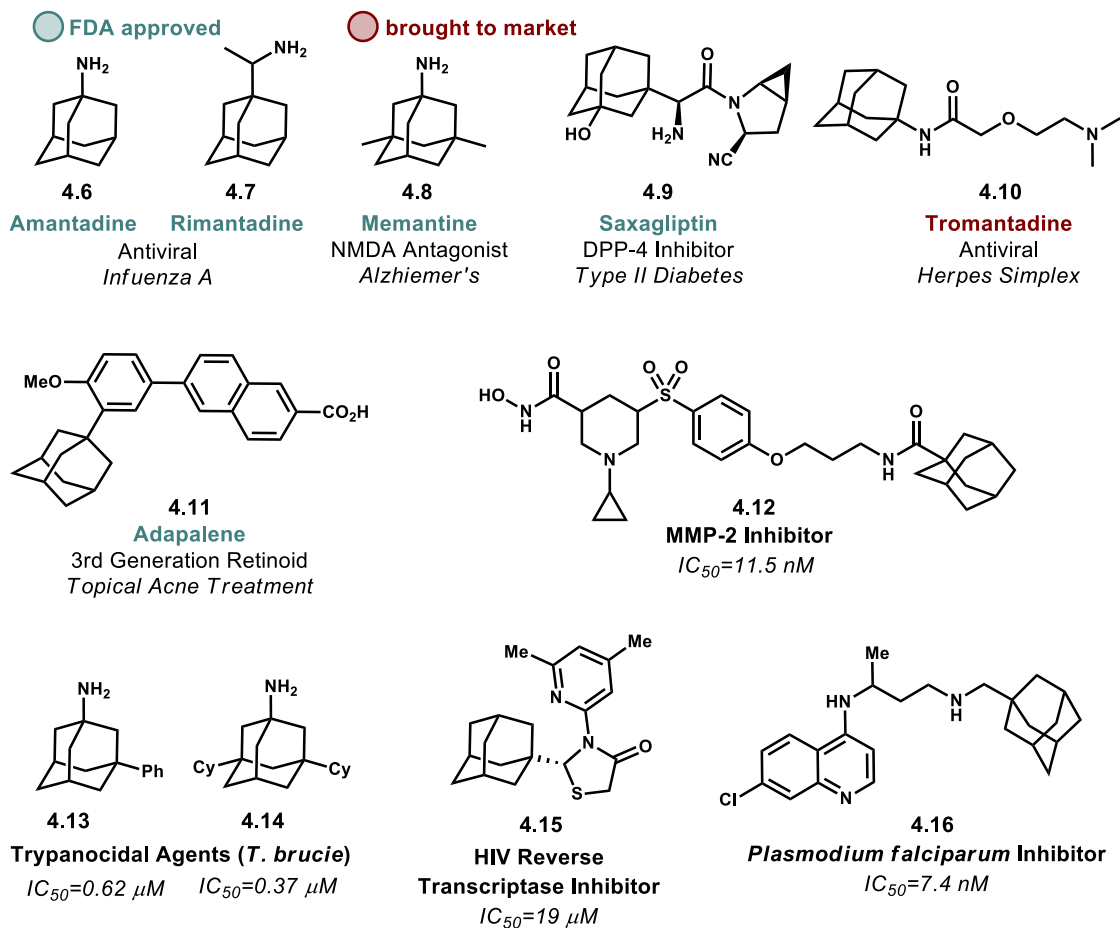


Figure 4.3 – Adamantane Containing Pharmaceutical Agents

1964.^[15] Amantadine was FDA approved in 1967 and the closely related Rimantadine (4.7) obtained FDA approval for the treatment of influenza A in 1993. Shortly after amantadine entered the market, Eli Lilly and Company patented memantine (4.8), which would ultimately be approved for use in the treatment of Alzheimer's disease in 2003. Several other FDA approved drugs contain adamantane such as saxagliptin 4.9 (antidiabetic) and adapalene (antiacne). Many other adamantanes are known to possess biological activity against a variety of serious human maladies such as *T. brucie* (African sleeping sickness), HIV, and *P. falciparum* (malaria).^[16]

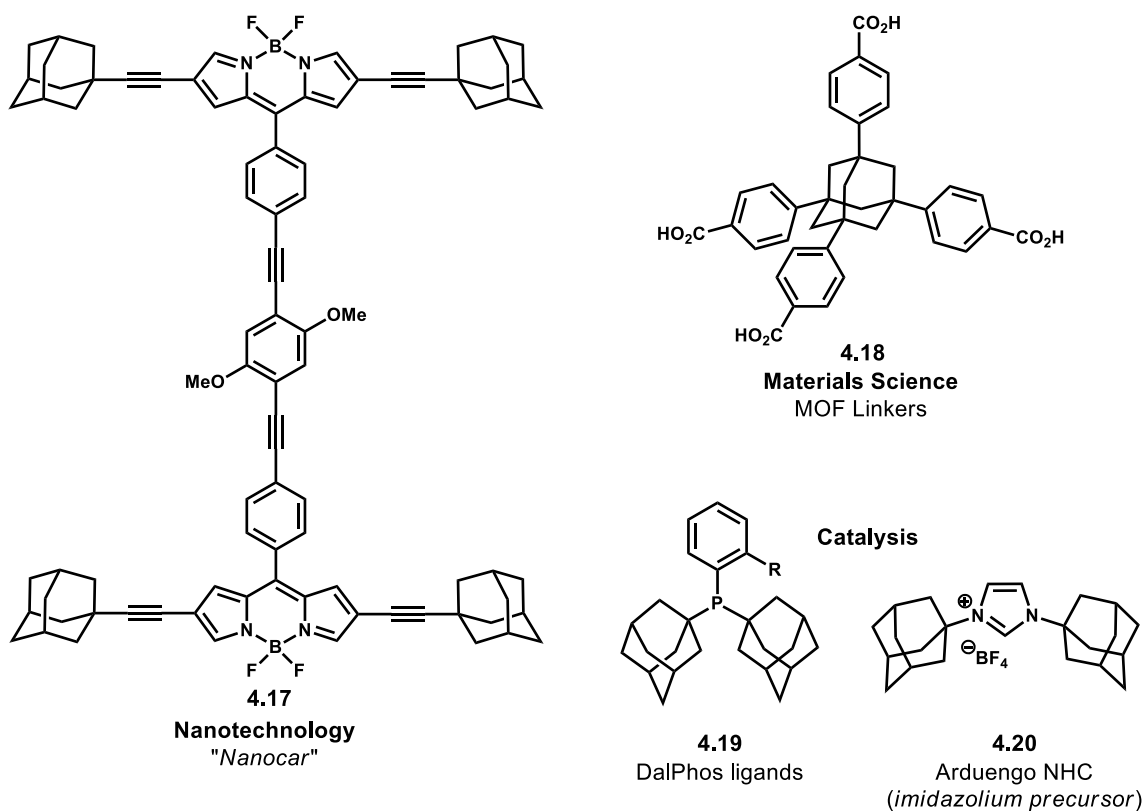


Figure 4.4 – Uses of Adamantanes in Non-Pharmaceutical Applications

Adamantanes have found useful applications in other areas as well (**Figure 4.4**). A particularly intuitive use is in the realm of nanotechnology where adamantanes have been used as the “wheels” of BODIPY based nanocars **4.17**. Adamantanes offer greater mobility on glass surfaces compared to nanocar designs using C₆₀ or carborane wheels.^[17] The steric bulk imparted by the adamantyl group have made it useful in catalytic applications.^[18] DalPhos ligands such as **4.19** have been used in palladium cross-coupling reactions between arylchlorides and hydrazine to afford aryl hydrazine products via in a Buchwald–Hartwig type process.^[19] The Arduengo NHC can be obtained by deprotonation of **4.20**, a crystalline and shelf-stable imidazolium carbene precursor first synthesized in 1991.^[20]

This NHC has been used in many applications such as a transesterification catalyst^[21] and in the synthesis of the second-generation Grubbs-type metathesis catalysts.^[22]

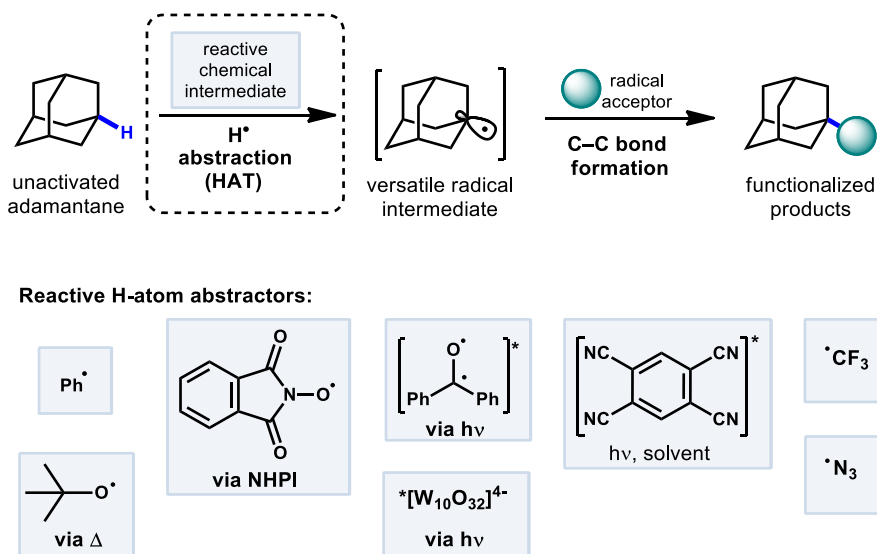


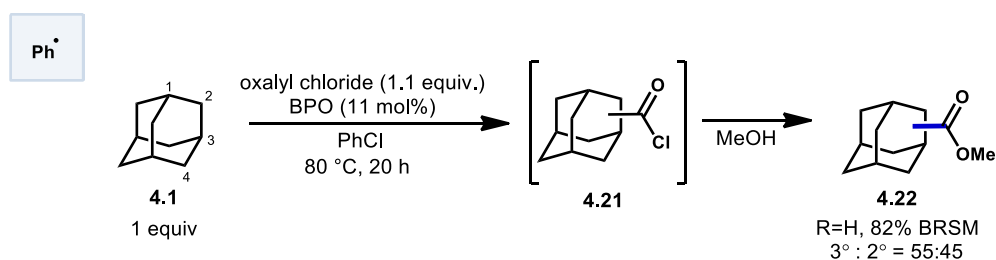
Figure 4.5 –A General HAT Reaction with Adamantane and Known Reactive Species

Typical functionalization of diamondoids relies on radical, ionic or oxidative transformations.^[23] Among these, single electron oxidations are usually the most selective.^[24] A vast body of work exists for reactions involving the adamantyl radical, many of which make use of prefunctionalized adamantanes. Rather than rely on these activated substrates, the direct C-H functionalization of diamondoids using HAT (hydrogen atom transfer, **Figure 4.5**) is more challenging and must contend with site-selectivity issues and incompatibility with redox-sensitive functional groups.^[25] However, adamantyl radicals generated these reactions are versatile intermediates capable of reacting with a wide array of radical acceptors. The generation of radicals on unactivated diamondoids requires the use of a high-energy H-atom abstractor, such as the species shown in **Figure 4.5**. The remainder of the chapter will focus on providing an overview of C–H to C–C transformations of adamantane and other diamondoids using HAT as the key radical generating step.

4.2 - Acylative Additions to Adamantane

Acyl adamantanes are defined here as a compound featuring a direct C–C bond between adamantane and the carbonyl of a ketone, ester or aldehyde. Compounds fitting this description are useful intermediates that can be further functionalized and while many methods have been developed to synthesize various acyladamanes over the years, most rely on a pre-functionalized adamantyl substrate and/or harsh conditions for accomplishing the necessary transformation. Therefore, direct methods for forging C–C bonds to adamantanes that eliminate the need for pre-functionalization are desirable. Use of the reactive adamantyl radical has been successful in achieving direct acylations in a variety of ways and shall be detailed herein.

4.2.1 - Chlorocarbonylation

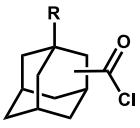


Scheme 4.1– Chlorocarbonylation Of Adamantane

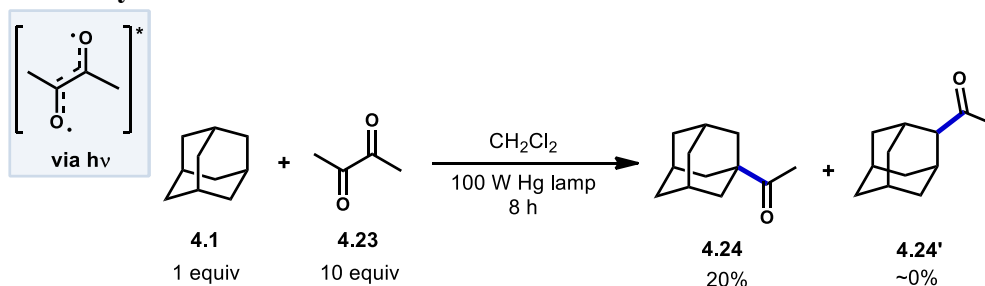
Early work by Tabushi in 1968 involving the radical chlorocarbonylation of adamantane using oxalyl chloride (**Scheme 4.1**). Using benzoyl peroxide as initiator, they were able to access chlorocarbonylated intermediate **4.21**.^[26] Following methanolysis, a mixture of adamantanecarboxylates **4.22** (55:45 rr) was obtained based on recovered starting material. After statistical correction, this distribution of regioisomers indicates a reactivity ratio of 3.67:1 favoring the tertiary adamantyl positions.^[27] This preferential

tertiary reactivity of adamantanes was also observed in prior radical halogenations by Smith and Williams as well.^[28] Tabushi went on to show that substituent effects of adamantyl chlorocarbonylation on the ratio of 3°:2° products differed from the ratio observed in radical brominations using bromine with carbon tetrachloride (**Table 4.1**).^[29] Substituent effects for such brominations followed a linear free-energy relationship while chlorocarbonylation behaved quite differently. A qualitative explanation offered by Tabushi was that bulky substituents in chlorocarbonylation reactions were more dependent on the strain at the 2° positions than the 3° positions than in bromination reactions.

Table 4.1 – Substituent Effects For Adamantane Chlorocarbonylation vs. Halogenation

R	Chloro-carbonylation	Halogenation via $\cdot\text{CCl}_3$
	3° : 2° ratio	3° : 2° ratio
	2.3 : 1	6.7 : 1
H	1.2 : 1	6.1 : 1
OCH ₃	5.7 : 1	vs. 5.7 : 1
CO ₂ CH ₃	4.4 : 1	4.9 : 1
CN	1.4 : 1	2.8 : 1
	steric basis	LFER basis (σ^*)

4.2.2 - Acetylations



Scheme 4.2 – Photoacetylation of Adamantane Using Biacetyl

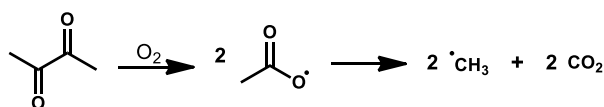
Adamantane can be selectively acetylated using an excess of biacetyl (**4.23**) under irradiation as demonstrated by Tabushi and Aoyama^[27] to give 1-acetyladamantane (**4.24**)

as the sole regioisomer (**Scheme 4.2**).^[30,31] The C–H abstracting species is believed to be triplet biacetyl since no acetylation occurred in the presence of pyrene, a known quencher of biacetyl phosphorescence via energy transfer (**Table 4.2**).^[32] Despite also being a quencher, oxygen instead increased rate of acetylation and both the 1- and 2-acetyladamantane products were observed as was 1-adamantanol, the autooxidation product. The increase in photoacetylation rate and loss of selectivity is attributed to the generation of reactive methyl radicals that form in a decarboxylative process after oxygen and biacetyl react. In higher ordered diamondoids, photoacetylation remains selective for methine positions. Schreiner *et al.* tested the acetylation of several larger members of the diamondoids family using biacetyl.^[33] However, unlike adamantane’s four equivalent methine positions, higher ordered diamondoids possess nonequivalent positions. For diamantane featuring apical and medial positions (occurring with a 1:3 apical:medial ratio), photoacetylation using biacetyl favored mono-acetylation at the apical position (**4.25a**, **Figure 4.6**) over the medial position in a 4.5:1 ratio (14:1 after statistical correction). Acetylation of the methylene positions and bis-addition products were not observed.

Table 4.2 – Biacetyl Quenching Studies

Conditions	1-acetyl adamantane (%)	2-acetyl adamantane (%)	1- adamantanol (%)
N ₂	13.8	--	--
N ₂ , pyrene	0	--	--
O ₂	28.6	12.3	8.3

Decarboxylative Generation of Methyl Radical



This apical selectivity is still maintained in even higher ordered tri-, tetra-, and pentamantanes despite an increase in the number of possible medial positions (**Figure 4.6**). For instance, despite the number of distinct C–H positions increasing from two in diamantane to four in triamantane **4.25b** and [121]tetramantane **4.25c**, acetylation of the apical position is still favored over the other medial positions in an ~5:1 ratio.^[10] Even higher apical selectivity is observed in [1(2)3]tetramantane **4.25d** and [123]tetramantane **4.25e** (despite **4.25e** having six distinct C–H positions).^[11] [1(2,3)4]pentamantane **4.25f** showed near complete apical selectivity and interestingly resulted in a significant amount of bis acetylated product as well.

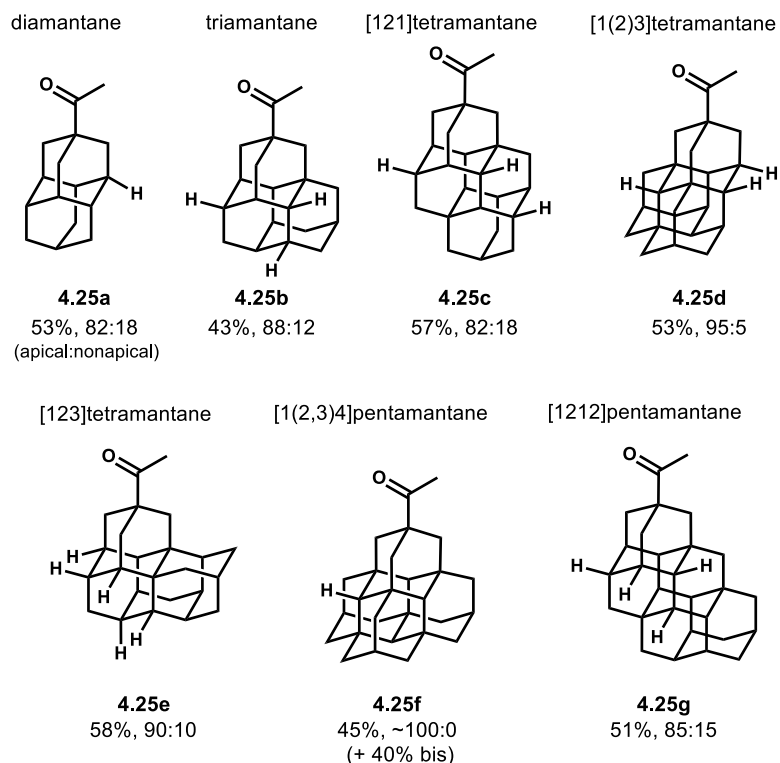
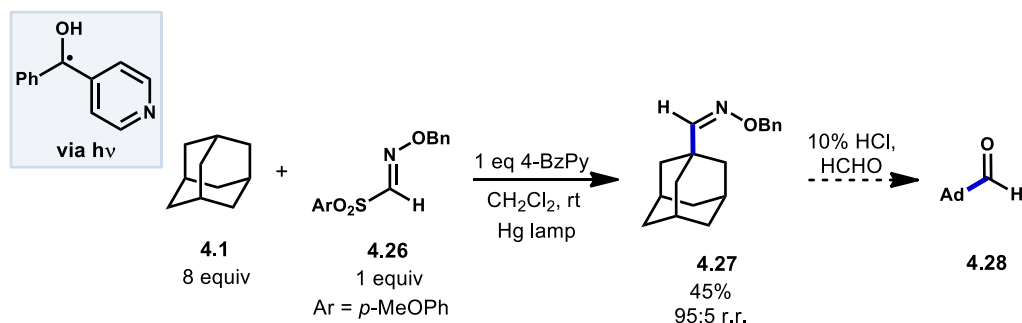


Figure 4.6 – Acetylation of Higher Order Diamondoids

Acetylation of diamondoids proceeds in an apical-selective manner. Reported yields are accompanied with the corresponding apical:non-apical product ratio. Other chemically distinct non-apical tertiary positions for each diamondoid are indicated with an explicitly drawn hydrogen.

4.2.3 - Formylation

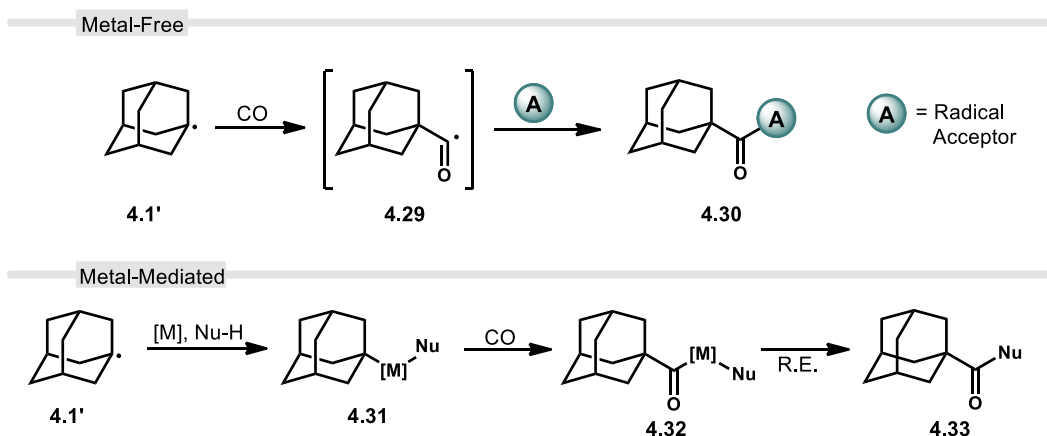
Recently, Kamijo et al. have reported a photochemically induced method for the formylation of unactivated C(sp³)–H bonds in many substrates including adamantane, albeit indirectly through an aldoxime intermediate.^[34] Using a mercury lamp to generate a photo-excited 4-benzoylpyridine (4-BzPy) to act as the C–H abstractor for adamantane, Kamijo showed that the resulting adamantyl radical can readily intercept an oxime derivative (**4.26**). Using an O-benzyl aldoxime with an arylsulfonyl substituent with good leaving group ability leads to an adamantyl O-benzylaldoxime precursor, **4.27**. The aldoxime can then be converted to the aldehyde **4.28** using a solution of formaldehyde in aqueous HCl, although the adamantyl aldoxime was not one of the substrates that was converted in this way in Kamijo's report (typical yield 70-80%). In the photochemical reaction, the methine position of adamantane was "formylated" with high regioselectivity (95:5).



Scheme 4.3 – Formylation of Adamantane via An Aldoxime Intermediate

4.3 - Carbonylations with CO

Carbonylation of adamantane using carbon monoxide (CO) technically falls under the purview of the acylative transformations described in the previous section. However, in the case of metal-free reactions of adamantyl radical **4.1'** with CO, another versatile intermediate, the adamantyl acyl radical (**4.29**, **Scheme 4.4**, top) is generated. Various strategies for arriving at this acyl radical have been developed and due to its use with various radical acceptors, these carbonylative transformations have been given their own section. The adamantyl radical can also incorporate CO through transition metal-catalyzed processes such as insertion (see **4.31** to **4.32**, **Scheme 4.4**, bottom) and reductive elimination to **4.33**.



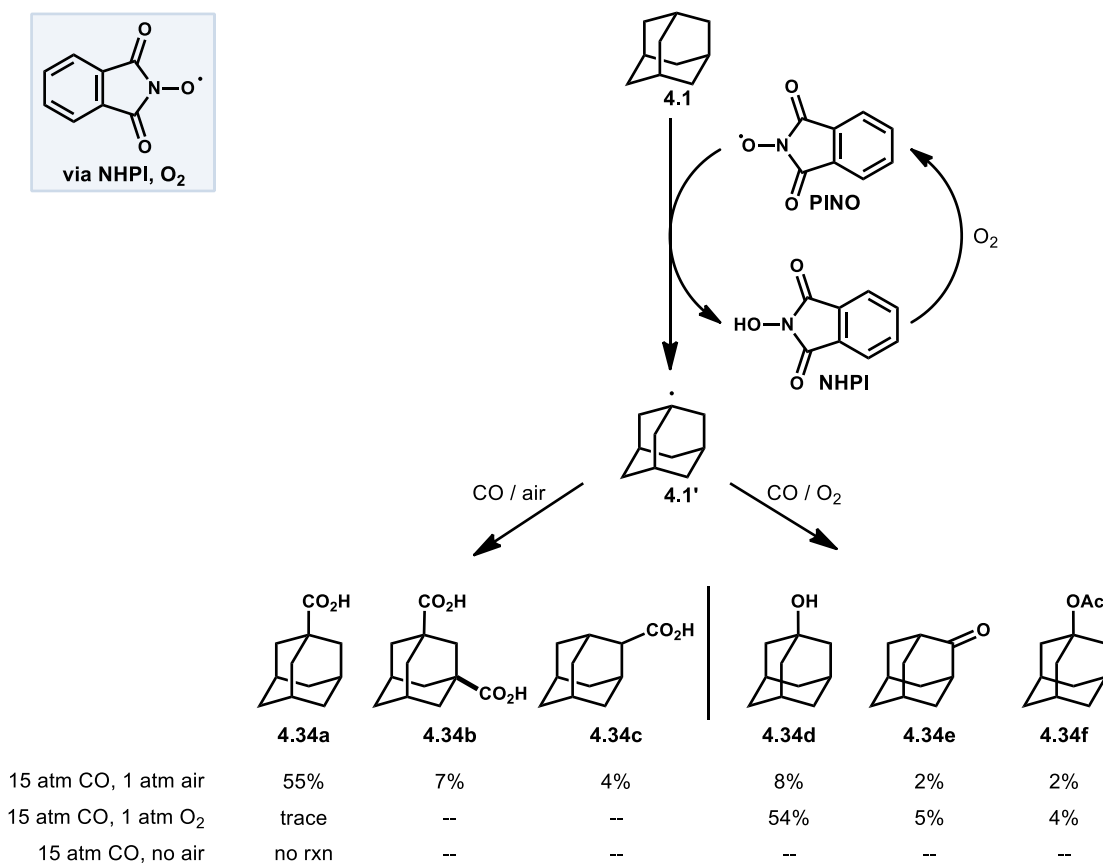
Scheme 4.4 –General Carbonylation of the Adamantyl Radical Using CO

4.3.1 - NHPI Mediated Carboxylation

C–H activation of saturated hydrocarbons using carbon monoxide, although attractive, is quite challenging due to the lack of selectivity and low conversion of starting material.^{[35–}

^{37]} Work done by Ishii in 1998 showed that oxidation of polycyclic alkanes in the presence

of air can produce carboxylated products using a catalytic free-radical method as shown in **Scheme 4.5**. *N*-hydroxyphthalimide (NHPI) is used as a radical catalyst to generate the PINO radical without photoactivation and under mild conditions.^[38] However, selectivity is quite poor when using adamantane as the hydrocarbon and a mix of both carboxylated and oxygenated species is formed.



Scheme 4.5 – Carbonylation and Other Oxidative Transformations of Adamantane via NHPI

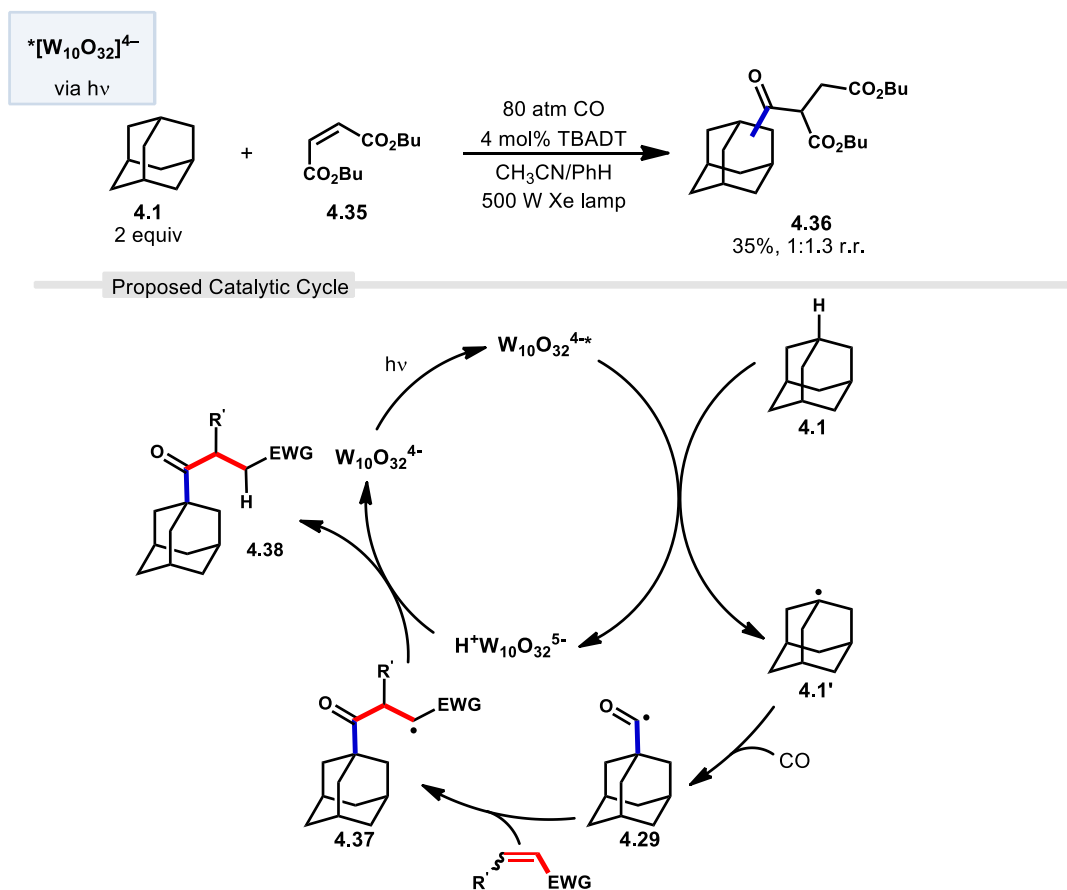
A conceivable mechanism begins with generating the reactive intermediate, phthalimide-*N*-oxyl (PINO) from NHPI in the presence of O₂. The PINO radical formed then goes on to do C–H abstraction preferentially at the tertiary position of adamantane to give the intermediate, adamantyl radical **4.1'**. This radical is readily trapped with CO, which upon subsequent reaction with O₂ eventually generates the carbonylated carboxylic acid products **4.34a-c**. The exact ratio of products varies depending on reaction conditions such as solvent and temperature and in all cases, there is recovery of starting material. When air is replaced by pure O₂, the oxygenated products 1-adamantanol **4.34d**, 2-adamantanone **4.34e**, and 1-adamantaneacetoxo **4.34f** are formed almost exclusively over the carboxylated products.

4.3.2 - Photocatalytic Carbonylation

In 2011, Ryu and Albini reported a three-component coupling reaction using photocatalytic methods.^[39] This multi-component process generated unsymmetrical ketones with tetrabutylammonium decatungstate (TBADT) as the photocatalyst and a xenon lamp as their UV light source. The carbonylation of adamantane proceeded using a 1:1 mixture of acetonitrile and benzene as solvent and 2 equivalents of adamantane although with poor selectivity and low yields (**Scheme 4.6**). A 1:1.3 mixture of the 1- and 2- carbonylated products **4.36** were obtained with an overall yield of 35% and 48% conversion of the alkene starting material. This is an unusual example of a reaction which appears to favor the 2° position of adamantane, for reasons which are not entirely obvious.

The proposed catalytic cycle for the C–H functionalization of adamantane using a three-component system in a tandem carbonylation-addition process is also illustrated in

Scheme 4.6 (bottom). Upon irradiation of TBADT, the excited photocatalyst abstracts a hydrogen from adamantane **4.1** generating adamantyl radical **4.1'**. Carbonylation results in the acyl radical **4.29** followed by a Giese-like addition to an electron deficient alkene to give intermediate **4.37**. The hydrogen from the reduced photocatalyst is finally donated to intermediate **4.37** turning over the catalyst affording the desired functionalized adamantane product **4.38**.

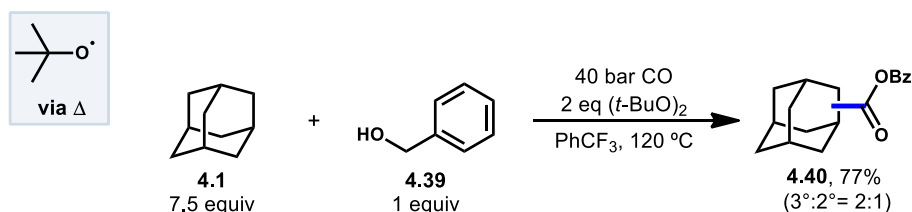


Scheme 4.6 – Tandem Carbonylation-Addition via TBADT Photocatalysis

The catalytic cycle shown is only for the tertiary product. The secondary product arises from carbonylation at the 2° position.

4.3.3 - Oxidative Radical Carbonylation

The use of radical carbonylation in the synthesis of carboxylates and esters via C–H activation is a useful alternative to similar approaches such as the Monsanto acetic acid synthesis^[40] that rely on transition metals.^[41] Lei et al. developed a metal-free oxidative carbonylation of alkanes via direct C–H bond activation using di-*tert*-butylperoxide (DTBP) in the presence of carbon monoxide and benzyl alcohol **4.39** to generate esters (Scheme 4.7).^[42] A variety of alkanes including adamantane underwent efficient



Scheme 4.7 – Oxidative Metal-Free Radical Carbonylation

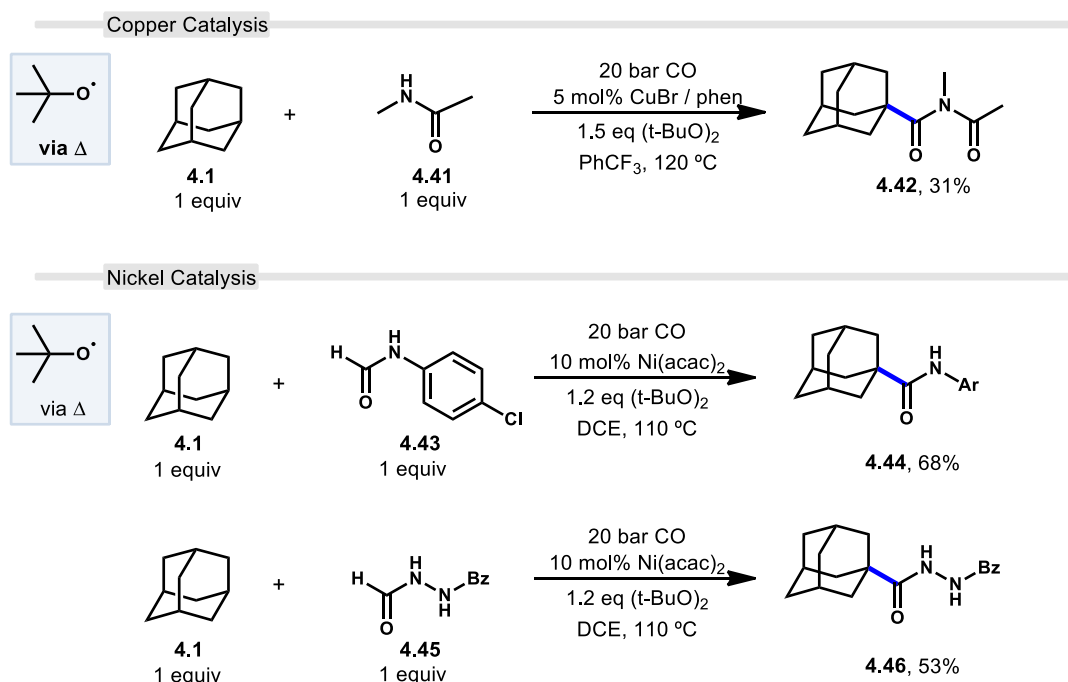
conversion to the corresponding benzyl ester product **4.40**. While the reaction proceeded in good yield, the regioselectivity of the carbonylation was rather low giving a 2:1 ratio of 3°:2° product in 77% yield.

4.3.4 - Transition Metal-Catalyzed Carbonylation

The use of transition metals for C–H activation via carbonylation is an attractive method for generating compounds containing carbonyl compounds. However, commonly used second- and third-row transition metals such as ruthenium and rhodium are expensive and can lead to complicated catalyst and ligand designs, limiting their use.^[43–45] First row transition metals like nickel and copper are favorable alternatives due to their low toxicity, abundance and low cost.^[46] Wu et al. reported the first copper-catalyzed carbonylative C–H activation in 2016 using a variety of alkanes and amides to generate imide products.^[47] Wu employed a Cu(I) precatalyst and di-*tert*-butyl peroxide (DTBP) to selectively

functionalize adamantane at the tertiary position; generating the imide in 31% yield (**Scheme 4.8, top**). While other alkanes were used in excess and cyclohexane as solvent, a 1:1 ratio of adamantane and *N*-methylacetamide **4.41** gave the desired product when (trifluoromethyl)benzene was solvent.

Nickel-based catalysis has also been reported to be successful in the activation of inert sp^3 C–H bonds.^[48] Recently, Yufeng et al. developed a Ni-catalyzed carbonylation

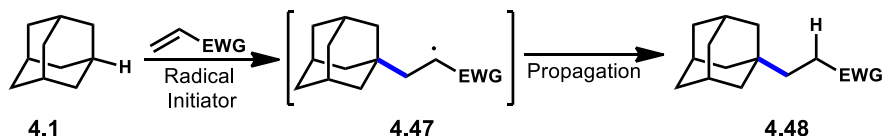


Scheme 4.8 – Transition Metal-Catalyzed Carbonylations of Adamantane

of unreactive alkanes with formamides to obtain amide products.^[49] Unlike Wu's work, the reaction generates an unstable formimide followed by thermal decomposition via loss of CO to give the final product. **Scheme 4.8** (bottom) illustrates two selective carbonylations both using adamantane and Ni(acac). The first reaction uses an equimolar amount of formanilide **4.43** to give a modest 68% yield while the second utilizes *N*-

formylbenzohydrazide **4.45** giving the corresponding diacylhydrazines **4.46** in 53% yield. In both cases, selectivity favored the methine position. Similar to the work done by Wu and coworkers, DTBP is homolytically cleaved with the help of the transition metal, to form the key reactive intermediate, the *tert*-butyloxy radical.

4.4 - Alkylation via Alkene Addition (Giese-Type Reaction)



Scheme 4.9 – General Giese Reaction with Adamantane

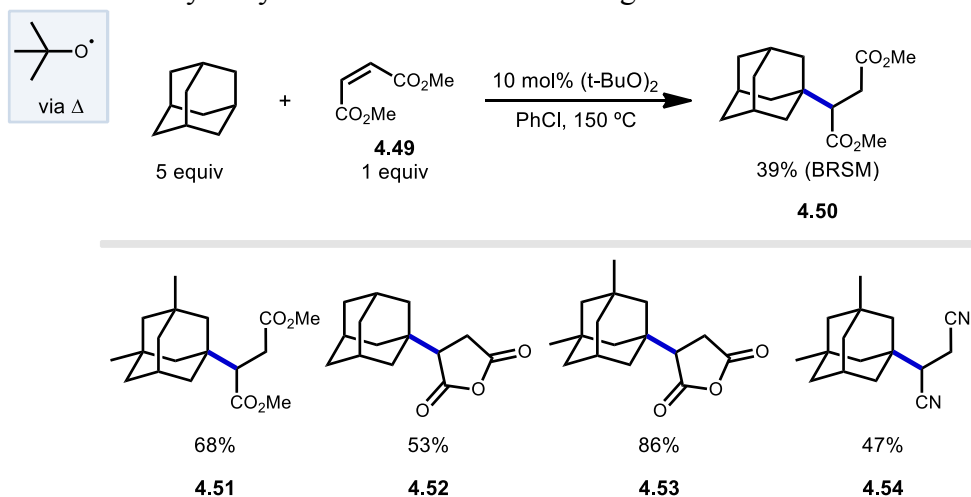
Giese-type reactions involve trapping of a carbon centered radical with an electrophilic alkene to form a new carbon-carbon bond (**Scheme 4.9, 4.47**). The α -carbon intermediate can go under further reaction in propagation or tandem addition steps. This opens the possibility for C–H functionalization of adamantanes to a diverse array of transformations.

4.4.1 - First Giese Addition with Adamantane

The addition of the adamantyl radical to alkenes can be achieved using pre-functionalized bromo- and iodo-adamantanes. Avoiding the need for preactivated starting materials through C–H activation of adamantane itself is an attractive option in terms of both atom-economy and step count, especially if the reaction proceeds with good regio- and diastereoselectivity. As such, there are many examples of Giese-type additions to alkenes that proceed by a radical C–H abstraction to generate the necessary adamantyl radical. The first of these Giese-type additions performed on adamantane and substituted adamantanes with different electron deficient alkenes was done by Fukunishi and Tabushi in 1988 and gave products (**4.50-4.54, Table 4.3**) in moderate yields and in regioselective

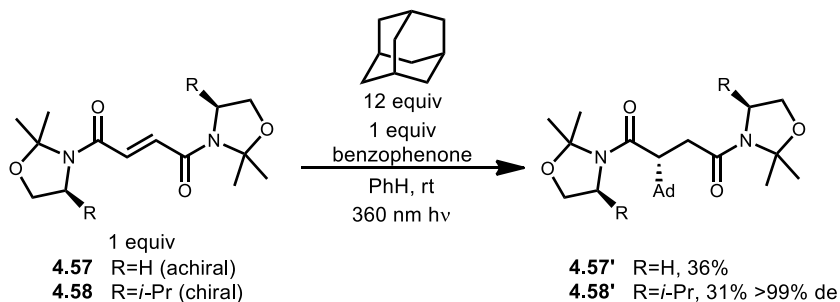
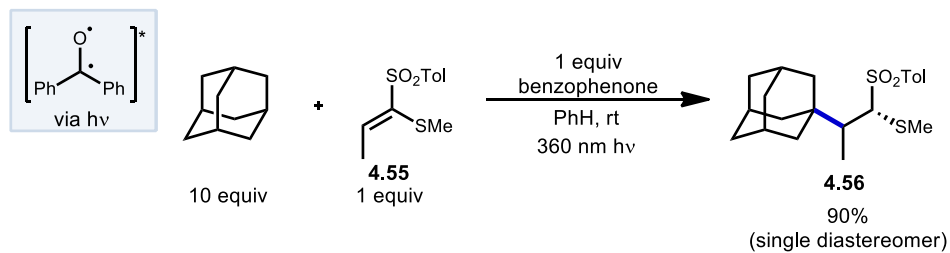
fashion for the 3° position. The reactive species is once again *tert*-butyloxy radical and is generated at high temperatures using di-*tert*-butylperoxide.^[50]

Table 4.3 – Early Alkylation of Adamantane Using Electron Withdrawn Alkenes



4.4.2 - Photochemically Driven Alkene Additions

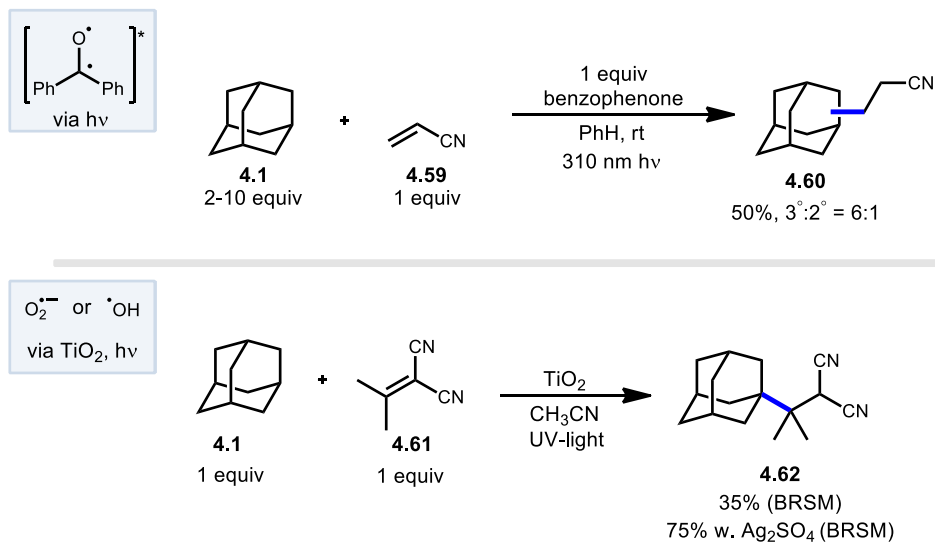
α -Thiosulfones are convenient synthetic intermediates that can be used for several key transformations. e.g. desulfurization^[51] and pyrolysis to obtain carbonyl derivatives.^[52] Albini and coworkers developed a photochemical radical alkylation to access α -thiosulfones from ketene dithioacetal S,S -dioxides.^[53] With stoichiometric amounts of benzophenone, 1 equiv of (*E*)-1-(methylthio)-1-[(4-methylphenyl)-sulfonyl]propene **4.55**, excess adamantane and UV light, the thiosulfone product **4.56** was obtained in 90% yield as a single diastereomer (**Scheme 4.10**, top). This stereoselectivity was found to be dependent on the steric bulk of the alkyl radical. Cyclohexane by comparison also proceeded efficiently in 89% yield but with lower diastereoselectivity (d.r.=82:18). Alkylation was selective for the tertiary bridgehead position and trace amounts



Scheme 4.10 – Photochemical Addition to Alkenes Using Benzophenone

of phenyladamantane, bis-adamantane, 1-adamantanol, and 2-adamantanone were also observed, the latter arising through reaction with residual oxygen.

Albini et al. used similar conditions to study radical additions to olefins with fumaric acid diamides and oxazolidine chiral auxiliaries to generate functionalized products with a high degree of diastereoselectivity.^[54] As shown in (Scheme 4.10, bottom), chiral **4.58** and achiral **4.57** oxazolidines were tested with excess adamantane and benzophenone as photosensitizer. As above, irradiation at 360 nm resulted in the triplet excited state of benzophenone and the formation of the adamantyl radical exclusively at the tertiary position. Addition to the fumaroyloxazolidines **4.57** and **4.58** gave desired functionalized adamantane products **4.57'** and **4.58'** in a stereoselective manner with moderate yields.

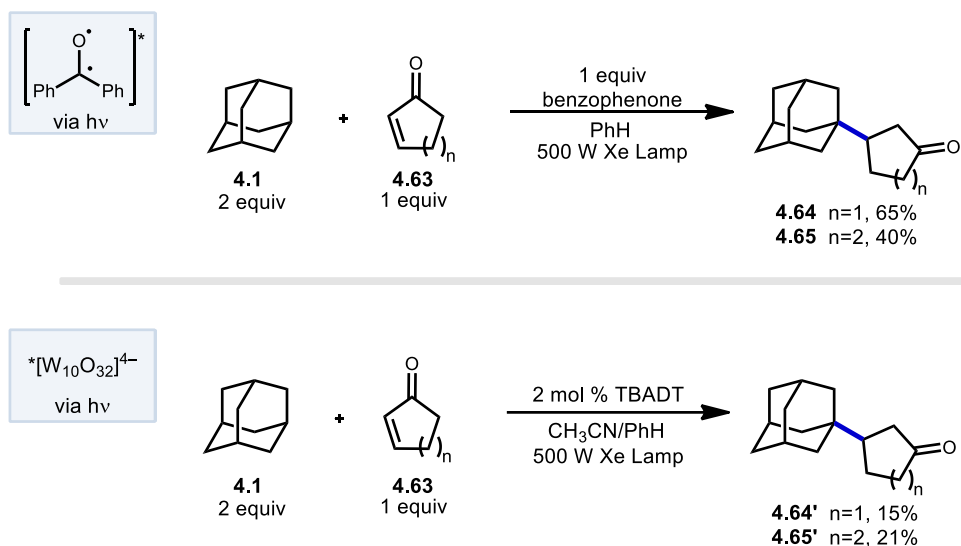


Scheme 4.11 – Additions to Alkenyl Nitriles

A common class of electronic deficient olefins are the α,β -unsaturated nitriles. These substrates commonly participate in Giese additions to produce natural products possessing nitrile moieties and other metabolites of interest. However, accessing them directly through radical methods has limitations due to toxicity of the organometallics and cyanide salts required.^[55–57] Albini's photochemical benzophenone platform provides a much safer route to the alkylation of these alkenyl nitriles. Using this approach, cyanoethyl adamantanes were synthesized using one equivalent photosensitizer, one equivalent of acrylonitrile **4.59**, and excess adamantane (**Scheme 4.11**). The resulting product **4.60** was formed as a mixture of regioisomers in a 6:1 ratio. Yields shown were determined by GC and the reported isolated yields were somewhat lower.

Albini also tested TiO_2 , a known heterogeneous photo-oxidant in the presence of oxygen or water. As shown in **Scheme 4.11**, isopropylidene malononitrile **4.61** and adamantane were treated with TiO_2 and irradiated under UV light. This reaction was subjected to longer irradiation times (3 h) than typically required for TiO_2 -mediated

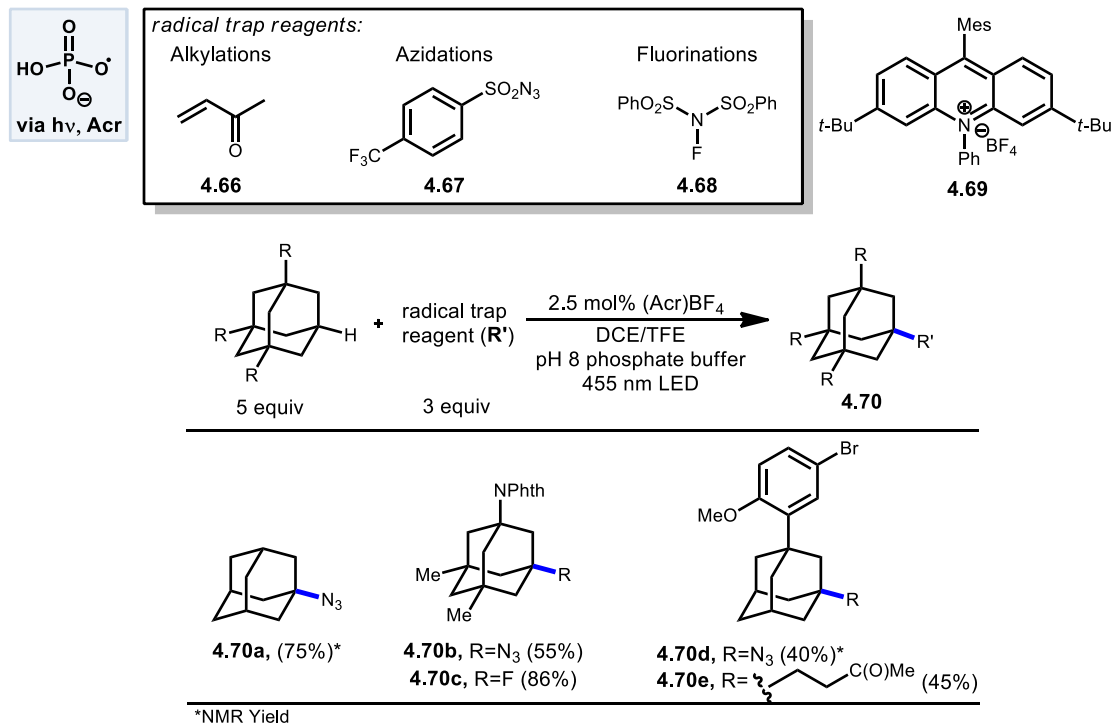
reactions in order to have conversions of above 30%. The alkylated adamantane product **4.62** was obtained in 35% yield based on recovered starting material. Oxygenated adamantane products were also observed and were attributed to remaining oxygen. A higher yield of 75% was obtained when using silver sulfate as a sacrificial oxidant.



Scheme 4.12 –Synthesis of β -Adamantylketones via Addition to Cyclic Enones

Later in 2006, Albini and coworkers went on to synthesize β -adamantylketones from cyclic enones **4.63** also using photomediated radical additions (**Scheme 4.12**).^[58] The adamantyl radical was generated via HAT by either benzophenone or TBADT. When using benzophenone as catalyst, only 1-adamantyl derivatives were observed and cyclopentanone product **4.64** was generated in 65% yield while the cyclohexanone product **4.65** was obtained in a lower 40% yield. Switching the photocatalyst to TBADT resulted in lower yields, with cyclopentanone product **4.64'** giving 15% yield and the cyclohexanone product **4.65'** giving 21% yield. The proposed reaction mechanism involves a direct hydrogen abstraction to the photocatalyst as opposed to energy or electron transfer pathways.

Table 4.4 – Additions to α,β -Unsaturated Ketones and Other Radical Trap Reagents



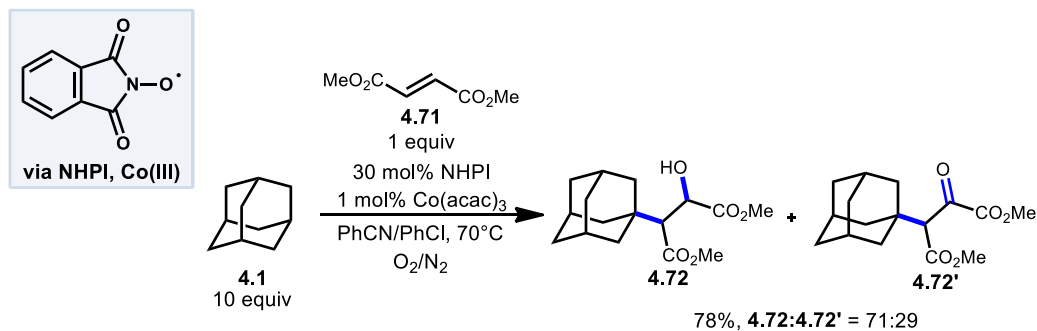
More recently, in 2018 Nicewicz and Alexanian developed a general strategy for organic photoredox-catalyzed C–H abstraction from a range of aliphatic substrates. They reported activation using an acridinium photocatalyst **4.69**, phosphate salt and blue light followed by trapping with a variety of radical acceptors **4.66–4.68** (Table 4.4). This allowed for the direct diversification of C–H bonds into new C–N, C–S, C–X and C–C bonds. Application of this methodology on substituted and unsubstituted adamantanes with highly oxidizing acridinium photocatalyst **4.69** was used to oxidatively generate oxygen-centered phosphate radicals capable of doing C–H abstraction of aliphatic compounds. When using an aryl substituted adamantane with 3-butenone **4.66**, product **4.70e** (a precursor to the acne medication adapalene) was formed in 45% yield. This reactivity

extended beyond Giese type reactions to non-alkene acceptors such as 4-(trifluoromethyl)benzenesulfonyl azide **4.67** and *N*-fluorobenzenesulfonimide (NFSI) **4.68**. *N*-phthalimidyl memantine underwent fluorination to give fluorinated product **4.70c** in 86% yield while azidation to **4.70b** was possible with 55% yield. Unsubstituted adamantane was also converted to azide **4.70a** in 75% yield.

4.4.3 - Non-Photochemical Alkene Additions

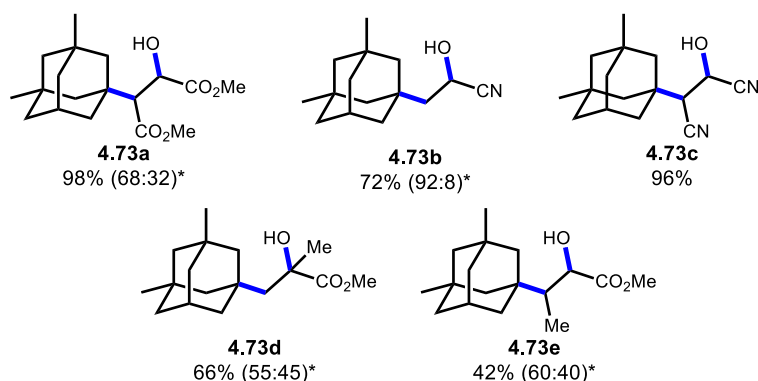
While Giese-type additions using photochemical methods are prevalent, other methods for accomplishing these additions have also been developed. A catalytic oxyalkylation of alkenes with adamantanes and other alkanes was reported by Ishii et.al.^[59] in 2001 using the PINO radical as the reactive intermediate with a cobalt co-catalyst in the presence of molecular oxygen. This reaction resulted in both oxyalkylated products in both the hydroxylated and carbonylated oxidation state (**Scheme 4.13**, top). Under optimized conditions, methyl fumarate **4.71** and adamantane gave 98% conversion with a 78% yield (71:29 ratio of hydroxy product **4.72** and ketone product **4.72'**). A variety of alkenes were also tested using dimethyl adamantane with yields ranging from modest to excellent however, in most cases, a mixture of products was observed (**Scheme 4.13**, **4.73a-e**).

A proposed mechanism is summarized in **Scheme 4.14**. These reactions are thought to be initiated by a single-electron transfer event to Co(acac)₃ to give a Co^{II} species that



Alkene Scope

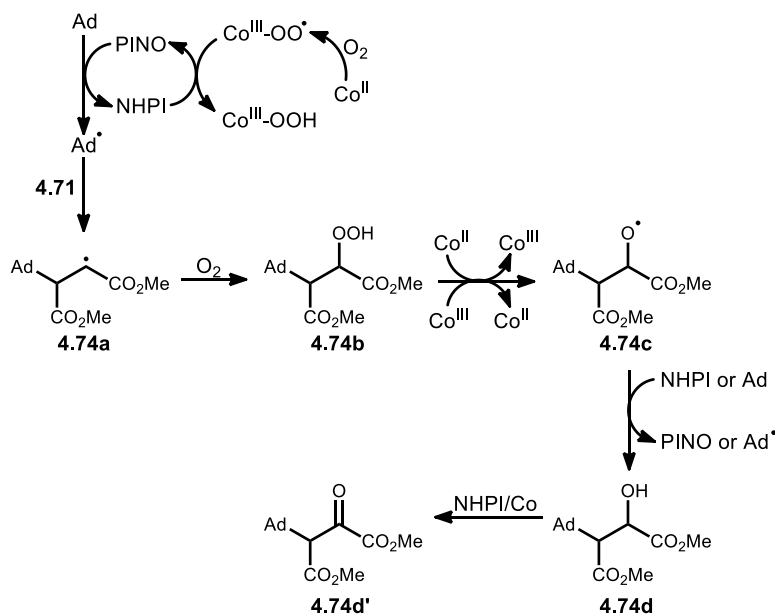
* α -hydroxy: α -keto ratio



Scheme 4.13 – Oxyalkylation of alkenes using Adamantane and O₂

undergoes reaction with O₂ to form a Co^{III}-OO[•] complex. HAT from NHPI to this oxygenated cobalt complex generates the incipient PINO radical and a cobalt hydroperoxide. PINO then goes on to generate the adamantyl radical via another HAT process. Adamantyl radical addition into alkene **4.71** affords alkyl radical intermediate **4.74a**, and is quickly trapped by O₂ with subsequent HAT from NHPI (or adamantane) leading to hydroperoxide **4.74b**. This hydroperoxide then undergoes decomposition by Co ions giving the alkoxy radical intermediate **4.74c**. Additional HAT from either NHPI or adamantane yields the hydroxylated product **4.74d**. Further oxidation to **4.74d'** is then possible in the presence of Co(acac)₃, NHPI, and O₂.

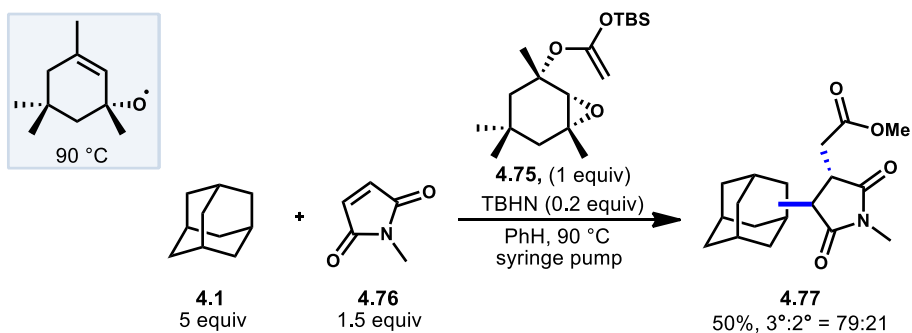
Proposed Mechanistic Summary



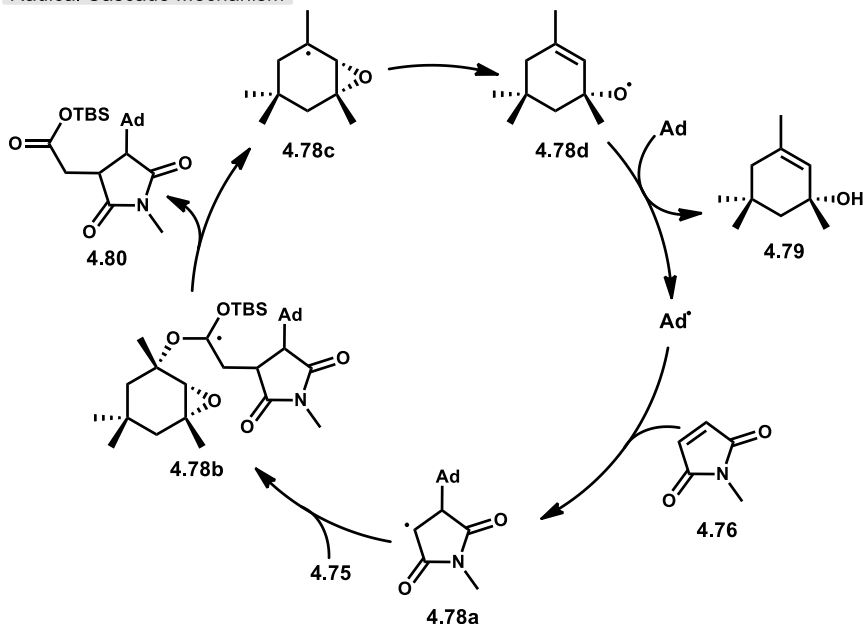
Scheme 4.14 – Mechanism for Co-Catalyzed Oxyallylation of Alkenes

A fascinating metal free radical-chain functionalization was investigated using oxiranylethylcarbinyl derivative **4.75** by Roberts and coworkers.^[60] Previously, Roberts used an analogue of this reagent as a source of allyloxy radicals with the intention of doing direct C–H abstraction.^[61] The reaction of interest involved excess adamantane, di-*tert*-butyl hyponitrite (TBHN) as a radical initiator, “acetal reagent A” **4.75**, and *N*-methylmaleimide (NMM) **4.76** as the acceptor (**Scheme 4.15**). With adamantane, a mixture of **4.77** isomers was obtained with a combined yield of 50% in a 79:21 regiochemical ratio favoring the tertiary position. Product formation proceeds as part of a complex radical cascade enabled by acetal reagent A. Following the initial formation of the adamantyl radical via TBHN, addition into NMM gives radical intermediate **4.78a**. Subsequent addition into acetal reagent A generates acetal radical **4.88b**, then fragments into silyl ester **4.80** and α -epoxy radical **7.78c**. Radical epoxide ring opening then gives oxyl radical **4.78d** and propagates

the reaction via HAT with adamantane. This particular acetal was used due to the commercial availability of starting material, isophorone oxide, and its inability to undergo undesirable rearrangements once the radical intermediate is generated.



Radical Cascade Mechanism

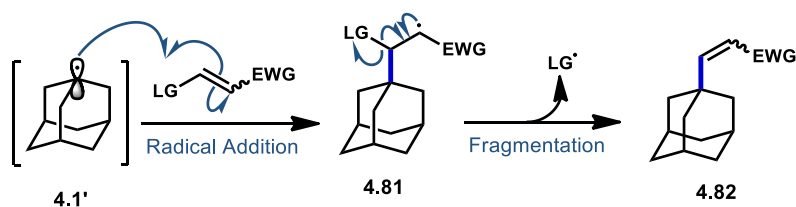


Scheme 4.15 – Metal-free Radical Addition Cascade with an Oxiranylcarbinyll Derivative

4.5 - Addition-Fragmentation

The addition-fragmentation sequence is well represented in the realm of radical chemistry^[62] and this mode of reactivity has been reported in a variety of cases involving the adamantyl radical. This process begins by using some means of C–H abstraction to

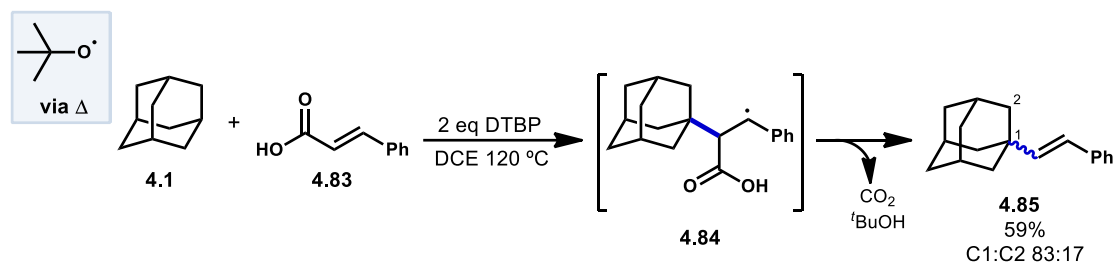
generate a reactive adamantyl radical (**Scheme 4.16, 4.1'**). This radical then adds into an appropriate radical accepting species leading to β -adamantyl radical intermediate (**4.81**). Common radical acceptors will feature an electron withdrawing group to aid in stabilizing radical intermediate **4.81** as well as a leaving group that promotes a facile fragmentation immediately following addition.



Scheme 4.16 – A General Addition-Fragmentation Sequence

4.5.1 - Decarboxylative Alkenylation

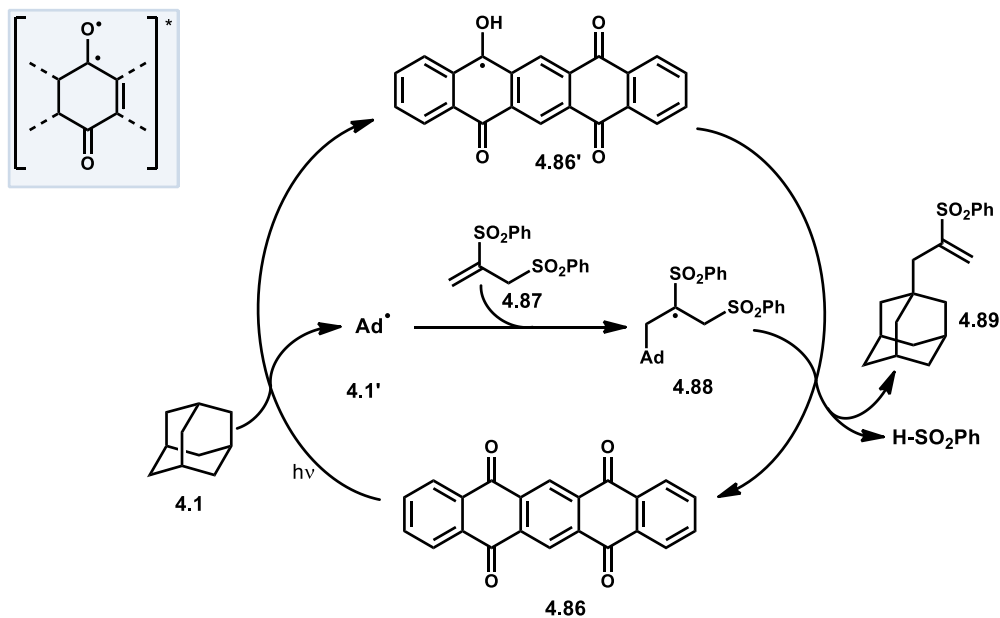
Sun et al. demonstrated that styrenyl adamantanes (**4.85**) can be made using cinnamic acids (**4.83**) in the presence of di-*tert*-butyl peroxide (DTBP) and heat (**Scheme 4.17**).^[63] In this case, homolytic thermolysis of DTBP results in *tert*-butoxy radical that acts as the C–H abstractor giving rise to the reactive adamantyl radical. This reaction is then thought to proceed through a decarboxylative fragmentation of **4.84** following the initial radical addition with loss of carbon dioxide. This addition-fragmentation process is selective for the tertiary adamantyl position, favoring it over the secondary position in an 83:17 ratio.



Scheme 4.17 – Decarboxylative Alkenylation of Adamantane with Cinnamic Acid

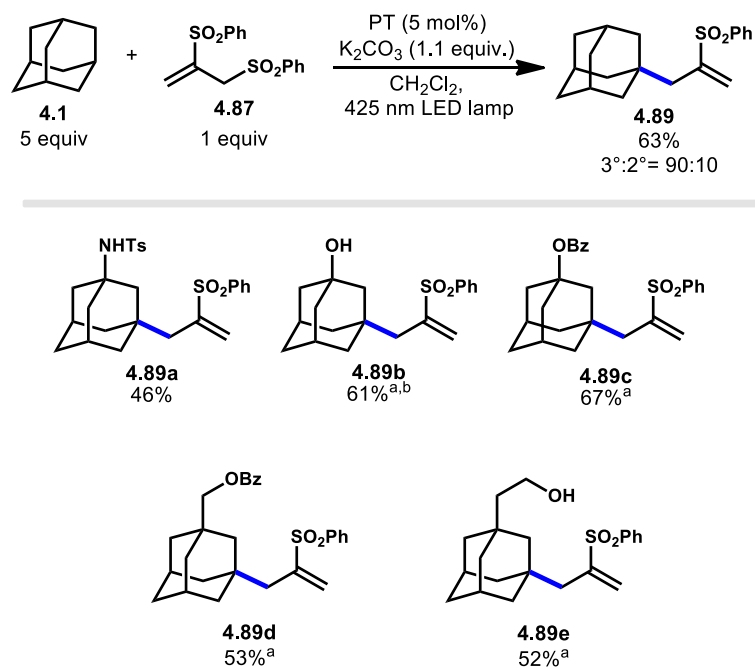
4.5.2 - Allylation

Adamantyl allylation has been demonstrated using 1,2-bis(phenylsulfonyl) propene as an allylating agent.^[64] The adamantyl radical is generated using 5,7,12,14-pentacenetetraone (PT, **4.86**, **Scheme 4.18**). The excited state generated by irradiating the PT catalyst has triplet biradical-type reactivity and is a competent C–H abstractor leading to semiquinone form, **C**.^[65–67] Adamantyl radical **4.1**' then intercepts bis-sulfonylated propene **4.87** to generate radical intermediate **4.88**. Fragmentation and re-oxidation of the PT catalyst results in allylated adamantyl sulphone product, **4.89**. Under these conditions, **4.89** was isolated in 63% yield with the allylated methine being favored in a 9:1 ratio over the methylene position. These conditions were also tolerated by a range of substituted adamantanes as shown in **Table 4.5**. Using substituted adamantanes **4.89a-e** generally favored C–H abstraction at one of the remaining methine positions in a ratio of >95:5.



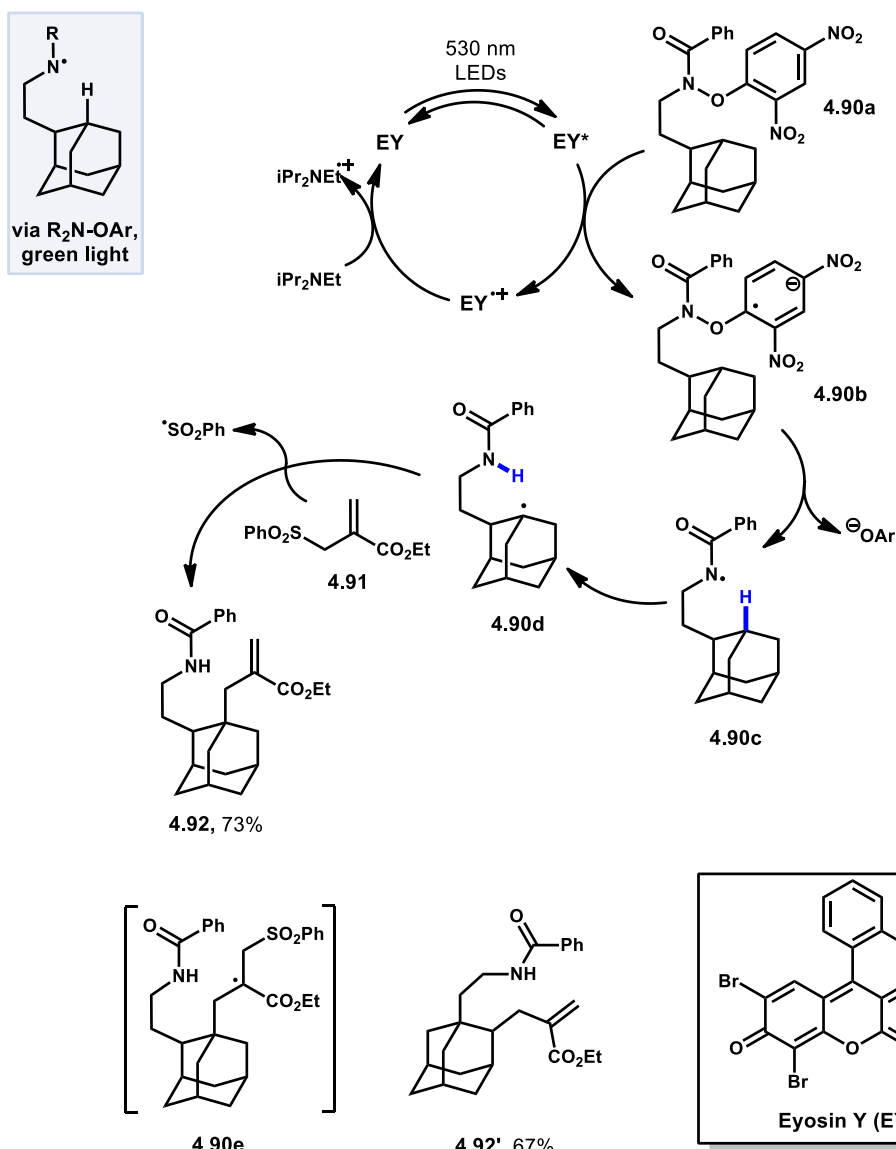
Scheme 4.18 – Photocatalytic Allylation of Adamantane with Sulfonylated Propene

Table 4.5 – Scope of Photocatalytic Allylation With Substituted Adamantanes



^aless than 4% of the methylene addition product observed. ^bran without use of K_2CO_3 .

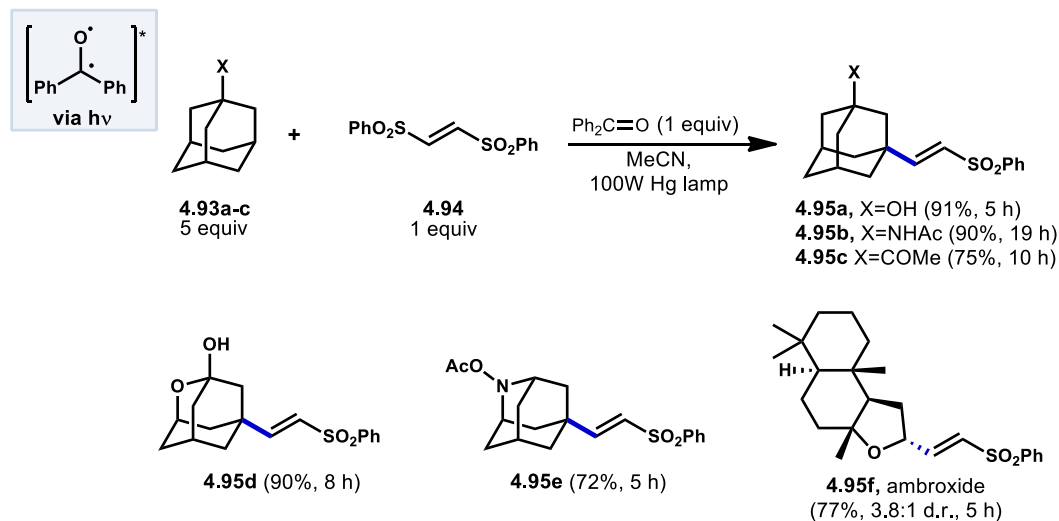
Wang and coworkers recently developed a method for the directed allylation of adamantane using a remote amidyl radical.^[47] This remote amidyl radical is generated photocatalytically using green LEDs to excite eosin Y (EY) and enables SET to a prefunctionalized adamantane featuring di-nitroaryloxy amide **4.90a** (Scheme 4.19). The resulting radical anion, **4.90b**, then fragments to give the key amidyl radical **4.90c**. Similar to a Hofmann–Löffler–Freitag reaction, remote amidyl radical **4.90c** was used to generate the adamantyl radical **4.90d** via a 1,5 H-atom abstraction.^[68] Interception of allyl sulfone **4.91** by the adamantyl radical and subsequent fragmentation of **4.90e** gives the final allylated adamantane **4.92**. Two features of this reaction are noteworthy. The first is the use of green light in the eventual production of the adamantyl radical, which is not typical due to the relatively high energy needed for the homolysis of C–H bonds. However, the use of the pre-functionalized hydroxamic acid derivative to generate the amidyl radical intermediate circumvents this issue and the reaction is possible without the need for the more commonly seen near-UV light used in C–H activation. Second is the reaction’s ability to regioselectively target the generation of either the 3° or 2° adamantyl radical. Since the radical is generated via a 1,5 intramolecular HAT, which is much faster than 1,6-HAT, its location is dictated by the amidyl substituents point of attachment to adamantane. In this way, the position of the adamantyl radical can be controlled by the choice of the pre-functionalized adamantane is used, leading to one of the two allylated product regioisomers (**4.92** or **4.92'**).



Scheme 4.19 – Photochemical Allylation Using an Amidyl Radical Cascade

4.5.3 - Photochemical Alkenylation

Addition/fragmentation sequences work well in the preparation of alkenylated adamantyl derivatives through the formation of a new $C(sp^3)-C(sp^2)$ bond. Inoue and Kamijo used benzophenone for the photochemical alkenylation of substituted adamantanes using *trans*-1,2-bis(phenylsulfonyl)ethylene **4.94** (Scheme 4.20) to give corresponding



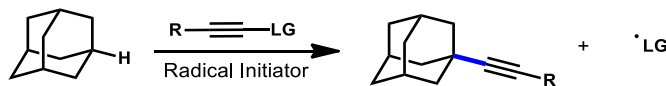
Scheme 4.20 – Photochemical Alkenylation of Substituted Adamantanes

sulfonyl-alkenylated adamantanes (**4.94a-e**). Substituted adamantanes **4.93a-c** proceeded with high selectivity for the methine positions with good yields in MeCN under irradiation from a 100W mercury lamp. The presence of proximal heteroatoms (X=O, N) typically activate adjacent C(sp³)-H bonds through hyperconjugation with the nearby lone pair.^[69] The C(sp³)-H bonds of heteroatom-substituted carbons are therefore typically selectively abstracted over other aliphatic positions as seen in ambroxide (**4.95f**). Interestingly, oxa- and azaadamantanes (**4.95d** and **4.95e**, respectively) were the only exceptions to this rule amongst the heteroatom bearing substrates tested by Inoue and Kamijo. Presumably this is because no hyperconjugation between the lone pair and C-H bond can occur with the rigid cage-like structure of adamantane.^[70]

4.6 - Alkynylation

Alkynes are valuable building blocks in organic synthesis and are important structural linkers in both materials science and chemical biology.^[71,72] The use of pre-functionalized substrates^[73,74] or transition metal-catalyzed alkynylations^[75-78] have been

extensively reported. However, metal-free conditions are of interest due to the current necessity of developing “greener” reactions.

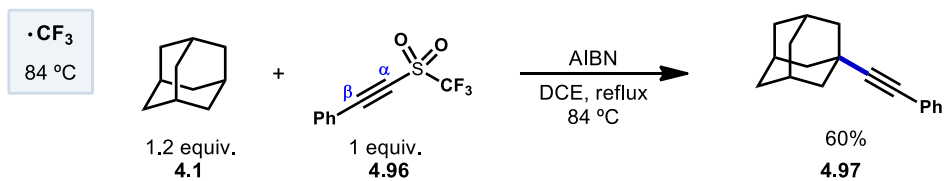


Scheme 4.21 – General Radical Alkynylation

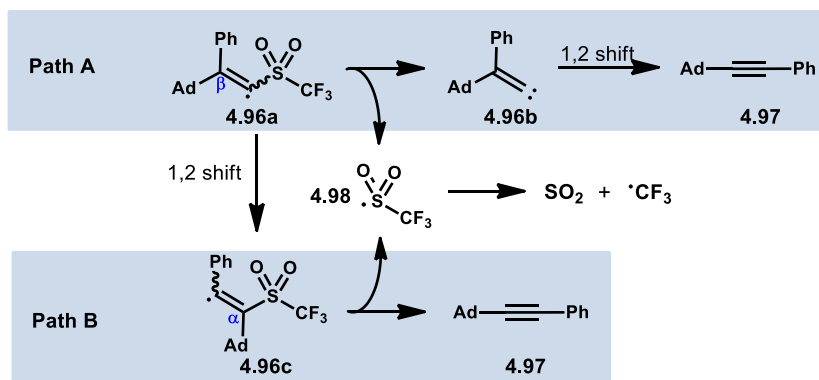
Alkynylations of adamantane can also be accomplished in both metal-free and metal-mediated radical processes and result in formation of a new C(sp³)–C(sp) bond. These reactions typically involve using a sufficiently electron deficient alkyne in the presence of a radical initiator (**Scheme 4.21**). Alkynes undergoing this kind of reaction often feature a leaving group that is involved in an addition-fragmentation sequence. In this fragmentation, the radical leaving group is ejected and usually propagates the reaction.

4.6.1 - Metal-Free Alkynylations

An early example of a metal-free alkynylation was reported by Fuchs using an alkynyl triflate to alkynylate of a variety of C–H bonds, including adamantane (see **Scheme 4.22**).^[79,80] Using AIBN and heat for initiation followed by subsequent adamantyl radical formation, the tertiary alkynylated adamantane was obtained in 60% yield. The authors note the possibility of two possible mechanistic pathways depending on



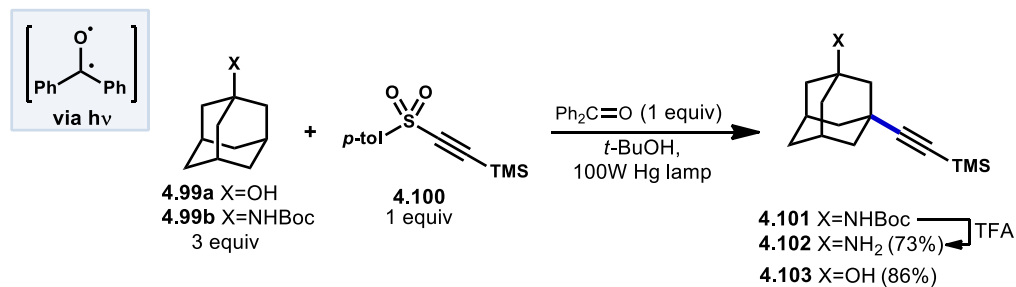
Possible Mechanistic Pathways



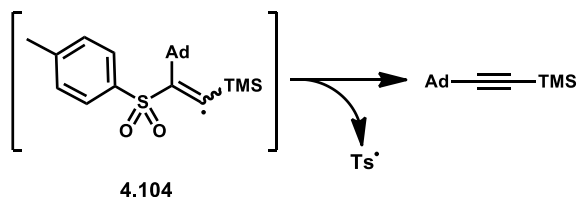
Scheme 4.22 – Alkenylation of Adamantane Using Alkynyl Triflones

the regiochemistry of the initial adamantyl radical addition to the alkyne. In the case of β -addition (Path A), vinyl sulfonyl radical **4.96a** undergoes homolytic fragmentation to give vinylidene carbene **4.96b**, and (trifluoromethyl)sulfonyl radical **4.98**. Once formed, vinylidene carbene **4.96b** undergoes a Fritsch–Buttenberg–Wiechell rearrangement^[81] to the alkenylated product. Alternatively, α -addition to the alkyne or a 1,2-shift from **4.96a** affords β -vinylsulfonyl radical **4.96c**. This intermediate then also loses (trifluoromethyl)sulfonyl radical to form the product. In both cases the transient (trifluoromethyl)sulfonyl radical undergoes further fragmentation to sulfur dioxide and trifluoromethyl radical to propagate the reaction.

Alkynylative transformations of substituted adamantanes using metal-free photocatalytic methods have also been demonstrated using tosyl-(trimethylsilyl)acetylene



Product Forming Step

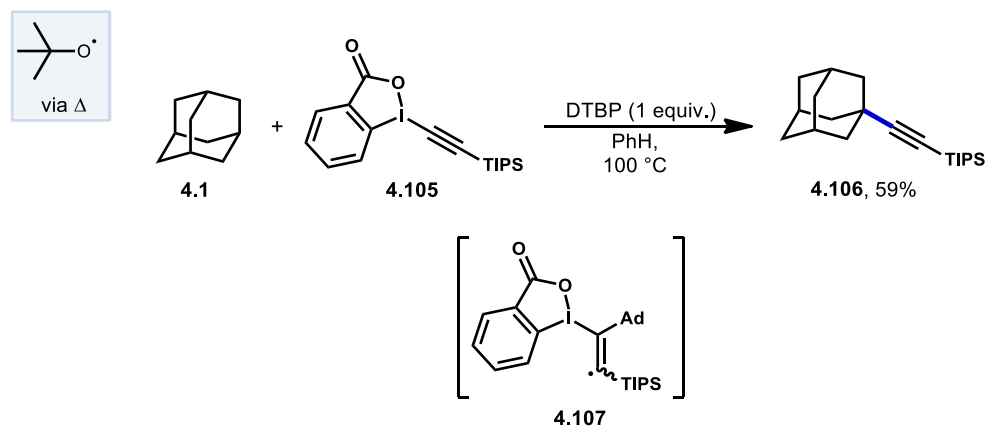


Scheme 4.23 – Photoinduced Alkynylation Using Tosyl-(trimethylsilyl)Acetylene

4.100 with benzophenone and a mercury lamp (Scheme 4.23).^[82] Upon excitation with UV light, an electrophilic oxyl radical is generated and abstracts a hydrogen atom from the tertiary position of adamantane generating the adamantyl radical. This intermediate then reacts with the electron-deficient alkyne and subsequent release of the toluenesulfinyl radical from alkenyl intermediate **4.104** generates the alkynylated adamantyl product. Under these conditions 1-adamantanol **4.99a** and Boc-protected adamantine **4.99b** were alkynylated in good yield.

Xu and coworkers investigated an efficient method for the direct alkynylation of substrates containing unactivated C(sp³)-H bonds under metal-free conditions using an ethynyl benziodoxole reagent (**4.105**, Scheme 4.24).^[83] When adamantane was used, C-H functionalization was selective for the tertiary position over the secondary and a 59% yield was reported for adamantyl product **4.106**. When performed in the presence of radical trapping agent TEMPO, the reaction was completely suppressed and the alkyl-TEMPO

product was observed, suggesting the reaction proceeds via an alkyl radical intermediate. A plausible mechanism begins with generation of the *tert*-butoxyradical from homolytic cleavage of di-*tert*-butylperoxide (DTBP) and then reacts with adamantane giving the adamantyl radical. This is followed by addition to the triple bond of the hypervalent iodine reagent to form radical intermediate **4.107**, which after subsequent β -elimination gives the final alkynylated product.

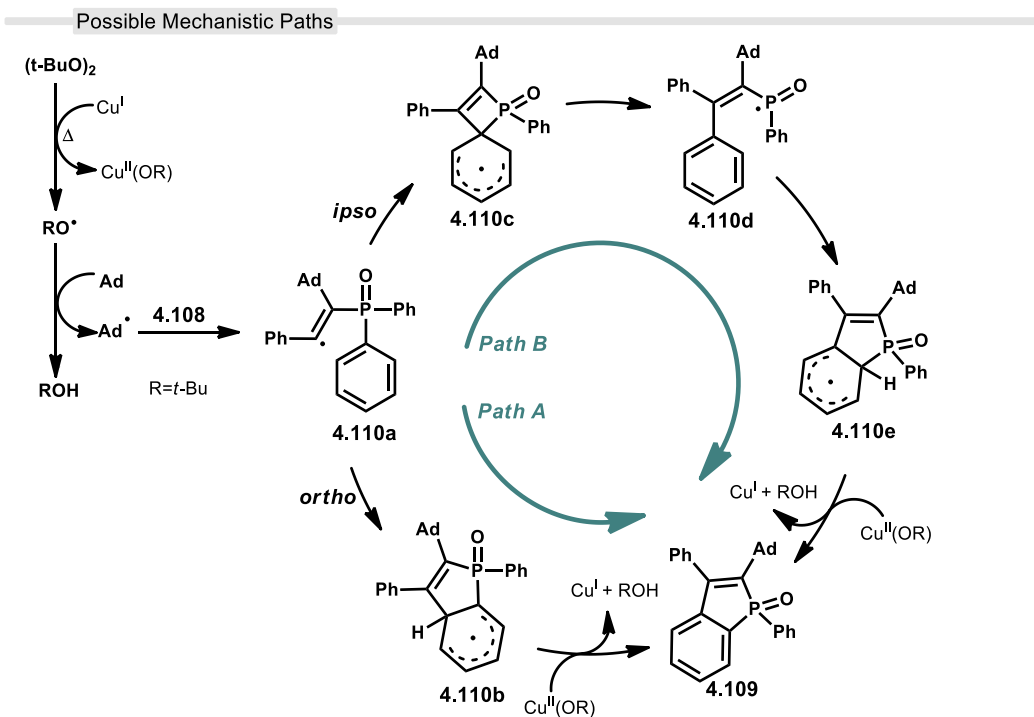
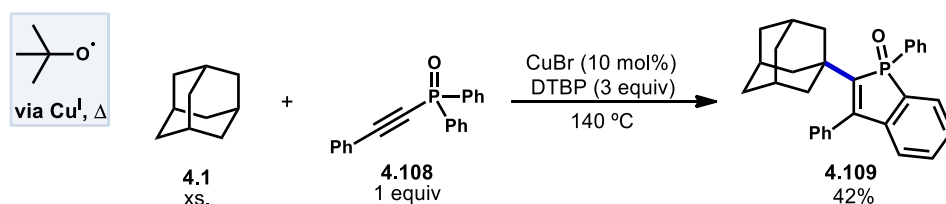


Scheme 4.24 – Radical Alkynylation Using an Ethynyl Benziiodoxole

4.6.2 - Metal-Catalyzed Alkynylation

A metal-mediated radical addition/cyclization of various unactivated cycloalkanes including adamantane with diaryl(arylethynyl)-phosphine oxides using copper was reported by Zhao et al. in 2018 (Scheme 4.25).^[84] The cyclic benzo[*b*]phosphole oxides products form from two sequential C–H abstractions and the formation of two new C–C bonds. The initial *tert*-butoxyl radical is formed after the Cu^I assisted homolysis of DTBP with heating. The adamantyl radical addition into alkyne **4.108** results in the key alkenyl radical intermediate **4.110a**. This radical can then follow two regiochemically determined paths both leading to the same product. In Path A ortho addition of the alkenyl radical leads

to aryl radical **4.110b**. In Path B, ipso addition of the alkenyl radical results in the 4-membered spirocyclic intermediate **4.110c**, which fragments to give phosphorus-centered radical **4.110d**. Ortho addition of the phosphorus radical gives radical **4.110e**, which in either pathway can be dehydrogenated with $\text{Cu}^{\text{II}}(\text{O}t\text{-Bu})$ to give the product and regenerate Cu^{I} .

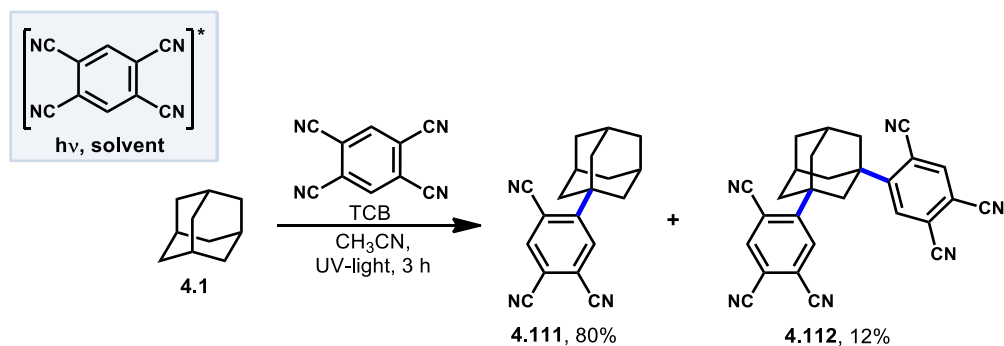


Scheme 4.25 – Alkyne Addition-Cyclization Using Alkynyl Diphenylphosphine Oxides

4.7 - Arylation

4.7.1 - Photooxidations Using TCB

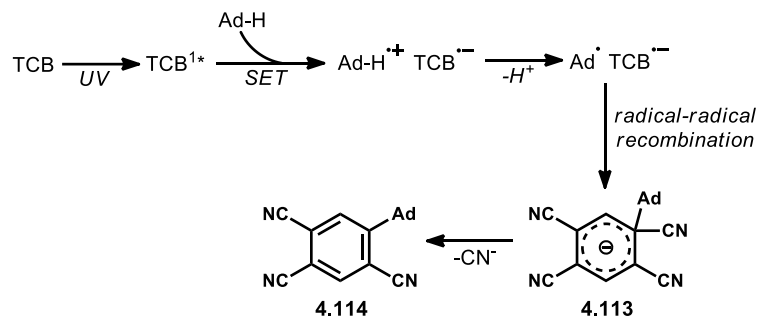
In 1996, Albini et al. used 1,2,4,5-benzenetetracarbonitrile (TCB) under UV-light to arylate adamantane.^[85,86] The mono-arylated product **4.111** was predominantly formed exclusively at the tertiary position while the bis-arylated product **4.112** was formed to a lesser degree (**Scheme 4.26**). Under UV-light Albini had previously shown that TCB in its singlet state is a strong oxidant capable of inducing SET from a variety of alkanes.^[87] After oxidation, an adamantyl radical cation/TCB radical anion pair is generated (**Figure 4.7**, top). The adamantyl radical cation then loses a proton to solvent to create the tertiary adamantyl radical that then quickly recombines with the radical anion of TCB to form aryl intermediate **4.113**. Re-aromatization through the loss of cyanide then gives the arylated adamantyl product **4.114**.



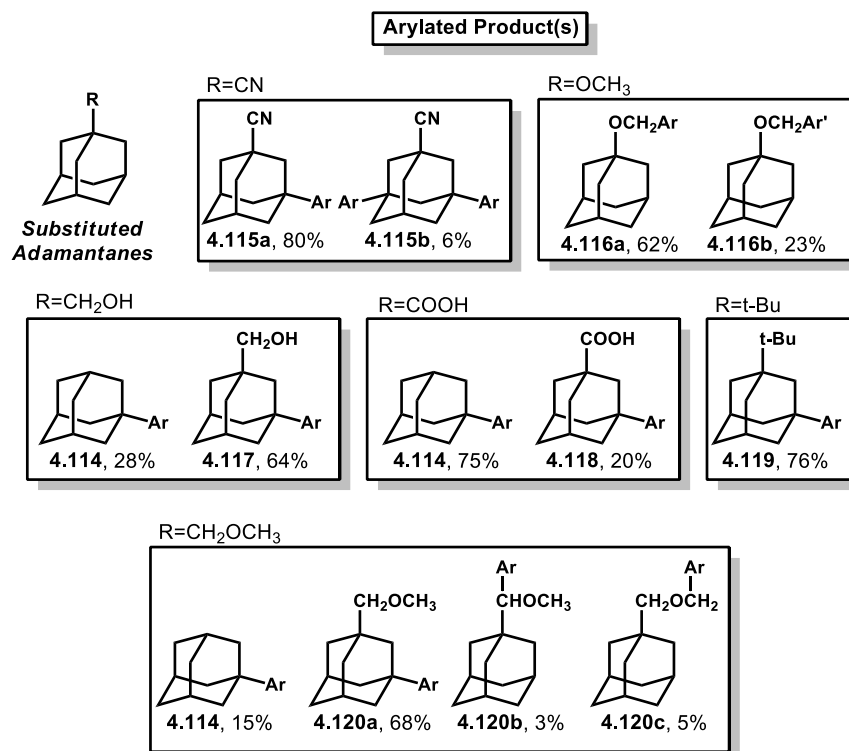
Scheme 4.26 – UV Arylation of Adamantanes Using TCB

Additionally, several substituted adamantanes were also tried (**Figure 4.7**, bottom) resulting in the formation of a varied array of products. 1-*tert*-Butyladamantane formed monoarylated product **4.119** exclusively. Mixtures of products were formed with

Mechanism for TCB Arylation



Scope with Substituted Adamantanes



Ar=2,4,5-tricyanophenyl
Ar'=2,3,4,5-tetracyanophenyl

Figure 4.7 – Mechanism and Scope for TCB Arylation of Adamantane

other substituents. Like unsubstituted adamantane, 1-adamantanecarbonitrile also resulted in formation of mono- and bis-arylated products (**4.115a, b**). 1-Methoxyadamantane reacted differently, with C–H abstraction at the methyl group rather than on the adamantyl moiety, giving two aryl ethers, with both tri- and tetra- benzenecarbonitrile products being

observed (**4.116a, b**). 1-Adamantylmethanol underwent monoarylation to **4.117**. Some substituent elimination was also observed leading to product **4.114**. Similarly, monoarylation of 1-adamantylmethyl methyl ether also proceeded with some substrate elimination, along with substitution on the sidechain (**4.120b, c**) also occurring in small amounts. 1-Adamantanecarboxylic acid proceeded mostly with decarboxylation to monoaryl adamantane product **4.114** with a minor amount retaining the carboxy group (**4.118**). Work by Schreiner, Fokin, and coworkers showed that arylation with TCB on higher order diamondoids (**4.121-4.124**) proceeds with 100% apical selectivity (**Figure 4.8**).^[10,88,89] Arylation beyond pentamantane has not been investigated.

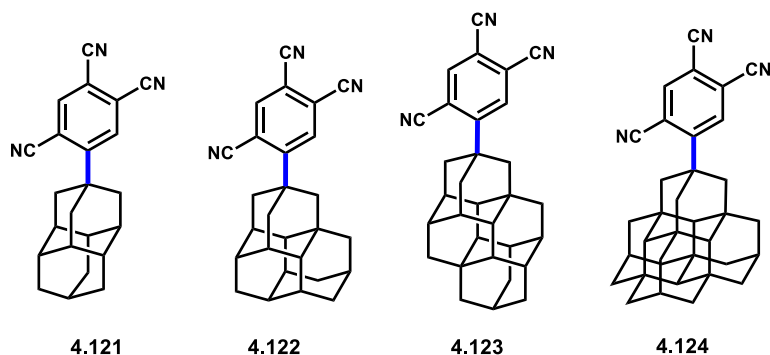
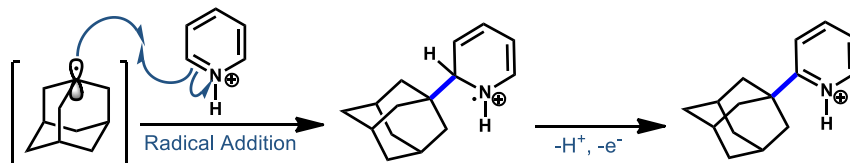


Figure 4.8 – TCB Arylation of Higher Order Diamondoids

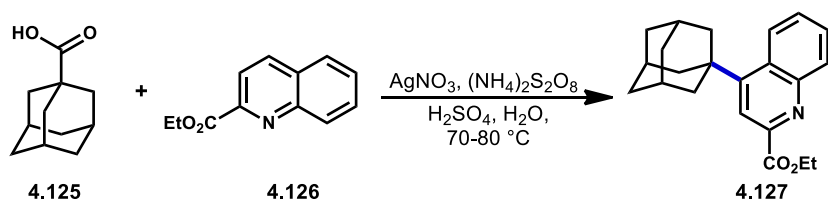
4.7.2 - Minisci-Type Arylations



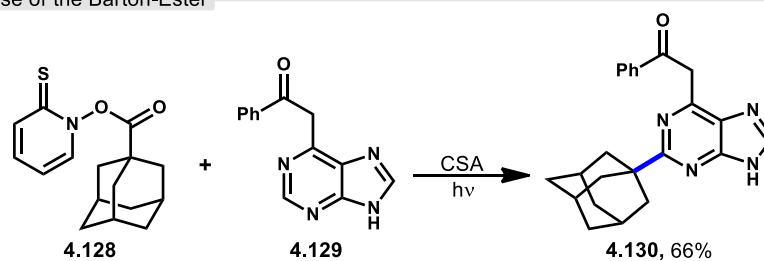
Scheme 4.27 – General Minisci Arylation Involving Adamantane

Minisci reactions like the one shown in **Scheme 4.27** are characterized by the addition of an alkyl radical to electron deficient heteroaromatic compound in an overall C–H to C–C substitution.^[90] Heteroaromatic adamantane containing nucleoside analogs have been known to possess antiherpetic^[91] and antifolate^[92] activity and can be synthesized using these Minisci-type reactions. Traditionally these reactions have used stoichiometric ammonium persulfate and silver nitrate to induce an oxidative decarboxylation to generate the alkyl radical.^[93] This decarboxylative approach was taken in the preparation of **4.127**, an adamantane containing antituberculosis precursor as shown in **Scheme 4.28**, top.^[94] Adamantane was also used in early work by Barton for the alkylation of caffeine and other purines with camphorsulfonic acid (CSA).^[95,96] Since then, several methods have been developed that are metal-free and/or do not rely on pre-functionalized adamantanes to arrive at the adamantyl radical intermediate. In 2013, Antonchick and coworkers developed a Minisci-type arylation reaction using a selective oxidative cross-coupling approach.^[97] One example, shown in **Scheme 4.29**, shows the arylation of adamantane using 4,7-dichloroquinoline in the presence of [bis(trifluoroacetoxy)iodo]benzene (PIFA) as oxidant and NaN₃, as a critical additive. The key H-atom abstractor is likely the azide radical and the corresponding arylated product **4.132** was obtained in an 84% yield as a single isomer. Overall, Antonchick et al. used this metal-free oxidative cross-coupling approach of heteroarenes and alkanes to obtain arylated products under mild, non-acidic conditions, with short reaction times and in high yields.

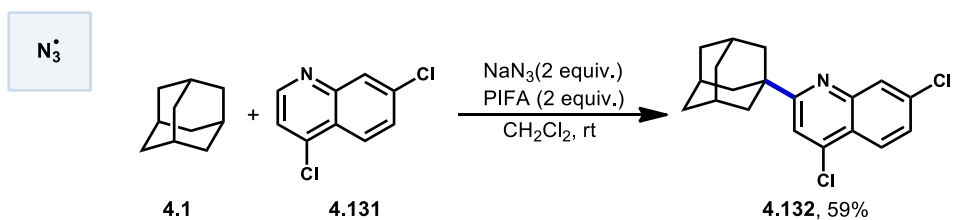
Direct Radical decarboxylation



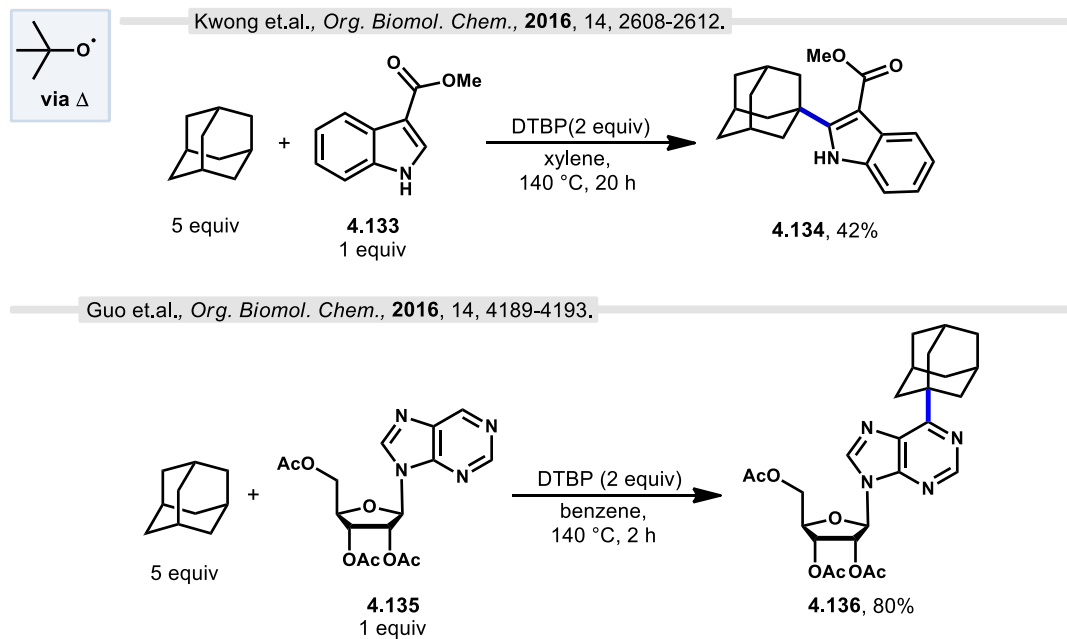
Use of the Barton-Ester



Scheme 4.28 – Early Minisci Arylations of Adamantane



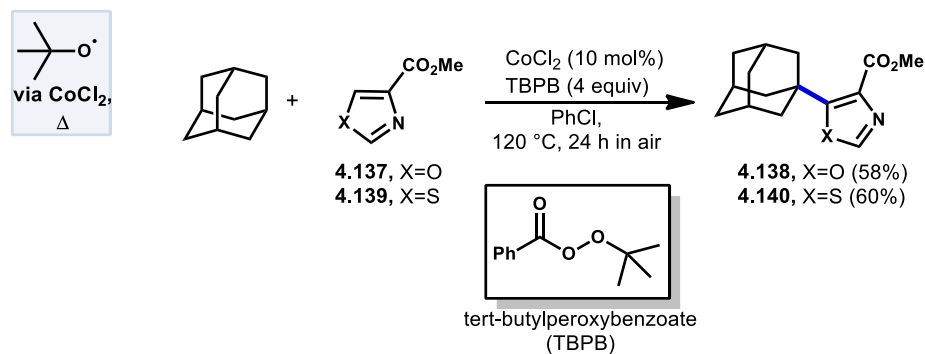
Scheme 4.29 – Oxidative Azide-Assisted Minisci Reaction with Adamantane



Scheme 4.30 – Use of DTBP in Minisci Reactions with Indoles and Purines

Kwong et al. and Guo et al. have also shown that DTBP can enable the oxidative cross-coupling of adamantane with indoles^[98] and purine nucleosides^[99] under similar reaction conditions (**Scheme 4.30**). Both methods were developed using neat cycloalkanes or cyclic ethers but the use of aromatic solvent such as xylene or benzene was required when using adamantane in order to dissolve it. In both cases, an excess of five equivalents of adamantane was enough for the reaction to proceed with moderate to good yield.

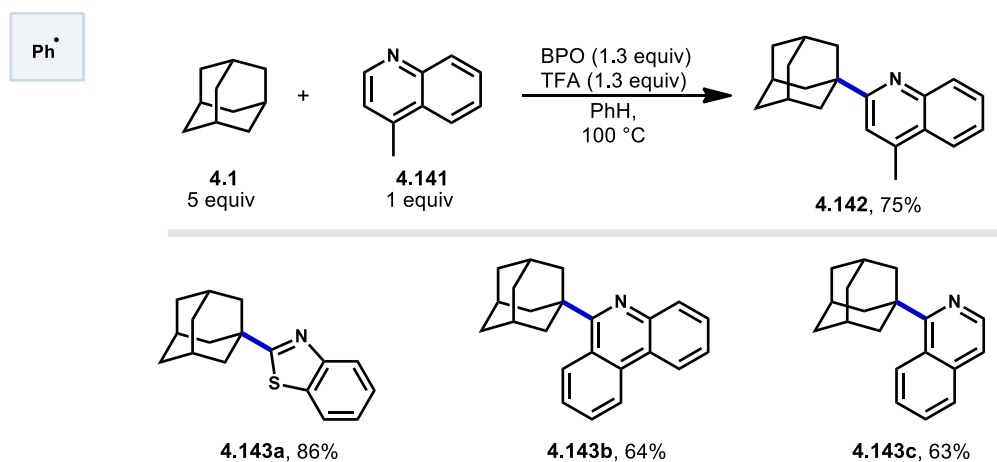
More recently in 2017, Li et al. also found the *tert*-butoxy radical was effective for oxidative cross-couplings of adamantane with oxazoles and thiazoles (**Scheme 4.31**).^[100] The *tert*-butoxy radical does not originate from DTBP and instead comes from the homolysis of *tert*-butylperoxybenzoate (TBPB) and uses catalytic cobalt(II) chloride to assist in radical generation through the formation of a cobalt(III) benzoate.



Scheme 4.31 – Cobalt-Catalyzed Cross-Couplings with Oxazoles and Thiazoles

Togo et al. showed that the introduction of heteroaromatic bases onto hydrocarbons can also be accomplished using benzoyl peroxide (BPO) in the absence transition metals and under irradiation free conditions (Table 4.6).^[101] When 5 equivalents of adamantane, 1.3 equivalents of BPO and trifluoroacetic acid in benzene was treated with the nitrogen containing compound lepidine (4.141), the desired methylquinoline product 4.142 was obtained in 75% yield. Other heteroaromatic bases also produced the arylated product in good yields (4.143a-c; 63%-86%). The reactive phenyl radical formed from BPO after undergoing decarboxylation abstracts a hydrogen from adamantane generating the

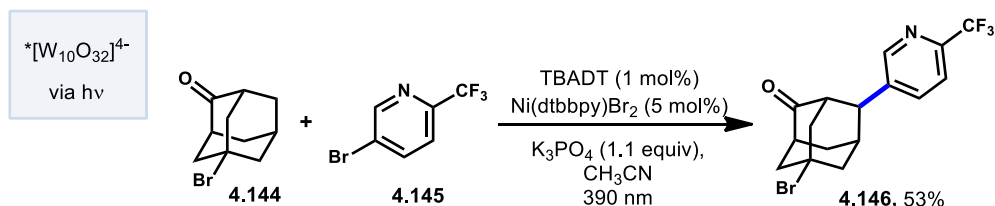
Table 4.6 – Arylation of Adamantane with Heteroaromatic Bases Using BPO



adamantyl radical. Subsequent nucleophilic radical addition to the protonated heteroaromatic base then occurs. After quenching with aqueous NaHCO_3 , the desired arylated product is obtained.

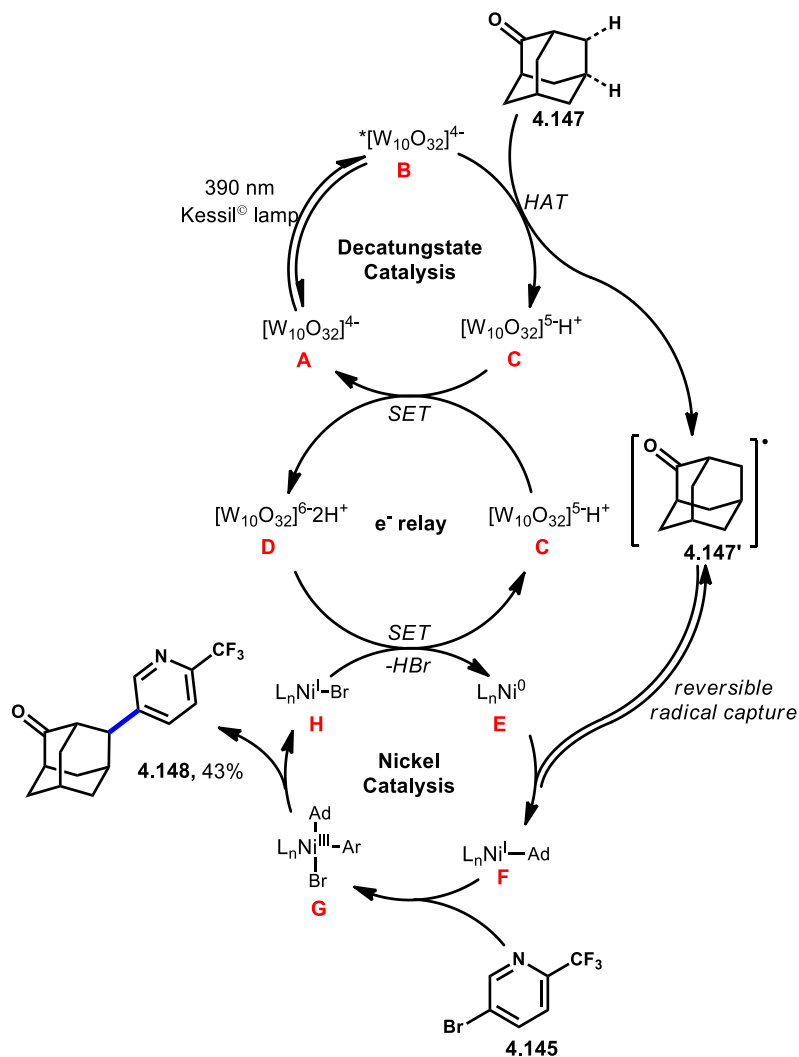
4.7.3 - Dual Catalytic Arylation

In 2018, another direct arylation was performed by MacMillan and coworkers using a dual catalytic system with decatungstate and a nickel catalyst (**Scheme 4.32**).^[102] Adamantane derivatives underwent arylation predominantly at the methylene position for both bromo-adamantanone (**4.144**) and 2-adamantanone (**4.147**) to give products **4.146** (53% yield) and **4.148** (48% yield), respectively. Interestingly, MacMillan and coworkers observed selective arylation at the methylene position of adamantane despite existing precedent that decatungstate-catalyzed functionalization occurs in a 1:1.3 ratio (refer to **Scheme 4.6**) only slightly favoring the methylene position.



Scheme 4.32 – Arylation of Bromo-adamantanone Using Ni/TBADT Catalysis

This difference in regioselectivity can be rationalized via reversible radical capture during nickel-catalysis with the selectivity being imparted by a preference for reductive elimination of the 2° aryl adamantane product.^[103] The proposed mechanism shown in **Scheme 4.33** begins with the photoexcitation of TBADT **A** followed by intersystem crossing giving the triplet excited state **B**. This is followed by HAT from a hydrocarbon



Scheme 4.33 – Adamantanone Arylation via Nickel/Decatungstate Dual Catalysis

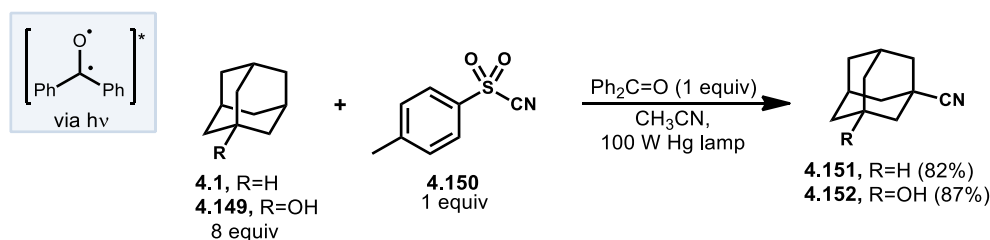
like adamantanone **4.147** by the excited TBADT catalyst ultimately reducing the catalyst to **C** and generating the adamantyl radical **4.147'**. A disproportionation event involving the singly reduced decatungstate **C** would regenerate the active HAT catalyst and form a doubly reduced decatungstate species **D**. The alkyl radical is captured by Ni⁰ **E** leading to alkyl Ni^I intermediate **F**. Oxidative addition of aryl bromide **4.145** then gives the key Ni^{III} intermediate **G** and undergoes reductive elimination to yield the desired cross-coupled

arylated product **4.148**. A final single-electron transfer step and loss of HBr between the active nickel catalyst and double-reduced TBADT catalyst completes both catalytic cycles.

4.8 - Amine and Nitrile Additions

4.8.1 - Cyanation

Classically, cyanation reactions are usually thought of in terms of the nucleophilic character of simple cyanides such as KCN adding to an electrophilic reaction partner. However, over the years, a variety of electrophilic cyanation reagents have been developed^[104] and pair well with the nucleophilic character of the adamantyl radical.



Scheme 4.34 – Photo Induced Cyanation of Adamantanes Using Tosyl Cyanide

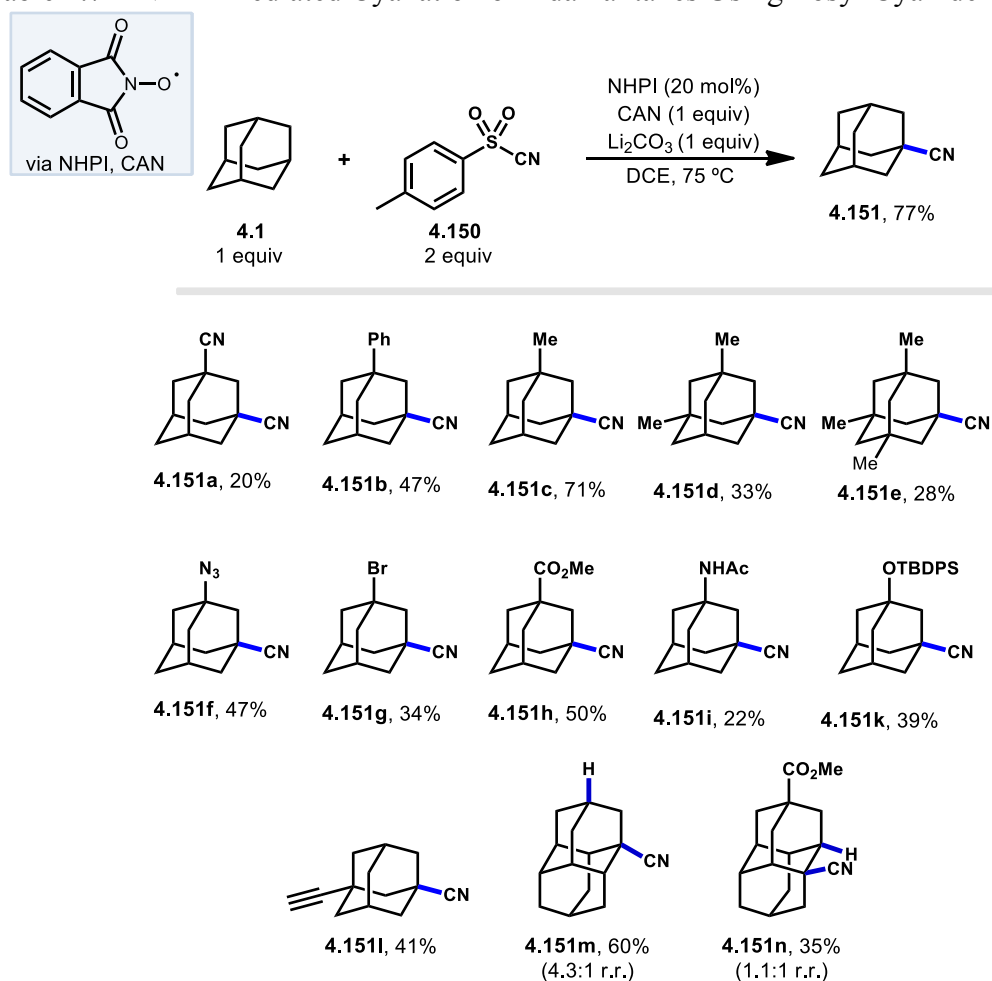
Inoue and coworkers showed that using benzophenone as a photocatalyst in conjunction with p-toluenesulfonyl cyanide (TsCN, **4.150**), adamantane and adamantanol could be cyanated in high yield (**Scheme 4.34**).^[105,106] The reaction proceeded to give exclusively the methine addition product. In this case the oxyl radical generated from excitation of benzophenone abstracts a hydrogen from the tertiary position on adamantane giving an adamantyl radical. This nucleophilic radical then goes on to react with TsCN generating the product and a sulfinyl radical. Catalytic turnover occurs with hydrogen atom abstraction by the sulfinyl radical from the ketyl intermediate giving sulfinic acid and the renewed photocatalyst. Although benzophenone was used stoichiometrically with

adamantane, the reaction proceeded when used in sub-stoichiometric quantities with other substrates such as 1,2-dioxane.

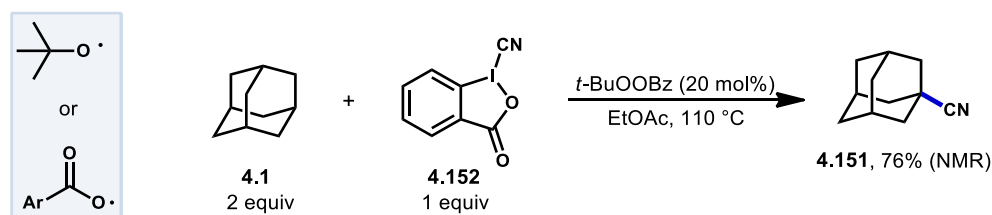
Schreiner et al. also found that using TsCN as an electrophilic cyanide source with a NHPI/PINO system effectively cyanated a variety of adamantanes and diamantanes.^[107] A few known reaction conditions were tried in order to access the PINO radical such as azobisisobutyronitrile (AIBN), Co(II/III) salts, and cerium(IV) nitrate (CAN). CAN was found to be superior in this regard giving the 1-cyanoadamantyl product **4.151** in 42% yield. The formation of significant amounts of 1-nitroadamantane as a side product was also observed with the use of CAN. The addition of base suppressed the formation of the undesired nitro product, with lithium carbonate giving the best result. Under this optimized TsCN/NHPI/CAN/Li₂CO₃ system, the cyanoadamantane was obtained in 77% yield. Other substituted adamantanes were obtained with varying degrees of success (**4.151a-n**). Notable among these reaction conditions is the use of only one equivalent of adamantane. Typically, most adamantane C–H activation reactions will use higher amounts of the adamantane in order to suppress further C–H activation of the product. The installation of the electron withdrawing cyano group deactivates the cage to further cyanation as evidenced by the difference in yield between the formation of mono- and di-cyanated products **4.151** and **4.151a**.

In 2018 Ma, Zhang and coworkers reported a metal-free cyanation reaction using a hypervalent cyanobenziodoxol reagent (**4.152**, **Scheme 4.35**).^[108] With *tert*-

Table 4.7 – NHPI-Mediated Cyanation of Adamantanes Using Tosyl Cyanide



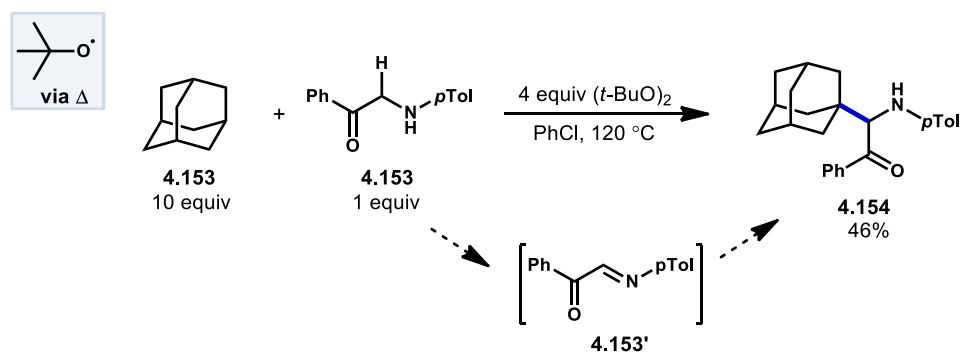
butylperoxybenzoate (TBPB) as a catalytic initiator, a very broad scope of cyclic hydrocarbons, ethers and amine derivatives underwent direct cyanation of C (sp³)–H bonds at elevated temperature, including adamantane in 76% yield as determined by ¹H NMR. The initial HAT occurs with the *tert*-butoxy or benzoyloxy radical at the most electronically activated position, while the chain-carrying radical is likely the aryloxy radical derived from 2-iodobenzoic acid. Spin-trapping and competition experiments were consistent with a radical mechanism for hydrocarbons and iminium ion.



Scheme 4.35 – Cyanation of Adamantane Using Cyanobenziodoxol

4.8.2 - Aminoalkylation

Di-*tert*-butyl peroxide (DTBP) was also used for the α -alkylation of α -amino carbonyls **4.153** with adamantane and other alkanes by Cheng et al.^[109] The *tert*-butoxy radical is thought to both facilitate the formation of the imine intermediate **4.153'** and generate the adamantyl radical that adds into the imine. Aminoalkylated product **4.154** was formed in 46% yield as a single regioisomer.



Scheme 4.36 – Aminoalkylations Using α -Amino Carbonyls

4.9 - Conclusion

Diamondoids are a special class of hydrocarbon with characteristics that have made them excellent substrates for the investigation C–H activation and HAT processes. Advances in this area continue to see improvement in terms of reaction efficiency, atom economy, and regioselectivity. A significant amount of progress has nevertheless been

achieved in this area since Schleyer's synthesis of adamantane in 1956 made the study of these reactions possible and today HAT reactions of diamondoids can be used for a variety of transformations. The focus of this chapter has been on C–C bond forming transformations including acylation, alkylation, alkenylation, alkynylation, allylation, arylation, aminoalkylation, and cyanation. However, many other transformations of adamantyl C–H bond exist and together contribute to the growing use of adamantane in a wide array of applications such as nanomaterials, catalysis and pharmaceutical agents.

4.10 - References

- (1) Landa, S.; Macháček, V. Sur l'adamantane, Nouvel Hydrocarbure Extrait Du Naphte. *Collect. Czechoslov. Chem. Commun.* **1933**, *5*, 1–5.
- (2) Shimoyama, A.; Yabuta, H. Mono- and Bicyclic Alkanes and Diamondoid Hydrocarbons in the Cretaceous/Tertiary Boundary Sediments at Kawaruppu, Hokkaido, Japan. *Geochem. J.* **2002**, *36*, 173–189.
- (3) Fort, R. C.; Schleyer, P. von Rague. Bridgehead Adamantane Carbonium Ion Reactivities. *J. Am. Chem. Soc.* **1964**, *86*, 4194–4195.
- (4) Mckerverey, M. A. Synthetic Approaches to Large Diamondoid Hydrocarbons. *Tetrahedron* **1980**, *36*, 971–992.
- (5) Prelog, V.; Seiwert, R. Über Die Synthese Des Adamantans. *Berichte Dtsch. Chem. Ges. B Ser.* **1941**, *74*, 1644–1648.
- (6) Stetter, H.; Schwarz, M.; Hirschhorn, A. Über Verbindungen mit Urotropin-Struktur, XII. Monofunktionelle Adamantan-Derivate. *Chem. Ber.* **1959**, *92*, 1629–1635.
- (7) von R. Schleyer, P. A Simple Preparation of Adamantane. *J. Am. Chem. Soc.* **1957**, *79*, 3292–3292.
- (8) Olah, G. A.; Prakash, G. K. S.; Shih, J. G.; Krishnamurthy, V. V.; Mateescu, G. D.; Liang, G.; Sipos, G.; Buss, V.; Gund, T. M.; Schleyer, P. v. R. Bridgehead Adamantyl, Diamantyl, and Related Cations and Dications. *J. Am. Chem. Soc.* **1985**, *107*, 2764–2772.
- (9) Olah, G. A.; Farooq, O. Chemistry in Superacids. 7. Superacid-Catalyzed Isomerization of Endo- to Exo-Trimethylenenorbornane (Tetrahydrodicyclopentadiene) and to Adamantane. *J. Org. Chem.* **1986**, *51*, 5410–5413.
- (10) Schreiner, P. R.; Fokina, N. A.; Tkachenko, B. A.; Hausmann, H.; Serafin, M.; Dahl, J. E. P.; Liu, S.; Carlson, R. M. K.; Fokin, A. A. Functionalized Nanodiamonds: Triamantane and [121]Tetramantane. *J. Org. Chem.* **2006**, *71*, 6709–6720.

- (11) Fokin, A. A.; Gunchenko, P. A.; Novikovskiy, A. A.; Shubina, T. E.; Chernyaev, B. V.; Dahl, J. E. P.; Carlson, R. M. K.; Yurchenko, A. G.; Schreiner, P. R. Photoacetylation of Diamondoids: Selectivities and Mechanism. *Eur. J. Org. Chem.* **2009**, *2009*, 5153–5161.
- (12) Schreiner, P. R.; Fokin, A. A.; Reisenauer, H. P.; Tkachenko, B. A.; Vass, E.; Olmstead, M. M.; Bläser, D.; Boese, R.; Dahl, J. E. P.; Carlson, R. M. K. [123]Tetramantane: Parent of a New Family of σ -Helicenes. *J. Am. Chem. Soc.* **2009**, *131*, 11292–11293.
- (13) Stetter, H.; Dieminger, K. Über Verbindungen mit Urotropin-Struktur, XIV. Komplexsalze mit Urotropin-Struktur. *Chem. Ber.* **1959**, *92*, 2658–2663.
- (14) Haaf, W. N-Formyl-Amine Aus Isoparaffinen. *Angew. Chem.* **1961**, *73*, 144–144.
- (15) Jackson, G.; Muldoon, R.; Akers, L. Serological Evidence For Prevention of Influenzal Infection in Volunteers by an Anti-Influenzal Drug Adamantanamine Hydrochloride. *Antimicrob. Agents Chemother.* **1963**, *161*, 703–707.
- (16) Wanka, L.; Iqbal, K.; Schreiner, P. R. The Lipophilic Bullet Hits the Targets: Medicinal Chemistry of Adamantane Derivatives. *Chem. Rev.* **2013**, *113*, 3516–3604.
- (17) Chu, P.-L. E.; Wang, L.-Y.; Khatua, S.; Kolomeisky, A. B.; Link, S.; Tour, J. M. Synthesis and Single-Molecule Imaging of Highly Mobile Adamantane-Wheeled Nanocars. *ACS Nano* **2013**, *7*, 35–41.
- (18) Agnew-Francis, K. A.; Williams, C. M. Catalysts Containing the Adamantane Scaffold. *Adv. Synth. Catal.* **2016**, *358*, 675–700.
- (19) Lundgren, R. J.; Stradiotto, M. Palladium-Catalyzed Cross-Coupling of Aryl Chlorides and Tosylates with Hydrazine. *Angew. Chem. Int. Ed.* **2010**, *49*, 8686–8690.
- (20) Arduengo, A. J.; Harlow, R. L.; Kline, M. A Stable Crystalline Carbene. *J. Am. Chem. Soc.* **1991**, *113*, 361–363.
- (21) Grasa, G. A.; Singh, R.; Scott, N. M.; Stevens, E. D.; Nolan, S. P. Reactivity of a N-Heterocyclic Carbene, 1,3-Di-(1-Adamantyl) Imidazol-2-Ylidene, with a Pseudo-

- Acid: Structural Characterization of Claisen Condensation Adduct. *Chem. Commun.* **2004**, No. 24, 2890–2891.
- (22) Dinger, M. B.; Niecypor, P.; Mol, J. C. Adamantyl-Substituted N-Heterocyclic Carbene Ligands in Second-Generation Grubbs-Type Metathesis Catalysts. *Organometallics* **2003**, *22*, 5291–5296.
- (23) Gunawan, M. A.; Hierso, J.-C.; Poinso, D.; Fokin, A. A.; Fokina, N. A.; Tkachenko, B. A.; Schreiner, P. R. Diamondoids: Functionalization and Subsequent Applications of Perfectly Defined Molecular Cage Hydrocarbons. *New J. Chem.* **2013**, *38*, 28–41.
- (24) Bagrii, E. I.; Nekhaev, A. I.; Maksimov, A. L. Oxidative Functionalization of Adamantanes (Review). *Pet. Chem.* **2017**, *57*, 183–197.
- (25) Newhouse, T.; Baran, P. S. If C-H Bonds Could Talk: Selective C-H Bond Oxidation. *Angew. Chem. Int. Ed.* **2011**, *50*, 3362–3374.
- (26) Tabushi, I.; Hamuro, J.; Oda, R. Chlorocarbonylation of Adamantane. *J. Org. Chem.* **1968**, *33*, 2108–2109.
- (27) Tabushi, I.; Aoyama, Y. Preparations of Some 1,2- and 1,4-Disubstituted Adamantanes. *J. Org. Chem.* **1973**, *38*, 3447–3454.
- (28) SMITH, G. W.; WILLIAMS, H. D. Some Reactions of Adamantane and Adamantane Derivatives. *J. Org. Chem.* **1961**, *26*, 2207–2212.
- (29) Tabushi, I.; Okada, T.; Aoyama, Y.; Oda, R. Product Ratio of Chlorocarbonylation of Substituted Adamantane. *Tetrahedron Lett.* **1969**, *10*, 4069–4072.
- (30) Tabushi, I.; Kojo, S.; Yoshida, Z. Photoacetylation of Substituted Adamantanes. Exclusive Bridgehead Substitution and a Large ρ Value. *Tetrahedron Lett.* **1973**, *14*, 2329–2332.
- (31) Tabushi, I.; Kojo, S.; Fukunishi, K. Mechanism of Photoacetylation of Substituted Adamantanes. *J. Org. Chem.* **1978**, *43*, 2370–2374.

- (32) Sandros, K.; Bäckström, H. L. J. Transfer of Triplet State Energy in Fluid Solutions. II. Further Studies of the Quenching of Biacetyl Phosphorescence in Solution. *Acta Chem. Scand.* **1962**, *16*, 958–968.
- (33) Tabushi, I.; Kojo, S.; Schleyer, P. v R.; Gund, T. M. Selective Functionalization of Unactivated Methine Positions. 4-Acetyldiamantane. *J. Chem. Soc. Chem. Commun.* **1974**, No. 15, 591–591.
- (34) Kamijo, S.; Takao, G.; Kamijo, K.; Hirota, M.; Tao, K.; Murafuji, T. Photo-Induced Substitutive Introduction of the Aldoxime Functional Group to Carbon Chains: A Formal Formylation of Non-Acidic C(Sp³)–H Bonds. *Angew. Chem. Int. Ed.* **2016**, *55*, 9695–9699.
- (35) Barton, D. H. R.; Doller, D. The Selective Functionalization of Saturated Hydrocarbons: Gif Chemistry. *Acc. Chem. Res.* **1992**, *25*, 504–512.
- (36) Sommer, J.; Bukala, J. Selective Electrophilic Activation of Alkanes. *Acc. Chem. Res.* **1993**, *26*, 370–376.
- (37) Arndtsen, B. A.; Bergman, R. G.; Mobley, T. A.; Peterson, T. H. Selective Intermolecular Carbon-Hydrogen Bond Activation by Synthetic Metal Complexes in Homogeneous Solution. *Acc. Chem. Res.* **1995**, *28*, 154–162.
- (38) Kato, S.; Iwahama, T.; Sakaguchi, S.; Ishii, Y. N-Hydroxyphthalimide-Catalyzed Carboxylation of Polycyclic Alkanes with Carbon Monoxide in the Presence of Dioxide. *J. Org. Chem.* **1998**, *63*, 222–223.
- (39) Ryu, I.; Tani, A.; Fukuyama, T.; Ravelli, D.; Fagnoni, M.; Albini, A. Atom-Economical Synthesis of Unsymmetrical Ketones through Photocatalyzed C–H Activation of Alkanes and Coupling with CO and Electrophilic Alkenes. *Angew. Chem. Int. Ed.* **2011**, *50*, 1869–1872.
- (40) Berre, C. L.; Serp, P.; Kalck, P.; Torrence, G. P. Acetic Acid. In *Ullmann's Encyclopedia of Industrial Chemistry*; American Cancer Society, 2014; pp 1–34.
- (41) Ryu, I. Radical Carboxylations of Iodoalkanes and Saturated Alcohols Using Carbon Monoxide. *Chem. Soc. Rev.* **2001**, *30*, 16–25.

- (42) Lu, L.; Cheng, D.; Zhan, Y.; Shi, R.; Chiang, C.-W.; Lei, A. Metal-Free Radical Oxidative Alkoxycarbonylation and Imidation of Alkanes. *Chem. Commun.* **2017**, *53*, 6852–6855.
- (43) Liu, Q.; Zhang, H.; Lei, A. Oxidative Carbonylation Reactions: Organometallic Compounds (R–M) or Hydrocarbons (R–H) as Nucleophiles. *Angew. Chem. Int. Ed.* **2011**, *50*, 10788–10799.
- (44) Wu, X.-F.; Neumann, H. Ruthenium and Rhodium-Catalyzed Carbonylation Reactions. *ChemCatChem* **2012**, *4*, 447–458.
- (45) Wu, X.-F.; Neumann, H.; Beller, M. Synthesis of Heterocycles via Palladium-Catalyzed Carbonylations. *Chem. Rev.* **2013**, *113*, 1–35.
- (46) Allen, S. E.; Walvoord, R. R.; Padilla-Salinas, R.; Kozlowski, M. C. Aerobic Copper-Catalyzed Organic Reactions. *Chem. Rev.* **2013**, *113*, 6234–6458.
- (47) Li, Y.; Dong, K.; Zhu, F.; Wang, Z.; Wu, X.-F. Copper-Catalyzed Carbonylative Coupling of Cycloalkanes and Amides. *Angew. Chem. Int. Ed.* **2016**, *55*, 7227–7230.
- (48) Castro, L. C. M.; Chatani, N. Nickel Catalysts/*N,N'*-Bidentate Directing Groups: An Excellent Partnership in Directed C–H Activation Reactions. *Chem. Lett.* **2015**, *44*, 410–421.
- (49) Han, Z.; Chaowei, D.; Lice, L.; Hongfei, M.; Hongzhong, B.; Yufeng, L. Nickel (II)-Catalyzed Efficient Aminocarbonylation of Unreactive Alkanes with Formanilides—Exploiting the Deformylation Behavior of Imides. *Tetrahedron* **2018**, *74*, 3712–3718.
- (50) Fukunishi, K.; Tabushi, I. Regioselective Radical Addition of Adamantanes to Dimethyl Maleate. *Synthesis* **1988**, *1988*, 826–827.
- (51) Ogura, K.; Kayano, A.; Sumitani, N.; Akazome, M.; Fujita, M. Efficient 1,2-Asymmetric Induction in Radical Reactions: Stereoselective Radical Addition to 3-Hydroxy-1-(Methylthio)-1-(*p*-Tolylsulfonyl)-1-Alkenes. *J. Org. Chem.* **1995**, *60*, 1106–1107.

- (52) Wladislaw, B.; Marzorati, L.; Uchôa, R. B. A Novel Thermal Decomposition of α -Methylthiobenzyl Phenyl Sulfones. Synthesis of p-Substituted 1-Deuteriobenzaldehydes. *Synthesis* **1986**, 1986, 964–965.
- (53) González-Cameno, A. M.; Mella, M.; Fagnoni, M.; Albini, A. Photochemical Alkylation of Ketene Dithioacetal S,S-Dioxides. An Example of Captodative Olefin Functionalization. *J. Org. Chem.* **2000**, 65, 297–303.
- (54) Campari, G.; Fagnoni, M.; Mella, M.; Albini, A. Diastereoselective Photosensitised Radical Addition to Fumaric Acid Derivatives Bearing Oxazolidine Chiral Auxiliaries. *Tetrahedron Asymmetry* **2000**, 11, 1891–1906.
- (55) Scheuer, P. J. Isocyanides and Cyanides as Natural Products. *Acc. Chem. Res.* **1992**, 25, 433–439.
- (56) Curran, D. P.; Hadida, S. Tris(2-(Perfluorohexyl)Ethyl)Tin Hydride: A New Fluorous Reagent for Use in Traditional Organic Synthesis and Liquid Phase Combinatorial Synthesis. *J. Am. Chem. Soc.* **1996**, 118, 2531–2532.
- (57) Tashtoush, H. I.; Sustmann, R. Chromium(II)-Mediated Intermolecular Free-Radical Carbon — Carbon Bond Formation. *Chem. Ber.* **1992**, 125, 287–289.
- (58) Dondi, D.; Cardarelli, A. M.; Fagnoni, M.; Albini, A. Photomediated Synthesis of β -Alkylketones from Cycloalkanes. *Tetrahedron* **2006**, 62, 5527–5535.
- (59) Hara, T.; Iwahama, T.; Sakaguchi, S.; Ishii, Y. Catalytic Oxyalkylation of Alkenes with Alkanes and Molecular Oxygen via a Radical Process Using N-Hydroxyphthalimide. *J. Org. Chem.* **2001**, 66, 6425–6431.
- (60) Cai, Y.; Dang, H.-S.; Roberts, B. P. Radical-Chain Functionalisation at C–H Centres Using an O-Oxiranylcarbinyl O-Silyl Ketene Acetal. *Tetrahedron Lett.* **2004**, 45, 4405–4409.
- (61) Cai, Y.; Roberts, B. P. Vicinal Alkylation–Carboxymethylation of Electron-Poor Alkenes by Radical-Chain Reactions with O-Alkyl O-Silyl Ketene Acetals and Their [3+2] Annulation by Reaction with O-Cyclopropylcarbinyl O-Silyl Ketene Acetals. *Tetrahedron Lett.* **2004**, 45, 1485–1488.

- (62) Studer, A.; Curran, D. P. Catalysis of Radical Reactions: A Radical Chemistry Perspective. *Angew. Chem. Int. Ed.* **2016**, *55*, 58–102.
- (63) Ji, J.; Liu, P.; Sun, P. Peroxide Promoted Tunable Decarboxylative Alkylation of Cinnamic Acids to Form Alkenes or Ketones under Metal-Free Conditions. *Chem. Commun.* **2015**, *51*, 7546–7549.
- (64) Kamijo, S.; Kamijo, K.; Maruoka, K.; Murafuji, T. Aryl Ketone Catalyzed Radical Allylation of C(Sp³)-H Bonds under Photoirradiation. *Org. Lett.* **2016**, *18*, 6516–6519.
- (65) Forkner, M. W.; Miller, L. L.; Rak, S. F. The Structure of a Conductive, Diamagnetic Diquinone Radical Anion Salt. *Synth. Met.* **1990**, *36*, 65–73.
- (66) Almlof, J. E.; Feyereisen, M. W.; Jozefiak, T. H.; Miller, L. L. Electronic Structure and Near-Infrared Spectra of Diquinone Anion Radicals. *J. Am. Chem. Soc.* **1990**, *112*, 1206–1214.
- (67) Baxter, I.; Cameron, D. W.; Titman, R. B. Formation of Some Linear Polycyclic Diquinones via a Novel Dimerization. *J. Chem. Soc. C Org.* **1971**, No. 0, 1253–1256.
- (68) Wolff, M. E. Cyclization of N-Halogenated Amines (The Hofmann-Löffler Reaction). *Chem. Rev.* **1963**, *63*, 55–64.
- (69) Fokin, A. A.; Schreiner, P. R. Selective Alkane Transformations via Radicals and Radical Cations: Insights into the Activation Step from Experiment and Theory. *Chem. Rev.* **2002**, *102*, 1551–1594.
- (70) Malatesta, V.; Ingold, K. U. Kinetic Applications of Electron Paramagnetic Resonance Spectroscopy. 36. Stereoelectronic Effects in Hydrogen Atom Abstraction from Ethers. *J. Am. Chem. Soc.* **1981**, *103*, 609–614.
- (71) Zhang, Z.-Z.; Liu, B.; Wang, C.-Y.; Shi, B.-F. Cobalt(III)-Catalyzed C2-Selective C-H Alkynylation of Indoles. *Org. Lett.* **2015**, *17*, 4094–4097.
- (72) Liu, W.; Chen, Z.; Li, L.; Wang, H.; Li, C.-J. Transition-Metal-Free Coupling of Alkynes with α -Bromo Carbonyl Compounds: An Efficient Approach towards β,γ -Alkynoates and Allenates. *Chem. – Eur. J.* **2016**, *22*, 5888–5893.

- (73) Cheung, C. W.; Ren, P.; Hu, X. Mild and Phosphine-Free Iron-Catalyzed Cross-Coupling of Nonactivated Secondary Alkyl Halides with Alkynyl Grignard Reagents. *Org. Lett.* **2014**, *16*, 2566–2569.
- (74) Russell, G. A.; Ngoviwachai, Preecha.; Tashtoush, H. I. Electron-Transfer Processes. 43. Attack of Alkyl Radicals upon 1-Alkenyl and 1-Alkynyl Derivatives of Tin and Mercury. *Organometallics* **1988**, *7*, 696–702.
- (75) Molander, G. A.; Traister, K. M. Pd-Catalyzed Alkynylation of 2-Chloroacetates and 2-Chloroacetamides with Potassium Alkynyltrifluoroborates. *Org. Lett.* **2013**, *15*, 5052–5055.
- (76) Ohmiya, H.; Yorimitsu, H.; Oshima, K. Cobalt-Mediated Cross-Coupling Reactions of Primary and Secondary Alkyl Halides with 1-(Trimethylsilyl)Ethenyl- and 2-Trimethylsilylethynylmagnesium Reagents. *Org. Lett.* **2006**, *8*, 3093–3096.
- (77) Yi, J.; Lu, X.; Sun, Y.-Y.; Xiao, B.; Liu, L. Nickel-Catalyzed Sonogashira Reactions of Non-Activated Secondary Alkyl Bromides and Iodides. *Angew. Chem. Int. Ed.* **2013**, *52*, 12409–12413.
- (78) Cahiez, G.; Gager, O.; Buendia, J. Copper-Catalyzed Cross-Coupling of Alkyl and Aryl Grignard Reagents with Alkynyl Halides. *Angew. Chem. Int. Ed.* **2010**, *49*, 1278–1281.
- (79) Gong, J.; Fuchs, P. L. Alkynylation of C–H Bonds via Reaction with Acetylenic Triflones. *J. Am. Chem. Soc.* **1996**, *118*, 4486–4487.
- (80) Xiang, J.; Jiang, W.; Fuchs, P. L. Scope and Limitations of Functionalized Acetylenic Triflones in the Direct Alkynylation of C-H Bonds.[1]. *Tetrahedron Lett.* **1997**, *38*, 6635–6638.
- (81) Jahnke, E.; Tykwinski, R. R. The Fritsch–Buttenberg–Wiechell Rearrangement: Modern Applications for an Old Reaction. *Chem. Commun.* **2010**, *46*, 3235–3249.
- (82) Hoshikawa, T.; Kamijo, S.; Inoue, M. Photochemically Induced Radical Alkynylation of C(Sp³)–H Bonds. *Org. Biomol. Chem.* **2012**, *11*, 164–169.

- (83) Cheng, Z.-F.; Feng, Y.-S.; Rong, C.; Xu, T.; Wang, P.-F.; Xu, J.; Dai, J.-J.; Xu, H.-J. Directed Alkynylation of Unactivated C(Sp³)–H Bonds with Ethynylbenziodoxolones Mediated by DTBP. *Green Chem.* **2016**, *18*, 4185–4188.
- (84) Ma, D.; Pan, J.; Yin, L.; Xu, P.; Gao, Y.; Yin, Y.; Zhao, Y. Copper-Catalyzed Direct Oxidative C-H Functionalization of Unactivated Cycloalkanes into Cycloalkyl Benzo[b]Phosphole Oxides. *Org. Lett.* **2018**, *20*, 3455–3459.
- (85) Mella, M.; Freccero, M.; Soldi, T.; Fasani, E.; Albini, A. Oxidative Functionalization of Adamantane and Some of Its Derivatives in Solution. *J. Org. Chem.* **1996**, *61*, 1413–1422.
- (86) Mella, M.; Freccero, M.; Albini, A. The Photochemical Approach to the Functionalization of Open-Chain and Cyclic Alkanes: 1. Single Electron Transfer Oxidation. *Tetrahedron* **1996**, *52*, 5533–5548.
- (87) Albini, A.; Mella, M.; Freccero, M. A New Method in Radical Chemistry: Generation of Radicals by Photo-Induced Electron Transfer and Fragmentation of the Radical Cation. *Tetrahedron* **1994**, *50*, 575–607.
- (88) Fokin, A. A.; Schreiner, P. R.; Fokina, N. A.; Tkachenko, B. A.; Hausmann, H.; Serafin, M.; Dahl, J. E. P.; Liu, S.; Carlson, R. M. K. Reactivity of [1(2,3)4]Pentamantane (Td-Pentamantane): A Nanoscale Model of Diamond. *J. Org. Chem.* **2006**, *71*, 8532–8540.
- (89) Fokin, A. A.; Tkachenko, B. A.; Gunchenko, P. A.; Gusev, D. V.; Schreiner, P. R. Functionalized Nanodiamonds Part I. An Experimental Assessment of Diamantane and Computational Predictions for Higher Diamondoids. *Chem. – Eur. J.* **2005**, *11*, 7091–7101.
- (90) Duncton, M. A. J. Minisci Reactions: Versatile CH-Functionalizations for Medicinal Chemists. *MedChemComm* **2011**, *2*, 1135–1161.
- (91) Shokova, E. A.; Kovalev, V. V. Adamantane Functionalization. Synthesis of Polyfunctional Derivatives with Various Substituents in Bridgehead Positions. *Russ. J. Org. Chem.* **2012**, *48*, 1007–1040.

- (92) Kawai, I.; Mead, L. H.; Drobniak, J.; Zakrzewski, S. F. Synthesis and Antifolate Activity of New Diaminopyrimidines and Diaminopurines in Enzymic and Cellular Systems. *J. Med. Chem.* **1975**, *18*, 272–275.
- (93) Anderson, J. M.; Kochi, J. K. Silver(I)-Catalyzed Oxidative Decarboxylation of Acids by Peroxydisulfate. Role of Silver(II). *J. Am. Chem. Soc.* **1970**, *92*, 1651–1659.
- (94) Nayyar, A.; Monga, V.; Malde, A.; Coutinho, E.; Jain, R. Synthesis, Anti-Tuberculosis Activity, and 3D-QSAR Study of 4-(Adamantan-1-Yl)-2-Substituted Quinolines. *Bioorg. Med. Chem.* **2007**, *15*, 626–640.
- (95) Barton, D. H. R.; Garcia, B.; Togo, H.; Zard, S. Z. Radical Decarboxylative Addition onto Protonated Heteroaromatic (and Related) Compounds. *Tetrahedron Lett.* **1986**, *27*, 1327–1330.
- (96) Castagnino, E.; Corsano, S.; Barton, D. H. R.; Zard, S. Z. Decarboxylative Radical Addition onto Protonated Heteroaromatic Systems Including Purine Bases. *Tetrahedron Lett.* **1986**, *27*, 6337–6338.
- (97) Antonchick, A. P.; Burgmann, L. Direct Selective Oxidative Cross-Coupling of Simple Alkanes with Heteroarenes. *Angew. Chem. Int. Ed.* **2013**, *52*, 3267–3271.
- (98) Yang, Q.; Choy, P. Y.; Wu, Y.; Fan, B.; Kwong, F. Y. Oxidative Coupling between C(Sp²)-H and C(Sp³)-H Bonds of Indoles and Cyclic Ethers/Cycloalkanes. *Org. Biomol. Chem.* **2016**, *14*, 2608–2612.
- (99) Wang, D.-C.; Xia, R.; Xie, M.-S.; Qu, G.-R.; Guo, H.-M. Synthesis of Cycloalkyl Substituted Purine Nucleosides via a Metal-Free Radical Route. *Org. Biomol. Chem.* **2016**, *14*, 4189–4193.
- (100) Wang, X.; Lei, B.; Ma, L.; Zhu, L.; Zhang, X.; Zuo, H.; Zhuang, D.; Li, Z. Cobalt-Catalyzed Cross-Dehydrogenative C(Sp²)-C(Sp³) Coupling of Oxazole/Thiazole with Ether or Cycloalkane. *Chem. – Asian J.* **2017**, *12*, 2799–2803.
- (101) Zhou, L.; Togo, H. Introduction of Heteroaromatic Bases onto Cycloalkanes with BPO. *Eur. J. Org. Chem.* **2019**, *2019*, 1627–1634.

- (102) Perry, I. B.; Brewer, T. F.; Sarver, P. J.; Schultz, D. M.; DiRocco, D. A.; MacMillan, D. W. C. Direct Arylation of Strong Aliphatic C–H Bonds. *Nature* **2018**, *560*, 70.
- (103) Gutierrez, O.; Tellis, J. C.; Primer, D. N.; Molander, G. A.; Kozlowski, M. C. Nickel-Catalyzed Cross-Coupling of Photoredox-Generated Radicals: Uncovering a General Manifold for Stereoconvergence in Nickel-Catalyzed Cross-Couplings. *J. Am. Chem. Soc.* **2015**, *137*, 4896–4899.
- (104) Schörghener, J.; Waser, M. New Strategies and Applications Using Electrophilic Cyanide-Transfer Reagents under Transition Metal-Free Conditions. *Org. Chem. Front.* **2016**, *3*, 1535–1540.
- (105) Kamijo, S.; Hoshikawa, T.; Inoue, M. Photochemically Induced Radical Transformation of C(Sp³)–H Bonds to C(Sp³)–CN Bonds. *Org. Lett.* **2011**, *13*, 5928–5931.
- (106) Hoshikawa, T.; Yoshioka, S.; Kamijo, S.; Inoue, M. Photoinduced Direct Cyanation of C(Sp³)–H Bonds. *Synthesis* **2013**, *45*, 874–887.
- (107) Berndt, J.-P.; Erb, F. R.; Ochmann, L.; Beppler, J.; Schreiner, P. R. Selective Phthalimido-N-Oxyl (PINO)-Catalyzed C–H Cyanation of Adamantane Derivatives. *Synlett* **2019**, *30*, 493–498.
- (108) Sun, M.-X.; Wang, Y.-F.; Xu, B.-H.; Ma, X.-Q.; Zhang, S.-J. A Metal-Free Direct C (Sp³)–H Cyanation Reaction with Cyanobenziodoxolones. *Org. Biomol. Chem.* **2018**, *16*, 1971–1975.
- (109) Peng, H.; Yu, J.-T.; Jiang, Y.; Yang, H.; Cheng, J. Di-Tert-Butyl Peroxide-Promoted α -Alkylation of α -Amino Carbonyl Compounds by Simple Alkanes. *J. Org. Chem.* **2014**, *79*, 9847–9853.

5 Photocatalytic C–H Aminoalkylation of Adamantanes

5.1 - Introduction

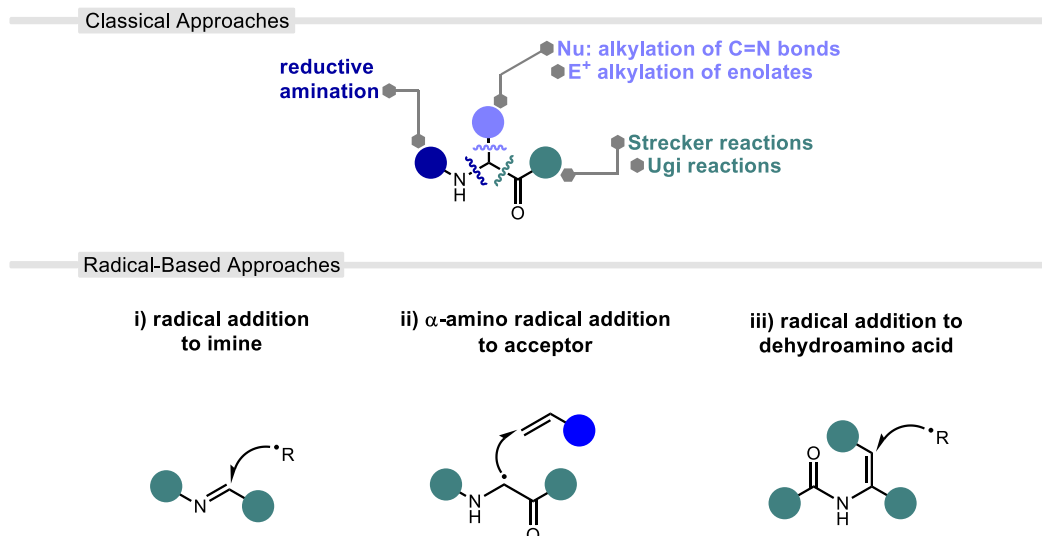


Figure 5.1 – Classical and Radical-Based Approaches to Aminoalkylation

Aminoalkylative transformations involving the simultaneous introduction of an amine and a new C–C bond are powerful due to the potential bioactivity of the products formed, particularly those featuring an α -aminoalkyl framework. Due to their resemblance to amino acids, many methods for the preparation of α -aminoalkylated compounds have been developed. These have predominantly relied upon the use of ionic approaches such as reductive amination or the Strecker and Ugi reactions.^[1,2] Radical-based approaches can proceed under milder conditions and offer compatibility with a wide range of functional groups, including a lower risk of racemization. Three main radical-based aminoalkylation strategies are commonly used: addition of an alkyl radical to an imine derivative^[3], radical conjugate addition into an α,β -dehydroamino acid precursor, or the addition of a captodative α -amino radical to a radical acceptor^[4–7] (**Figure 5.1**).

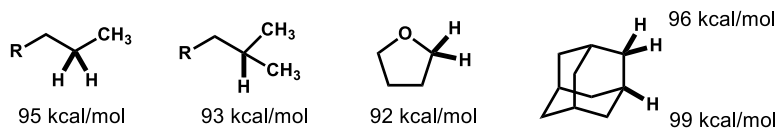


Figure 5.2 – BDE Comparison of Activated and Unactivated C–H Bonds with Adamantane

The use of imine derivatives as radical acceptors has grown steadily in recent years and typically involves the use of an alkyl halide in conjunction with a radical initiation system. The most widespread means of initiation has traditionally been the use of triethylborane or diethylzinc in the presence of air, however, other initiations involving the use of zinc metal^[8,9], tributyltin hydride^[10], and $\text{Mo}_2(\text{CO})_{10}$ ^[11] have also been explored.

Over the past 30 years, organometallic photoredox catalysis has emerged as a popular means of enabling or initiating radical processes smoothly under visible light irradiation.^[12] Ruthenium and iridium polypyridyl complexes are most commonly used for this purpose due to their ability to enter long-lived photo-excited states and their proficiency at engaging in either oxidative or reductive SET.^[13] Both metals form coordinatively saturated, 18-electron, d^6 complexes with a full set of t_{2g} orbitals.^[14] This makes these complexes extraordinarily stable and resistant to ligand exchange. While ruthenium complexes tend to be homoleptic, iridium complexes can be adorned with different ligands and still undergo efficient metal-to-ligand charge transfer (MLCT). For this reason, iridium complexes have a greater flexibility in the tunability of their redox potentials based on heteroleptic ligand substitutions. In general, electron deficient ligands

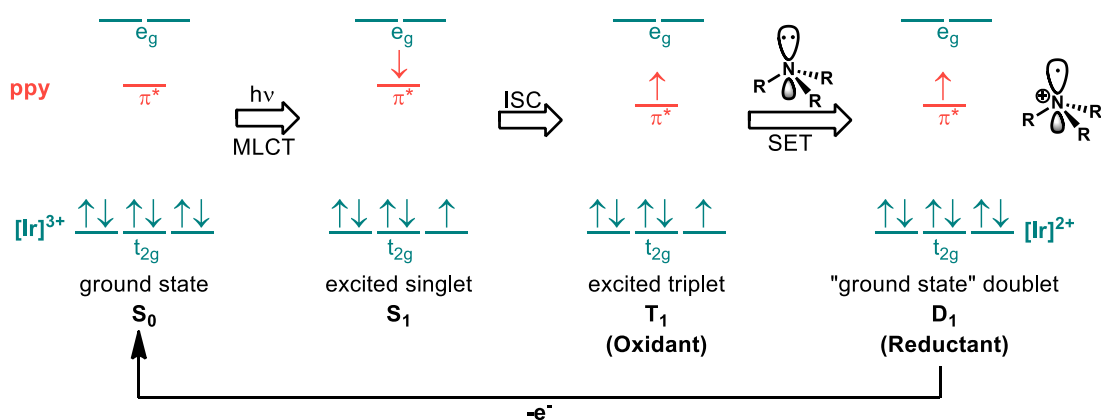


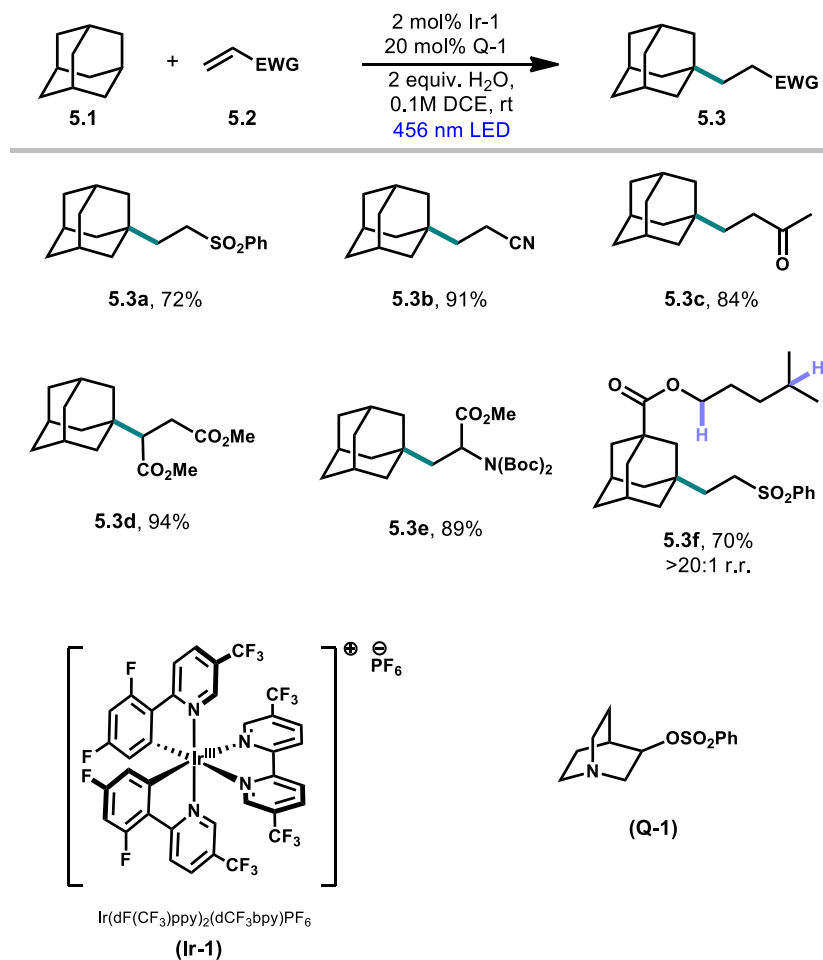
Figure 5.3 –Excitation of an Ir Photocatalyst and SET From a Tertiary Amine

give rise to more oxidizing complexes, while more electron-rich ligands lead to stronger reductants. **Figure 5.3** illustrates a light-induced MLCT to short-lived excited singlet state S_1 . This singlet quickly undergoes intersystem crossing (ISC) to the long-lived excited triplet state T_1 . It is this triplet that can interact with an appropriate substrate, in this case an amine, and oxidize it to a radical cation. The resulting Ir^{2+} doublet complex can revert back to the Ir^{3+} singlet ground state by acting as a reductant in a subsequent SET process (not shown). The ability of these organometallic photoredox catalysts to perform both oxidative and reductive operations explains their remarkable utility.

Proper pairing of redox partners is necessary to ensure efficient SET and minimize alternative relaxation modes such as fluorescence or energy transfer. The aminoalkylation of hydrocarbons via direct C–H functionalization remains challenging due to strength of un-activated alkyl C–H bonds and their associated bond dissociation energies. In particular, adamantane possesses unusually high BDE's that have traditionally required the use of either preactivated adamantane scaffolds or high energy light. However, previous work in

Table 5.1 – Previous Work: Adamantane Alkylations with Electron Deficient Alkenes

Previous work by Dr. Abigail Fecue and Dr. Hai-Bin Yang:



our lab determined that tertiary adamantyl C–H bonds could be selectively activated using a quinuclidine-based HAT catalyst (**Q-1**) driven by an iridium photoredox co-catalyst (**Ir-1**). This dual catalytic system was used for the alkylation of adamantane using a variety of electron deficient alkenes (**Table 5.1**). Under these conditions, adamantane was selectively alkylated even in the presence of other weaker C–H bonds (**5.3f**). As seen in the previous

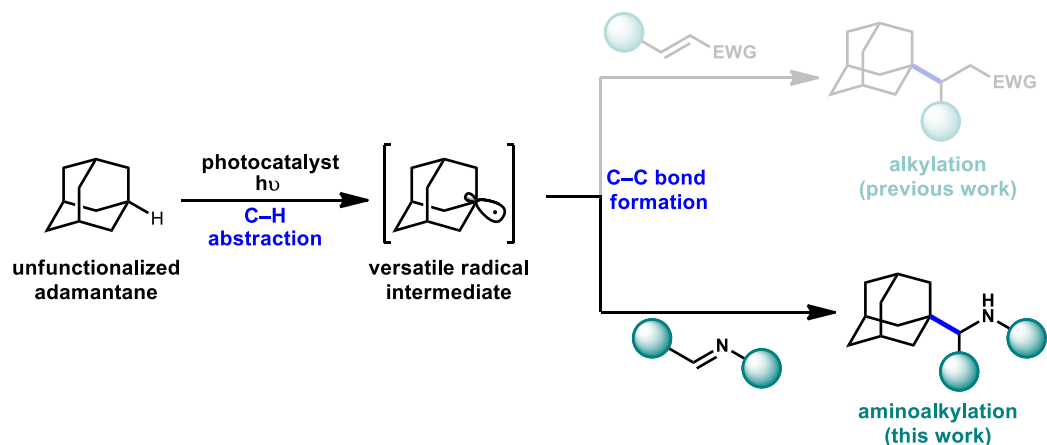


Figure 5.4 – Photocatalytic Alkylation and Aminoalkylation of Adamantane

chapter, many methods of direct adamantane C–H activation exhibit poor selectivity for the secondary and tertiary positions.

Expanding this work from alkenes to include aldimines would prove useful in the preparation of aminoalkyl adamantane derivatives (**Figure 5.4**). Such a method would enable the direct functionalization of adamantane where existing methods accomplishing the same transformation rely on reductive amination of formylated or acylated adamantanes (**Figure 5.5**). The aminoalkyl adamantanes generated by this direct functionalization are important biologically active compounds and are featured in at least two clinically approved drugs, saxagliptin (antidiabetic) and rimantadine (antiviral). Furthermore, no other singular hydrocarbon moiety (other than the methyl group) has had the success rate of adamantane in improving the activity of existing pharmaceuticals.^[15]

We

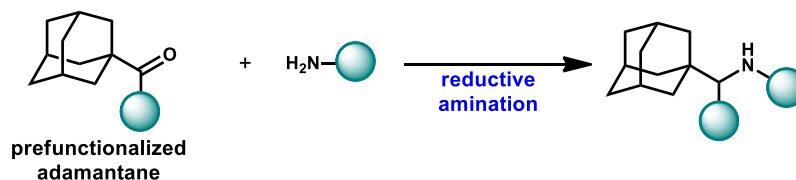


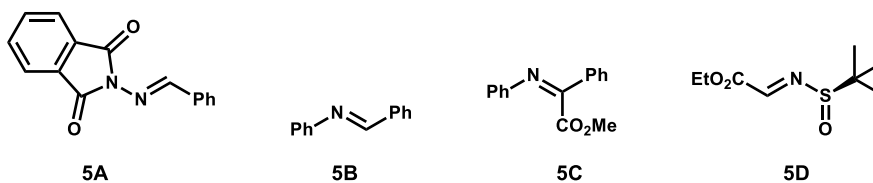
Figure 5.5 –Adamantane Aminoalkylation using Reductive Amination

therefore endeavored to further develop this photocatalytic method of adamantane C–H activation to include aldimine substrates with a specific focus on demonstrating the applicability to compounds of medicinal relevance such as saxagliptin and rimantadine.

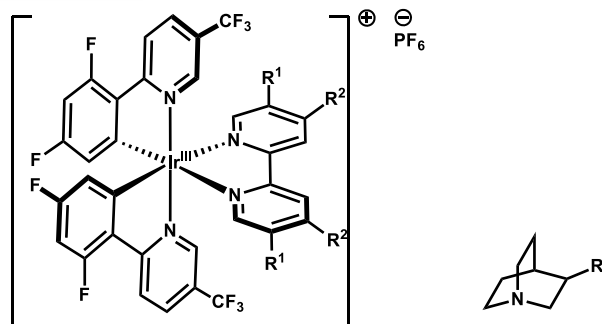
5.2 - Reaction Optimization

The standard conditions developed in our prior alkylation work with alkenes provided the basis investigating the ideal reaction conditions for aminoalkylation. An initial survey of potential imine substrates and photocatalysts (**Figure 5.6**) was performed by Prof. Martin and Dr. Yang. Imine substrates **5B** and **5C** did not readily show signs of productive product conversion, however, Dr. Yang found phthalimido derivative **5A** underwent reaction with adamantane using both iridium and acridinium based photocatalysts. In short, the optimal catalyst system was **Ir-1/Q-1** in 1,2-dichloroethane (DCE) as solvent with visible light irradiation (456 nm LEDs). Dr. Yang also determined that 5,7,12,14-pentacenetetraone (**PT**) worked with chiral sulfinimine **5D** to give the amino alkylated adamantane product in moderate yield and 1.3:1 dr. After the investigation of several more imine substrate classes, we were happy to find that these standard conditions also worked on appropriately N-substituted imines (**Scheme 5.1**). However, we were interested in determining if modifications to the conditions could further improve our

Early Test Substrates



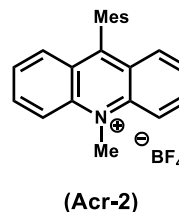
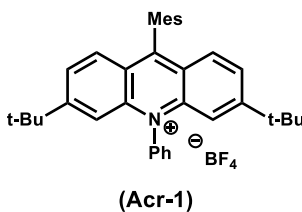
Tested Photocatalytic Systems



Dual Cat. Systems



Acridiniums



Quinones

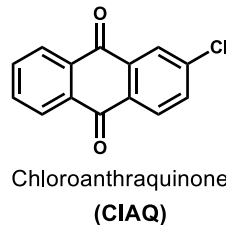
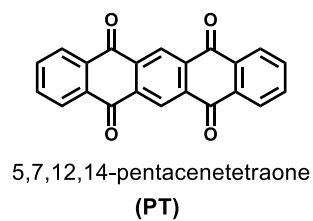
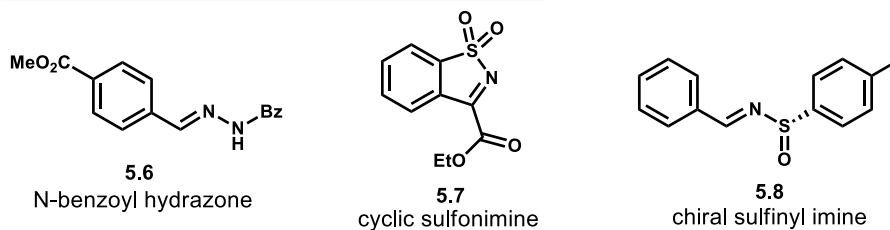
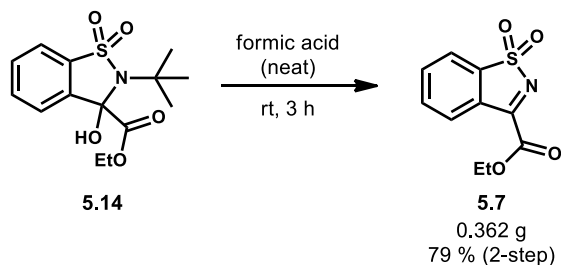
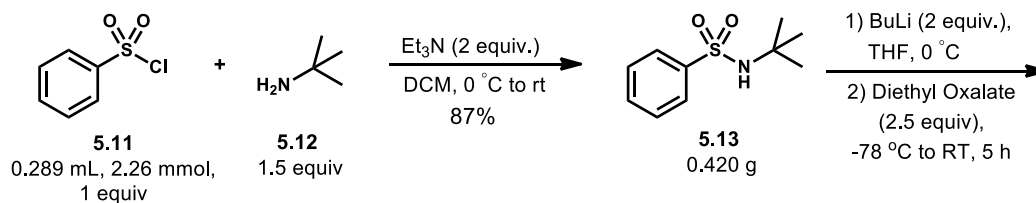
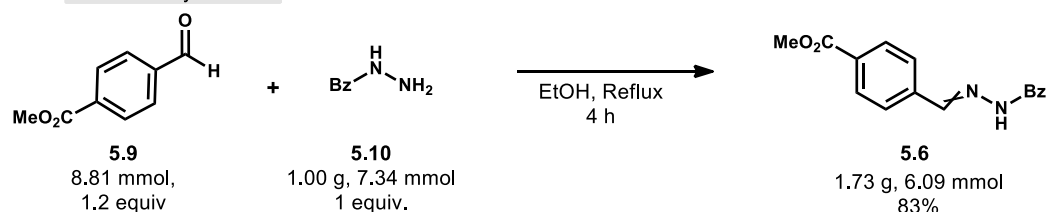


Figure 5.6 – Initial Survey of Imine Substrates and Photocatalysts

Early Test Substrates Using the Ir-1/Q-1 Catalyst System



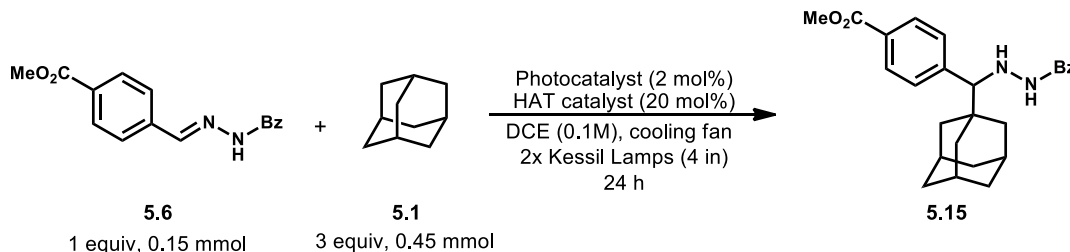
Substrate Synthesis



Scheme 5.1 – Synthesis of Early Test Substrates for the Ir-1/Q-1 Catalyst System results. The focus of my optimization studies of these reactions predominantly was focused on three imine substrate classes, *N*-benzoyl hydrazone **5.6**, cyclic sulfonimine **5.7**, and chiral sulfinyl imine **5.8**, shown in **Scheme 5.1** (top). These substrates were chosen in part for their ease of synthesis and analysis of crude NMR data.

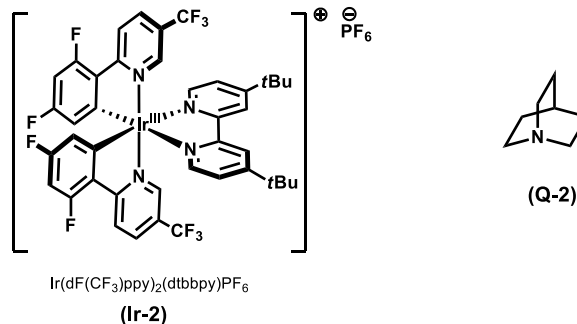
The *N*-benzoyl hydrazone is easily synthesized via condensation of benzohydrazide **5.10** onto the corresponding benzaldehyde. Methyl 4-formylbenzoate **5.9** in this case was chosen due to the methyl group's usefulness as a diagnostic reporter in crude NMR analysis with an internal standard. The chiral sulfinyl imine **5.8** was prepared in a similar manner using benzaldehyde and (*S*)-4-methylbenzene sulfinamide using a small amount of pyrrolidine as an organocatalyst.^[16] Cyclic sulfonimine **5.7** was synthesized in 3 steps

Table 5.2 – Variation of Catalytic Systems with *N*-Benzoyl-Hydrazone



Entry	Catalyst System	Light Source	Yield (NMR)*
1	Ir-1, Q-1	456 nm	85 %
2	Ir-2, Q-2	456 nm	24 %
3	Ir-2, Q-2	427 nm	14 %
4	Ir-1, no HAT	456 nm	0 %
5	Q1, No photocat.	456 nm	0 %
6	Ir-1, Q-1	no light	0 %

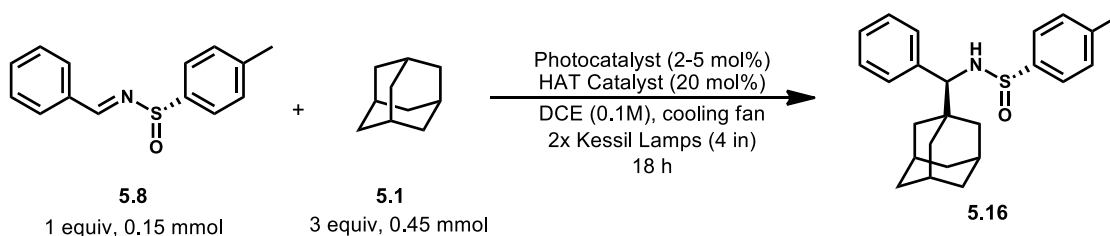
*NMR analysis done using Bn₂O as internal standard.



from benzenesulfonyl chloride **5.11**, *tert*-butyl amine **5.12**, and diethyl oxalate.^[17] While the synthesis was more laborious, the cyclic sulfonimine substrate was a reliable reaction partner with a variety of substituted adamantanes.

Initially a survey of alternative dual catalytic systems using different photocatalysts, HAT catalysts, and light sources was conducted. **Ir-1/Q-1** was initially tried with *N*-benzoyl hydrazone **5.6** (entry 1) and met with good results and gave an NMR yield of 85% (**Table 5.2**). Using **Ir-2/Q-2**, a less oxidizing catalytic system, both 456 nm and 427 nm light (entries 2 and 3) resulted in much lower NMR yields. Entries 4-6 demonstrate that a photocatalyst, HAT catalyst, and light source are each required components of the reaction.

Table 5.3 – Variation of Catalytic Systems with a Chiral Sulfinimine



Entry	Catalyst System	Light Source	Yield (NMR) ^b
1	Ir-1, Q-1	456 nm	44 % (9:1 d.r.)
2	Ir-2, Q-2	456 nm	18 % ^c
3	CIAQ ^a	427 nm	<5 % ^c
4	PT ^a	427 nm	53 % (9:1 d.r.)
5	PT ^a	390 nm	77 % (9:1 d.r.)
6	PT ^a	no light	0 %

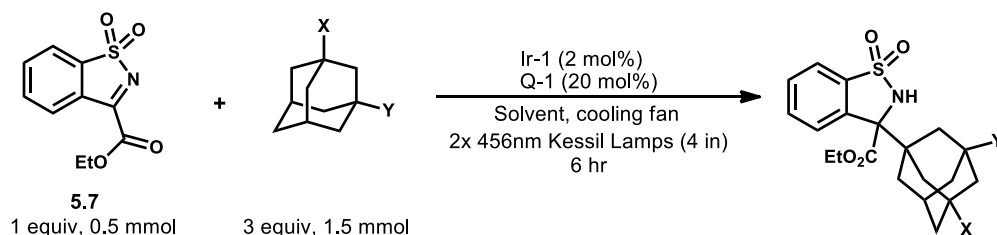
^a No dedicated HAT catalyst added.

^b NMR analysis done using Bn₂O as internal standard.

^c d.r. not determined.

The use of the **Ir-1/Q-1** system was much less effective when used on chiral sulfinyl imine **5.8** (entry 1, **Table 5.3**) while even poorer performance was seen using **Ir-2/Q-2** (entry 2). Kamijo and coworkers demonstrated that the adamantyl radical can be generated using 2-chloroanthraquinone (CIAQ) and pentacenetetraone (PT).^[18] These quinone based photocatalysts facilitate HAT in their excited states (under irradiation) and are therefore capable of directly engaging adamantane. We found that while CIAQ gave

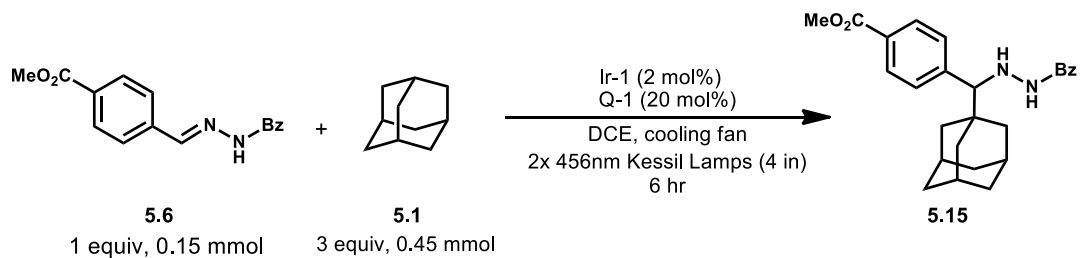
Table 5.5 – Solvent Studies with Substituted Adamantanes and Cyclic Sulfonimine



Entry	X	Y	Solvent	Yield (Isolated)
1	H	H	DCE	83%
2	Cl	H	DCE	66%
3	Cl	H	MeCN	74%
4	CN	H	DCE	27%
5	CN	H	MeCN	40%
6	Ac	H	DCE	66%
7	Ac	H	MeCN	62%
8	Me	Me	DCE	80%
9	OH	H	DCE	77%

Both solvent choice (**Table 5.5**) and concentration (**Table 5.6**) were observed to have a moderate effect on product conversion. In cases where lower yields were observed, modification of these variables is often able to improve results. For example, in **Table 5.5**, switching solvents from 1,2-dichloroethane to acetonitrile improved yields from 66% to 74% with 1-chloroadamantane (entries 2-3) and from 27% to 40% with 1-adamantane-carbonitrile (entries 4-5). Based on qualitative examination, a large amount of the adamantane used in these reactions goes undissolved (although by reaction completion, complete solvation is observed). Some adamantanes appear to be more soluble in acetonitrile than 1,2-dichloroethane and this likely explains the improvements in yield.

Table 5.6 – Effect of Reaction Concentration for *N*-Benzoyl-Hydrazone



Entry	DCE (mL)	DCE (M)	% Yield (NMR)*
1	1.0	0.15	47%
2	1.5	0.10	63%
3	3.0	0.05	56%

*NMR analysis done using Bz₂O as internal standard.

5.3 - Proposed Catalytic Cycles

Photocatalytically driven HAT processes can proceed according to two general routes and are categorized by the nature of the catalytic species performing HAT on the substrate. These routes can be described as being either a direct or indirect process resulting in the generation of alkyl radical \mathbf{R}^{\bullet} through a hydrogen atom abstraction step (**Figure 5.7**). In a direct catalytic HAT process, the catalyst is capable of both undergoing photoexcitation to \mathbf{PC}^* and subsequent hydrogen atom abstraction from the substrate \mathbf{RH} leading to $\mathbf{PC-H}^{\bullet}$ and the alkyl radical \mathbf{R}^{\bullet} . Albini's use of benzophenone,^[19–21] Kamijo's use of quinone-based catalysts^[22–24] and Dilman's use of a decatungstate catalyst^[25] in the C–H activation of alkanes proceed according to direct HAT.

In an indirect process, the species undergoing photoexcitation does not directly engage in HAT chemistry. Instead, the excited photocatalyst interacts with HAT catalyst \mathbf{A} , and enables it to perform H-atom abstraction.^[26–28] After HAT, the resulting $\mathbf{A-H}^{\bullet}$ species can donate a proton and an electron elsewhere and resume catalysis. These events often aid in the turnover of the deactivated photocatalyst \mathbf{PC}_D returning it to its ground state ready for

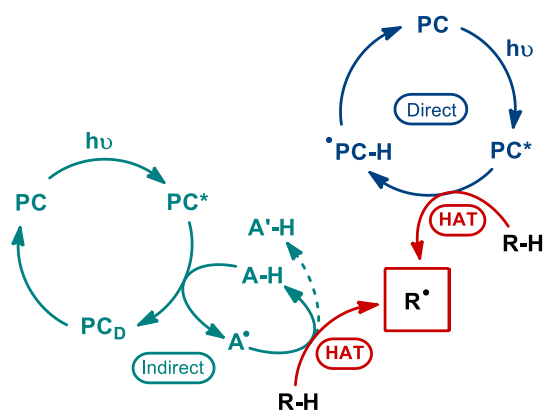


Figure 5.7 – Direct vs. Indirect Photocatalytic HAT Processes

photoexcitation. Alternatively, the hydrogen atom abstractor may be used stoichiometrically with $A^{\bullet}-H$ forming as a reaction byproduct. **Figure 5.8** shows several examples of the catalytic species used in direct and indirect photocatalytic HAT reactions.

Our previously reported alkylation of adamantanes via radical addition to alkene acceptors is believed to proceed in an indirect HAT process facilitated by iridium photocatalyst **Ir-1** and quinuclidine HAT catalyst **Q-1**. The same catalytic system is believed to be operational with imine radical acceptors in aminoalkylative transformations as well. 5,7,12,14-Pentacenetetraone offers an alternative route to generate the adamantyl

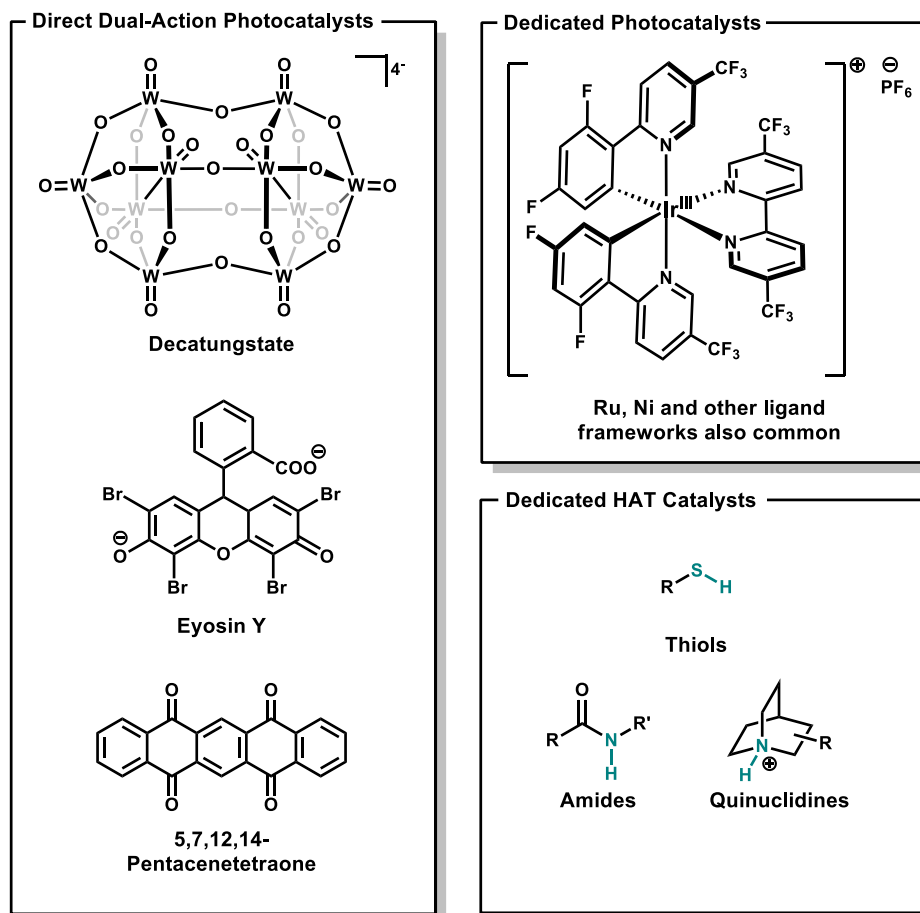


Figure 5.8 – Examples of Direct and Indirect HAT Catalysts

radical using a direct HAT process and was found to be more efficient in reactions involving chiral sulfinyl imines.

5.3.1 - Indirect Dual Photocatalytic-HAT System

A plausible mechanism for adamantane aminoalkylation with **Ir-1/Q-1** is shown in **Figure 5.9**. Starting with excitation of Ir^{III} to *Ir^{III} (**I**→**II**) under blue light, the excited iridium complex oxidizes the quinuclidine to its radical cation (**III**→**IV**). Adamantane then undergoes HAT to give the adamantyl radical (**A1**→**A2**) and quinuclidinium **V**. This adamantyl radical then adds into imine substrate **B** to afford amino radical intermediate **A3** and is quickly reduced by Ir^{II} back to Ir^{III} (**VI**→**I**) to give the anionic penultimate intermediate **A4**. Protonation of anion **A4** by quinuclidinium **V** completes the catalytic

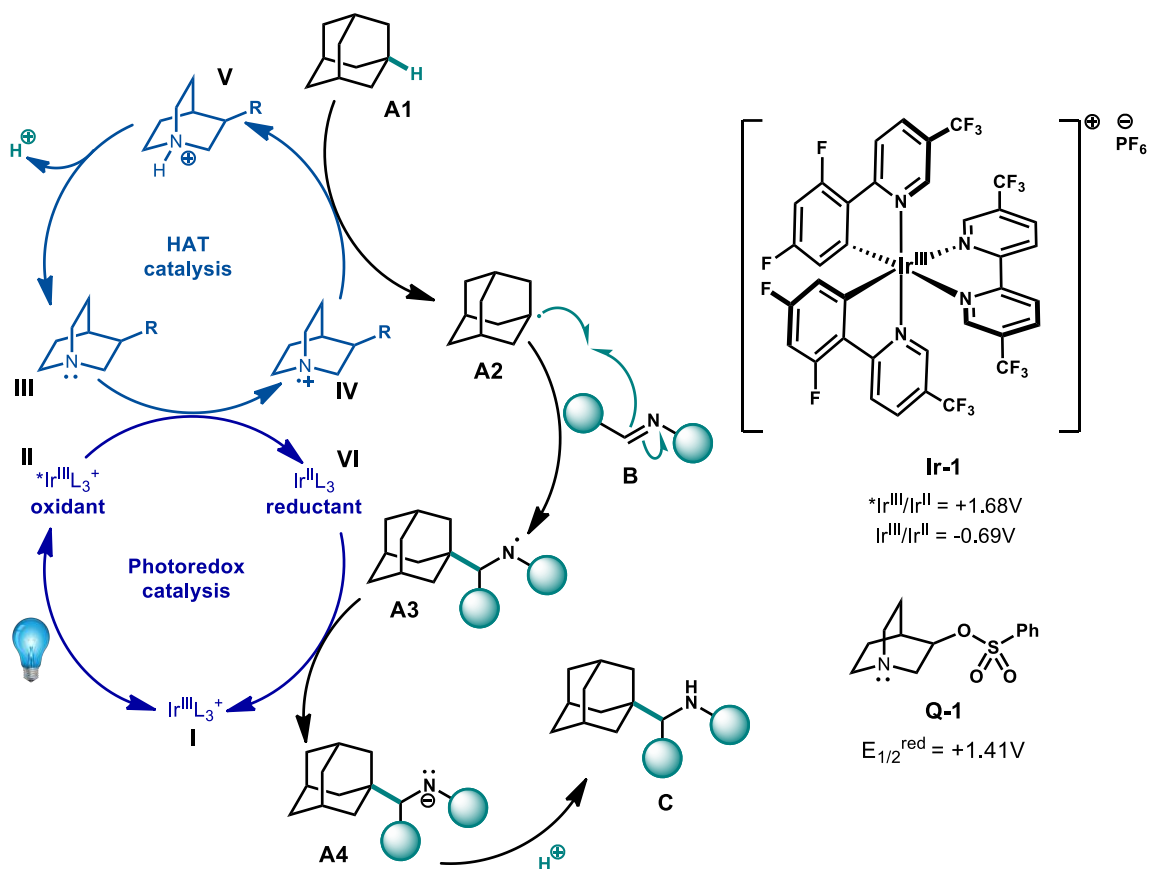


Figure 5.9 – Proposed Catalytic Cycle for Indirect Aminoalkylation of Adamantane

cycle in a redox neutral fashion. Previous work conducted by Feceu and Yang on adamantane alkylation using the same catalyst system established that the reaction is inhibited by the addition of radical scavengers such as TEMPO and BHT and significant fluorescence quenching of **Ir-1** occurs with the addition of **Q-1**.^[28] Reactions ran in the presence of D₂O showed deuterium incorporation in only the products, with no deuterium incorporation into the C–H bonds of adamantane or the alkene. This is suggestive of an irreversible HAT process.

Table 5.7 – Competition Experiments with Non-Adamantyl Substrates

$\text{R-H} + \text{5.1} \xrightarrow[\text{Q-1 (20 mol\%)}]{\text{Ir-1 (2 mol\%)}} \text{R-CH}_2\text{-CH}_2\text{-SO}_2\text{Ph (5.16)} + \text{5.17}$

Intermolecular Competition		Intramolecular Competition	
R	C-H BDE	% Yield (5.16)	% Yield (5.17)
 (non-competitive)	99 kcal/mol	--	80%
	86 kcal/mol	0%	80%
	98 kcal/mol	2%	73%
	H ¹ : 106 kcal/mol H ² : 99 kcal/mol	2%	61%
	89 kcal/mol	14%	63%
	92 kcal/mol	28%	46%

5.18 70% (>20:1 r.r.)
5.19 70% (>20:1 r.r.)

Previous competition studies by Dr. Abigail Feceu and Dr. Hai-bin Yang

The **Ir-1/Q-1** catalyst system is remarkably selective for the tertiary adamantyl position, with no HAT being observed from the secondary adamantyl position. Feceu and Yang also demonstrated this selectivity remains even in the presence of other C–H bonds. Direct competition experiments with a variety of other hydrocarbon substrates featuring C–H bonds of differing BDEs in an alkylation reaction with vinyl phenylsulfone demonstrates this impressive selectivity (**Table 5.7**). The origin of this selectivity may be due in part to adamantane's unique cage-like structure, which minimizes the extent of rehybridization in the sp^3 centers that occurs during the C–H abstraction transition state.^[29] Adamantane is also thought to undergo HAT more favorably than non-caged alkanes based on comparative carbocation stability.^[30] A higher degree of stabilization is possible for a developing positive charge at the tertiary adamantyl position due to the favorable hyperconjugative effects of the adjacent C–H bonds^[31] The use of the phenylsulfonate substituent on the quinuclidine HAT catalyst is therefore thought to benefit more significantly than other substrates from the stabilization that occurs during charge transfer in the polarity matched transition state with adamantane (**Figure 5.10**). The electron withdrawing nature of the phenylsulfonate increases the reactivity of the quinuclidinium intermediate and strengthens the N–H bond which is thought to increase the rate of HAT with adamantane.

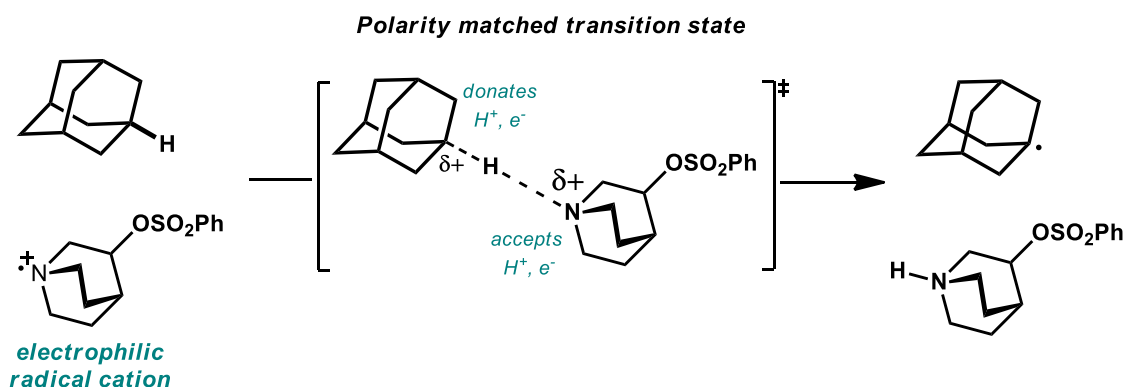


Figure 5.10 – Polar Effects During Charge Transfer in the HAT Transition State

5.3.2 - Direct HAT Cycle Using Pentacenetetraone (PT)

Based on the previous mechanistic investigations on the indirect **Ir-1/Q-1** catalytic system and work by Kamijo and coworkers with quinone-based photocatalysts,^[18] we propose the following catalytic cycle shown in **Figure 5.11**. In this direct HAT cycle, **PT** is excited to **PT*** and abstracts an H-atom from adamantane to give radical **A2** and **PT-H**.

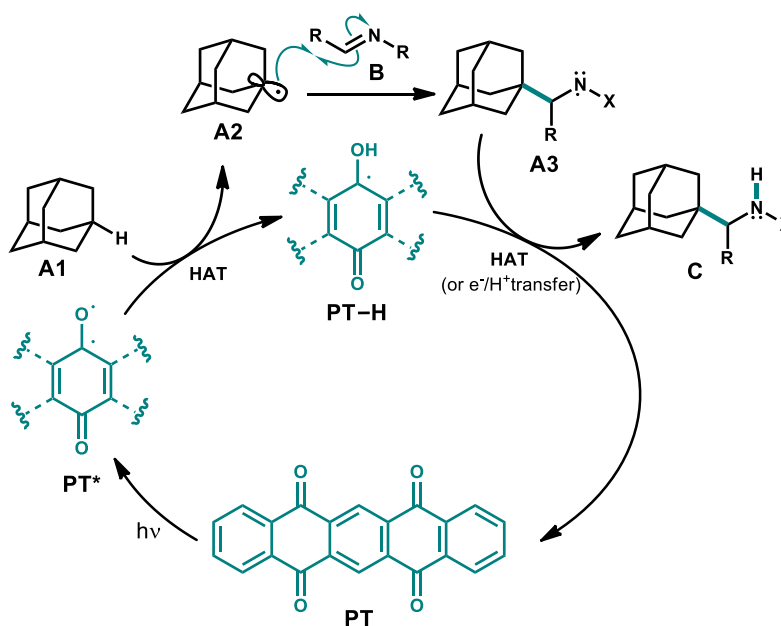


Figure 5.11 – Proposed Catalytic Cycle for Direct Aminoalkylation of Adamantane

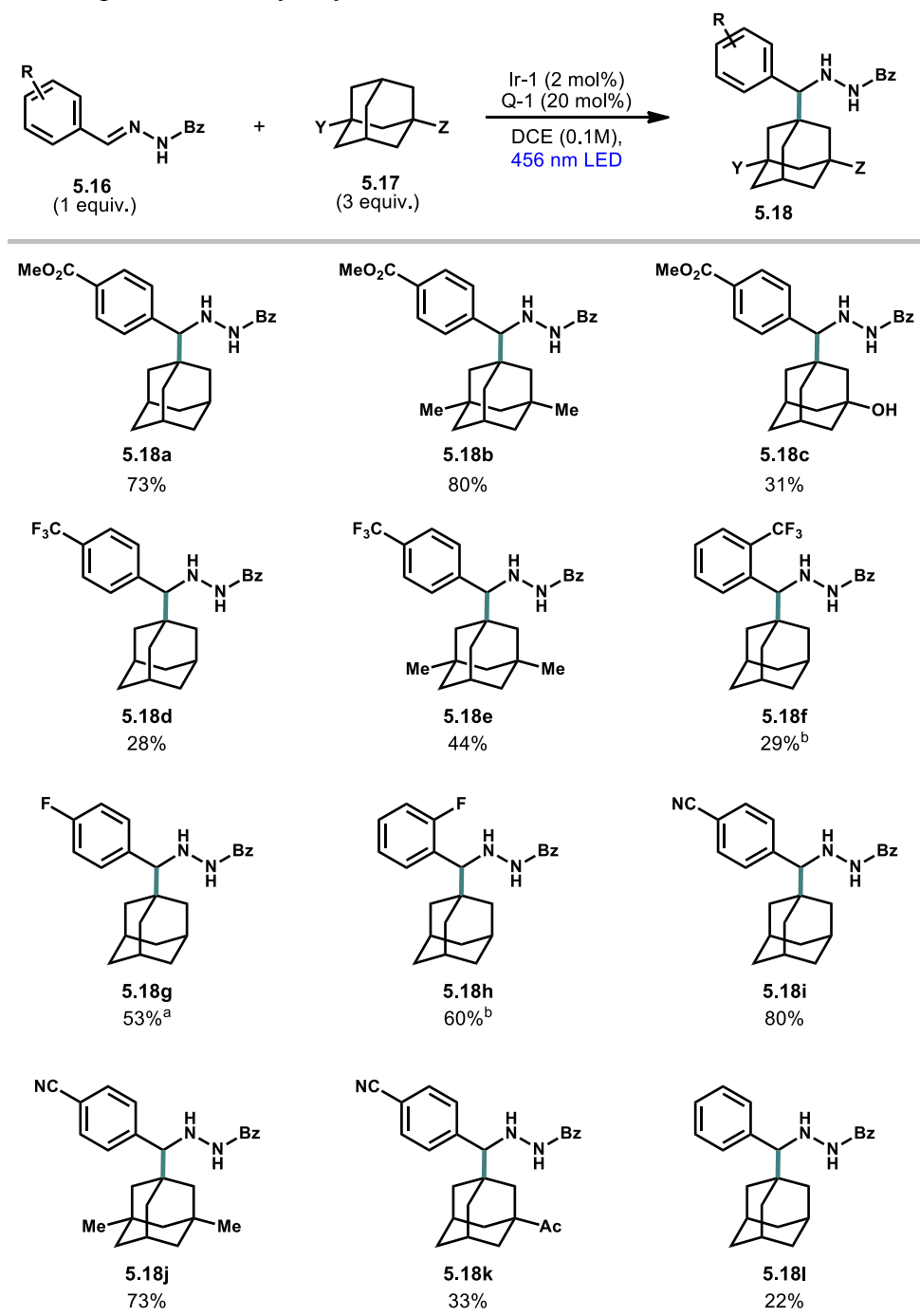
The adamantyl radical then adds into imine **B** to generate aminyl radical **A3**. Turn over then occurs through HAT or by single electron reduction followed proton transfer to reach the final product **C**.

5.4 - Substrate Scope

5.4.1 - *N*-Benzoyl Hydrazones

Due to the ease of the synthesis and the relative abundance of aldehyde starting materials available, the first class of imine radical acceptors we examined were *N*-benzoyl hydrazones (**Table 5.8**). This reaction tested with a variety of imines featuring an electron withdrawing substituent (-CO₂ Me, -CN, -CF₃, -F) at either *meta* or *para* positions. These were tested in conjunction with electron rich adamantanes (unsubstituted and dimethyl) and electron poor adamantanes (-OH, -Ac). We found that pairings of an imine featuring a resonance withdrawing aryl substituent with an electron rich adamantane worked best (**5.18a** and **b**, **5.18i** and **j**, 73-80%). Imines with inductive withdrawing groups (e.g CF₃) were almost uniformly less efficient (**5.18d-f**, 28-44%; **5.18g-h**, 53-60%). Poor results also were observed with electron withdrawn adamantanes (**5.18c** and **k**).

Table 5.8 – Scope of *N*-Benzoyl-Hydrazones with Various Adamantanes

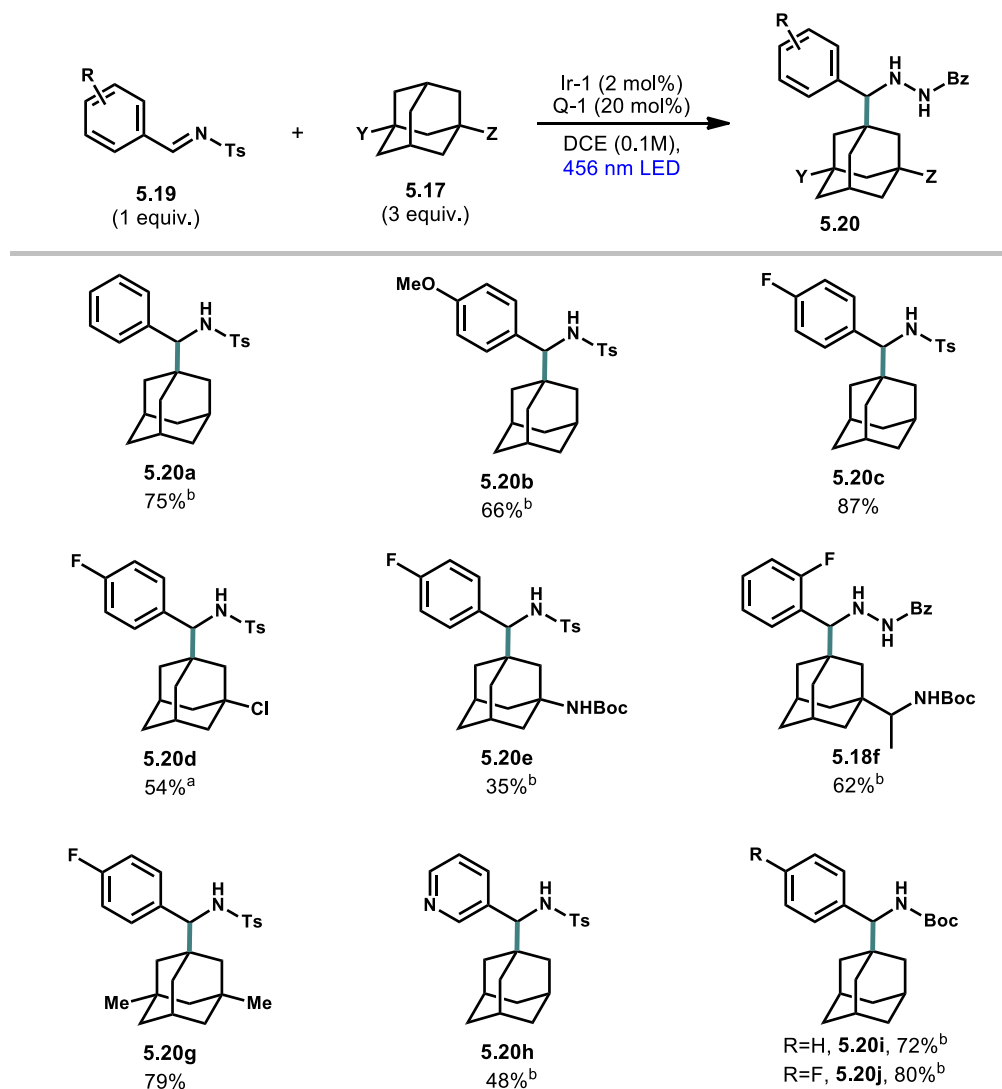


Reactions performed on a 0.5 mmol scale using 2 x 40W 456nm lamps over 24-72 h. All yields are isolated yields. a) Solvent is CH₃CN. b) Synthesized by coworker Hoang Dang

5.4.2 - *N*-Tosyl Imines

N-Tosyl imines were generally more reactive than the benzoyl hydrazones due to the more electron withdrawing nature of the toluenesulfonyl group. Moderate to high yields were obtained even with more electron rich aryl groups. Phenyl tosyl imine **5.20a** resulted in a 75% yield while its benzoyl hydrazone analog **5.18l**, only gave a yield of 22%. Similarly, *para*-fluoro tosyl imine **5.20c** proceeded to give a higher yield than the benzoyl hydrazone variant **5.18g** (87% compared to 53%, respectively). Electron rich aryl substituents such as a *para*-anisaldehyde derived imine **5.20b** worked in moderate yield. A Ts-imine featuring a pyridine substituent resulted in a 48% yield. Like the benzoyl hydrazones, electron withdrawn chloro- and NHBoc-adamantanes (**5.20d** and **5.20e**) were less efficient and gave yields of only 54% and 35%, respectively. The use of dimethyl adamantane did not increase the yield over unsubstituted adamantane (compare **5.20c** and **5.20g**). Two *N*-Boc imines were tried and gave products **5.20i** and **5.20j** in yields of 72% and 80%, respectively.

Table 5.9 – Scope of *N*-Tosyl Imines with Various Adamantanes



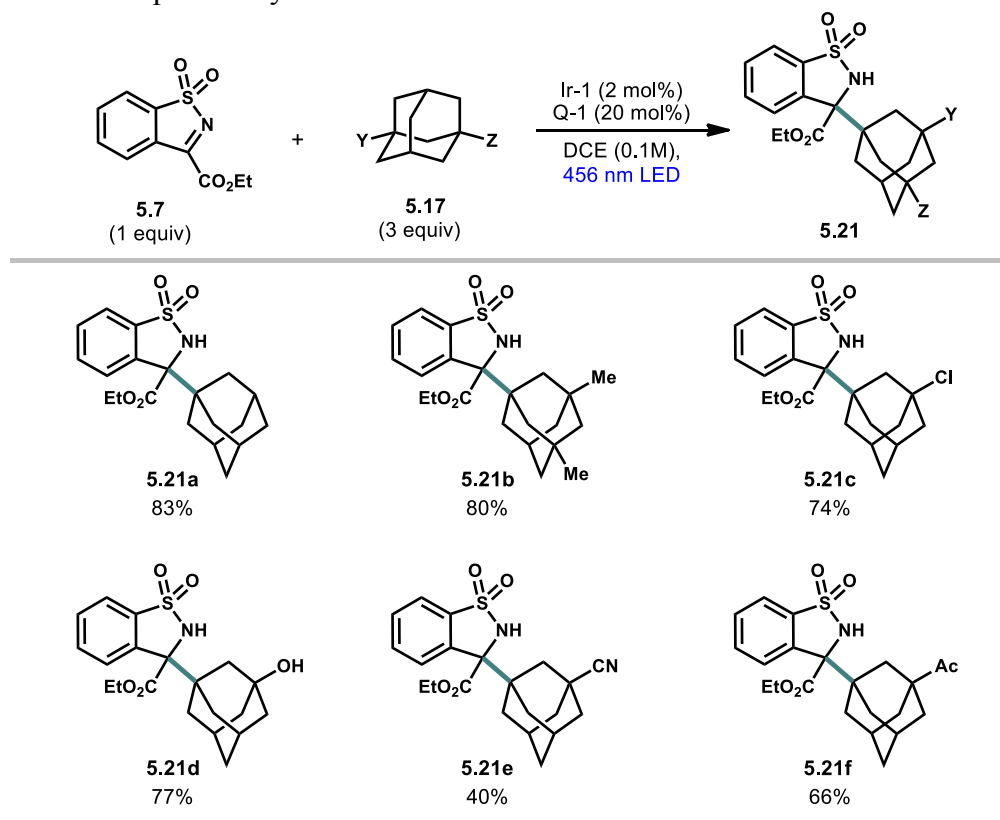
Reactions performed on a 0.5 mmol scale using 2 x 40W 456nm lamps over 24-72 h. All yields are isolated yields. a) Solvent is CH₃CN. b) Synthesized by coworker Hoang Dang

5.4.3 - Cyclic Sulfonimine

Reactions involving cyclic sulfonimine **5.7** were found to work well with a variety of substituted adamantanes (**5.21a-e**, Table 5.10). The bond forming step leads to two

adjacent fully-substituted centers, highlighting the ability of this reaction to create sterically congested products. Unsubstituted adamantane **5.21a** and electron rich dimethyladamantane **5.21b** were highest yielding (83% and 80%, respectively). Introduction of inductively withdrawing hydroxy or chloro substituents resulted in small drops in yield (**5.21c,d**). More significant decreases in yield were seen with withdrawing nitrile and acetyl substituents (**5.21e,f**).

Table 5.10 – Scope of a Cyclic Sulfonimine with Various Adamantanes



Reactions performed on a 0.5 mmol scale using 2 x 40W 456nm lamps over 24-48 h. All yields are isolated yields.

Electron-deficient adamantanes result in lower yields than with electron rich or unsubstituted adamantanes. The decreases in reaction efficiency observed with sulfonimine **5.7** and the various electron deficient adamantane substrates are also observed with other imines. During C–H abstraction, the developing positive charge on adamantane is

destabilized by the presence of electron withdrawing substituents. This likely reduces the rate of the HAT step leading to the formation of the adamantyl radical intermediate and explains the poorer results seen with electron deficient adamantane substrates.

5.4.4 - Chiral Sulfinyl Imines

The chiral adamantyl methanamino scaffold is present in at least two clinically approved pharmaceuticals: saxagliptin, an antidiabetic, and rimantadine, an antiviral (Figure 5.12).

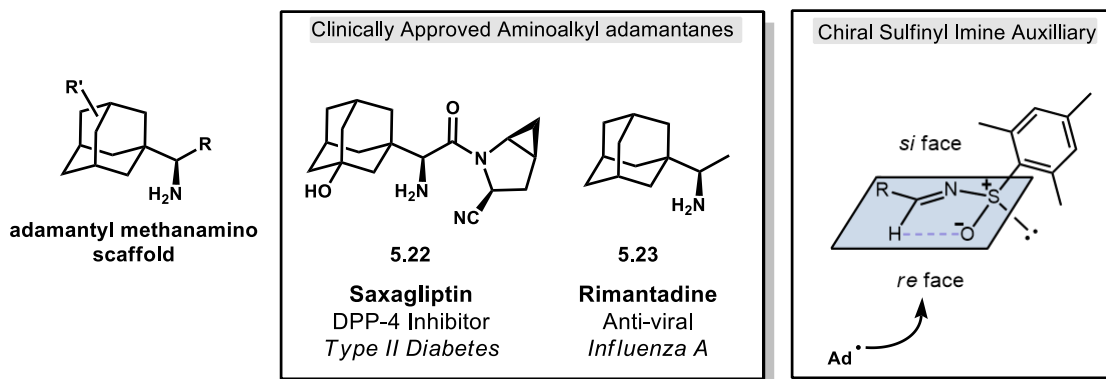
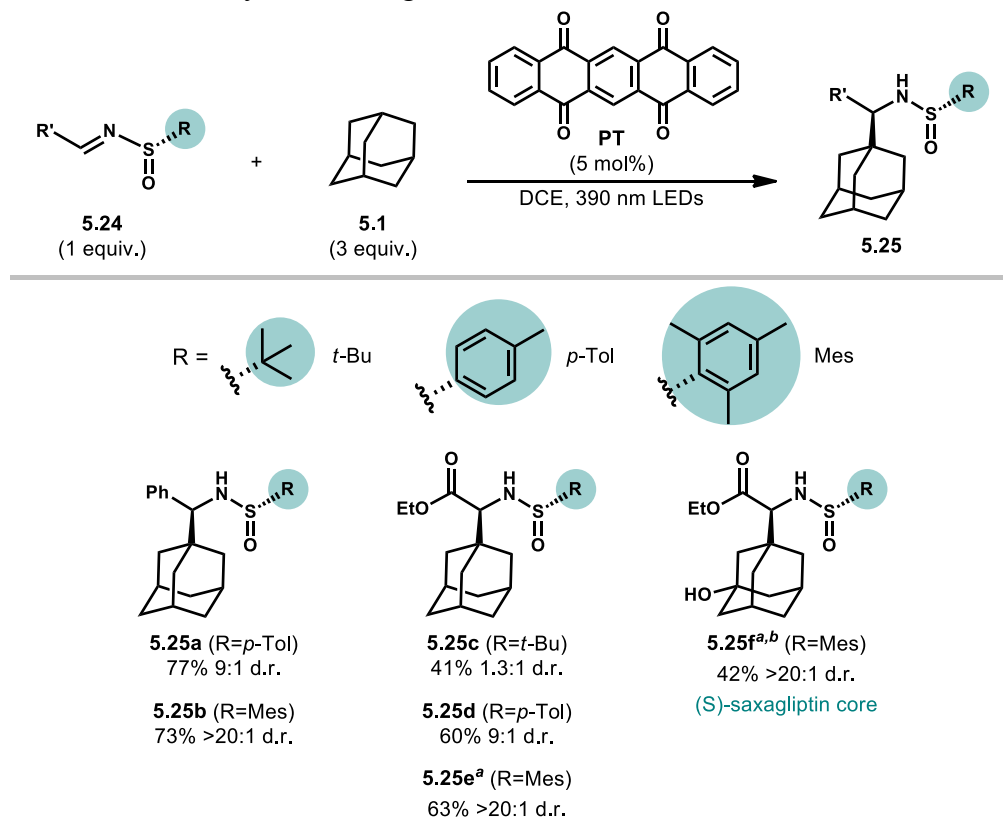


Figure 5.12 – Amino adamantanes of Medicinal Relevance

As such, an enantioselective route to these products is valuable. The use of chiral sulfinyl imines such as the Ellman *N-tert*-butylsulfinyl auxiliary is effective in asymmetric amine synthesis.^[32–37] In particular, glyoxylate-derived chiral sulfinimines have been used for the preparation of enantiopure α -amino acids.^[37–40] Because of the chiral α -amino core present in saxagliptin, we set out to investigate the viability of using chiral sulfinimines to obtain enantioenriched amino adamantanes.

The chiral sulfinimines were found to be less efficient with the **Ir-1/Q-1** catalytic system due to slower rates of conversion which resulted in higher degree of hydrolysis

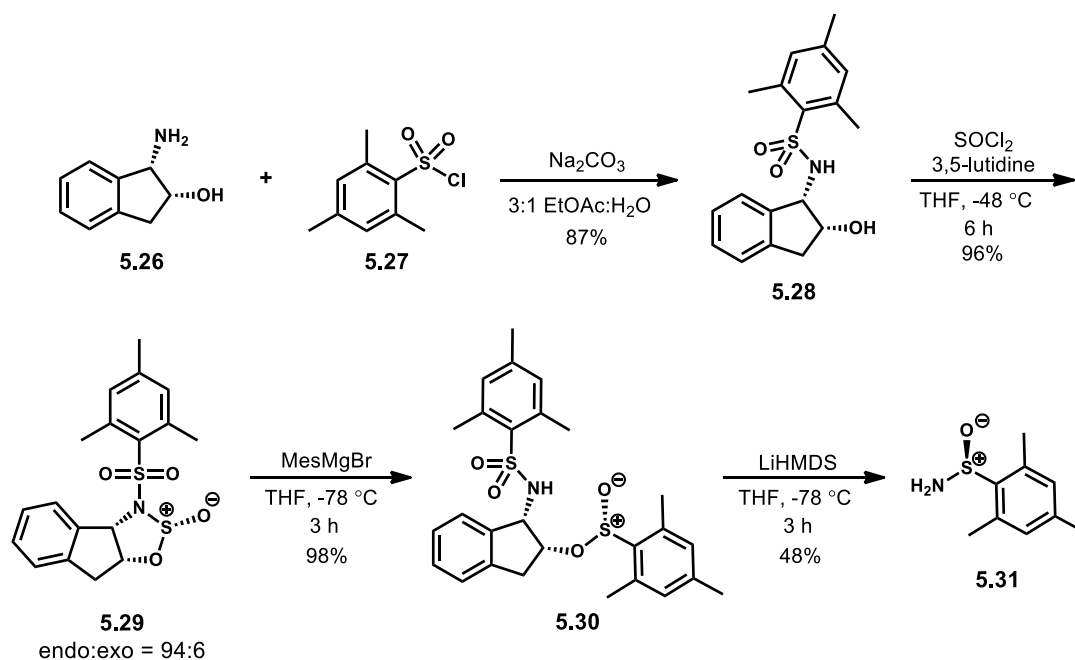
Table 5.11 – Aminoalkylation Using Chiral Sulfinimines



Reactions performed on a 0.3 mmol scale using 2 x 40W 390 nm lamps over 48-72 h. All yields are isolated yields. d.r. values obtained by ¹H NMR analysis of crude reaction mixture a) Performed on 0.5 mmol scale. b) Performed using 1:1 DCE:PhCl as solvent.

back to the starting aldehyde and sulfinamide. This undesired hydrolysis was found to be significantly mitigated by using 5,7,12,14-pentacenetetraone (**PT**) as a photocatalyst instead. Initial testing with a glyoxylate-derived Ellman *tert*-butyl sulfinimine resulted in only a slight asymmetric induction in aminoalkylated product **5.25c**, d.r. 1.3:1 (**Table 5.11**Table 1.1). However, a large improvement in diastereoselectivity was obtained after switching to the Davis *para*-tolyl auxiliary, which is more commonly used in radical reactions.^[40–42] Both benzaldehyde- and glyoxylate- derived *para*-tolylsulfinimines (**5.25a** and **5.25d**, respectively) showed an increase in d.r. to 9:1 as confirmed by ¹H NMR analysis of the product mixture (**Figure 5.13**).

It was theorized that further increasing the steric bulk of the auxiliary might boost the reaction's diastereoselectivity again. However, while *tert*-butyl and *para*-tolyl sulfinamides are commercially available at reasonable cost, the mesityl sulfinamide recently used by Baran and coworkers^[37] is much more costly (~\$50/mg). The mesitylsulfinamide (**5.31**) was therefore synthesized over four steps starting with *cis*-aminoindanol according to a procedure by Han and Senanayake^[43] (**Scheme 5.2**). With mesitylsulfinamide in hand, it was used to synthesize the corresponding benzaldehyde and glyoxylate sulfinimines for use in photochemical aminoalkylation reactions with adamantane. Gratifyingly, the resulting mesitylsulfinamide products **5.25b** and **5.25e** in moderate yield and >20:1 d.r. The (*S*)-saxagliptin core (**5.25f**) was also assembled with >20:1 d.r. using 1-adamantanol.



Scheme 5.2 – Synthesis of Chiral Mesitylsulfinamide

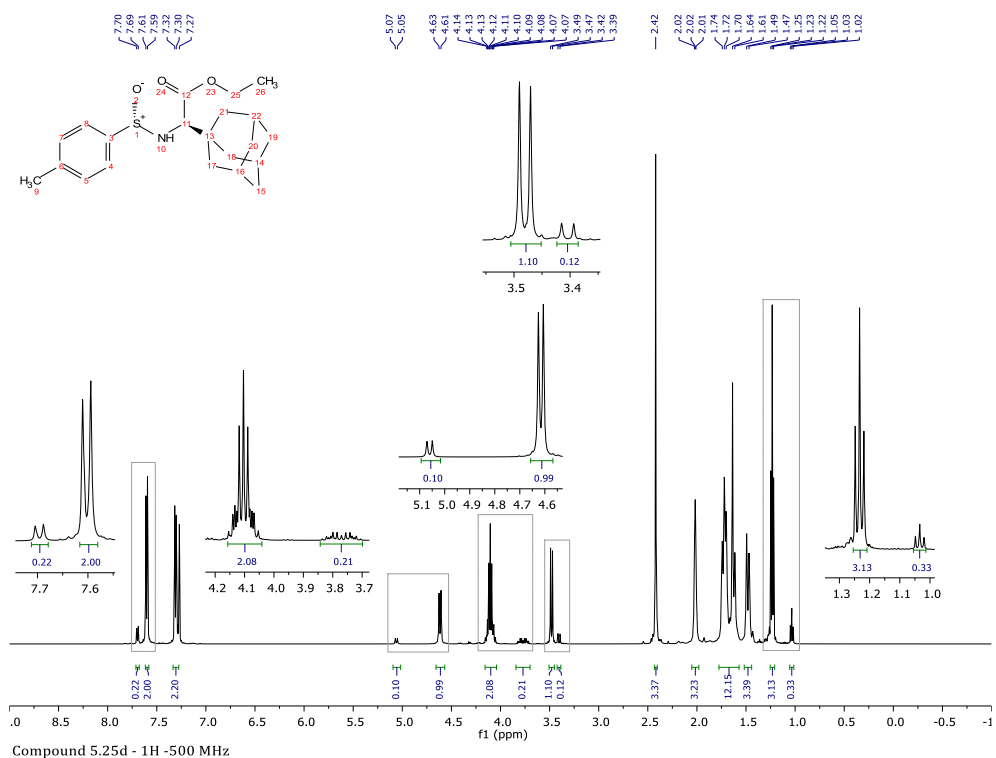


Figure 5.13 – ^1H NMR of a Diastereomeric Mixture of Aminoalkyl Tosylsulfonimines
5.4.5 - Non-Adamantyl Substrates

The aminoalkylations presented here have focused on using conditions that favor the selective functionalization of adamantane. However, we were also interested in their efficacy with non-adamantyl substrates such as cyclohexane and tetrahydrofuran. Tetrahydrofuran was able to be functionalized using the **Ir-1/Q-1** and cyclic sulfonimine **5.7** to give **5.32** isolated as a mixture of diastereomers in 50% yield. The PT system was also found to be capable of functionalizing cyclohexane to a small extent making tosylsulfonamide **5.33** in 30% yield. Notably, while the catalyst systems we describe here are the most efficient for adamantane by a significant margin, other methods such as decatungstate currently provide a better solution for the direct aminoalkylation of other hydrocarbons and ether substrates.^[4,25,44,45]

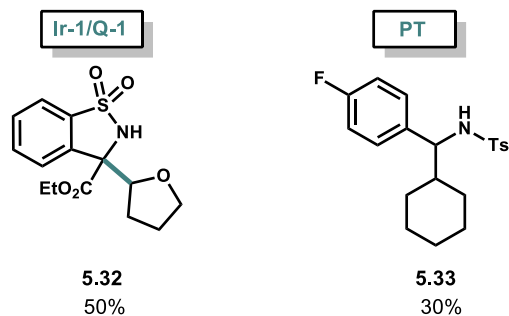
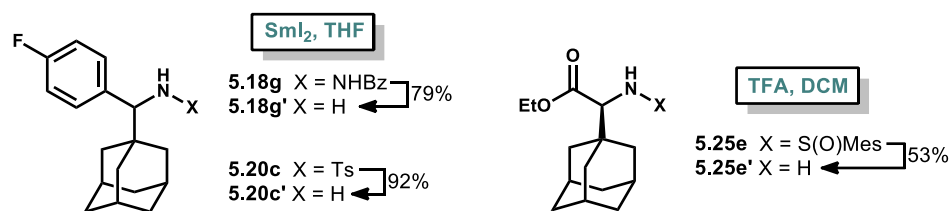


Figure 5.14 – Examples of Non-Adamantyl Aminoalkylated Products

5.5 - Deprotections

In order to expand the application of these amino adamantane products, we set out to demonstrate the viability of deprotection to the free amine for a few representative examples. Free amines with α -adamantyl substituents such as rimantadine commonly possess antiviral or other activities.^[15] Free amines are also useful functional handles for further synthetic diversification which is useful in pharmaceutical drug development and design.



Scheme 5.3 – Deprotection to Free Amine Products Using SmI_2 and TFA

Samarium diiodide was found to be useful in the deprotection of hydrazone **5.18g** and toluenesulfonamide **5.20c**. Sodium metal and sodium naphthalenide were also tried but caused significant decomposition for both the hydrazone and sulfonamide starting materials. Using samarium diiodide, the deprotected free amine products **5.18g'** and **5.20c'** were obtained in yields of 79% and 92% respectively. The sulfinyl group in **5.25e** was

removed under acidic conditions using a mixture of TFA and DCM to obtain the adamantylglycine ethyl ester **5.25e'**. To confirm that the deprotection process using these conditions did not compromise the enantiopurity of the starting materials, optical rotations were taken using both **5.25e'** enantiomers (from the correspondent deprotections of the S,S- and R,R-**5.25e** sulfinimines). Equal but opposite $[\alpha]_D$ values of -33.6 and 33.5 deg·mL/g⁻¹·dm⁻¹ were obtained for the S and R enantiomers which implies their stereochemistry remains fixed throughout this deprotection procedure.

5.6 - Conclusions

The photocatalytic aminoalkylation of a wide variety of imines using adamantane has been demonstrated through selective hydrogen atom abstraction. The use of an iridium photocatalyst together with a quinuclidine co-catalyst was used for the aminoalkylation of *N*-benzoyl hydrazones, *N*-tosyl imines, and a cyclic sulfonimine. A variety of substituted adamantanes were also compatible with this methodology although in general, electron withdrawing substituents resulted in decreased yields. A quinone based catalyst, pentacenetetraone, enables the enantioselective aminoalkylation of unnatural α -adamantyl amino acid derivatives which are present in approved pharmaceuticals such as saxagliptin. Other non-adamantyl substrates such as cyclohexane and tetrahydrofuran were able to be used with these catalytic systems, although with diminished yields. Overall, this work provides a stable platform for the synthesis of a diverse array of potential biologically active adamantane derivatives. In the future, expanding this methodology to include more than just adamantane would be of use. Additionally, undertaking work to identify the

antiviral effects of these aminoalkylated analogs is promising due to the similar structure of these derivatives to rimantadine, a known antiviral.

5.7 - Experimental

5.7.1 - General Methods

The general methods used in this chapter are the same as those listed in chapter 3 with the exception of the following: ^1H and ^{13}C NMR spectra were recorded on a Bruker Avance NEO 400, Bruker Avance III 500. High resolution mass spectrometry data was recorded on an Agilent LCTOF instrument using direct injection of samples in dichloromethane into the electrospray source (ESI) with positive ionization.

5.7.2 - General Procedures

General Procedure A: Photochemical Reactions with Ir-1/Q-1

To an 8-mL glass vial equipped with a magnetic stir bar were sequentially added imine (0.50 mmol, 1.0 equiv), photoredox catalyst Ir-1 (2 mol%), hydrogen atom transfer catalyst (20 mol%), adamantane (1.50 mmol, 3.0 equiv), and 1,2-dichloroethane (5.0 mL, 0.2 M). The vial was sealed with a Teflon septum and screw-top cap. The resulting mixture was degassed by freezing the vial contents in a dry ice/acetone bath, placing the vial under a static vacuum, then allowing the frozen mixture to thaw (this cycle was repeated 3 times) then backfilled with N_2 . The vials were then placed on a stir plate and irradiated between two 456nm Kessil® PR160 LED lamps (<http://www.kessil.com/photoredox/Products.php>) 4 inches away from the diode source on each side. A single small desktop fan was aimed directly at the vial to facilitate heat dissipation (experiments set up in this manner operate at just over room temperature at approx. 27 °C).

General Procedure B: Photochemical Reactions with PT

To an 8-mL glass vial equipped with a magnetic stir bar were sequentially added chiral sulfinimine (1.0 equiv), pentacenetetraone photoredox catalyst PT (5-10 mol%), adamantane (3.0 equiv), and 1,2-dichloroethane (0.1 M). The vial was sealed with a Teflon septum and screw-top cap. The resulting mixture was degassed by freezing the vial contents in a dry ice/acetone bath, placing the vial under a static vacuum, then allowing the frozen mixture to thaw (this cycle was repeated 3 times) then backfilled with N₂. The vials were then placed on a stir plate and irradiated between two 390nm Kessil® PR160 LED lamps (<http://www.kessil.com/photoredox/Products.php>) 4 inches away from the diode source on each side. A single small desktop fan was aimed directly at the vial to facilitate heat dissipation (experiments set up in this manner operate at just over room temperature at approx. 30 °C).

General Procedure C: Hydrazone Condensations

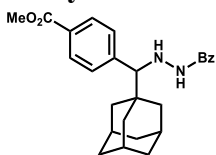
To a round bottom flask equipped with a magnetic stir bar were added N-acylhydrazide (7.00 mmol, 1 equiv) followed by 14 mL ethanol. The aldehyde/ketone (8.40 mmol, 1.2 equiv) was then added and the flask was fitted with a reflux condenser and sparged with nitrogen for 5 mins. The reaction was then heated to 95 °C and stirred for 4-8 hours at reflux until the reaction was judged complete by TLC. The reaction mixture was allowed to cool to room temperature and was then stored in the freezer (-4 °C) overnight to allow the product to crystallize. The crystals were then collected via vacuum filtration and rinsed with cold ethanol then cold hexanes.

Synthesis of Chiral N-Sulfinyl imines Chiral N-Sulfinyl imines were prepared via condensation on to the respective aldehyde according to known literature procedure^[16] from the commercially available chiral sulfinamides or synthesized in the case of mesitylsulfinamide according to the following procedure.^[43]

Synthesis of Iridium Photocatalysts The iridium photocatalyst was synthesized following known literature preparations.^[46,47]

Synthesis of Quinuclidine HAT Catalyst The quinuclidine sulfonate HAT catalyst was synthesized using the procedure used previously by our group.^[28]

methyl 4-adamantan-1-yl((2-benzoylhydrazinyl)methyl)benzoate (5.18a):

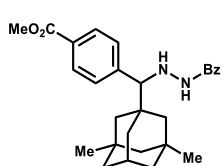


5.18a

According to *General Procedure A*, methyl 4-((2-benzoylhydrazono)methyl)benzoate (0.141 g, 0.50 mmol, 1.0 equiv), photoredox catalyst **Ir-1** (0.011 g, 2 mol%), quinuclidine phenylsulfonate (0.026 g, 20 mol%), adamantane **5.1** (0.204 g, 1.50 mmol, 3.0 equiv), and 1,2-dichloroethane (5.0 mL) reacted for 24 hours. The dark brown reaction mixture was then reduced to dryness under vacuum and the resulting solid was purified using column chromatography (gradient from 5-40% ethyl acetate in a 2:1 mixture of hexane : dichloromethane) to give a tan solid (0.161 g, 76%). ¹H NMR (400 MHz,) δ 8.01 (d, $J = 8.0$ Hz, 2H), 7.52 – 7.40 (m, 4H), 7.37 – 7.29 (m, 2H), 7.18 (d, $J = 7.2$ Hz, 1H), 5.56 (dd, $J = 7.2, 2.1$ Hz, 1H), 3.93 (s, 3H), 3.80 (s, 1H), 1.99 (p, $J = 3.2$ Hz, 3H), 1.77 – 1.65 (m, 6H), 1.65 – 1.58 (m, 6H). ¹³C NMR (100 MHz, Chloroform-*d*) δ 167.2, 167.2, 144.9, 132.9, 131.8, 129.3, 129.1, 128.7, 126.8, 74.8, 52.2, 39.1, 37.0, 36.4, 28.5.

IR (ATR) 3366, 2900, 2847, 1708, 1664 cm^{-1} **HRMS** (ESI) m/z calcd for $\text{C}_{26}\text{H}_{31}\text{N}_2\text{O}_3$ $(\text{M}+\text{H})^+ = 419.2329$, found 419.2327.

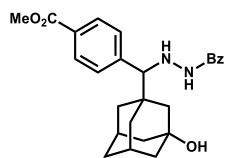
methyl 4-((3,5-dimethyladamantan-1-yl)2-benzoylhydrazinyl)methyl benzoate



(5.18b):

According to *General Procedure A*, methyl 4-((2-benzoylhydrazono)methyl)benzoate (0.141 g, 0.50 mmol, 1.0 equiv), photoredox catalyst **Ir-1** (0.011 g, 2 mol%), quinuclidine phenylsulfonate (0.026 g, 20 mol%), 3,5-dimethyladamantane (0.278 mL, 1.50 mmol, 3.0 equiv), and 1,2-dichloroethane (5.0 mL) were reacted for 24 hours. The dark brown reaction mixture was then reduced to dryness under vacuum and the resulting solid was purified using column chromatography (3:2:1 hexanes: dichloromethane: ethyl acetate) to give an off-white solid (0.180 g, 80%). **¹H NMR** (400 MHz, Chloroform-*d*) δ 7.97 (d, $J = 8.3$ Hz, 2H), 7.52 – 7.39 (m, 5H), 7.34 – 7.28 (m, 2H), 5.52 (s, 1H), 3.90 (s, 3H), 3.83 (s, 1H), 2.09 – 2.01 (m, 1H), 1.52 (d, $J = 12.0$ Hz, 1H), 1.41 (d, $J = 12.0$ Hz, 1H), 1.36 – 1.16 (m, 8H), 1.11 (d, $J = 12.3$ Hz, 1H), 1.02 (d, $J = 12.3$ Hz, 1H), 0.79 (s, 6H). **¹³C NMR** (100 MHz, Chloroform-*d*) δ 167.2, 167.1, 144.9, 132.8, 131.8, 129.2, 129.1, 128.6, 126.9, 74.2, 52.2, 51.1, 45.3, 45.2, 43.2, 38.2, 37.7, 31.2, 31.2, 30.8, 29.5. **IR** (ATR) 3367, 3306, 3056, 2901, 2846, 1709 cm^{-1} **HRMS** (ESI) m/z calcd for $\text{C}_{28}\text{H}_{35}\text{N}_2\text{O}_3$ $(\text{M}+\text{H})^+ = 447.2642$, found 447.2632.

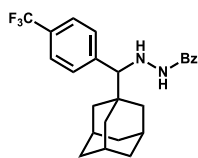
methyl 4-((3-hydroxyadamantan-1-yl)methyl)benzoylhydrazinyl)methyl)benzoate (5.18c):



5.18c

According to *General Procedure A*, methyl 4-((2-benzoylhydrazono)methyl)benzoate (0.141 g, 0.50 mmol, 1.0 equiv), photoredox catalyst **Ir-1** (0.011 g, 2 mol%), quinuclidine phenylsulfonate (0.026 g, 20 mol%), 1-hydroxyadamantane (0.228 g, 0.90 mmol, 3.0 equiv), and 1,2-dichloroethane (5.0 mL) were reacted for 24 hours. The dark brown reaction mixture was then reduced to dryness under vacuum and the resulting solid was purified using column chromatography (3:2:1 hexanes: dichloromethane: ethyl acetate) to give an off-white solid (0.180 g, 31%). ¹H NMR (500 MHz, Chloroform-*d*) δ 7.99 (d, *J* = 8.1 Hz, 2H), 7.48 (d, *J* = 7.2 Hz, 2H), 7.47 – 7.40 (m, 2H), 7.36 – 7.30 (m, 4H), 5.49 (d, *J* = 5.1 Hz, 1H), 3.91 (s, 3H), 3.89 (s, 1H), 2.22 (s, 2H), 1.75 (s, 1H), 1.68 – 1.63 (m, 4H), 1.62 – 1.50 (m, 7H), 1.49 – 1.43 (m, 1H). ¹³C NMR (100 MHz, Chloroform-*d*) δ 167.3, 167.2, 144.4, 132.7, 131.9, 129.5, 129.3, 128.7, 126.9, 73.8, 68.9, 52.3, 46.5, 44.8, 44.7, 40.0, 38.3, 37.6, 35.4, 30.5, 30.4.

***N'*-adamantan-1-yl((4-(trifluoromethyl)phenyl)methyl)benzohydrazide (5.18d):**

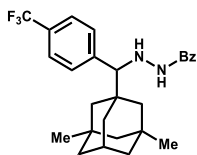


5.18d

According to *General Procedure A*, *N'*-(4-(trifluoromethyl)benzylidene)benzohydrazide (0.146 g, 0.50 mmol, 1.0 equiv), photoredox catalyst **Ir-1** (0.011 g, 2 mol%), quinuclidine phenylsulfonate (0.026 g, 20 mol%), adamantane **5.1** (0.204 g, 1.50 mmol, 3.0 equiv), and 1,2-dichloroethane (5.0 mL) were reacted for 24 hours. The dark brown reaction mixture was then reduced to dryness under vacuum and the resulting solid was purified using column chromatography (gradient from 1:2 ethyl acetate: hexanes to 3:2 ethyl acetate: hexanes) to give an off white solid (0.060 g, 28%). ¹H NMR (400 MHz,

) δ 7.60 (d, $J = 7.9$ Hz, 2H), 7.55 – 7.42 (m, 5H), 7.39 – 7.32 (m, 2H), 7.16 (s, 1H), 3.80 (s, 1H), 2.00 (s, 3H), 1.77 – 1.67 (m, 6H), 1.65 – 1.55 (m, 6H). ^{13}C NMR (100 MHz, Chloroform- d) δ 167.3, 132.8, 132.0, 129.9 (m, obscured), 129.6 (q, $J = 32.5$ Hz), 128.8, 126.8, 124.8, 124.8, 124.4 (q, $J = 272.1$ Hz), 74.7, 39.1, 37.0, 36.4, 28.5. IR (ATR) 3306, 3242, 2925, 2883, 2850, 1623 cm^{-1} HRMS (ESI) m/z calcd for $\text{C}_{25}\text{H}_{28}\text{F}_3\text{N}_2\text{O}$ ($\text{M}+\text{H}$) $^+ = 429.2148$, found 429.2137.

***N'*-(3,5-dimethyladamantanyl)((4-(trifluoromethyl)phenyl)methyl) benzohydrazide (5.18e):**

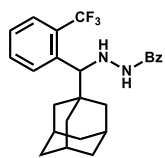


5.18e

According to *General Procedure A*, *N'*-(4-(trifluoromethyl)benzylidene)benzohydrazide (0.146 g, 0.50 mmol, 1.0 equiv), photoredox catalyst **Ir-1** (0.011 g, 2 mol%), quinuclidine phenylsulfonate (0.026 g, 20 mol%), 3,5-dimethyladamantane (0.278 mL, 1.50 mmol, 3.0 equiv), and 1,2-dichloroethane (5.0 mL) were reacted for 24 hours. The dark brown reaction mixture was then reduced to dryness under vacuum and the resulting solid was purified using column chromatography (product dry loaded on silica support followed by elution with 200 mL hexanes then 1:9 ethyl acetate: toluene) to give a light brown solid (0.101 g, 44%). ^1H NMR (500 MHz, Chloroform- d) δ 7.60 (d, $J = 8.0$ Hz, 2H), 7.52 – 7.44 (m, 5H), 7.36 (t, $J = 7.7$ Hz, 2H), 7.17 (s, 1H), 5.55 (s, 1H), 3.85 (s, 1H), 2.10 – 2.05 (m, 1H), 1.54 (d, $J = 12.1$ Hz, 1H), 1.43 (d, $J = 12.1$ Hz, 1H), 1.37 – 1.19 (m, 8H), 1.14 (d, $J = 12.3$ Hz, 1H), 1.05 (d, $J = 12.3$ Hz, 1H), 0.82 (s, 6H). ^{13}C NMR (100 MHz, Chloroform- d) δ 167.3, 143.6, 132.8, 132.0, 129.9 (m, obscured), 129.6 (q, $J = 32.3$ Hz), 128.8, 126.8, 124.9, 124.9, 124.4 (q, $J = 271.9$ Hz), 74.2, 51.1, 45.4, 45.2, 43.2, 38.2, 37.7, 31.3, 30.8,

29.5. **IR** (ATR) 3319, 3261, 2920, 2865, 2839, 1628 cm^{-1} **HRMS** (ESI) m/z calcd for $\text{C}_{27}\text{H}_{32}\text{F}_3\text{N}_2\text{O}$ ($\text{M}+\text{H}$) $^+$ = 457.2461, found 457.2463.

***N'*-(adamantan-1-yl(2-(trifluoromethyl)phenyl)methyl)benzohydrazide (5.18f):**

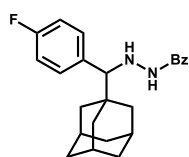


5.18f

According to *General Procedure A*, *N'*-(2-(trifluoromethyl)benzylidene)benzohydrazide (0.146 g, 0.50 mmol, 1.0 equiv), photoredox catalyst **Ir-1** (0.012 g, 2 mol%), quinuclidine phenylsulfonate (0.026 g, 20 mol%), adamantane **5.1** (0.204 g, 1.50 mmol,

3.0 equiv) and 1,2-dichloroethane (5.0 mL) were reacted for 24 hours (cooling fan was omitted for this reaction). The dark brown reaction mixture was then reduced to dryness under vacuum and the resulting solid was purified using column chromatography (0-10% ethyl acetate gradient in hexanes) to give a white solid (0.061 g, 29%). **^1H NMR** (400 MHz, Chloroform-*d*) δ 7.94 (d, J = 8.0 Hz, 1H), 7.66 (d, J = 8.0 Hz, 1H), 7.60 (t, J = 7.6 Hz, 1H), 7.49 (d, J = 7.1 Hz, 2H), 7.42 (p, J = 7.6 Hz, 2H), 7.34 (t, J = 7.6 Hz, 2H), 7.00 (s, 1H), 5.63 (s, 1H), 4.24 (s, 1H), 2.00 (s, 3H), 1.93 (d, J = 11.7 Hz, 3H), 1.67 (q, J = 12.4 Hz, 6H), 1.61 – 1.42 (m, 3H). **^{13}C NMR** (100 MHz, Chloroform-*d*) δ 167.3, 139.5, 133.2, 131.7, 131.2, 130.8, 128.7, 127.4, 126.8, 126.1 – 125.9 (m, obscured), 125.9, 124.44 (d, J = 275.0 Hz) 68.5, 39.3, 37.2, 37.0, 28.7. **IR** (ATR) 3317, 3214, 3081, 2929, 2904, 2849, 1633 cm^{-1} **^1H HRMS** (ESI) m/z calcd for $\text{C}_{25}\text{H}_{27}\text{F}_3\text{N}_2\text{O}$ ($\text{M}+\text{H}$) $^+$ = 428.2075, found 428.2086.

***N*'-(adamantan-1-yl(4-fluorophenyl)methyl)benzohydrazide (5.18g):**



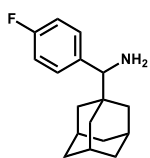
5.18g

According to *General Procedure A*, *N*'-(4-fluorobenzylidene)benzohydrazide (0.121 g, 0.50 mmol, 1.0 equiv), photoredox catalyst **Ir-1** (0.012 g, 2 mol%), quinuclidine phenylsulfonate (0.026 g, 20 mol%), adamantane **5.1** (0.204 g, 1.50 mmol, 3.0 equiv) and acetonitrile (5.0 mL) were reacted for 48 hours (cooling fan was omitted for this reaction). The dark brown reaction mixture was then reduced to dryness under vacuum and the resulting solid was purified using column chromatography (0-7% ethyl acetate gradient in hexanes) to give a white solid (0.100 g, 53%). with spectra matching known literature .¹ **¹H NMR** (400 MHz, Chloroform-*d*) δ 7.50 (d, $J = 7.7$ Hz, 2H), 7.45 (d, $J = 7.4$ Hz, 1H), 7.34 (dd, $J = 16.1, 8.5$ Hz, 4H), 7.13 (s, 1H), 7.04 (t, $J = 8.6$ Hz, 2H), 5.55 (s, 1H), 3.71 (s, 1H), 2.15 – 1.94 (m, 3H), 1.70 (t, $J = 9.3$ Hz, 6H), 1.60 (d, $J = 13.0$ Hz, 6H). **¹³C NMR** (126 MHz, Chloroform-*d*) δ 167.0, 162.3 (d, $J = 245.2$ Hz), 134.8 (d, $J = 3.2$ Hz), 133.1, 131.8, 130.9 (d, $J = 7.7$ Hz), 128.8, 126.8, 114.8 (d, $J = 20.9$ Hz), 74.4, 39.1, 37.1, 36.3, 28.6. **IR** (ATR) 3304, 3223, 3065, 2902, 2849, 1640 cm^{-1} **HRMS** (ESI) m/z calcd for $\text{C}_{24}\text{H}_{27}\text{FN}_2\text{O}$ ($\text{M}+\text{H}$)⁺ = 378.2107, found 378.2102.

***N*'-(adamantan-1-yl(4-fluorophenyl)methanamine (5.18g'):**

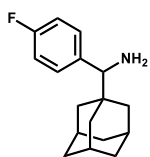
From *N,N*-benzoyl and *N*-tosyl adamantyl amines, deprotected amine (**51**) was prepared according to previously reported procedures^[2,49], with some modifications.

¹ [48]



5.18g'

A flame-dried flask containing 0.050 g adamantane product **20** (0.121 mmol, 1.0 equiv) was degassed and loaded with 0.50 mL tetrahydrofuran, samarium diiodide (9.30 mL of 1.0 M solution in THF, 10.0 equiv) and water (0.058 mL, 30.0 equiv) under nitrogen. To the dark blue mixture was added pyrrolidine (0.198 mL, 20.0 equiv), causing an amalgamation and rapid discoloration from dark blue to white. After stirring for 10 minutes at room temperature, the mixture was diluted with methylene chloride and washed with 5 mL of potassium sodium tartrate and 5 mL potassium carbonate (10% w/v each). The organic layer was washed with 5 mL brine, dried over sodium sulfate, and concentrated under vacuum. The residue was purified on preparatory TLC (1:2:4 chloroform : ethyl acetate : hexanes), and the resulting product was further flushed through a short plug of silica (hexanes wash then slow increase to 100% ethyl acetate) to afford an off-white solid. (0.034 g, 92%). ¹H NMR (500 MHz, Chloroform-*d*) δ 7.25 – 7.14 (m, 2H), 6.99 (t, *J* = 8.7 Hz, 2H), 3.51 (s, 1H), 1.97 (s, 3H), 1.67 (d, *J* = 11.1 Hz, 3H), 1.61 – 1.53 (m, 6H), 1.53 – 1.37 (m, 3H). ¹³C NMR (125 MHz, Chloroform-*d*) δ 161.9 (d, *J* = 244.4 Hz), 130.6, 129.9, 114.2, 114.2, 65.5, 38.8, 37.2, 28.6. IR (ATR) 2900, 2848, 1665, 1603 cm⁻¹ HRMS (ESI) *m/z* calcd for C₁₇H₂₂FN (M+H)⁺ = 260.1815, found 260.1807.

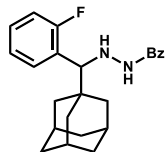


5.20c'

A flame-dried flask containing 0.050 g adamantane product **27** (0.132 mmol, 1.0 equiv) was degassed and loaded with 0.50 mL methanol, samarium diiodide (4.0 mL of 1.0 M solution in THF, 3.0 equiv) under nitrogen. After stirring for 10 minutes at room temperature, the mixture was diluted with methylene chloride and washed with 5 mL of potassium sodium tartrate and 5 mL potassium carbonate (10% w/v each). The organic layer was washed with 5 mL brine, dried over sodium sulfate,

and concentrated under vacuum. The residue was purified on preparatory TLC (1:1:5 chloroform : ethyl acetate : hexanes), and the resulting product was further flushed through a short plug of silica (hexanes wash then slow increase to 100% ethyl acetate) to afford an off-white solid. (0.020 g, 79%). **HRMS** (ESI) m/z calcd for $C_{17}H_{22}FN$ ($M+H$)⁺ = 260.1815, found 260.1808.

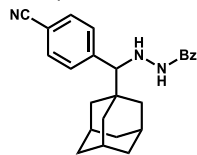
***N'*-(adamantan-1-yl(2-fluorophenyl)methyl)benzohydrazide (5.18h):**



5.18h

According to *General Procedure A*, *N'*-(2-fluorobenzylidene)benzohydrazide (0.121 g, 0.50 mmol, 1.0 equiv), photoredox catalyst **Ir-1** (0.012 g, 2 mol%), quinuclidine phenylsulfonate (0.026 g, 20 mol%), adamantane **5.1** (0.204 g, 1.50 mmol, 3.0 equiv) and 1,2-dichloroethane (5.0 mL) were reacted for 24 hours (cooling fan was omitted for this reaction). The dark brown reaction mixture was then reduced to dryness under vacuum and the resulting solid was purified using column chromatography (0-7% ethyl acetate gradient in hexanes) to give a white solid (0.114 g, 60%). **¹H NMR** (400 MHz, Chloroform-*d*) δ 7.69 – 7.61 (m, 1H), 7.52 (d, J = 7.6 Hz, 2H), 7.45 (t, J = 7.4 Hz, 1H), 7.35 (t, J = 7.6 Hz, 2H), 7.31 – 7.23 (m, 1H), 7.20 (t, J = 7.5 Hz, 1H), 7.14 (s, 1H), 7.03 (t, J = 9.2 Hz, 1H), 5.57 (s, 1H), 4.20 (s, 1H), 2.00 (t, J = 3.3 Hz, 3H), 1.82 (d, J = 12.4 Hz, 3H), 1.74 – 1.57 (m, 9H). **¹³C NMR** (126 MHz, Chloroform-*d*) δ 167.0, 162.3 (d, J = 247.3 Hz), 133.0, 131.8, 129.9, 128.7, 128.6 (d, J = 8.4 Hz), 126.9, 123.7 (d, J = 3.4 Hz), 115.3 (d, J = 23.2 Hz), 66.2, 38.7, 37.1, 37.0, 28.6. **IR** (ATR) 3309, 3281, 2904, 2847, 1634 cm^{-1} **HRMS** (ESI) m/z calcd for $C_{24}H_{27}FN_2O$ ($M+H$)⁺ = 378.2107, found 378.2103.

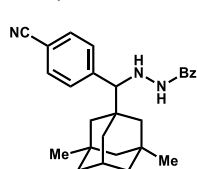
***N'*-(adamantan-1-yl)((4-(cyanophenyl))methyl)benzohydrazide (5.18i):**



5.18i

According to *General Procedure A*, *N'*-(4-cyanobenzylidene)benzohydrazide (0.124 g, 0.50 mmol, 1.0 equiv), photoredox catalyst **Ir-1** (0.011 g, 2 mol%), quinuclidine phenylsulfonate (0.026 g, 20 mol%), adamantane **5.1** (0.204 g, 1.50 mmol, 3.0 equiv), and 1,2-dichloroethane (5.0 mL) were reacted for 24 hours. The dark brown reaction mixture was then reduced to dryness under vacuum and the resulting solid was purified using column chromatography (product dry loaded on silica support followed by elution with 200 mL hexanes then 1:9 ethyl acetate: toluene) to give a light brown solid (0.151 g, 78%). **¹H NMR** (400 MHz, Chloroform-*d*) δ 7.63 (d, *J* = 8.1 Hz, 2H), 7.53 – 7.43 (m, 5H), 7.36 (t, *J* = 7.6 Hz, 2H), 7.25 (d, *J* = 5.8 Hz, 1H), 5.51 (d, *J* = 6.0 Hz, 1H), 3.80 (s, 1H), 2.00 (s, 3H), 1.70 (d, *J* = 11.9 Hz, 6H), 1.59 (d, *J* = 11.9 Hz, 6H). **¹³C NMR** (100 MHz, Chloroform-*d*) δ 167.4, 145.3, 132.7, 132.0, 131.6, 128.8, 126.8, 119.1, 111.2, 74.8, 39.1, 36.9, 36.5, 28.4. **IR** (ATR) 3307, 3242, 3066, 2917, 2851, 2228, 1622 cm⁻¹ **HRMS** (ESI) *m/z* calcd for C₂₅H₂₈N₃O (M+H)⁺ = 386.2227, found 386.2221.

***N'*-(3,5-dimethyladamantan-1-yl)((4-(cyanophenyl))methyl)benzohydrazide (5.18j):**

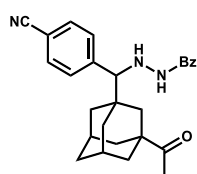


5.18j

According to *General Procedure A*, *N'*-(4-cyanobenzylidene)benzohydrazide (0.124 g, 0.50 mmol, 1.0 equiv), photoredox catalyst **Ir-1** (0.011 g, 2 mol%), quinuclidine phenylsulfonate (0.026 g, 20 mol%), 3,5-dimethyladamantane (0.278 mL, 1.50 mmol, 3.0 equiv), and 1,2-dichloroethane (5.0 mL) were reacted for 18 hours. The dark brown reaction mixture was then reduced to dryness under vacuum and the resulting solid was purified using column chromatography (product dry loaded on silica support followed by

elution with 200 mL hexanes then 1:9 ethyl acetate: toluene) to give a light brown solid (0.150 g, 73%). **¹H NMR** (400 MHz, Chloroform-*d*) δ 7.61 (d, J = 8.3 Hz, 2H), 7.53 – 7.43 (m, 4H), 7.35 (t, J = 7.6 Hz, 3H), 5.49 (s, 1H), 3.84 (s, 1H), 2.13 – 2.01 (m, 1H), 1.51 (d, J = 12.0 Hz, 1H), 1.40 (d, J = 12.1 Hz, 1H), 1.35 – 1.00 (m, 11H), 0.81 (s, 6H). **¹³C NMR** (100 MHz, Chloroform-*d*) δ 167.4, 145.3, 132.6, 132.0, 131.6, 128.8, 126.8, 119.1, 111.2, 74.2, 51.0, 45.3, 45.1, 43.1, 38.3, 37.7, 31.2, 30.8, 29.4. **IR** (ATR) 3360, 3306, 3059, 2897, 2842, 2228, 1706 cm^{-1} **HRMS** (ESI) m/z calcd for $\text{C}_{27}\text{H}_{31}\text{N}_3\text{ONa}$ ($\text{M}+\text{Na}$)⁺ = 436.2359, found 436.2347.

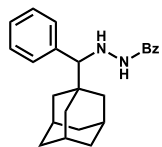
***N'*-(3-acetyladamantan-1-yl)((4-(cyanophenyl)methyl)benzohydrazide (5.18k):**



5.18k

According to *General Procedure A*, *N'*-(4-cyanobenzylidene)benzohydrazide (0.124 g, 0.50 mmol, 1.0 equiv), photoredox catalyst Ir-1 (0.011 g, 2 mol%), quinuclidine phenylsulfonate (0.026 g, 20 mol%), 1-acetyladamantane (0.267 g, 1.50 mmol, 3.0 equiv), 1,2-dichloroethane (5.0 mL) were reacted for 24 hours. The dark brown reaction mixture was then reduced to dryness under vacuum and the resulting solid was purified using column chromatography dry loaded on silica support, gradient from 35-45% ethyl acetate in toluene to give a white powder (0.070 g, 33%). **¹H NMR** (400 MHz,) δ 7.63 (d, J = 7.9 Hz, 2H), 7.48 (dd, J = 17.6, 7.4 Hz, 4H), 7.36 (t, J = 7.4 Hz, 3H), 5.47 (d, J = 5.3 Hz, 1H), 3.88 (s, 1H), 2.16 (s, 2H), 2.08 (s, 3H), 1.88 – 1.44 (m, 12H). **¹³C NMR** (100 MHz, Chloroform-*d*) δ 213.2, 167.6, 144.7, 132.5, 132.1, 131.8, 128.8, 126.8, 118.9, 111.5, 74.2, 47.0, 39.1, 38.5, 38.2, 37.8, 36.9, 35.8, 28.1, 24.6.

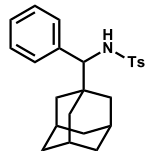
***N'*-(adamantan-1-yl(phenyl)methyl)benzohydrazide (5.18l):**



5.18l

According to *General Procedure A*, *N'*-benzylidenebenzohydrazide (0.112 g, 0.50 mmol, 1.0 equiv), photoredox catalyst **Ir-1** (0.011 g, 2 mol%), quinuclidine phenylsulfonate **Q-1** (0.026 g, 20 mol%), adamantane **5.1** (0.204 g, 1.50 mmol, 3.0 equiv), and 1,2-dichloroethane (5.0 mL) were reacted for 24 hours. The dark brown reaction mixture was then reduced to dryness under vacuum and the resulting solid was purified using column chromatography (4:1 hexanes: ethyl acetate) to give an off-white solid (0.040 g, 22%) with spectra matching known literature ². **¹H NMR** (500 MHz, Chloroform-*d*) δ 7.50 – 7.47 (m, 2H), 7.44 (t, *J* = 7.4 Hz, 1H), 7.39 – 7.29 (m, 6H), 7.20 (s, 1H), 5.60 (s, 1H), 3.71 (s, 1H), 1.99 (s, 3H), 1.77 – 1.66 (m, 6H), 1.65 – 1.58 (m, 6H). **¹³C NMR** (125 MHz, Chloroform-*d*) δ 166.9, 139.1, 133.1, 131.7, 128.7, 127.9, 127.4, 126.8, 75.1, 39.1, 37.1, 36.3, 28.5. **IR** (ATR) 3244, 3063, 2889, 2845, 1643 cm⁻¹. **HRMS** (ESI) *m/z* calcd. for C₂₄H₂₉N₂O (M+H)⁺ = 361.2274, found 361.2265.

***N*-adamantan-1-yl(phenyl)methyl-4-methylbenzenesulfonamide (5.20a)**



5.20a

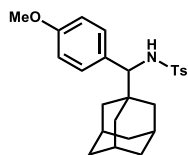
According to *General Procedure A*, *N*-benzylidene-4-methylbenzenesulfonamide (0.198 g, 0.50 mmol, 1.0 equiv), photoredox catalyst (0.011 g, 2 mol%), quinuclidine phenylsulfonate (0.026 g, 20 mol%), adamantane **5.1** (0.204 g, 1.50 mmol, 3.0 equiv) and 1,2-dichloroethane (5.0 mL) were reacted for 24 hours. The crude residue was purified by column chromatography on silica gel (EtOAc/Hexanes = 1/5) to afford **5.20a** (149.0 mg, 75% yield) with spectra matching known literature ³. **¹H NMR** (400 MHz, Chloroform-*d*) δ 7.45 (d, *J* = 8.4 Hz, 2H),

² [48]

³ [50]

7.08- 7.01 (m, 3H), 6.95 (d, $J = 8.0$ Hz, 2H), 6.87-6.85 (m, 2H), 5.82 (d, $J = 9.6$ Hz, 1H), 3.85 (d, $J = 9.6$ Hz, 1H), 2.27 (s, 3H), 1.93 (brs, 3H), 1.68-1.60 (m, 6H), 1.51 (d, $J = 12.1$ Hz, 3H), 1.36 (d, $J = 12.1$ Hz, 3H). ^{13}C NMR (100 MHz, Chloroform- d) δ 142.6, 137.5, 137.4, 129.0, 128.5, 127.4, 127.1, 126.7, 67.9, 38.8, 36.8, 28.4, 21.5.

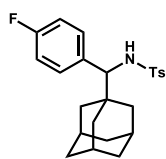
***N*-(adamantan-1-yl(4-methoxyphenyl)methyl)-4-methylbenzenesulfonamide (5.20b):**



5.20b

According to *General Procedure A*, *N*-(4-methoxybenzylidene)-4-methylbenzene sulfonamide (0.145 g, 0.50 mmol, 1.0 equiv), photoredox catalyst **Ir-1** (0.012 g, 2 mol%), quinuclidine phenylsulfonate (0.026 g, 20 mol%), adamantane **5.1** (0.204 g, 1.50 mmol, 3.0 equiv) and 1,2-dichloroethane (5.0 mL) were reacted for 48 hours. The crude residue was purified by column chromatography on silica gel (EtOAc/Hexanes = 1/4) to afford **3** (130.2 mg, 61% yield), ^1H NMR (400 MHz, Chloroform- d) δ 7.45 (d, $J = 8.3$ Hz, 2H), 6.98 (d, $J = 8.3$ Hz, 2H), 6.77 (d, $J = 8.7$ Hz, 2H), 6.57 (d, $J = 8.7$ Hz, 2H), 5.77 (d, $J = 9.4$ Hz, 1H), 3.82 (d, $J = 9.4$ Hz, 1H), 3.72 (s, 3H), 2.29 (s, 3H), 1.98 – 1.87 (m, 3H), 1.71 – 1.57 (m, 6H), 1.54 – 1.46 (m, 3H), 1.41 – 1.29 (m, 3H) ^{13}C NMR (100 MHz, Chloroform- d) δ 158.5, 142.5, 137.7, 129.6, 129.5, 129.0, 127.2, 112.9, 67.4, 55.3, 38.8, 36.8, 28.4, 21.5.

***N*-(adamantan-1-yl(4-fluorophenyl)methyl)-4'-methylbenzenesulfonamide (5.20c):**

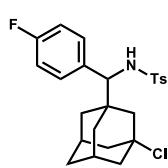


5.20c

According to *General Procedure A*, *N*-(4-fluorobenzylidene)-4'-methylbenzenesulfonamide (0.139 g, 0.50 mmol, 1.0 equiv), photoredox catalyst **Ir-1** (0.012 g, 2 mol%), quinuclidine phenylsulfonate (0.026 g, 20 mol%), adamantane **5.1** (0.204 g, 1.50 mmol, 3.0 equiv) and 1,2-

dichloroethane (5.0 mL) were reacted for 24 hours. The dark brown reaction mixture was then reduced to dryness under vacuum and the resulting solid was purified using column chromatography (20% ethyl acetate in 2:3 toluene : hexanes) to give a tan solid (0.180 g, 87%). $^1\text{H NMR}$ (400 MHz, Chloroform-*d*) δ 7.41 (d, $J = 8.3$ Hz, 2H), 7.02 (d, $J = 8.0$ Hz, 2H), 6.88 – 6.70 (m, 4H), 5.10 (d, $J = 8.3$ Hz, 1H), 3.87 (d, $J = 8.8$ Hz, 1H), 2.32 (s, 3H), 1.99 – 1.92 (m, 3H), 1.69 – 1.48 (m, 9H), 1.36 – 1.24 (m, 3H). $^{13}\text{C NMR}$ (126 MHz, Chloroform-*d*) δ 161.8 (d, $J = 245.5$ Hz), 143.0, 137.5, 133.3 (d, $J = 3.1$ Hz), 129.9 (d, $J = 8.0$ Hz), 129.2, 127.2, 114.4 (d, $J = 21.4$ Hz), 67.2, 38.8, 36.7, 36.7, 28.3, 21.5. **IR** (ATR) 3272, 2943, 2894, 2838, 1603 cm^{-1} **HRMS** (ESI) m/z calcd for $\text{C}_{24}\text{H}_{28}\text{FNO}_2\text{S}$ ($\text{M}+\text{H}$) $^+$ = 413.1825, found 413.1824.

***N*-(3-chloroadamantan-1-yl(4-fluorophenyl)methyl)-4'-methylbenzenesulfonamide (5.20d):**

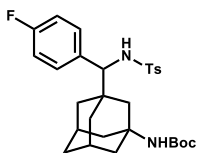


5.20d

According to *General Procedure A*, *N*-(4-fluorobenzylidene)-4'-methylbenzenesulfonamide (0.139 g, 0.50 mmol, 1.0 equiv), photoredox catalyst **Ir-1** (0.012 g, 2 mol%), quinuclidine phenylsulfonate (0.026 g, 20 mol%), 1-chloroadamantane (0.256 g, 1.50 mmol, 3.0 equiv) and acetonitrile (5.0 mL) were reacted for 72 hours (cooling fan was omitted for this reaction). The dark brown reaction mixture was then reduced to dryness under vacuum and the resulting solid was purified using column chromatography (7.5% ethyl acetate in mixture of 3:5 toluene : hexanes) to give an off-white solid (0.120 g, 53%). $^1\text{H NMR}$ (400 MHz, Chloroform-*d*) δ 7.41 (d, $J = 8.1$ Hz, 2H), 7.02 (d, $J = 8.0$ Hz, 2H), 6.88 – 6.72 (m, 4H), 5.14 (d, $J = 9.4$ Hz, 1H), 3.95 (d, $J = 9.5$ Hz, 1H), 2.32 (s, 3H), 2.23 – 2.16 (m, 2H), 2.04

(d, $J = 12.2$ Hz, 2H), 1.99 – 1.85 (m, 3H), 1.72 – 1.58 (m, 4H), 1.47 (d, $J = 13.1$ Hz, 1H), 1.32 (d, $J = 10.1$ Hz, 2H). ^{13}C NMR (126 MHz, Chloroform-*d*) δ 162.0 (d, $J = 246.5$ Hz), 143.3, 137.2, 132.5 (d, $J = 3.1$ Hz), 129.8 (d, $J = 7.9$ Hz), 129.3, 127.1, 114.8 (d, $J = 21.5$ Hz), 68.2, 66.3, 48.8, 46.9, 46.8, 41.1, 37.1, 36.8, 34.7, 31.2, 21.5. IR (ATR) 3272, 2936, 2905, 2856, 1598 cm^{-1} HRMS (ESI) m/z calcd for $\text{C}_{24}\text{H}_{27}\text{ClFNO}_2\text{S}$ (M+H) $^+$ = 447.1435, found 447.1428.

***N*-(3-(*N'*-*tert*-butoxycarbonyl-amino)-adamantyl(4-fluorophenyl)methyl)-4'-methyl**



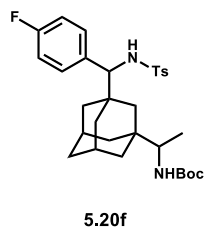
5.20e

benzenesulfonamide (5.20e):

According to *General Procedure A*, *N*-(4-fluorobenzylidene)-4'-methylbenzenesulfonamide (0.139 g, 0.50 mmol, 1.0 equiv), photoredox catalyst **Ir-1** (0.012 g, 2 mol%), quinuclidine phenylsulfonate (0.026 g, 20 mol%), *tert*-butyl-adamantan-1-ylcarbamate (0.419 g, 1.50 mmol, 3.0 equiv) and 1,2-dichloroethane (5.0 mL) were reacted for 48 hours. The light brown reaction mixture was then reduced to dryness under vacuum and the resulting solid was purified using column chromatography (15-30% ethyl acetate gradient in mixture of 3:5 toluene : hexanes) to give a brown solid (0.100 g, 35%). ^1H NMR (400 MHz, Chloroform-*d*) δ 7.42 (d, $J = 8.1$ Hz, 2H), 7.02 (d, $J = 8.0$ Hz, 2H), 6.83 (dd, $J = 8.6, 5.5$ Hz, 2H), 6.76 (t, $J = 8.7$ Hz, 2H), 5.39 (d, $J = 9.5$ Hz, 1H), 4.35 (s, 1H), 3.91 (d, $J = 9.1$ Hz, 1H), 2.32 (s, 3H), 2.11 (t, $J = 3.5$ Hz, 2H), 1.85 (d, $J = 11.7$ Hz, 2H), 1.72 (d, $J = 9.2$ Hz, 3H), 1.55 (d, $J = 12.1$ Hz, 3H), 1.41 (s, 11H), 1.34 – 1.21 (m, 2H). ^{13}C NMR (126 MHz, Chloroform-*d*) δ 162.0 (d, $J = 245.8$ Hz), 143.1, 137.4, 133.1 (d, $J = 3.3$ Hz), 129.9 (d, $J = 7.7$ Hz), 129.2, 127.2, 126.6, 114.6 (d, $J = 21.4$ Hz), 66.5, 51.2, 43.2, 41.1, 38.9, 37.8, 29.2, 28.6, 21.5. IR (ATR) 3169, 2978, 2935, 2908, 2858,

1671 cm^{-1} **HRMS** (ESI) m/z calcd for $\text{C}_{29}\text{H}_{37}\text{FN}_2\text{O}_4\text{S}$ $(\text{M}+\text{H})^+ = 528.2458$, found 528.2465.

***N*-(3-(1'-(*N*'-*tert*-butylcarbonyl)-ethyl)adamantyl(4-fluorophenyl)methyl)-4'-methyl**



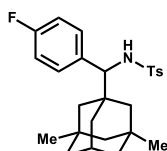
benzenesulfonamide (5.20f):

According to *General Procedure A*, *N*-(4-fluorobenzylidene)-4'-methylbenzenesulfonamide (0.139 g, 0.50 mmol, 1.0 equiv), photoredox catalyst **Ir-1** (0.012 g, 2 mol%), quinuclidine phenylsulfonate (0.026 g, 20 mol%), *tert*-butyl-((adamantan-1-yl)ethyl)carbamate (0.419 g, 1.50 mmol, 3.0 equiv) and 1,2-dichloroethane (5.0 mL) were reacted for 24 hours. The brown reaction mixture was then reduced to dryness under vacuum and the resulting solid was purified using column chromatography (5-25% ethyl acetate gradient in mixture of 3:5 toluene : hexanes) to give a tan solid which was an inseparable, complex mixture of diastereomers (0.173 g, 62%). **$^1\text{H NMR}$** (400 MHz, Chloroform-*d*) First Diastereomer: δ 5.42 (d, $J = 8.8$ Hz, 1H); Second Diastereomer: δ 5.30 (d, $J = 8.8$ Hz, 1H); Both Diastereomers: δ 7.43 (d, $J = 6.2$ Hz, 2H), 7.02 (dd, $J = 8.0, 5.4$ Hz, 2H), 6.86 – 6.77 (m, 2H), 6.75 (td, $J = 8.5, 5.6$ Hz, 2H), 4.27 (dd, $J = 19.4, 10.0$ Hz, 1H), 3.89 (dd, $J = 9.2, 5.9$ Hz, 1H), 3.31 (q, $J = 8.6$ Hz, 1H), 2.34 – 2.29 (m, 2H), 2.08 – 2.00 (m, 2H), 1.65 (s, 2H), 1.46 (s, 9H), 1.43 – 1.16 (m, 9H), 1.02 (d, $J = 12.0$ Hz, 2H), 0.94 (t, $J = 6.4$ Hz, 3H). **$^{13}\text{C NMR}$** (126 MHz, Chloroform-*d*) δ 161.9 (d, $J = 245.8$ Hz), 155.8, 143.1 (d, $J = 10.0$ Hz), 137.5, 133.3 (d, $J = 3.5$ Hz), 129.9 (d, $J = 8.2$ Hz), 129.2 (d, $J = 5.4$ Hz), 128.4, 127.2, 114.5 (d, $J = 21.4$ Hz), 114.5 (d, $J = 21.3$ Hz), 67.0, 54.3, 39.1, 38.9, 38.4, 38.2, 37.4, 36.9, 36.1, 28.6, 28.3, 21.5, 15.1. **IR** (ATR) 3339,

3294, 2976, 2932, 2850, 1678 cm^{-1} **HRMS** (ESI) m/z calcd for $\text{C}_{31}\text{H}_{41}\text{FN}_2\text{O}_4\text{S}$ ($\text{M}+\text{H}$) $^+$ = 556.2771, found 556.2748.

***N*-(3,5-dimethyladamantan-1-yl)((4-fluorophenyl)methyl)-4'-methylbenzene**

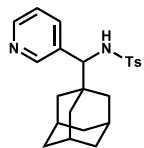
sulfonamide (5.20g):



5.20g

According to *General Procedure A*, *N*-(4-fluorobenzylidene)-4'-methylbenzenesulfonamide (0.139 g, 0.50 mmol, 1.0 equiv), photoredox catalyst **Ir-1** (0.012 g, 2 mol%), quinuclidine phenylsulfonate (0.026 g, 20 mol%), 1,3-dimethyl adamantane (0.246 g, 1.50 mmol, 3.0 equiv) and 1,2-dichloroethane (5.0 mL) were reacted for 24 hours. The dark brown reaction mixture was then reduced to dryness under vacuum and the resulting solid was purified using column chromatography (3% ethyl acetate in mixture of 2:3 toluene : hexanes) to give a white solid (0.221 g, 79%). **^1H NMR** (400 MHz, Chloroform-*d*) δ 7.44 (d, J = 8.0 Hz, 2H), 7.01 (d, J = 7.9 Hz, 2H), 6.86 – 6.78 (m, 2H), 6.79 – 6.68 (m, 2H), 5.49 (d, J = 9.1 Hz, 1H), 3.92 (d, J = 9.1 Hz, 1H), 2.31 (s, 3H), 2.09 – 1.93 (m, 1H), 1.44 (d, J = 12.7 Hz, 1H), 1.24 (d, J = 2.3 Hz, 2H), 1.23 – 1.11 (m, 6H), 1.06 (d, J = 12.4 Hz, 1H), 0.99 – 0.85 (m, 2H), 0.74 (s, 6H). **^{13}C NMR** (101 MHz, Chloroform-*d*) δ 161.8 (d, J = 245.3 Hz), 143.0, 137.5, 133.3 (d, J = 2.3 Hz), 129.9 (d, J = 8.2 Hz), 129.2, 127.2, 114.4 (d, J = 21.4 Hz), 66.7, 50.9, 45.1, 44.9, 43.0, 38.6, 37.5, 31.2, 30.6, 29.8, 29.4, 21.5. **IR** (ATR) 3273, 2942, 2893, 2861, 2838, 1603 cm^{-1} **HRMS** (ESI) m/z calcd for $\text{C}_{26}\text{H}_{32}\text{FNO}_2\text{S}$ ($\text{M}+\text{H}$) $^+$ = 441.2138, found 441.2137.

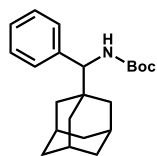
***N*-(3-adamantan-1-yl(pyridin-3-yl)methyl)-4'-methylbenzenesulfonamide (5.20h):**



5.20h

According to *General Procedure A*, 4-methyl-*N*-(pyridin-3-ylmethylene)benzenesulfonamide (0.143 g, 0.50 mmol, 1.0 equiv), photoredox catalyst **Ir-1** (0.012 g, 2 mol%), quinuclidine phenylsulfonate (0.026 g, 20 mol%), adamantane **5.1** (0.204 g, 1.50 mmol, 3.0 equiv) and acetonitrile (5.0 mL) were reacted for 48 hours. The dark brown reaction mixture was then reduced to dryness under vacuum and the resulting solid was purified using column chromatography (10-40% ethyl acetate gradient in mixture of 3:5 toluene : hexanes) to give a tan solid (0.095 g, 48%). **¹H NMR** (400 MHz, Chloroform-*d*) δ 8.35 (d, *J* = 3.9 Hz, 1H), 8.16 (d, *J* = 2.4 Hz, 1H), 7.44 (d, *J* = 8.2 Hz, 2H), 7.25 – 7.15 (m, 1H), 7.10 – 6.95 (m, 3H), 5.11 (d, *J* = 8.5 Hz, 1H), 3.91 (d, *J* = 8.5 Hz, 1H), 2.31 (s, 3H), 1.97 (s, 3H), 1.66 (d, *J* = 15.4 Hz, 6H), 1.52 (d, *J* = 12.5 Hz, 3H), 1.32 (d, *J* = 12.2 Hz, 3H). **¹³C NMR** (126 MHz, DMSO-*d*₆) δ 149.4, 147.4, 141.8, 138.2, 135.4, 133.1, 128.8, 126.3, 122.2, 64.8, 38.0, 36.3, 36.1, 27.6, 20.8; peaks at 129.3 and 125.6 do not correspond to product **22**. **IR** (ATR) 3023, 2902, 2852, 2748, 1595 cm⁻¹ **HRMS** (ESI) *m/z* calcd for C₂₃H₂₈N₂O₂S (M+H)⁺ = 396.1871, found 396.1881.

***tert*-Butyl(-adamantan-1-yl(phenyl)methyl)carbamate (5.20i):**

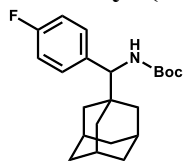


5.20i

According to *General Procedure A*, *tert*-butyl benzylicidencarbamate (0.103 g, 0.50 mmol, 1.0 equiv), photoredox catalyst **Ir-1** (0.012 g, 2 mol%), quinuclidine phenylsulfonate (0.026 g, 20 mol%), adamantane **5.1** (0.204 g, 1.50 mmol, 3.0 equiv) and 1,2-dichloroethane (5.0 mL) were reacted for 24 hours. The dark brown reaction mixture was then reduced to dryness under vacuum and

the resulting solid was purified using column chromatography (0-2% ethyl acetate gradient in mixture of 1:6 chloroform : hexanes) to give a tan solid (0.123 g, 72%). **¹H NMR** (500 MHz, Chloroform-*d*) δ 7.30 (t, $J = 7.4$ Hz, 2H), 7.25 (t, $J = 7.3$ Hz, 1H), 7.14 (d, $J = 7.4$ Hz, 2H), 5.23 – 5.06 (m, 1H), 4.39 – 4.07 (m, 1H), 1.97 (s, 3H), 1.72 – 1.60 (m, 6H), 1.57 (d, $J = 10.9$ Hz, 4H), 1.48 – 1.30 (m, 11H). **¹³C NMR** (126 MHz, Chloroform-*d*) δ 155.7, 139.7, 128.4, 127.7, 126.9, 79.3, 64.2, 38.9, 36.9, 36.5, 28.5, 28.4. **IR** (ATR) 3349, 2910, 2848, 1679 cm^{-1} **HRMS** (ESI) m/z calcd for $\text{C}_{22}\text{H}_{31}\text{NO}_2$ (M+H)⁺ = 364.2254, found 364.2256.

***tert*-Butyl-(adamantan-1-yl(4-fluorophenyl)methyl)carbamate (5.20j):**

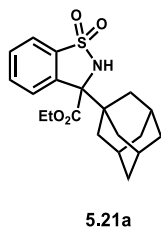


5.20j

According to *General Procedure A*, *tert*-butyl 4-fluorobenzylidene carbamate (0.112 g, 0.50 mmol, 1.0 equiv), photoredox catalyst **Ir-1** (0.012 g, 2 mol%), quinuclidine phenylsulfonate (0.026 g, 20 mol%), adamantane **5.1** (0.204 g, 1.50 mmol, 3.0 equiv) and 1,2-dichloroethane (5.0 mL) were reacted for 44 hours. The brown reaction mixture was then reduced to dryness under vacuum and the resulting solid was purified using column chromatography (0-2% ethyl acetate gradient in mixture of 1:4 chloroform : hexanes) to give an orange-white solid (0.144 g, 80%). **¹H NMR** (500 MHz, Chloroform-*d*) δ 7.10 (dd, $J = 8.4, 5.4$ Hz, 2H), 6.99 (t, $J = 8.7$ Hz, 2H), 5.15 – 5.04 (m, 1H), 4.26 (d, $J = 9.2$ Hz, 1H), 1.97 (p, $J = 3.2$ Hz, 3H), 1.67 (dt, $J = 12.5, 2.6$ Hz, 3H), 1.64 – 1.52 (m, 7H), 1.45 – 1.35 (m, 11H). **¹³C NMR** (126 MHz, Chloroform-*d*) δ 161.9 (d, $J = 244.6$ Hz), 155.7, 135.5, 129.7 (d, $J = 7.9$ Hz), 114.5 (d, $J = 21.1$ Hz), 79.5, 63.7, 38.9, 36.9, 36.3, 28.5, 28.4. **IR**

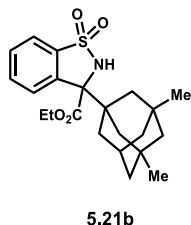
(ATR) 3254, 2903, 2848, 1698 cm^{-1} **HRMS** (ESI) m/z calcd for $\text{C}_{22}\text{H}_{30}\text{FNO}_2$ ($\text{M}+\text{H}$) $^+$ = 382.2160, found 382.2159.

ethyl 3-(adamantan-1-yl)-2,3-dihydrobenzo[d]isothiazole-3-carboxylate 1,1-dioxide (5.21a):



According to *General Procedure A*, cyclic sulfonylimine **5.7** (0.119 g, 0.50 mmol, 1.0 equiv), photoredox catalyst **Ir-1** (0.011 g, 2 mol%), quinuclidine phenylsulfonate (0.026 g, 20 mol%), adamantane **5.1** (0.204 g, 1.50 mmol, 3.0 equiv), 1,2-dichloroethane (5.0 mL) and deionized water (18 μL , 0.50 mmol, 1.0 equiv) were reacted for 18 hours. The dark brown reaction mixture was then reduced to dryness under vacuum and the resulting solid was purified using column chromatography (2:1 hexanes:ethyl acetate) to give a tan solid (0.156 g, 83%). $^1\text{H NMR}$ (500 MHz, Chloroform-*d*) δ 7.89 (d, $J = 7.9$ Hz, 1H), 7.73 (d, $J = 7.6$ Hz, 1H), 7.66 – 7.55 (m, 2H), 5.84 (s, 1H), 4.42 – 4.22 (m, 2H), 2.02 – 1.97 (m, 3H), 1.82 – 1.76 (m, 3H), 1.66 – 1.59 (m, 6H), 1.58 – 1.51 (m, 3H), 1.35 (t, $J = 7.2$ Hz, 3H). $^{13}\text{C NMR}$ (100 MHz, Chloroform-*d*) δ 169.3, 136.1, 134.9, 132.3, 130.2, 128.2, 121.4, 76.0, 63.3, 42.3, 37.0, 36.4, 28.5, 14.3. **HRMS** (ESI) m/z calcd for $\text{C}_{20}\text{H}_{26}\text{NO}_4\text{S}$ ($\text{M}+\text{H}$) $^+$ = 376.1577, found 376.1580.

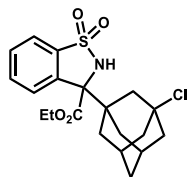
ethyl 3-(3,5-dimethyladamantyl)-2,3-dihydrobenzo[d]isothiazole-3-carboxylate 1,1-dioxide (5.21b):



According to *General Procedure A*, cyclic sulfonylimine **5.7** (0.119 g, 0.50 mmol, 1.0 equiv), photoredox catalyst **Ir-1** (0.011 g, 2 mol%), quinuclidine phenylsulfonate (0.026 g, 20 mol%), 2,4-dimethyladamantane (0.278 mL, 1.50 mmol, 3.0 equiv), 1,2-dichloroethane (5.0 mL) and deionized water (18 μL , 0.50 mmol, 1.0 equiv) were reacted for 18 hours. The dark brown

reaction mixture was then reduced to dryness under vacuum and the resulting solid was purified using column chromatography (2:1 hexanes:ethyl acetate) to give an off-white solid (0.163 g, 80%). **¹H NMR** (500 MHz, Chloroform-*d*) δ 7.89 (d, J = 8.0 Hz, 1H), 7.75 (d, J = 7.7 Hz, 1H), 7.66 – 7.57 (m, 2H), 5.81 (s, 1H), 4.38 – 4.25 (m, 2H), 2.11 – 2.07 (m, 1H), 1.66 (d, J = 11.7 Hz, 1H), 1.42 (d, J = 11.7 Hz, 2H), 1.29 – 1.22 (m, 7H), 1.11 (d, J = 12.4 Hz, 1H), 1.02 (d, J = 12.3 Hz, 1H), 0.81 (s, 3H), 0.80 (s, 3H). **¹³C NMR** (100 MHz, Chloroform-*d*) δ 169.3, 136.1, 135.0, 132.4, 130.3, 128.2, 121.5, 63.4, 50.6, 44.3, 43.3, 43.2, 42.7, 42.6, 35.6, 31.5, 31.4, 30.8, 30.7, 29.5, 14.3. **HRMS** (ESI) m/z calcd for C₂₂H₃₀NO₄S (M+H)⁺ = 404.1890, found 404.1892.

ethyl 3-(3-chloroadamantyl)-2,3-dihydrobenzo[d]isothiazole-3-carboxylate 1,1-dioxide (5.21c):

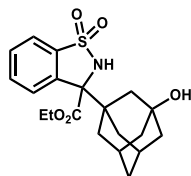


5.21c

According to *General Procedure A*, cyclic sulfonylimine **5.7** (0.119 g, 0.50 mmol, 1.0 equiv), photoredox catalyst **Ir-1** (0.011 g, 2 mol%), quinuclidine phenylsulfonate **Q-1** (0.026 g, 20 mol%), 1-chloroadamantane (0.256 g, 1.50 mmol, 3.0 equiv), 1,2-dichloroethane (5.0 mL) and deionized water (18 μ L, 0.50 mmol, 1.0 equiv) were reacted for 18 hours. The dark brown reaction mixture was then reduced to dryness under vacuum and the resulting solid was purified using column chromatography (2:1 hexanes:ethyl acetate) to give a white solid (0.150 g, 74%). **¹H NMR** (500 MHz, Chloroform-*d*) δ 7.88 (d, J = 8.1 Hz, 1H), 7.75 (d, J = 8.0 Hz, 1H), 7.68 – 7.59 (m, 2H), 5.91 (s, 1H), 4.39 – 4.27 (m, 2H), 2.24 – 2.19 (m, 2H), 2.17 – 2.09 (m, 2H), 2.05 – 1.91 (m, 4H), 1.84 – 1.77 (m, 1H), 1.74 – 1.68 (m, 1H), 1.60 – 1.45 (m, 4H), 1.35 (t, J = 7.1 Hz, 3H). **¹³C NMR** (100 MHz, Chloroform-*d*) δ 168.8, 136.1, 134.2, 132.7, 130.6, 128.0, 121.6, 75.0, 68.0, 63.7, 47.1, 46.5, 46.5, 46.0, 35.3, 35.1, 34.3,

31.1, 14.2. **HRMS** (ESI) m/z calcd for $C_{20}H_{25}ClNO_4S$ $(M+H)^+ = 409.1115$, found 409.1119.

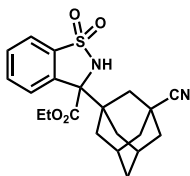
ethyl 3-(3-hydroxyadamantyl)-2,3-dihydrobenzo[d]isothiazole-3-carboxylate 1,1-dioxide (5.21d):



5.21d

According to *General Procedure A*, cyclic sulfonylimine **5.7** (0.119 g, 0.50 mmol, 1.0 equiv), photoredox catalyst **Ir-1** (0.011 g, 2 mol%), quinuclidine phenylsulfonate (0.026 g, 20 mol%), 1-hydroxyadamantane (0.228 g, 1.50 mmol, 3.0 equiv), 1,2-dichloroethane (5.0 mL) and deionized water (18 μ L, 0.50 mmol, 1.0 equiv) were reacted for 18 hours. The dark brown reaction mixture was then reduced to dryness under vacuum and the resulting solid was purified using column chromatography (2:1 hexanes:ethyl acetate) to give a tan solid (0.140 g, 80%). **¹H NMR** (500 MHz, Chloroform-*d*) δ 7.89 (d, $J = 8.0$ Hz, 1H), 7.75 (d, $J = 7.7$ Hz, 1H), 7.66 – 7.57 (m, 2H), 5.81 (s, 1H), 4.38 – 4.25 (m, 2H), 2.11 – 2.07 (m, 1H), 1.66 (d, $J = 11.7$ Hz, 1H), 1.42 (d, $J = 11.7$ Hz, 2H), 1.29 – 1.22 (m, 7H), 1.11 (d, $J = 12.4$ Hz, 1H), 1.02 (d, $J = 12.3$ Hz, 1H), 0.81 (s, 3H), 0.80 (s, 3H). **¹³C NMR** (100 MHz, Chloroform-*d*) δ 169.3, 136.1, 135.0, 132.4, 130.3, 128.2, 121.5, 63.4, 50.6, 44.3, 43.3, 43.2, 42.7, 42.6, 35.6, 31.5, 31.4, 30.8, 30.7, 29.5, 14.3. **HRMS** (ESI) m/z calcd for $C_{20}H_{26}NO_4S$ $(M+H)^+ = 392.1526$, found 392.1519.

ethyl 3-(3-cyanoadamantyl)-2,3-dihydrobenzo[d]isothiazole-3-carboxylate 1,1-dioxide (5.21e):

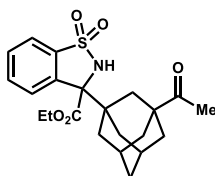


5.21e

According to *General Procedure A*, cyclic sulfonylimine **5.7** (0.119 g, 0.50 mmol, 1.0 equiv), photoredox catalyst **Ir-1** (0.011 g, 2 mol%), quinuclidine phenylsulfonate **Q-1** (0.026 g, 20 mol%), 1-

adamantanecarbonitrile (0.242 g, 1.50 mmol, 3.0 equiv), 1,2-dichloroethane (5.0 mL) and deionized water (18 μ L, 0.50 mmol, 1.0 equiv) were reacted for 18 hours. The dark brown reaction mixture was then reduced to dryness under vacuum and the resulting solid was purified using column chromatography (2:1 hexanes:ethyl acetate) to give a tan solid (0.080 g, 40%). **¹H NMR** (500 MHz,) δ 7.86 (d, J = 7.9 Hz, 1H), 7.76 (d, J = 7.3 Hz, 1H), 7.73 – 7.57 (m, 2H), 5.91 (s, 1H), 4.34 (p, J = 7.0 Hz, 2H), 2.20 – 1.47 (m, 14H), 1.36 (t, J = 7.1 Hz, 3H). **¹³C NMR** (100 MHz, Chloroform-*d*) δ 168.6, 136.2, 133.9, 132.8, 130.8, 127.9, 124.4, 121.8, 75.1, 63.9, 41.9, 39.5, 38.9, 38.9, 35.6, 35.3, 34.5, 31.2, 27.4, 27.4, 14.3. **HRMS** (ESI) m/z calcd. for C₂₁H₂₅N₂O₄S (M+H)⁺ = 401.1530, found 401.1525.

ethyl 3-(3-acetyladamantyl)-2,3-dihydrobenzo[d]isothiazole-3-carboxylate 1,1-dioxide (5.21f):



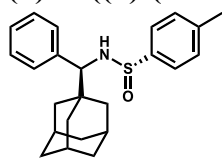
5.21f

According to *General Procedure A*, cyclic sulfonylimine **5.7** (0.119 g, 0.50 mmol, 1.0 equiv), photoredox catalyst **Ir-1** (0.011 g, 2 mol%), quinuclidine phenylsulfonate (0.026 g, 20 mol%), 1-acetyladamantane (0.267 g, 1.50 mmol, 3.0 equiv), 1,2-dichloroethane (5.0 mL) and deionized water (18 μ L, 0.50 mmol, 1.0 equiv) were reacted for 18 hours. The dark brown reaction mixture was then reduced to dryness under vacuum and the resulting solid was purified using column chromatography (2:1 hexanes:ethyl acetate) to give a white solid (0.136 g, 66%). **¹H NMR** (500 MHz, Chloroform-*d*) δ 7.89 (d, J = 7.9 Hz, 1H), 7.75 (d, J = 7.7 Hz, 1H), 7.68 – 7.57 (m, 2H), 5.90 (s, 1H), 4.40 – 4.25 (m, 2H), 2.17 (t, J = 3.1 Hz, 2H), 2.08 (s, 3H), 1.85 – 1.78 (m, 2H), 1.76 – 1.69 (m, 4H), 1.64 – 1.54 (m, 6H), 1.35 (t, J = 7.1 Hz, 3H). **¹³C NMR** (100 MHz, Chloroform-*d*) δ 213.0, 169.0, 136.2, 134.5, 132.6,

130.5, 128.2, 121.6, 75.7, 63.6, 47.2, 42.8, 37.7, 37.5, 37.3, 36.1, 35.4, 28.2, 24.7, 14.3.

HRMS (ESI) m/z calcd for $C_{22}H_{28}NO_5S$ ($M+H$)⁺ = 418.1683, found 418.1677.

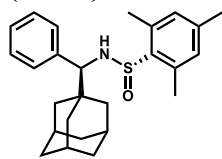
(S)-N-((S)-(adamantan-1-yl)(phenyl)methyl)-4-methylbenzenesulfinamide (5.25a):



5.25a

According to *General Procedure B*, (S)-N-benzylidene-4-methylbenzenesulfinamide (0.036 g, 0.15 mmol, 1.0 equiv), photoredox catalyst **PT** (0.0025 g, 5 mol%), adamantane (0.061 g, 0.45 mmol, 3.0 equiv), 1,2-dichloroethane (1.5 mL) were reacted for 24 hours. The reaction mixture was then reduced to dryness under vacuum and the resulting solid was purified using column chromatography (1:6 hexane:ethyl acetate) to give a white powder as a 9:1 mixture of diastereomers (0.044 g, 77%). **¹H NMR** (major diastereomer, (500 MHz,) δ 7.37 (d, J = 8.2 Hz, 2H), 7.12 (dd, J = 5.0, 1.9 Hz, 3H), 7.03 (d, J = 8.3 Hz, 2H), 6.91 – 6.86 (m, 2H), 4.62 (d, J = 7.2 Hz, 1H), 3.88 (d, J = 7.1 Hz, 1H), 2.30 (s, 3H), 1.98 (s, 3H), 1.69 – 1.62 (m, 7H), 1.55 (d, J = 10.9 Hz, 3H), 1.39 (dd, J = 12.3, 2.7 Hz, 3H). **¹³C NMR** (100 MHz, Chloroform-d) δ 141.2, 140.9, 140.2, 129.0, 128.6, 127.4, 126.6, 125.9, 65.9, 39.2, 36.9, 36.6, 28.5, 21.4. **HRMS** (ESI) m/z calcd for $C_{24}H_{30}NOS$ ($M+H$)⁺ = 380.2043, found 380.2047

(S)-N-((S)-(adamantan-1-yl)(phenyl)methyl)-2,4,6-trimethylbenzene sulfinamide (5.25b):

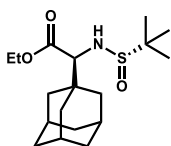


5.25b

According to *General Procedure B*, (S)-N-benzylidene-2,4,6-trimethylbenzene sulfinamide (0.081 g, 0.30 mmol, 1.0 equiv), photoredox catalyst **PT** (0.0051 g, 5 mol%), adamantane **5.1** (0.122 g, 0.90 mmol, 3.0 equiv), 1,2-dichloroethane (3.0 mL) were reacted for 48 hours. The reaction mixture was then reduced to dryness under vacuum and the resulting solid was purified

using column chromatography (3:1 hexane:ethyl acetate) to give a pale yellow oil as a single apparent diastereomer (0.089 g, 73%). **¹H NMR** (single diastereomer, 400 MHz,) δ 7.32 – 7.20 (m, 3H), 7.11 (d, J = 8.0 Hz, 2H), 4.69 (d, J = 7.7 Hz, 1H), 3.88 (d, J = 7.7 Hz, 1H), 2.50 (s, 6H), 2.26 (s, 3H), 1.95 (s, 3H), 1.68 – 1.61 (m, 6H), 1.57 – 1.49 (m, 3H), 1.44 – 1.35 (m, 3H). **¹³C NMR** (125 MHz, Chloroform-d) δ 140.5, 139.9, 138.5, 136.7, 130.8, 128.2, 127.8, 127.2, 69.6, 39.0, 37.2, 36.9, 28.5, 21.1, 19.6. **HRMS** (ESI) m/z calcd for C₂₆H₃₄NOS (M+H)⁺ = 408.2356, found 408.2359.

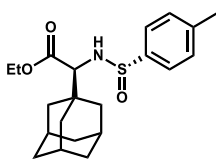
(S)-ethyl 2-(adamantan-1-yl)-2-((S)-1,1-dimethylethylsulfinamido)acetate (5.25c):



5.25c

According to *General Procedure B*, (S)-ethyl 2-((*tert*-butylsulfinyl)imino)acetate (0.061 g, 0.30 mmol, 1.0 equiv), photoredox catalyst **PT** (0.0051 g, 5 mol%), adamantane 5.1 (0.122 g, 0.90 mmol, 3.0 equiv), 1,2-dichloroethane (3.0 mL) were reacted for 24 hours. The reaction mixture was then reduced to dryness under vacuum and the resulting solid was purified using Yamazen Smart-Flash chromatography using gradient elution (100% hexanes to 4:1 hexane:ethyl acetate) to give a clear oil as a 1.3:1 mixture of diastereomers (0.065 g, 63%).

(S)-ethyl 2-(adamantan-1-yl)-2-((S)-4-methylphenylsulfinamido)acetate (5.25d):

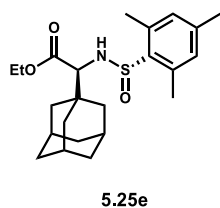


5.25d

According to *General Procedure B*, (S)-ethyl 2-((*p*-tolylsulfinyl)imino)acetate (0.072 g, 0.30 mmol, 1.0 equiv), photoredox catalyst **PT** (0.0051 g, 5 mol%), adamantane 5.1 (0.122 g, 0.90 mmol, 3.0 equiv), 1,2-dichloroethane (3.0 mL) were reacted for 24 hours. The reaction mixture was then reduced to dryness under vacuum and the resulting solid was purified using Yamazen Smart-Flash chromatography using gradient elution (100%

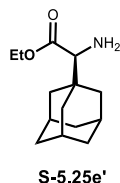
hexanes to 4:1 hexane:ethyl acetate) to give a clear oil as a 9:1 mixture of diastereomers (0.046 g, 41%). **¹H NMR** (Major diastereomer, 500 MHz, Chloroform-*d*) δ 7.60 (d, *J* = 8.1 Hz, 2H), 7.31 (d, *J* = 8.0 Hz, 2H), 4.62 (d, *J* = 9.8 Hz, 1H), 4.16 – 4.05 (m, 2H), 3.48 (d, *J* = 9.8 Hz, 1H), 2.42 (s, 3H), 2.06 – 1.99 (m, 3H), 1.77 – 1.61 (m, 9H), 1.53 – 1.45 (m, 3H), 1.23 (t, *J* = 7.2 Hz, 3H). **¹³C NMR** (125 MHz, Chloroform-*d*) δ 172.0, 142.2, 141.6, 129.7, 125.6, 65.7, 61.1, 38.8, 36.8, 36.5, 28.4, 28.3, 21.5, 14.3. **HRMS** (ESI) *m/z* calcd for C₂₁H₃₀NO₃S (M+H)⁺ = 376.1941, found 376.1943.

(S)-ethyl 2-(adamantan-1-yl)-2-((S)-2,4,6-trimethylphenylsulfinamido)acetate (5.25e):



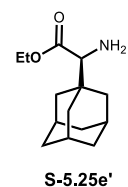
According to *General Procedure B*, (S)-ethyl 2-((mesitylsulfinyl)imino)acetate (0.080 g, 0.30 mmol, 1.0 equiv), photoredox catalyst **PT** (0.0051 g, 5 mol%), adamantane **5.1** (0.122 g, 0.90 mmol, 3.0 equiv), 1,2-dichloroethane (3.0 mL) were reacted for 48 hours. The reaction mixture was then reduced to dryness under vacuum and the resulting solid was purified using Yamazen Smart-Flash chromatography using gradient elution (100% hexanes to 9:1 hexane:ethyl acetate) to give a clear oil as a single apparent diastereomer (0.077 g, 63%). **¹H NMR** (single diastereomer, 400 MHz, Chloroform-*d*) δ 6.88 (s, 2H), 4.98 (d, *J* = 10.3 Hz, 1H), 4.33 – 4.18 (m, 2H), 3.46 (d, *J* = 10.3 Hz, 1H), 2.58 (s, 6H), 2.30 (s, 3H), 1.98 (s, 3H), 1.72 – 1.65 (m, 6H), 1.64 – 1.57 (m, 3H), 1.52 – 1.46 (m, 3H), 1.32 (t, *J* = 7.1 Hz, 3H). **¹³C NMR** (100 MHz, Chloroform-*d*) δ 172.3, 141.0, 138.2, 136.9, 130.9, 67.5, 61.3, 38.8, 36.8, 36.7, 28.4, 21.2, 19.5, 14.4. **HRMS** (ESI) *m/z* calcd for C₂₃H₃₄NO₃S (M+H)⁺ = 404.2254, found 404.2250.

(S)-ethyl 2-(adamantanyl)-2-aminoacetate (S-5.25e')



To a round bottom flask containing a stir bar was added mesitylsulfonamide product **49** (0.075 g, 0.185 mmol), 1 mL dichloromethane, and 1 mL trifluoroacetic acid. The head space was flushed with N₂ and then the flask was sealed and stirred at room temperature for 24 h. The volatiles were removed under vacuum and the resulting residue was dissolved in 3 mL of ethyl acetate and extracted with 3 mL saturated aqueous sodium bicarbonate. The organic layer was then washed with 3 mL water, followed by 3 mL brine, then dried over sodium sulfate. The organic layer was reduced under vacuum and the residue was purified using column chromatography. Fractions were collected using 7:3 ethyl acetate: hexanes until a UV active spot was observed by TLC. Then a 3% methanol in ethyl acetate mixture was used until product fractions were detected on TLC using KMnO₄ stain. These fractions were rotovapped down to give a white foam (0.031 g, 70%). ¹H NMR (400 MHz,) δ 4.18 (q, J = 7.1 Hz, 2H), 3.00 (s, 1H), 2.06 – 1.93 (m, 3H), 1.76 – 1.60 (m, 10H), 1.54 – 1.47 (m, 2H), 1.29 (t, J = 7.1 Hz, 3H). ¹³C NMR (100 MHz, Chloroform-d) δ 174.5, 64.4, 60.4, 38.6, 37.1, 36.2, 28.5, 14.5. HRMS (ESI) m/z calcd for C₁₄H₂₄NO₂ (M+H)⁺ = 238.1802, found 238.1803. [α]_D = -33.6 (l=1 dm, c= 0.0032 g/mL, α= -0.1075).

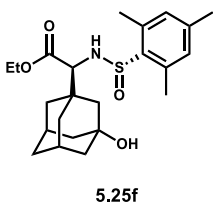
(R)-ethyl 2-(adamantanyl)-2-aminoacetate (R-5.25e')



Prepared according to the same procedure used with S-52 from the corresponding R-mesitylsulfonamide (0.068 g, 0.167 mmol) to afford the product as a clear oil (0.024 g, 62%). ¹H NMR (400 MHz,) δ 4.18 (q, J = 7.2

Hz, 2H), 3.00 (s, 1H), 2.03 – 1.90 (m, 3H), 1.71 – 1.60 (m, 10H), 1.54 – 1.47 (m, 2H), 1.29 (t, J = 7.2 Hz, 3H). $[\alpha]_{\text{D}} = 33.5$ (l=1 dm, c= 0.001 g/mL, $\alpha = -0.0335$).

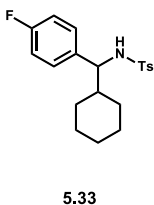
(S)-ethyl 2-(3-hydroxyadamantan-1-yl)-2-((S)-2,4,6-trimethylphenylsulfinamido)acetate (5.25f):



According to *General Procedure B*, (S)-ethyl 2-((mesitylsulfinyl)imino)acetate (0.119 g, 0.50 mmol, 1.0 equiv), photoredox catalyst **PT** (0.0085 g, 5 mol%), 1-hydroxyadamantane (0.228 g, 0.90 mmol, 3.0 equiv), 1,2-dichloroethane (5.0 mL) were reacted for 48 hours.

The reaction mixture was then reduced to dryness under vacuum and the resulting solid was purified using Yamazen Smart-Flash chromatography using gradient elution (95:5 hexanes:ethyl acetate to 4:1 hexane:ethyl acetate) to give a clear oil as a single apparent diastereomer (0.0885 g, 42%). $^1\text{H NMR}$ (single diastereomer, 400 MHz, Chloroform- d) δ 6.88 (s, 2H), 5.00 (d, $J = 10.2$ Hz, 1H), 4.29 – 4.19 (m, 2H), 3.54 (d, $J = 10.2$ Hz, 1H), 2.57 (s, 6H), 2.30 (s, 3H), 2.25 – 2.18 (m, 3H), 1.68 – 1.38 (m, 12H), 1.31 (t, $J = 7.1$ Hz, 3H). $^{13}\text{C NMR}$ (100 MHz, Chloroform- d) δ 171.9, 141.0, 137.9, 136.8, 130.8, 68.7, 66.4, 61.4, 46.2, 44.5, 44.4, 40.1, 37.4, 35.2, 30.2, 21.1, 19.4, 14.2. **HRMS** (ESI) m/z calcd for $\text{C}_{23}\text{H}_{34}\text{NO}_4\text{S}$ ($\text{M}+\text{H}$) $^+$ = 420.2204, found 420.2201.

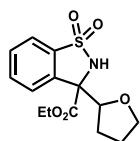
***N*-(cyclohexyl(4-fluorophenyl)methyl)-4'-methylbenzenesulfonamide (5.33):**



According to *General Procedure B*, *N*-(4-fluorobenzylidene)-4'-methylbenzenesulfonamide (0.50 mmol, 1.0 equiv), photoredox catalyst **PT** (0.017 g, 5 mol%), cyclohexane (0.162 mL, 1.50 mmol, 3.0 equiv), 1,2-dichloroethane (5.0 mL) were reacted for 52 hours. The reaction mixture was then reduced to dryness under vacuum and the resulting solid was purified using column chromatography (0-5% ethyl acetate gradient in 1:1 chloroform : hexanes) to give a brown solid. $^1\text{H NMR}$ (500 MHz,) δ 7.46 (d, $J = 8.3$ Hz, 2H), 7.09 (d, $J = 8.4$ Hz, 2H), 6.92 –

6.85 (m, 2H), 6.80 (t, $J = 8.7$ Hz, 2H), 4.74 (d, $J = 7.8$ Hz, 1H), 4.05 (t, $J = 7.8$ Hz, 1H), 2.35 (s, 3H), 1.91 (d, $J = 14.0$ Hz, 1H), 1.81 – 1.71 (m, 1H), 1.66 – 1.60 (m, 2H), 1.54 – 1.46 (m, 1H), 1.28 (d, $J = 13.4$ Hz, 1H), 1.18 – 1.04 (m, 3H), 0.98 – 0.76 (m, 2H).

ethyl 3-(tetrahydrofuran-2-yl)-2,3-dihydrobenzo[d]isothiazole-3-carboxylate 1,1-dioxide (5.32):



5.32

According to *General Procedure A*, cyclic sulfonylimine **5.7** (0.035 g, 0.15 mmol, 1.0 equiv), photoredox catalyst **Ir-1** (0.003 g, 2 mol%), quinuclidine phenylsulfonate (0.008 g, 20 mol%), tetrahydrofuran (0.036 mL, 0.45 mmol, 3.0 equiv), and 1,2-dichloroethane (1.5 mL) were reacted for 24 hours. The dark brown reaction mixture was then reduced to dryness under vacuum and the resulting solid was purified using column chromatography (2:1 hexanes:ethyl acetate) to give a tan solid (0.023 g, 50%). $^1\text{H NMR}$ (500 MHz, Chloroform-*d*) First Diastereomer: δ 5.63 – 5.60 (m, 1H), 4.43 – 4.19 (m, 2H), 2.82 – 2.73 (m, 1H), 1.39 (td, $J = 7.1, 2.7$ Hz, 1H); Second Diastereomer: δ 5.54 – 5.51 (m, 1H), 4.06 – 3.83 (m, 2H), 2.54 – 2.46 (m, 1H), 1.27 (td, $J = 8.7, 2.7$ Hz, 1H); Both Diastereomers: δ 7.80 (d, $J=7.0$ Hz, 1H), 7.66 – 7.56 (m, 3H), 5.26 (d, $J = 11.5$ Hz, 1H), 2.30 – 2.14 (m, 2H), 2.05 – 1.96 (m, 1H), 1.35 – 1.23 (m, 3H). **HRMS** (ESI) m/z calcd for $\text{C}_{14}\text{H}_{18}\text{NO}_5\text{S}$ ($\text{M}+\text{H}$) $^+$ = 312.0900, found 312.0908.

5.8 - References

- (1) Duthaler, R. O. Recent Developments in the Stereoselective Synthesis of α -Aminoacids. *Tetrahedron* **1994**, *50*, 1539–1650.
- (2) Kobayashi, S.; Hirabayashi, R. Highly Stereoselective Synthesis of Homoallylic Amines Based on Addition of Allyltrichlorosilanes to Benzoylhydrazones under Neutral Conditions. *J. Am. Chem. Soc.* **1999**, *121*, 6942–6943.
- (3) Friestad, G. K. Addition of Carbon-Centered Radicals to Imines and Related Compounds. *Tetrahedron* **2001**, *57*, 5461–5496.
- (4) Nakajima, K.; Miyake, Y.; Nishibayashi, Y. Synthetic Utilization of α -Aminoalkyl Radicals and Related Species in Visible Light Photoredox Catalysis. *Acc. Chem. Res.* **2016**, *49*, 1946–1956.
- (5) Miyabe, H.; Ushiro, C.; Ueda, M.; Yamakawa, K.; Naito, T. Asymmetric Synthesis of α -Amino Acids Based on Carbon Radical Addition to Glyoxylic Oxime Ether. *J. Org. Chem.* **2000**, *65*, 176–185.
- (6) Miyabe, H.; Ueda, M.; Naito, T. Carbon-Carbon Bond Construction Based on Radical Addition to C=N Bond. *Synlett* **2004**, *2004*, 1140–1157.
- (7) Miyabe, H.; Shibata, R.; Sangawa, M.; Ushiro, C.; Naito, T. Intermolecular Alkyl Radical Addition to the Carbon-Nitrogen Double Bond of Oxime Ethers and Hydrazones. *Tetrahedron* **1998**, *54*, 11431–11444.
- (8) Yamada, K.; Fujihara, H.; Yamamoto, Y.; Miwa, Y.; Taga, T.; Tomioka, K. Radical Addition of Ethers to Imines Initiated by Dimethylzinc. *Org. Lett.* **2002**, *4*, 3509–3511.
- (9) Ueda, M.; Miyabe, H.; Nishimura, A.; Sugino, H.; Naito, T. Zinc-Mediated Radical Reaction of Glyoxylic Oxime Ether and Hydrazone in Aqueous Media: Asymmetric Synthesis of α -Amino Acids. *Tetrahedron Asymmetry* **2003**, *14*, 2857–2859.
- (10) Naito, T.; Nakagawa, K.; Nakamura, T.; Kasei, A.; Ninomiya, I.; Kiguchi, T. Radical Cyclization in Heterocycle Synthesis. 6.1 A New Entry to Cyclic Amino Alcohols via Stannyl Radical Cyclization of Oxime Ethers Connected with Aldehydes or Ketones. *J. Org. Chem.* **1999**, *64*, 2003–2009.

- (11) Slater, K. A.; Friestad, G. K. Mn-Mediated Radical-Ionic Annulations of Chiral N-Acylhydrazones. *J. Org. Chem.* **2015**, *80*, 6432–6440.
- (12) Teegardin, K.; Day, J. I.; Chan, J.; Weaver, J. Advances in Photocatalysis: A Microreview of Visible Light Mediated Ruthenium and Iridium Catalyzed Organic Transformations. *Org. Process Res. Dev.* **2016**, *20*, 1156–1163.
- (13) Prier, C. K.; Rankic, D. A.; MacMillan, D. W. C. Visible Light Photoredox Catalysis with Transition Metal Complexes: Applications in Organic Synthesis. *Chem. Rev.* **2013**, *113*, 5322–5363.
- (14) Lowry, M. S.; Bernhard, S. Synthetically Tailored Excited States: Phosphorescent, Cyclometalated Iridium(III) Complexes and Their Applications. *Chem. – Eur. J.* **2006**, *12*, 7970–7977.
- (15) Wanka, L.; Iqbal, K.; Schreiner, P. R. The Lipophilic Bullet Hits the Targets: Medicinal Chemistry of Adamantane Derivatives. *Chem. Rev.* **2013**, *113*, 3516–3604.
- (16) Morales, S.; Guijarro, F. G.; García Ruano, J. L.; Cid, M. B. A General Aminocatalytic Method for the Synthesis of Aldimines. *J. Am. Chem. Soc.* **2014**, *136*, 1082–1089.
- (17) Wang, H.; Jiang, T.; Xu, M.-H. Simple Branched Sulfur–Olefins as Chiral Ligands for Rh-Catalyzed Asymmetric Arylation of Cyclic Ketimines: Highly Enantioselective Construction of Tetrasubstituted Carbon Stereocenters. *J. Am. Chem. Soc.* **2013**, *135*, 971–974.
- (18) Kamijo, S.; Kamijo, K.; Maruoka, K.; Murafuji, T. Aryl Ketone Catalyzed Radical Allylation of C(Sp³)–H Bonds under Photoirradiation. *Org. Lett.* **2016**, *18*, 6516–6519.
- (19) González-Cameno, A. M.; Mella, M.; Fagnoni, M.; Albini, A. Photochemical Alkylation of Ketene Dithioacetal S,S-Dioxides. An Example of Captodative Olefin Functionalization. *J. Org. Chem.* **2000**, *65*, 297–303.

- (20) Albini, A.; Mella, M.; Freccero, M. A New Method in Radical Chemistry: Generation of Radicals by Photo-Induced Electron Transfer and Fragmentation of the Radical Cation. *Tetrahedron* **1994**, *50*, 575–607.
- (21) Dondi, D.; Cardarelli, A. M.; Fagnoni, M.; Albini, A. Photomediated Synthesis of β -Alkylketones from Cycloalkanes. *Tetrahedron* **2006**, *62*, 5527–5535.
- (22) Hoshikawa, T.; Kamijo, S.; Inoue, M. Photochemically Induced Radical Alkynylation of C(Sp³)–H Bonds. *Org. Biomol. Chem.* **2012**, *11*, 164–169.
- (23) Kamijo, S.; Hoshikawa, T.; Inoue, M. Photochemically Induced Radical Transformation of C(Sp³)–H Bonds to C(Sp³)–CN Bonds. *Org. Lett.* **2011**, *13*, 5928–5931.
- (24) Amaoka, Y.; Nagatomo, M.; Watanabe, M.; Tao, K.; Kamijo, S.; Inoue, M. Photochemically Induced Radical Alkenylation of C(Sp³)–H Bonds. *Chem. Sci.* **2014**, *5*, 4339–4345.
- (25) Supranovich, V. I.; Levin, V. V.; Dilman, A. D. Radical Addition to N-Tosylimines via C–H Activation Induced by Decatungstate Photocatalyst. *Org. Lett.* **2019**, *21*, 4271–4274.
- (26) Skubi, K. L.; Blum, T. R.; Yoon, T. P. Dual Catalysis Strategies in Photochemical Synthesis. *Chem. Rev.* **2016**, *116*, 10035–10074.
- (27) Shaw, M. H.; Twilton, J.; MacMillan, D. W. C. Photoredox Catalysis in Organic Chemistry. *J. Org. Chem.* **2016**, *81*, 6898–6926.
- (28) Yang, H.-B.; Feceu, A.; Martin, D. B. C. Catalyst-Controlled C–H Functionalization of Adamantanes Using Selective H-Atom Transfer. *ACS Catal.* **2019**, *9*, 5708–5715.
- (29) Fort, R. C.; Schleyer, P. von Rague. Bridgehead Adamantane Carbonium Ion Reactivities. *J. Am. Chem. Soc.* **1964**, *86*, 4194–4195.
- (30) Kruppa, G. H.; Beauchamp, J. L. Energetics and Structure of the 1- and 2-Adamantyl Radicals and Their Corresponding Carbonium Ions by Photoelectron Spectroscopy. *J. Am. Chem. Soc.* **1986**, *108*, 2162–2169.

- (31) Schleyer, P. von R.; Fort, R. C.; Watts, W. E.; Comisarow, M. B.; Olah, G. A. Stable Carbonium Ions. VIII. The 1-Adamantyl Cation. *J. Am. Chem. Soc.* **1964**, *86*, 4195–4197.
- (32) Robak, M. T.; Herbage, M. A.; Ellman, J. A. Synthesis and Applications of Tert-Butanesulfinamide. *Chem. Rev.* **2010**, *110*, 3600–3740.
- (33) Ellman, J. A.; Owens, T. D.; Tang, T. P. N-Tert-Butanesulfinyl Imines: Versatile Intermediates for the Asymmetric Synthesis of Amines. *Acc. Chem. Res.* **2002**, *35*, 984–995.
- (34) Ellman, J. A. Applications of Tert-Butanesulfinamide in the Asymmetric Synthesis of Amines. *Pure Appl. Chem.* **2003**, *75*, 39–46.
- (35) Akindele, T.; Yamamoto, Y.; Maekawa, M.; Umeki, H.; Yamada, K.; Tomioka, K. Asymmetric Radical Addition of Ethers to Enantiopure N-p-Toluenesulfinyl Aldimines, Mediated by Dimethylzinc–Air. *Org. Lett.* **2006**, *8*, 5729–5732.
- (36) Lacôte, E.; Delouvrié, B.; Fensterbank, L.; Malacria, M. Radical Cyclization/ β -Elimination Tandem Reactions: Enantiopure Sulfoxides as Temporary Chiral Auxiliaries. *Angew. Chem. Int. Ed.* **1998**, *37*, 2116–2118.
- (37) Ni, S.; Garrido-Castro, A. F.; Merchant, R. R.; de Gruyter, J. N.; Schmitt, D. C.; Mousseau, J. J.; Gallego, G. M.; Yang, S.; Collins, M. R.; Qiao, J. X.; Yeung, K.-S.; Langley, D. R.; Poss, M. A.; Scola, P. M.; Qin, T.; Baran, P. S. A General Amino Acid Synthesis Enabled by Innate Radical Cross-Coupling. *Angew. Chem. Int. Ed.* **2018**, *57*, 14560–14565.
- (38) Ling, Z.; Singh, S.; Xie, F.; Wu, L.; Zhang, W. Copper-Catalyzed Asymmetric Alkynylation of Cyclic N-Sulfonyl Ketimines. *Chem. Commun.* **2017**, *53*, 5364–5367.
- (39) Miyabe, H.; Ushiro, C.; Ueda, M.; Yamakawa, K.; Naito, T. Asymmetric Synthesis of α -Amino Acids Based on Carbon Radical Addition to Glyoxylic Oxime Ether. *J. Org. Chem.* **2000**, *65*, 176–185.

- (40) Davis, F. A.; Chen, B.-C. Asymmetric Synthesis of Amino Acids Using Sulfinimines (Thiooxime S-Oxides). *Chem. Soc. Rev.* **1998**, *27*, 13–18.
- (41) Friestad, G. K. Control of Asymmetry in the Radical Addition Approach to Chiral Amine Synthesis. *Top. Curr. Chem.* **2014**, *343*, 1–32.
- (42) F. Garrido-Castro, A.; Choubane, H.; Daaou, M.; Carmen Maestro, M.; Alemán, J. Asymmetric Radical Alkylation of N -Sulfinimines under Visible Light Photocatalytic Conditions. *Chem. Commun.* **2017**, *53*, 7764–7767.
- (43) Han, Z.; Krishnamurthy, D.; Grover, P.; Fang, Q. K.; Senanayake, C. H. Properly Designed Modular Asymmetric Synthesis for Enantiopure Sulfinamide Auxiliaries from N-Sulfonyl-1,2,3-Oxathiazolidine-2-Oxide Agents. *J. Am. Chem. Soc.* **2002**, *124*, 7880–7881.
- (44) Amaoka, Y.; Kamijo, S.; Hoshikawa, T.; Inoue, M. Radical Amination of C(Sp³)–H Bonds Using N-Hydroxyphthalimide and Dialkyl Azodicarboxylate. *J. Org. Chem.* **2012**, *77*, 9959–9969.
- (45) McNally, A.; Prier, C. K.; MacMillan, D. W. C. Discovery of an α -Amino C–H Arylation Reaction Using the Strategy of Accelerated Serendipity. *Science* **2011**, *334*, 1114–1117.
- (46) Choi, G. J.; Zhu, Q.; Miller, D. C.; Gu, C. J.; Knowles, R. R. Catalytic Alkylation of Remote C–H Bonds Enabled by Proton-Coupled Electron Transfer. *Nature* **2016**, *539*, 268–271.
- (47) Lowry, M. S.; Hudson, W. R.; Pascal, R. A.; Bernhard, S. Accelerated Luminophore Discovery through Combinatorial Synthesis. *J. Am. Chem. Soc.* **2004**, *126*, 14129–14135.
- (48) Nam, T. K.; Jang, D. O. Radical “On Water” Addition to the C=N Bond of Hydrazones: A Synthesis of Isoindolinone Derivatives. *J. Org. Chem.* **2018**, *83*, 7373–7379.
- (49) Ankner, T.; Hilmersson, G. Instantaneous Deprotection of Tosylamides and Esters with SmI₂/Amine/Water. *Org. Lett.* **2009**, *11*, 503–506.

- (50) Chen, J.; Zhang, Z.; Li, B.; Li, F.; Wang, Y.; Zhao, M.; Gridnev, I. D.; Imamoto, T.; Zhang, W. Pd(OAc)₂-Catalyzed Asymmetric Hydrogenation of Sterically Hindered N-Tosylimines. *Nat. Commun.* **2018**, *9*, 5000.

6 Synthesis of Small Molecule Inhibitors for the SUMO E1 Enzyme

6.1 - Introduction

Protein post-translational modifications such as methylation, acetylation, glycosylation, ubiquitination, and sumoylation are critical to normal cell regulation and function. The latter is mediated by small ubiquitin-like modifier (SUMO) proteins which are enzymatically conjugated to hundreds of known target substrates and control a wide array of metabolic processes such as stress response, transcription, cellular proliferation, and apoptosis.^[1] In recent years, studies have linked the dysregulation of the sumoylation pathway to numerous diseases, especially carcinogenesis and increased chemotherapeutic resistance for a variety of cancers.^[2,3] As such, there has been a growing interest in elucidating the exact mechanisms involved with sumoylation and devising methods to control this pathway using small molecule inhibitors.

The process of sumoylation uses three sequentially interacting enzymes known as SUMO E1, E2, and E3; their names being indicative of their order of involvement in the pathway. SUMO E1 naturally binds ATP which is used to form a SUMO-AMP adenylate complex. This activated substrate complex is then used to transfer SUMO to the E2 complex and continue on in the sumoylation process. The competitive inhibition of ATP by another small molecule halts production of the SUMO/SUMO E1 conjugate and by extension, the entire sumoylation pathway. Anacardic and ginkgolic acids have been found to be effective inhibitors of SUMO E1 despite their simplicity, causing complete desumoylation at *in-vitro* concentrations of 10 μ M.^[4] This desumoylation activity has been applied to overcome chemotherapeutic resistant acute myeloid leukemia (AML) which is associated with over-sumoylation.^[5] The same studies were also able to demonstrate that

desumoylation reduces tumor size in mice. Anacardic acid is therefore a promising starting point for the development of cancer treatments despite lacking the typical chemical features associated with drugs such as oxidative stability, rigidity, and low logP. Currently there is no reported co-crystal structure between SUMO E1 and anacardic acid and its exact mode of binding is still unclear. However, the SUMO E1/ATP-Mg²⁺ co-crystal structure has been solved (PDB code 1Y8Q)^[6] and this crystal structure remains the most used starting point for E1 inhibitor design. Our computational docking calculations using anacardic acid have assumed anacardic acid occupies the ATP active site when bound which has provided a theoretical basis for its mode of binding. Anacardic acid's carboxyl group is predicted to interact with the arginine and lysine residues normally interactive with ATP's phosphate oxygens while the alkyl tail curls around to fill the hydrophobic pocket. Fukuda and coworkers have determined that anacardic acid's alkyl tail and carboxylate are necessary for inhibition, while the phenol is not essential.^[4] Docking studies do not show any interaction between anacardic acid and the highly conserved aspartate that appears in the center of most ATP active sites.^[7] For this reason, anacardic acid derivatives specifically target SUMO E1 without interfering with other kinase activity.

6.2 - Background

6.2.1 - Sumoylation Cycle

The process of protein sumoylation begins with the maturation of the SUMO protein through cleavage of a tetrapeptide from the C-terminus to reveal the diglycine motif used in SUMO conjugation (A1 to A2, **Figure 6.1**). SUMO then undergoes activation through

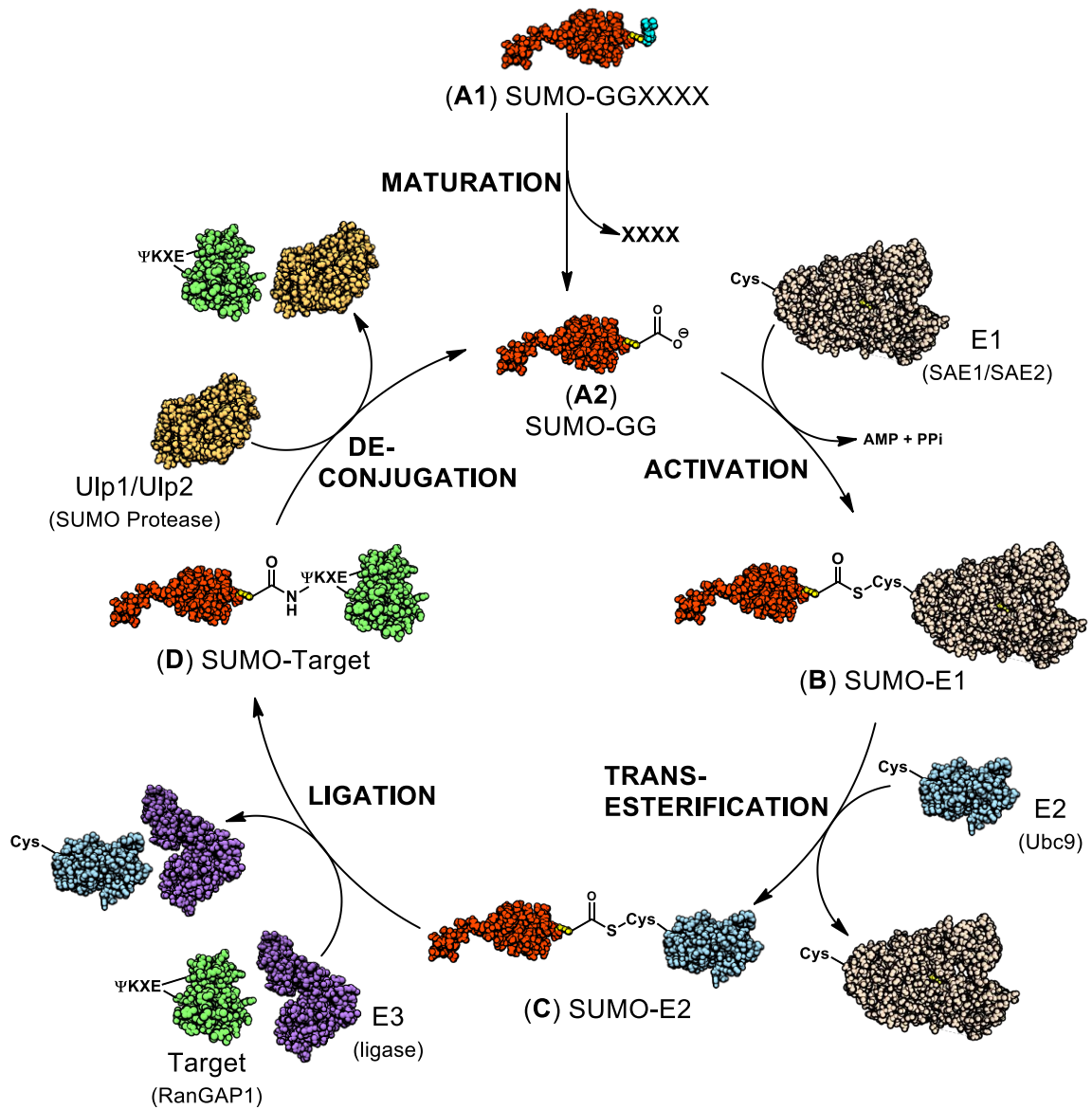


Figure 6.1 – The Sumoylation Cycle

conjugation to the E1 enzyme, **(B)**.^[8] The E1 enzyme catalyzes the formation of a SUMO adenylate on SUMO's C-terminal end from ATP via loss of pyrophosphate. Thioester bond formation to a nearby catalytic cysteine through loss of AMP covalently links SUMO to the E1 enzyme. Transesterification between cysteine residues to the E2 enzyme then occurs **(C)**.^[9] The E2 enzyme is critical in the recognition of the protein target undergoing

sumoylation. Many proteins are subject to sumoylation due to E2 recognition and this occurs at specific sites featuring the SUMO conjugation motif ψ KxE (where ψ is a large hydrophobic residue and x is any residue).^[10] An E3 ligase then ligates SUMO to a lysine residue to its protein target through an isopeptide bond (**D**). Commonly, the ligation occurs on the lysine within the consensus motif although it is also possible that another surrounding lysine can serve as the point of conjugation. However, not all proteins containing a ψ KxE sequence are capable of undergoing sumoylation due to steric inaccessibility. E2 recognition of protein targets is one of the features that distinguishes the sumoylative process from ubiquitination where target recognition is instead mediated by the Ub E3 ligase.



Figure 6.2 – Poly-Sumoylation of Protein Target

Pre-SUMO processing and SUMO deconjugation is performed in bacteria by SUMO specific proteases Ulp1 and Ulp2.^[11,12] One of eight proteins bearing significant sequence homology to Ulp1 in humans is believed to be responsible for this same activity.^[13] The process of sumoylation and desumoylation is a complex and tightly controlled dynamic pathway that modulates enzymatic activity by turning enzymes “on” or “off.” Sumo proteins themselves are able to undergo sumoylation giving rise to poly-sumoylated chains (**Figure 6.2**).

6.2.2 - Role of SUMO E1 in Carcinogenesis

Due to the role of protein sumoylation in cellular regulation, the dysregulation of the sumoylation cycle can lead to the development of cancer or be exploited to further the proliferation of cancer cells.^[2] Several oncogenes have been identified that capitalize on this dysregulation of the SUMO cycle and are dependent on it for cancer-causing behavior. This relationship is termed “non-oncogene addiction” as the cancer cells are dependent on the behavior of non-oncogenic genes.^[14]

For example, the oncogene Myc is a proliferative transcription factor associated with regulation of mitotic spindle function.^[15] Sumoylation takes an active role in controlling which genes governing spindle function are able to be activated by Myc.^[16] It has been shown that in the absence of sumoylation, Myc reverts to activating a different set of genes leading to irregular spindle behavior during mitosis and ultimately results in catastrophic cellular damage.^[17] Notably, interference with proper spindle function during mitosis by “spindle poisons” such as Taxol has long been a therapeutic approach for the treatment of many cancers.^[18] The taxane class of therapeutics has major limitations due to their toxicity to non-tumor organ systems. Targeting the sumoylation process may be a possible way to mimic the effect of spindle poisons without the serious disadvantages of taxane compounds.

Sumoylation is also a significant contributor to the chemotherapeutic resistance within many cancers such as AML. Cancer cells undergo abnormally rapid cellular division so their DNA is often unpacked to facilitate replication. In this unpacked state, DNA is much more susceptible to damage. Many chemotherapeutic agents are therefore designed

to take advantage of this by inducing DNA damage which act as a trigger for apoptosis. Sumo controls the activation of the DNA damage induced transcription factor (DDIT3) gene that acts as proapoptotic regulator. Cancer cells with abnormal levels of sumoylation activity are thus more chemoresistant since they are unable to induce an apoptotic response to DNA damage.^[19] This elevated level of chemoresistance translates into the need for higher therapeutic doses and effectively eliminates the possibility of chemotherapeutic treatment for the young, elderly, or individuals in poor health for whom treatment would be fatal.^[20] By inhibiting the sumoylation pathway, chemoresistant variants of AML cancer cells were rendered vulnerable to chemotherapies at much lower dosages.^[5]

6.3 - Molecular Docking Studies

Before beginning any chemical synthesis, a considerable amount of time was first invested in performing computational protein-ligand docking studies. This allowed for more informed decision making when determining which compounds warranted further synthetic consideration. Virtual screening is commonly used in the early stages of drug discovery where it is used to narrow down a large library of compounds to a few hits (**Figure 6.3**). Our approach did not require the screening of an immense library because anacardic acid is already known to interact with SUMO E1. Instead we used anacardic acid as a starting point for the rational design of a few hundred derivatives based on established structure-activity relationships (SAR) and used computational docking to identify promising structures. Many software packages are available for this purpose and they were evaluated before AutoDock Vina was eventually chosen for its combination of high accuracy, low computational demand, and low cost.^[21]

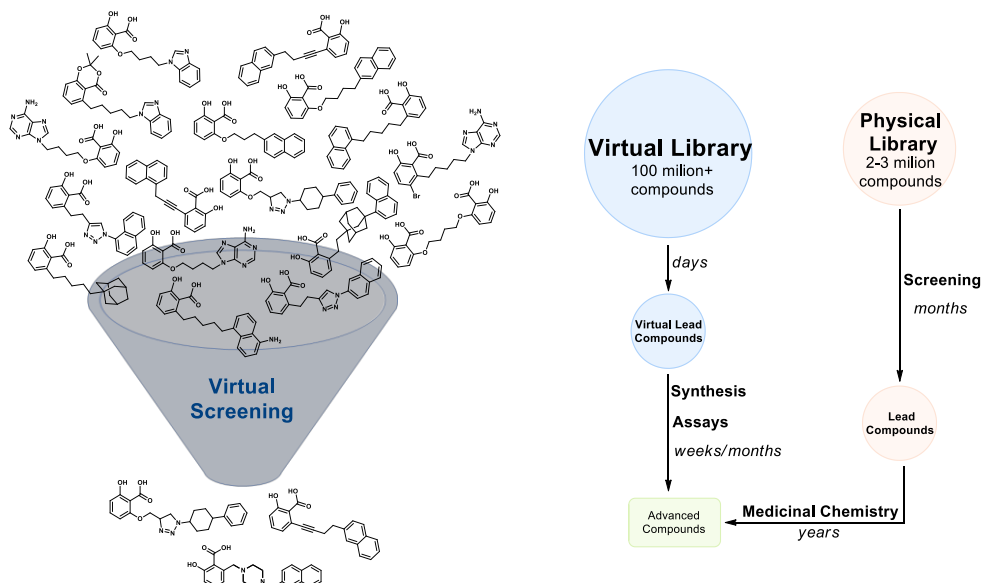


Figure 6.3 – Virtual Screening of Potential Inhibitors

Vina works by first using a user-defined 3D “search box” centered around the desired docking area (**Figure 6.4B**). A grid function is then run that fills the box space with virtual carbon atoms; any carbons that experience overlap (based on van der Waals radii) are rejected leaving only a 3D array of “allowable” carbon positions. These positions are then used to approximate if a given ligand in a specific conformation and orientation will fit within this allowable space. If the ligand fits, Vina then uses a semi-empirical free energy forcefield to evaluate each conformation. This calculation considers steric repulsion, electrostatic interactions, hydrogen bonding, desolvation, and entropic differences of the ligand in its bound/unbound state to generate an estimated free energy of binding. There are many computational parameters that need to be accounted for when setting up a docking calculation such as the size of the search space, protein/ligand protonation states, setting up flexible residues that are allowed to move, and number of

docking repetitions to use for a single ligand, just to name a few. The more parameters used, the more computationally intensive the docking job will generally be.

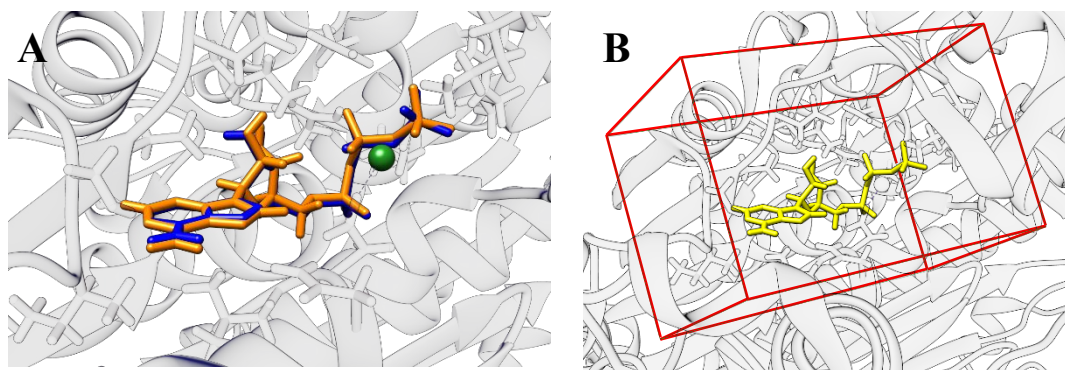


Figure 6.4 – ATP Docking Study With SUMO E1

A) ATP from crystal structure (orange) and the docked confirmation (blue) match very closely B) ATP centered in the search box. Ligands will be docked within this area.

A known crystal structure of SUMO E1 with bound ATP is freely available from the Protein Databank (PDB id= 1Y8Q).^[6] This structure was used as the starting point for our docking calculations. To determine the proper algorithm search parameters, Vina was first used to calculate the binding conformation of ATP within the active site. Once the calculated binding conformation of ATP matched the known conformation from the crystal structure (seen in **Figure 6.4A**), that set of parameters could then be confidently used with other non-native ligands.

Over 200 compounds were docked with SUMO E1 using rational design based on the structures of anacardic acid and ATP. As anticipated, much of the compound library was rejected based on low ligand binding affinity or poor clustering within the active site. Low ligand binding affinity occurs due to poor- or even repulsive interaction with active site residues. Clustering analysis is possible after running many repeated docking calculations with the same ligand. If a docking pose is returned repeatedly, it is very likely

the pose is the result of a significant (non-random) interaction or set of interactions between the protein and the ligand. Referring to **Figure 6.5**, an ideal ligand has high clustering around a high calculated binding affinity while ligands that did not show clustering, or have clustering around lower binding affinities are less desirable. The best binding derivatives that gave good clustering results are discussed in the following section.



Figure 6.5 – Clustering Analysis Examples

6.3.1 - Docking Results

The docking energy of ATP itself was calculated to be -10.4 kcal/mol. This value is only semi-empirical and is not intended to be predictive of its real free energy of binding. However, being the natural substrate of SUMO E1, this value does serve as a useful reference point when assessing the predicted binding ability of other ligands. The docking scores for the library of potential ligands designed to resemble anacardic acid were then compared to the score for native ATP. As can be seen in **Figure 6.6**, the salicylate moiety is always positioned on the right-hand side of the active site where the benzoic acid group interacts with either a lysine (LYS.346 or LYS.72) or arginine (ARG.21) which are normally reserved for ATP's phosphate groups. **Figure 6.6A** shows the hydrophobic tail

of anacardic acid curling around to fill the left-hand side of the active site typically occupied by adenine. However, the calculated binding energy for anacardic acid was -7.5 kcal/mol (2.9 kcal/mol less favorable than ATP). For this reason, one of the first derivatives we tried docking was anacardic acid with a truncated tail replaced with an adenine ring (**B**) which did increase the free energy of binding to -8.8 kcal/mol. Replacing the adenine ring with a naphthyl ring (**C**) resulted in a further increase in binding affinity to -9.8 kcal/mol. This increase may be attributed to the more hydrophobic nature of the naphthyl group and/or the slightly larger size of the bicyclic ring system.

Further reducing the number of rotatable bonds by using a butyne linker rather than a butane linker offered a slight improvement in binding (**D**). However, a large jump in binding affinity (-10.2 kcal/mol) was observed by completely replacing the butane linker with a piperazine linker (**E**). This derivatives binding was the first that nearly matched that of the native substrate ATP. As shown in **Figure 6.6E**, the piperazine occupies more “vertical” space inside the binding pocket filling it more completely thereby displacing more water which is favorable. This observation can also be made with the highest binding target we identified featuring a triazole linkage (**F**). This triazole was calculated to have a binding free energy of -11.1 kcal/mol, even exceeding ATP's.

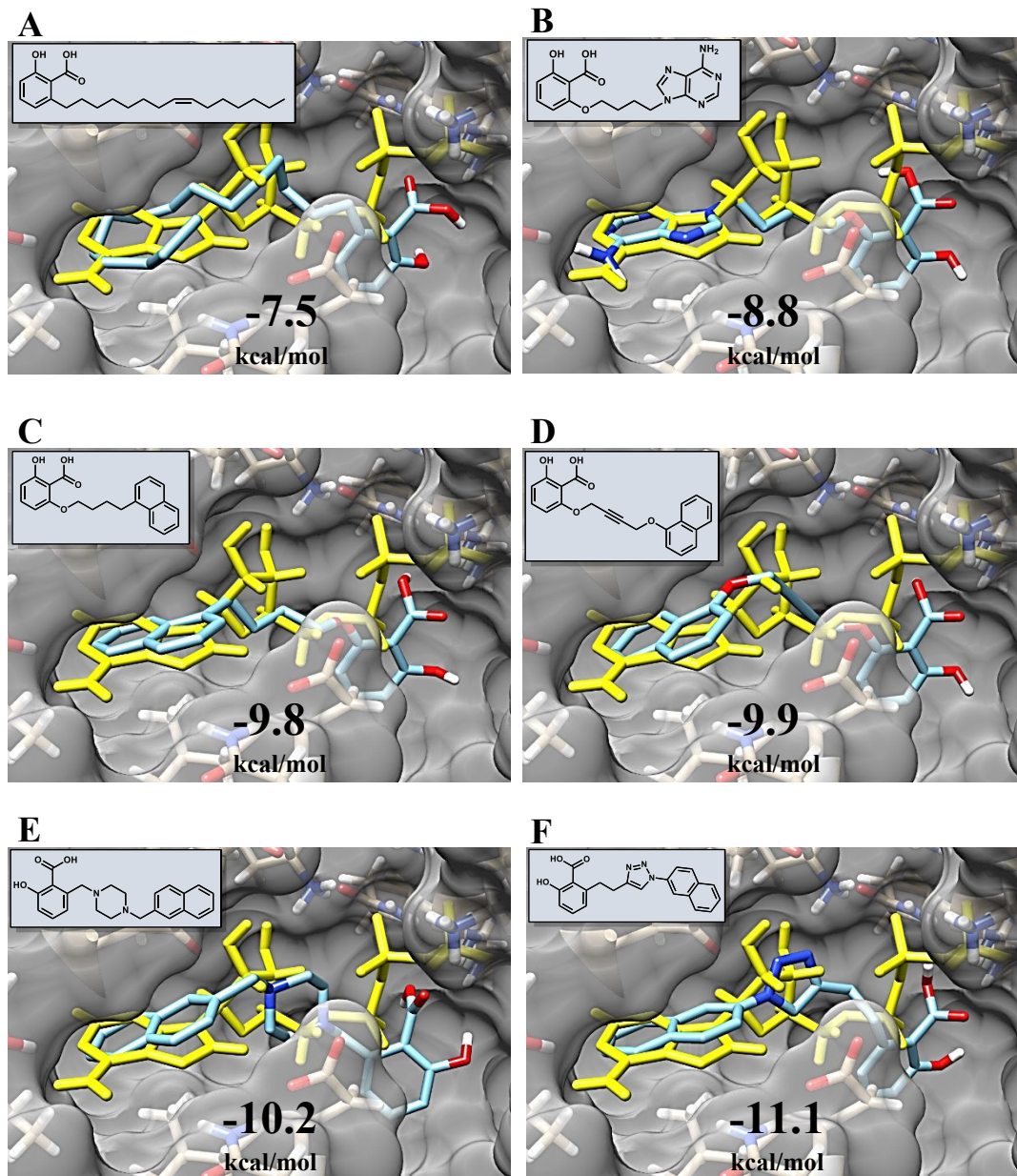


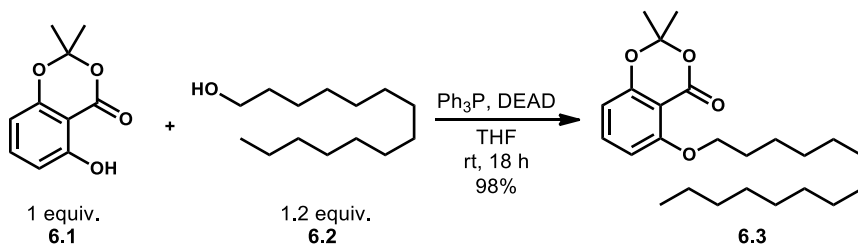
Figure 6.6 – Ligand Docking Studies With SUMO E1
 Docked ligand poses and associated binding free energies calculated using AutoDock Vina. The values are the results of Vina's docking algorithm and are meant to be used comparatively, not interpreted as real-world predictions. As a point of reference, the free energy for docked ATP is -10.4 kcal/mol.

One of the attractive features of using anacardic acid as a starting point for design is its ability to target SUMO E1 while being dramatically different from ATP. While many features of ATP binding sites are biologically conserved, the active site of SUMO E1 is thought to be unique enough from other kinases to bind anacardic competitively alongside ATP. When designing these derivatives, it was important to avoid mimicry of ATP to a large degree. Otherwise, the chances of hitting other off-target protein kinases increases dramatically. For example, none of the derivatives that were designed considered targeting a highly conserved asparagine residue in most ATP binding pockets that interacts with the dihydroxy moiety of ATP's ribose. In this way, targeting other members of the kinome which are usually critical for proper cell function is minimized.

6.4 - Design and Synthesis of Anacardic Acid Derivatives

6.4.1 - Aryl Ether Anacardic Acid Derivatives

Acetonide-protected dihydroxybenzoic acid **6.1** is able to be used in Mitsunobu reactions with other alcohols to reliably construct a variety of anacardic acid derivatives featuring an aryl ether linkage. To test the viability of the acetonide to participate in Mitsunobu reactions, we first set out to synthesize a 15:0 anacardic acid derivative with tetradecanol **6.2** (Scheme 6.1). Reaction with triphenylphosphine

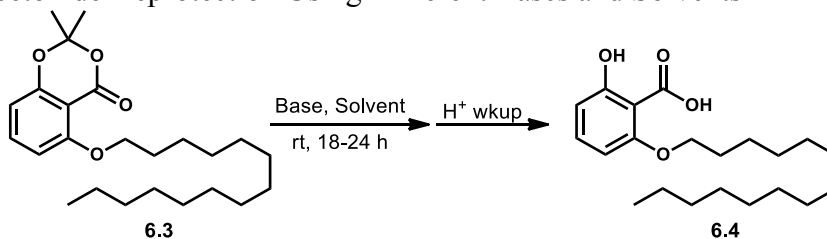


Scheme 6.1 – Mitsunobu Synthesis of an Aryl Ether Anacardic Acid Derivative

and diethyl azodicarboxylate (DEAD) gave the desired aryl ether product **6.3** in excellent yield.

To reach the final anacardic acid derivative **6.4**, different basic conditions were tried to determine the best method for acetonide deprotection (**Table 6.1**). Existing methods often use aqueous base for this purpose although we found that these approaches were ineffective without the addition of an organic co-solvent. Even then, the reactions proceeded slowly and with low conversion. This was attributed to poor interaction at the biphasic interface due to the high ionic strength of the aqueous base and the organic phase containing the acetonide with high hydrophobicity. Ultimately, 1,4 dioxane combined with vigorous stirring proved to be quite effective at giving full deprotection of the acetonide over a reasonable time period of approximately 24 hours.

Table 6.1 – Acetonide Deprotection Using Different Bases and Solvents



Base	Solvent	Conversion (%)	Isolated Yield (%)
5M KOH	THF	58	--
1M KOH	THF	71	--
5M KOH	THF, MeOH	62	--
5M KOH	1,4 dioxane	100	91
2M NaOH	1,4 dioxane	99	97
5M KOH	1,4 dioxane, MeOH	72	--

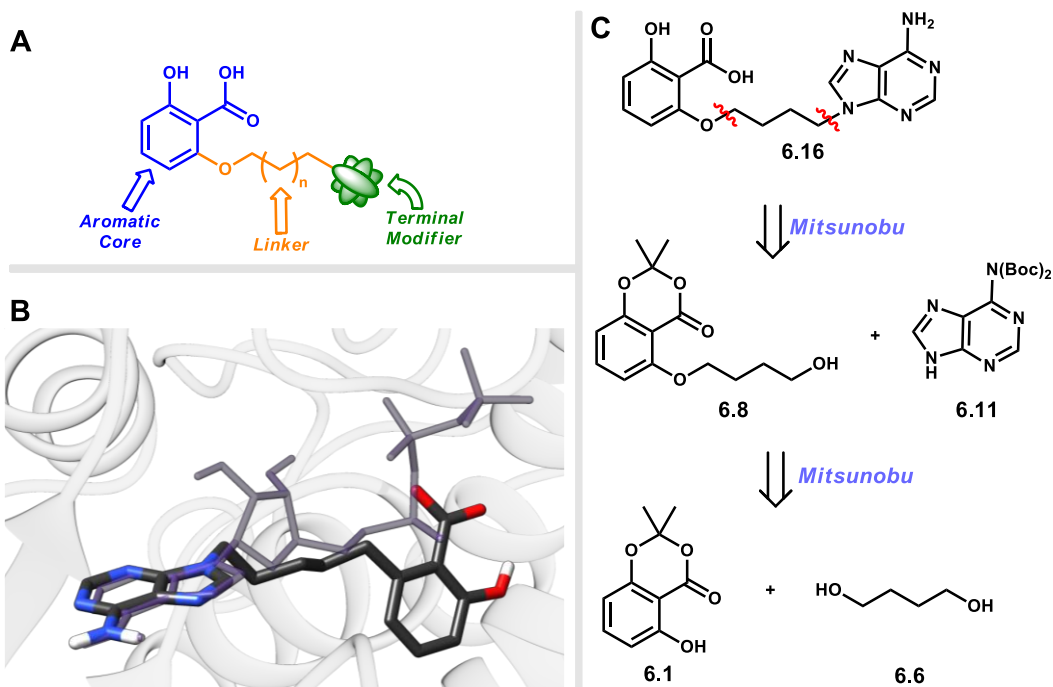
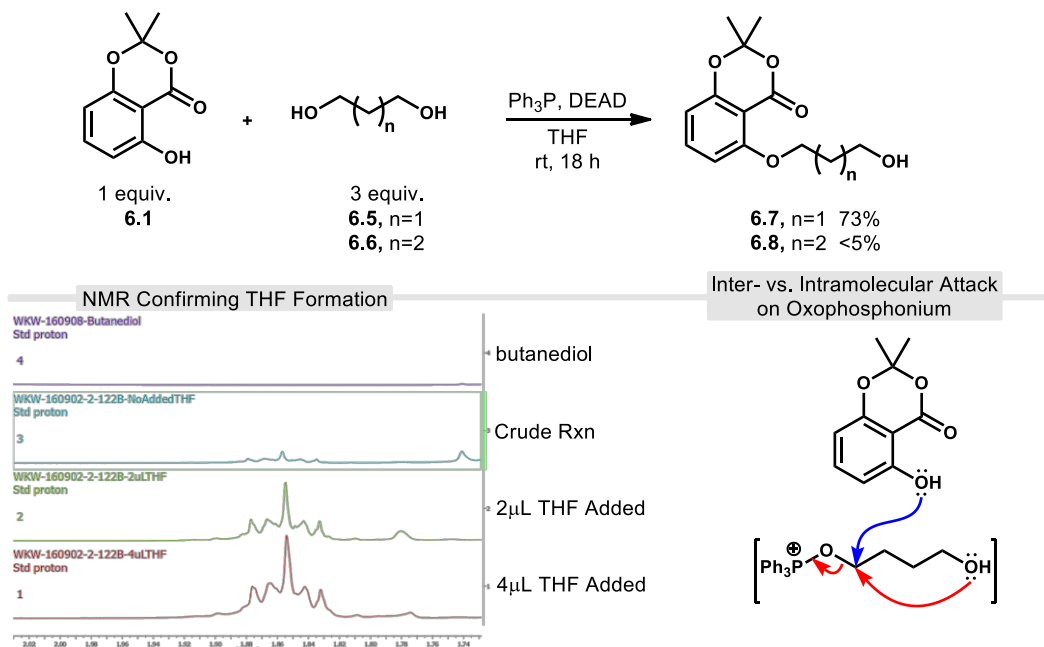


Figure 6.7 – Mitsunobu-based Assembly of Anacardic Acid Derivatives

A) Use of variable sections allows for the modular assembly of derivatives. B) Overlay of known the ATP geometry (purple) with the a computationally predicted conformation of an anacardic acid derivative C) Retrosynthesis via sequential Mitsunobu reactions.

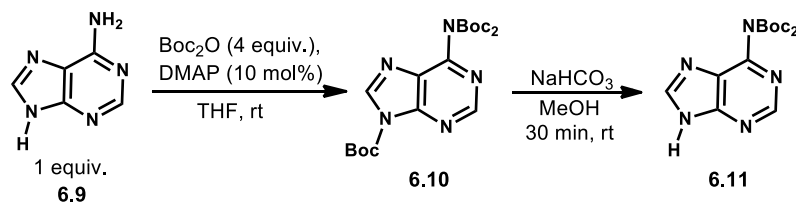


Scheme 6.2 – Mitsunobu Reactions with 1,3-Propanediol and 1,4-Butanediol

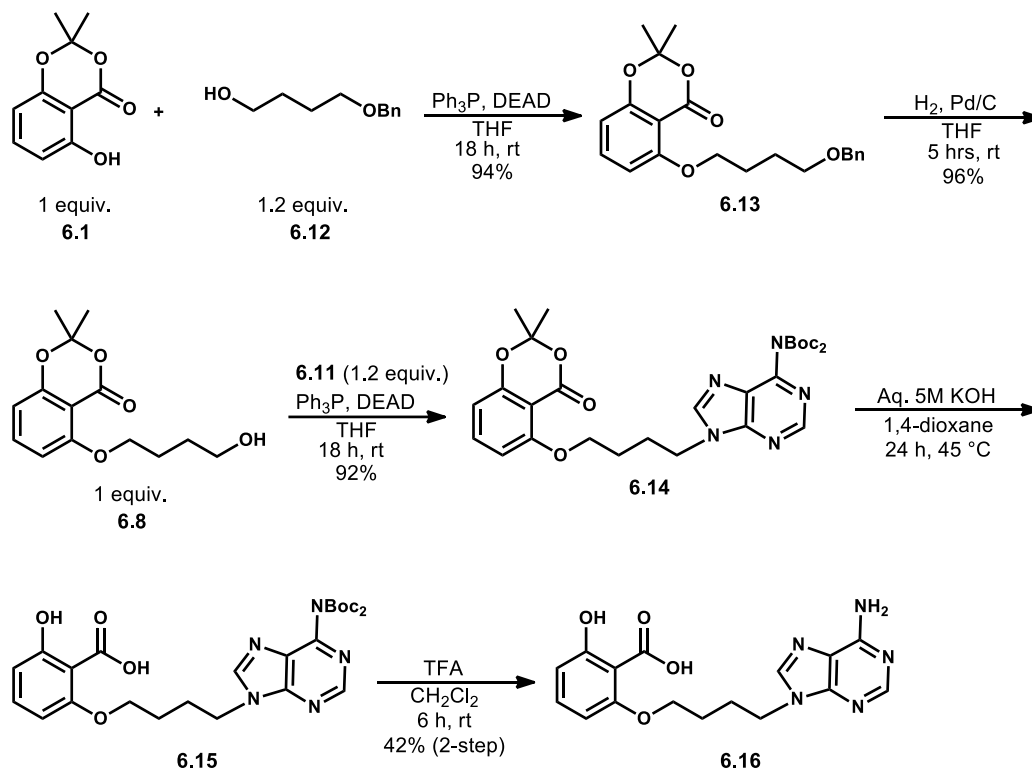
Considering how efficiently the Mitsunobu reaction worked for creating the aryl ether linkage to the acetonide, we considered the possibility of using a dual Mitsunobu strategy with straight-chain diols. These diols would serve as a linker region between the aromatic core and a variable terminal modifier as shown in **Figure 6.7A** and allow for the assembly of these components in a modular fashion. We were most intrigued by the use of adenine as a terminal modifier (**6.16**, **Figure 6.7B and C**) due to its similarity to the natural SUMO E1 substrate (ATP). Adenine itself is also capable of participating in Mitsunobu reactions. Based on computational docking calculations (see previous section), we predicted that a 5-atom linker would be the ideal length to position the adenylyl moiety so it mimics the natural binding confirmation of ATP. With this in mind, we began with a Mitsunobu reaction between the acetonide-protected phenol **6.1** (**Scheme 6.2**) and 1,4-butane-diol **6.6** to give the aryl ether product **6.8**. However, the yield of this reaction was extremely low for such a well preceded reaction (<5%). When the analogous reaction was performed with propane diol **6.5**, the resulting yield was significantly better (78%). We surmised that the creation of the oxophosphonium intermediate from butane diol undergoes rapid intramolecular cyclization to form THF before the desired intermolecular attack by the phenol, while oxetane formation from propane diol is slower. Because of the widespread use of THF as the solvent of choice in Mitsunobu reactions, as was the case in our reaction, the formation of THF was essentially invisible. To test this theory, the reaction was performed in another solvent, 1,4-dioxane, inside an NMR tube to see if the formation of THF was observed. An ^1H NMR peak consistent with the expected THF “crown” at 1.85

ppm was present in the crude reaction mixture and definitively confirmed by the growth of this peak after titration of pure THF into the reaction mixture.

Preparation of Bis-Boc Adenine



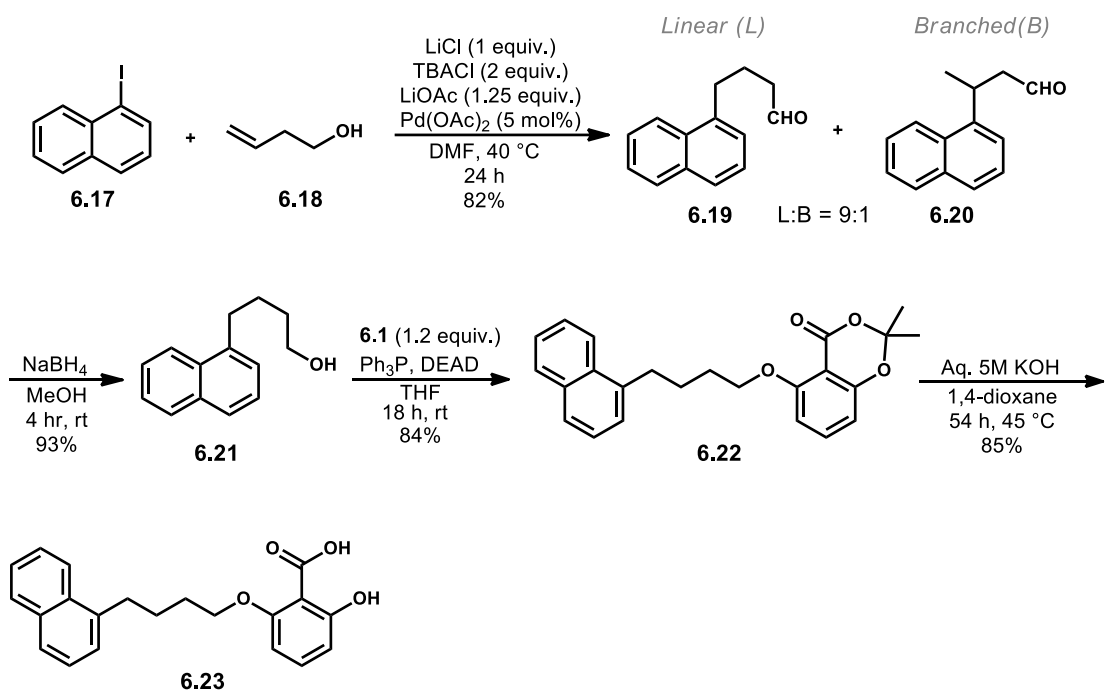
Main Synthetic Sequence



Scheme 6.3 – Synthesis of an Adenylated Anacardic Acid Derivative

To prevent this unwanted cyclization, we opted to use benzyloxy butanol **6.12** (Scheme 6.3) which proceeded to give the aryl ether product **6.13** in excellent yield (94%) Hydrogenolysis was then used to remove the benzyl group which afforded alcohol **6.8**, also

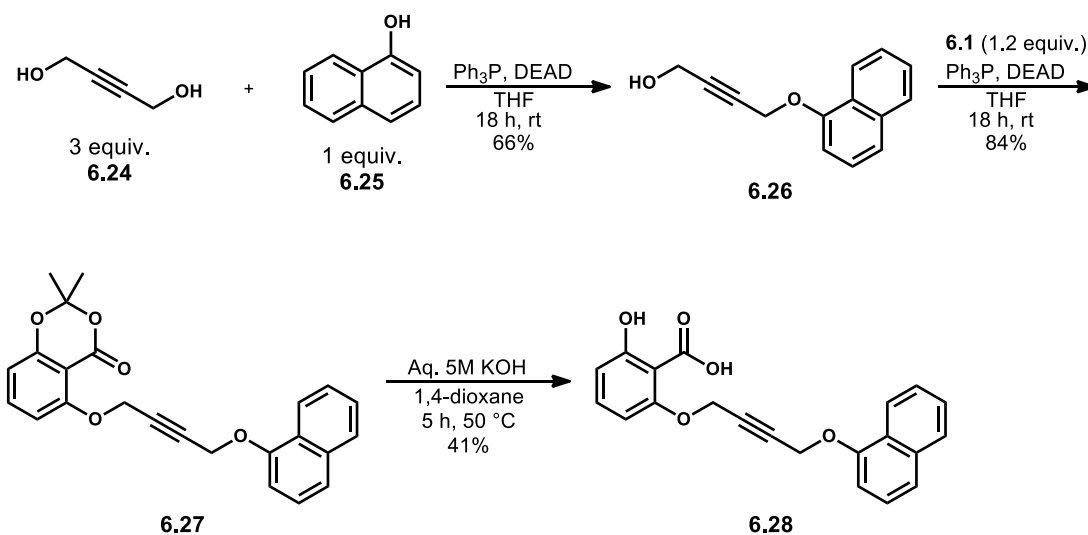
in excellent yield (96%). This butane-linked alcohol was then subjected to a second Mitsunobu reaction with bis-Boc adenine **6.11** to give the protected adenylated derivative **6.14**. Bis-Boc adenine **6.11** was synthesized by first tris-Boc protecting adenine, followed by a selective mono Boc removal procedure using sodium bicarbonate and methanol. Using aqueous KOH for acetonide removal and then TFA for Boc removal gave the final adenylated anacardic acid derivative **6.16** in 46% over the two deprotection steps.



Scheme 6.4 – Synthesis of a Naphthylated Anacardic Acid Derivative

Many of the residues surrounding adenine in the active site of SUMO E1 are hydrophobic and therefore we were interested to see if a nonpolar terminal modifier such as naphthalene may have stronger hydrophobic interactions and thus a better binding affinity. To synthesize the naphthylated derivative **6.23** (Scheme 6.4), a Heck relay reaction between naphthyl iodide **6.17** and 3-buten-ol was used to obtain a mixture of linear

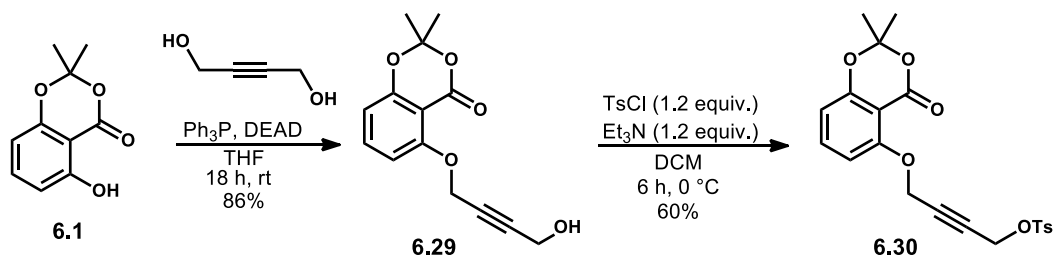
and branched aldehyde products (**6.19**:**6.20**, L:B 9:1). Aldehyde reduction with NaBH₄ to give alcohol **6.21** proceeded smoothly. While the linear and branched isomers were difficult to separate as aldehydes, after conversion to alcohols separation via chromatography was much more successful. A Mitsunobu was again used to construct an aryl ether linkage with phenol **6.1**, forming the butoxy-linked intermediate **6.22**. Acetonide deprotection gave the final naphthylated anacardic acid derivative **6.33**.



Scheme 6.5 – Synthesis of a Butyne-Linked Naphthylated Anacardic Acid Derivative

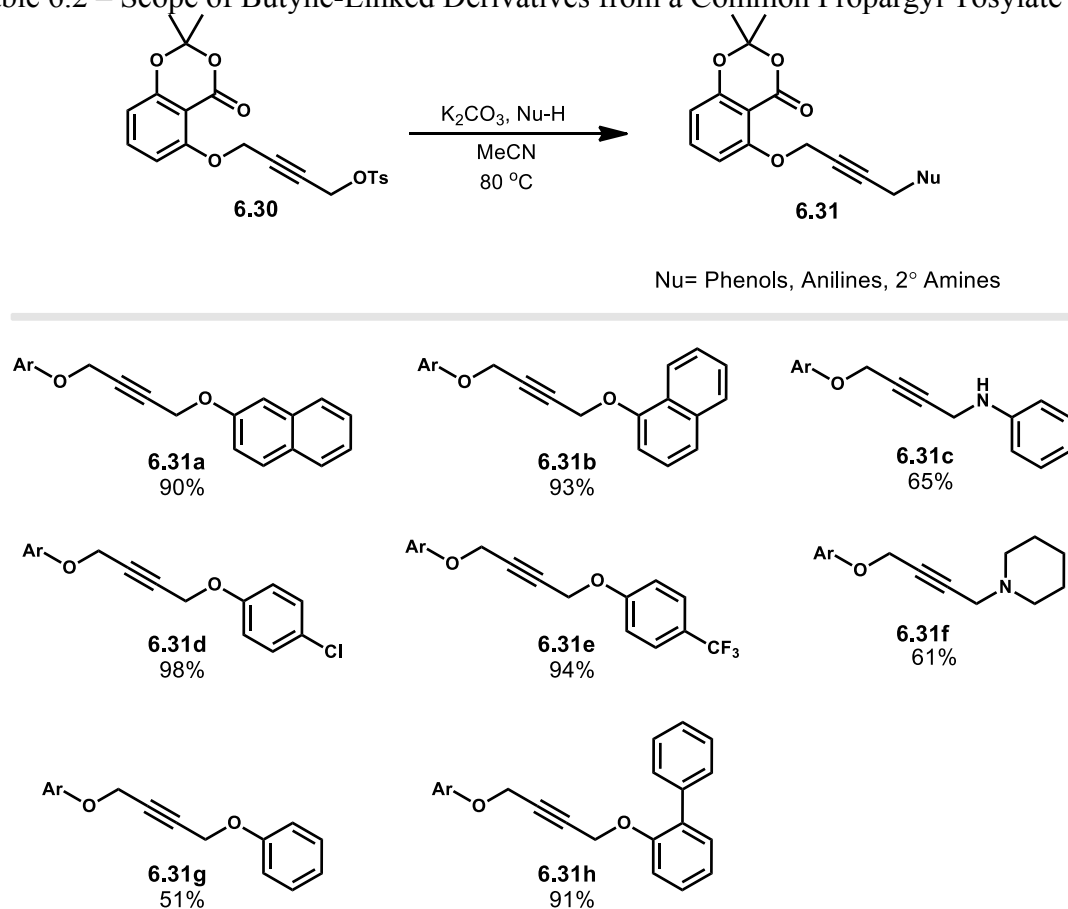
We theorized that this naphthylated derivative should mimic how anacardic acid is predicted to fit in the active site of SUMO E1. The flexible tail of anacardic acid extends across the active site before it curls up on the hydrophobic side of the binding pocket. In terms of space occupied, the naphthyl moiety fills the same area as the curled tail of anacardic acid (refer to **Figure 6.6C**). However, being locked in a ring, the naphthyl group significantly increases molecular rigidity by reducing the number of rotatable bonds and reduces the entropic cost of active site occupation. With this in mind, we next considered the use of butyne linkers to further increase molecular rigidity.

To accomplish this, a double Mitsunobu sequence akin to the one used with the butane diol linker was used with butyne diol. However, benzyl protection/deprotection steps were unnecessary due the presence of the alkyne (making cyclization unfavorable) and made the overall reaction sequence more direct (**Scheme 6.5**). In this case, two Mitsunobu reactions were used in sequence, first with butyne diol (**6.24**) and 1-naphthol (**6.25**) and again with the aryl acetonide **6.1** with good yields. Deprotection with aqueous base gave the butyne-linked naphthyl derivative **6.28**. Reversing the order of these Mitsunobu reactions and doing the reaction with butyne diol and the aryl acetonide to give propargyl alcohol **6.29** was also used as the first step in a divergent synthesis of butyne-linked derivatives (**Scheme 6.6**). Through conversion of the propargyl alcohol to the tosylate **6.30** with tosyl chloride, a common intermediate is reached that can then be reacted with a variety of nucleophiles such as phenols, anilines, and amines. A scope with a variety of nucleophiles is shown in **Table 6.2**. Most phenolic and naphtholic derivatives proceeded in excellent yield with the more electron deficient *para*-chloro **6.31d** and trifluoromethyl **6.31e** products performing most efficiently. The aniline **6.31c** and piperidine **6.31f** derivatives were lower yielding and gave only moderate yields.



Scheme 6.6 – Synthesis of a Divergent Propargyl Tosylate Intermediate

Table 6.2 – Scope of Butyne-Linked Derivatives from a Common Propargyl Tosylate



6.4.1.1 - Biochemical Evaluation of Selected Aryl Ether-Linked Derivatives

Working in collaboration with Dr. Jeff Perry's lab (UCR, Biochemistry) and Dr. Jaiyu Liao's lab (UCR, Bioengineering), a small library of aryl ether linked derivatives (**Figure 6.8A**) was tested for SUMO E1 inhibition using a gel electrophoresis assay^[22,23] and a Förster resonance energy transfer (FRET) assay^[24,25] (**Figure 6.8 B and C**).

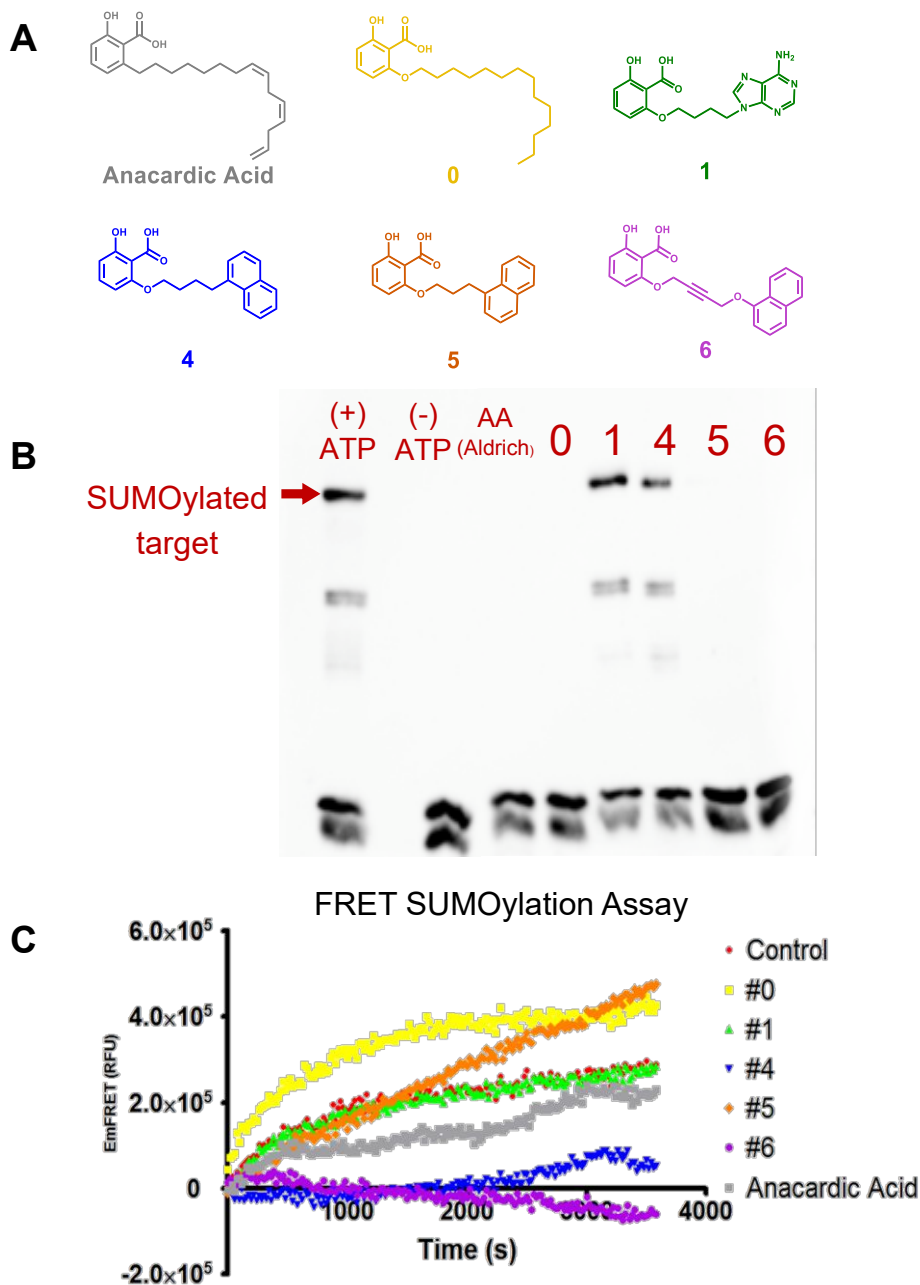


Figure 6.8 – Sumo Inhibition Studies Using Aryl Ether Anacardic Acid Derivatives

A) Derivatives used in SUMOylation assays. Anacardic Acid purchased from Aldrich. B) Gel electrophoresis assay performed by the Perry Lab, UCR Biochemistry at 1mM inhibitor. Successful inhibition of E1 enzymatic activity is indicated by lack of SUMOylated protein target band. C) FRET assay performed by Liao Lab, UCR Bioengineering at 300 μ M. Cypet-SUMO1, E1(Aos1/Uba2), Ypet-Ubc9 were mixed in SUMOylation buffer. After 1mM ATP was added, the conjugation of Cypet-SUMO1 to Ypet-Ubc9 resulted in FRET signal increase over time. Lower fluorescence indicates more effective inhibition of the SUMO/E1 complex.

The far-left lane in **Figure 6.8B** serves as the positive control with ATP present together with SUMO E1, SUMO, and a sumoylation target. The next lane to the right is the negative control where ATP was omitted. The dark band at the top of the left lane is the sumoylated protein target and no sumoylation was observed in the absence of ATP. No sumoylation was seen when a commercial sample of anacardic acid was used indicating inhibition of SUMO E1. The results of this assay indicate that compounds 5 and 6 act as inhibitors while 1 and 4 do not. First, and most surprisingly, the adenine derivative (4, blue), proved to be ineffective at inhibiting the SUMO E1 enzyme despite its structural similarity to ATP. The length of the linker for the naphthyl derivatives was determined to have a large impact on inhibitory ability. The three-carbon linker (5, orange) displayed inhibition while the four-carbon variant (4, blue) did not. The four-carbon butyne linker (6, purple) did exhibit inhibition suggesting that the positioning of the terminal modifier and linker within the active site may be an additional factor to consider rather than just the number of atoms in the linker.

Interestingly, the FRET assay results are at odds with the conclusions reached using the electrophoresis assay. For example, in the FRET assay, the tetradecanol-derived derivative (0, yellow) is the worst at inhibiting sumoylation even though the gel electrophoresis assay suggests inhibition. The dramatic difference between the anacardic acid standard (grey) and its aryl ether variant (yellow) is indeed surprising given that they differ by only a single carbon-to-oxygen substitution and it may be possible that this derivative destabilizes protein elements involved with FRET emission. The FRET assay also indicates that derivative 4 (blue) is a good inhibitor which is contrary to the result

obtained in the electrophoresis assay. Both assay methods suggest that the butyne linked derivative 6 (purple) effectively inhibits the sumoylation process. Given that derivative 6 is the most rigid of the derivatives tested, it offers the largest departure from anacardic acid. While these inhibitors are predicted to occupy roughly the same amount of space within the ATP binding pocket (**Figure 6.9**, the number of rotatable bonds in anacardic acid goes from 15 to only 6 in the butyne-linked naphthyl derivative significantly reducing the entropic cost of adopting the correct binding conformation within the active site.

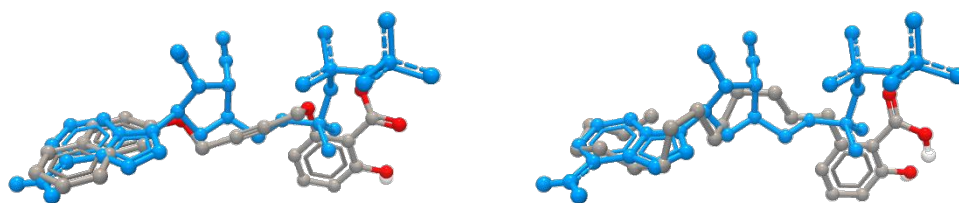
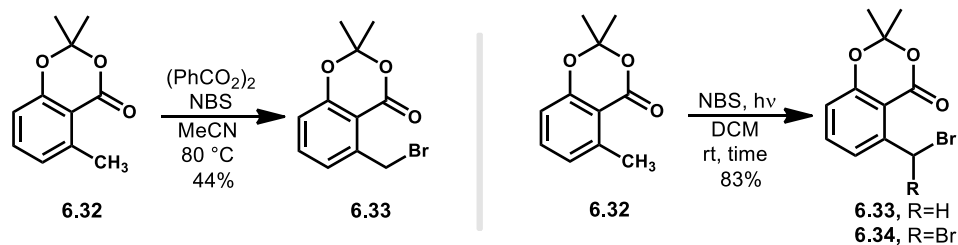


Figure 6.9 – Space Occupation of The ATP Binding Pocket by Anacardic Acid and a Butyne-Linked Derivative

6.4.2 - Piperazine and Piperidine-Linked Anacardic Acid Derivatives

Piperazines are a common moiety found in a large number of pharmaceuticals and are used in a wide range of therapeutic areas such as antifungals, antivirals, antihistamines, antidepressants.^[26] For this reason, piperazines are considered “privileged structures” within the realm of medicinal chemistry and are considered a common combinatorial building block used in drug discovery.^[27] Computational docking calculations suggested that derivatives featuring a piperazine linker fit well inside the ATP binding pocket of SUMO E1.

Table 6.3 –Benzylic Radical Bromination Optimization



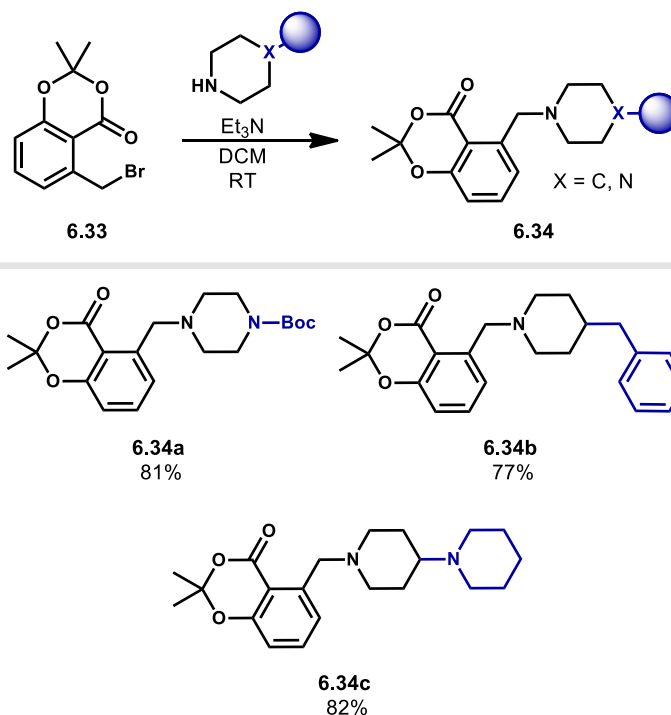
[NBS] (M)	Light Src.	time (h)	Isolated Yield (%)	6.33:6.34*
0.2	2x 100W CFL	6	70	--
0.15	2x 100W CFL	6	75	94:6
0.1	2x 100W CFL	6	45	91:9
0.2	UV Reactor	1	42*	--
0.2	UV Reactor	3	83	93:7
0.2	UV Reactor	6	77	88:12

NBS (1.15 equiv.), (PhCO₂)₂ (15 mol%)

*Determined using HNMR with Bn₂O as internal std.

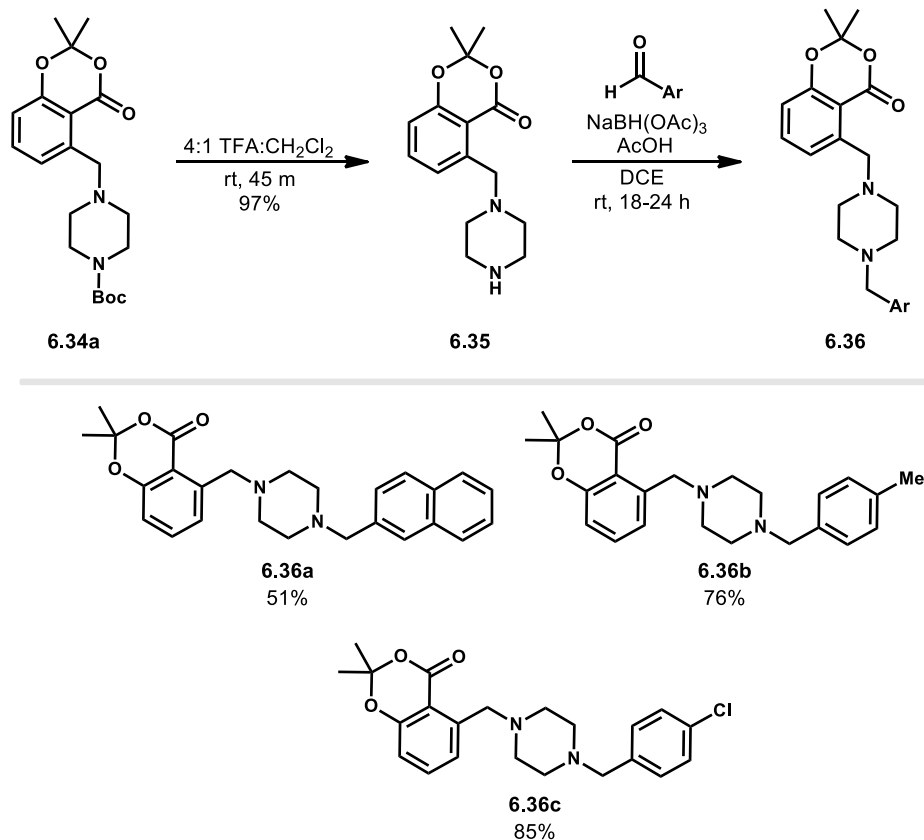
Rather than begin with the 2,6-dihydroxybenzoic acid derived acetonide, the starting material used in the synthesis of the piperazine derivatives instead started from the 6-methylsalicylic acid acetonide (**6.32**, **Table 6.3**). In preparation for substitution with piperazine, the benzylic position first needed to be brominated (**6.33**). Initially, a radical bromination was attempted using *N*-bromosuccinimide (NBS) with benzoyl peroxide and heating for radical initiation. However, only moderate yields were obtained using this method and tedious re-additions of benzoyl peroxide were required to sustain the reaction. An alternative light-initiated method was then tried using 2x 100 W CFL bulbs. These conditions were much more convenient and improved product yield. The production of the undesired dibrominated product **6.34** proved to be somewhat problematic because of the difficulty separating it from the monobrominated product. It was later found that use of a

photoreactor using UV light reduced reaction times although the ratio of dibromo and monobromo products was not appreciably affected.



Scheme 6.7 – Benzyl Substitution of Aryl Acetonide With Piperidines and N-Boc Piperazine

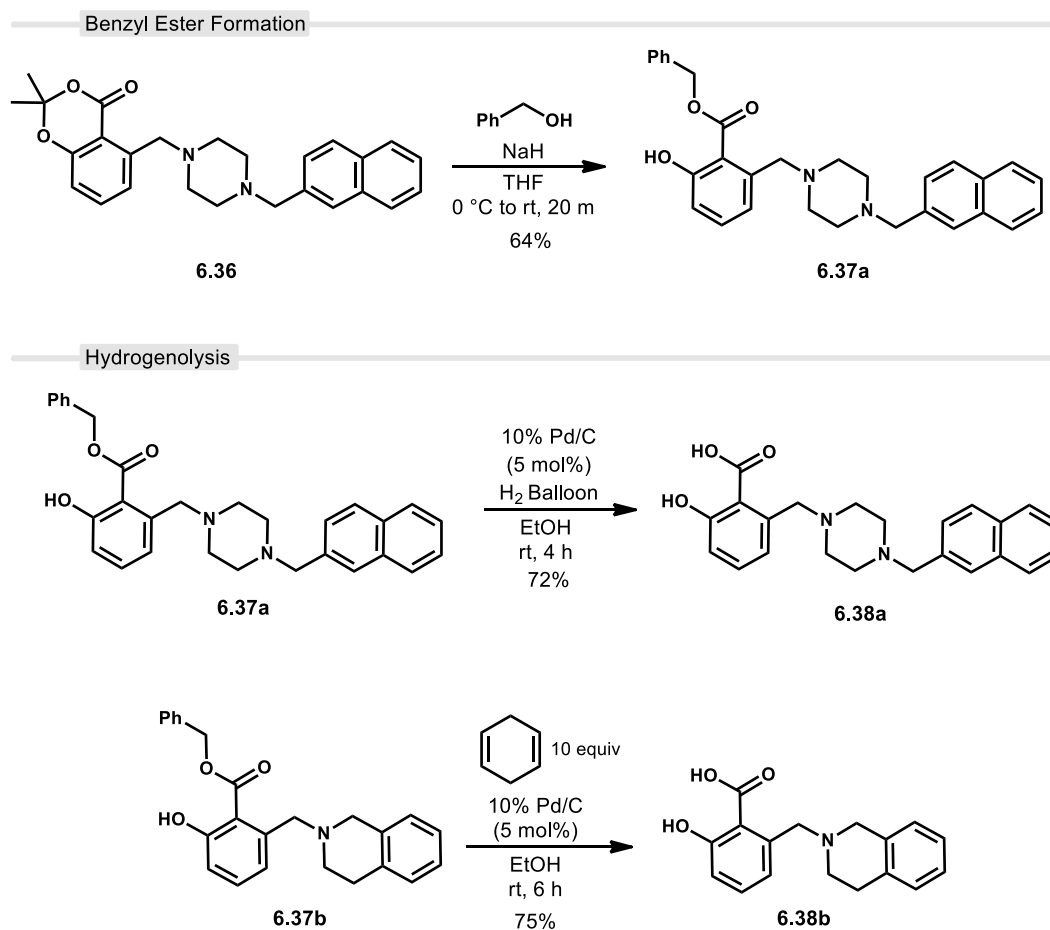
The brominated acetonide was then used in substitution reactions with various piperazines to obtain piperazine-linked products **6.34a-c** with good results (Scheme 6.7). *N*-Boc piperazine **6.34a** was deprotected using TFA to afford the benzyl piperazine intermediate **6.35** in excellent yield (Scheme 6.8) and used in reductive aminations with different aryl aldehydes using sodium triacetoxyborohydride (STAB). This approach was used to create another set of piperazine-linked acetonides (**6.36a-c**) in moderate to good yield.



Scheme 6.8 – Piperazine-Linked Derivatives Using Reductive Amination

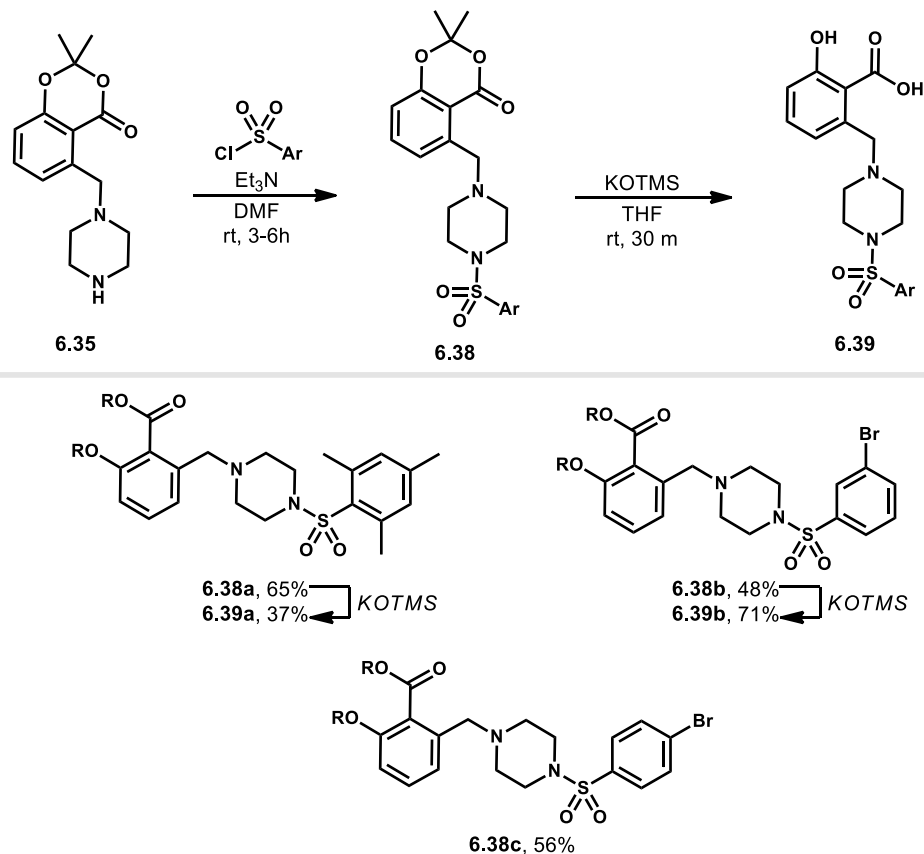
Deprotection of the piperazine derivatives using aqueous KOH was problematic due to the amphoteric character of these molecules. Organic extraction of the products, which may form zwitterionic salts, was very inefficient under both the basic reaction conditions and upon acidification. Another deprotection strategy was then tried which relied on hydrogenolysis in the final step. The use of heterogeneous hydrogenolysis is advantageous due to the ease of workup which simply involves filtration of the reaction mixture to remove the heterogeneous catalyst. Not only does this eliminate the need for an extraction, in some cases, subsequent purification can be avoided altogether.

First, the acetonide was opened using benzyl alcohol and sodium hydride to afford benzyl ester **6.37a** (Scheme 6.9). This benzyl ester was then subjected to hydrogenolysis using palladium on carbon in the presence of hydrogen gas. This afforded the deprotected product **6.38a** in 72% yield after passage through a short pad of silica. A similar approach



Scheme 6.9 – Alternative Acetonide Deprotection Strategy Using Hydrogenolysis

was used in the deprotection of tetrahydroisoquinoline acetonide **6.37b**. Instead of hydrogen gas being used to activate the Pd/C surface, 1,4-cyclohexadiene was used for this purpose and gave comparable results.



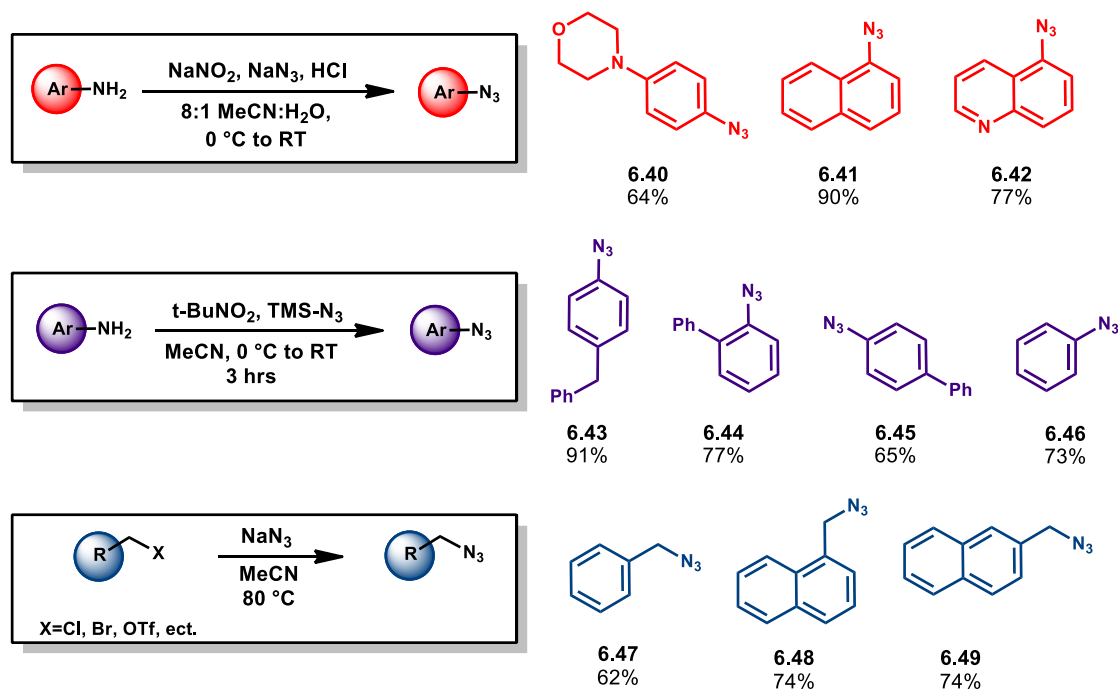
Scheme 6.10 –Piperazine Sulfonamide-Linked Anacardic Acid Derivatives

The unrotected piperazine **6.35** was also used to make sulfonamides from the corresponding arylsulfonyl chlorides, which proceeded to give products **6.38a-c** in moderate yield (**Scheme 6.10**). A new deprotection strategy was tried using potassium trimethylsilanolate (KOTMS) and was a significant improvement over the previous approaches with aq. KOH in dioxane and hydrogenolysis. These deprotections with KOTMS were complete by TLC in under 30 minutes and the precipitated potassium carboxylate could be filtered off and then rinsed or sonicated with water to obtain the mesityl product **6.39a** in 37% yield and the m-bromobenzene product **6.39b** in 71% yield. The dramatic increase in reaction efficiency is attributed the good solubility of KOTMS in organic solvent resulting in more nucleophile in solution compared to the biphasic aq.

KOH/dioxane mixture. The silanol byproduct can also be easily removed under vacuum which further simplified purification.

6.4.3 - Triazole-Linked Anacardic Acid Derivatives

1,2,3-Triazole based linkers were initially considered due to their facile and reliable synthesis using a Cu(I)-catalyzed alkyne-azide cycloaddition (CuAAC). These reactions proceed in the presence of copper(I) to give the same products as Huisgen-type 1,3-dipolar cycloaddition between an alkyne and an azide.^[28] Due to their versatility this is one of the



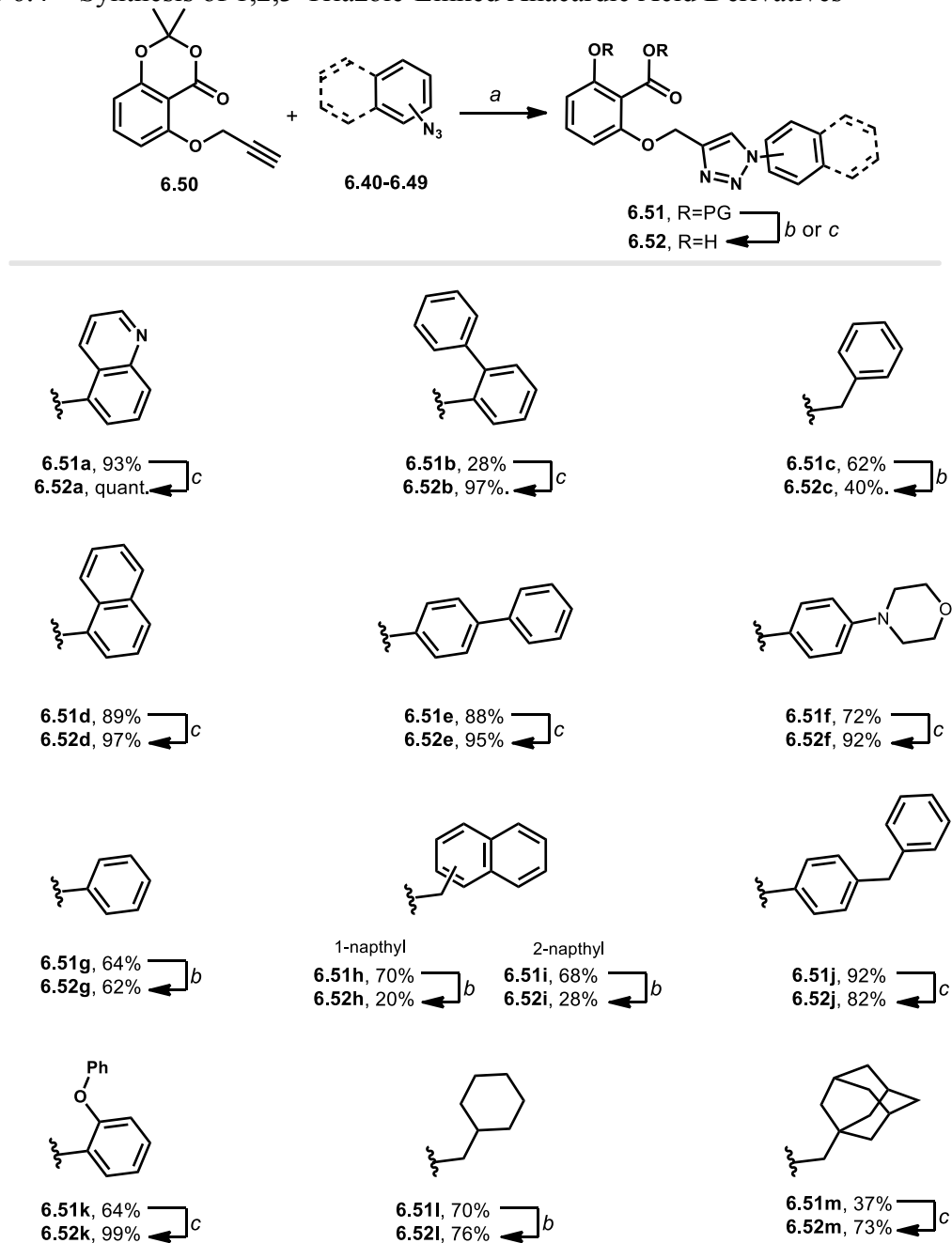
Scheme 6.11 – Synthesis of Azides For Use in Click-Reactions most used and well known of the so-called “click” reactions.^[29,30] Additionally, the triazole linker was predicted to bind well by computational docking studies.

To create a library of triazole-linked derivatives, a number of azides were first synthesized. Many were made from anilines by conversion to their aryl diazoniums followed by treatment with either sodium azide or TMS azide (6.40-6.46, Scheme 6.11). A small handful of aliphatic azides were also made via simple substitution with sodium

azide (**6.47-6.49**). The alkyne used in these reactions, **6.50**, was made using a Mitsunobu reaction with phenolic acetonide **6.1** and propargyl alcohol. A wide range of triazole derivatives were then synthesized using CuAAC click reactions (**Table 6.4**).

The yields obtained from these click reactions were generally high and did not require any optimization around specific azides which expedited the assembly of a large collection of triazole products (**6.51a-m**). In most cases, acetonide deprotection of these triazoles was accomplished using KOTMS. A few deprotections were carried out using aqueous KOH before finding that KOTMS was a superior alternative. The differences in the two deprotection methods is evident by looking at the yields of the deprotected products (**6.52a-m**); the yields for derivatives using KOTMS are uniformly higher.

Table 6.4 – Synthesis of 1,2,3-Triazole-Linked Anacardic Acid Derivatives



a) sodium ascorbate (10 mol%), CuSO₄•5H₂O (4 mol%), 1:3 H₂O:CH₂Cl₂, rt, 3-8 h b) 5M aq. KOH, 1,4-Dioxane 40 °C, 24 h c) KOTMS (1.2 equiv.), THF, rt, 30 m

6.4.3.1 - Biochemical Evaluation of Triazole-Based Anacardic Acid Derivatives

In collaboration with the Liao lab, the library of triazoles was tested using an in-situ FRET assay to quantify SUMO E1 inhibition (**Figure 6.10**).^[25] Biphenyl derivative #155 and diphenylmethane derivative #158 were the most effective inhibitors. Compared to the biphenyl and diphenylmethane derivatives, the phenyl and naphthyl derivatives performed poorly suggesting that their size and limited points of free rotation may be detrimental. Interestingly, adamantyl derivative #170 performed notably better than its phenyl and cyclohexyl variants (#127 and #168, respectively).

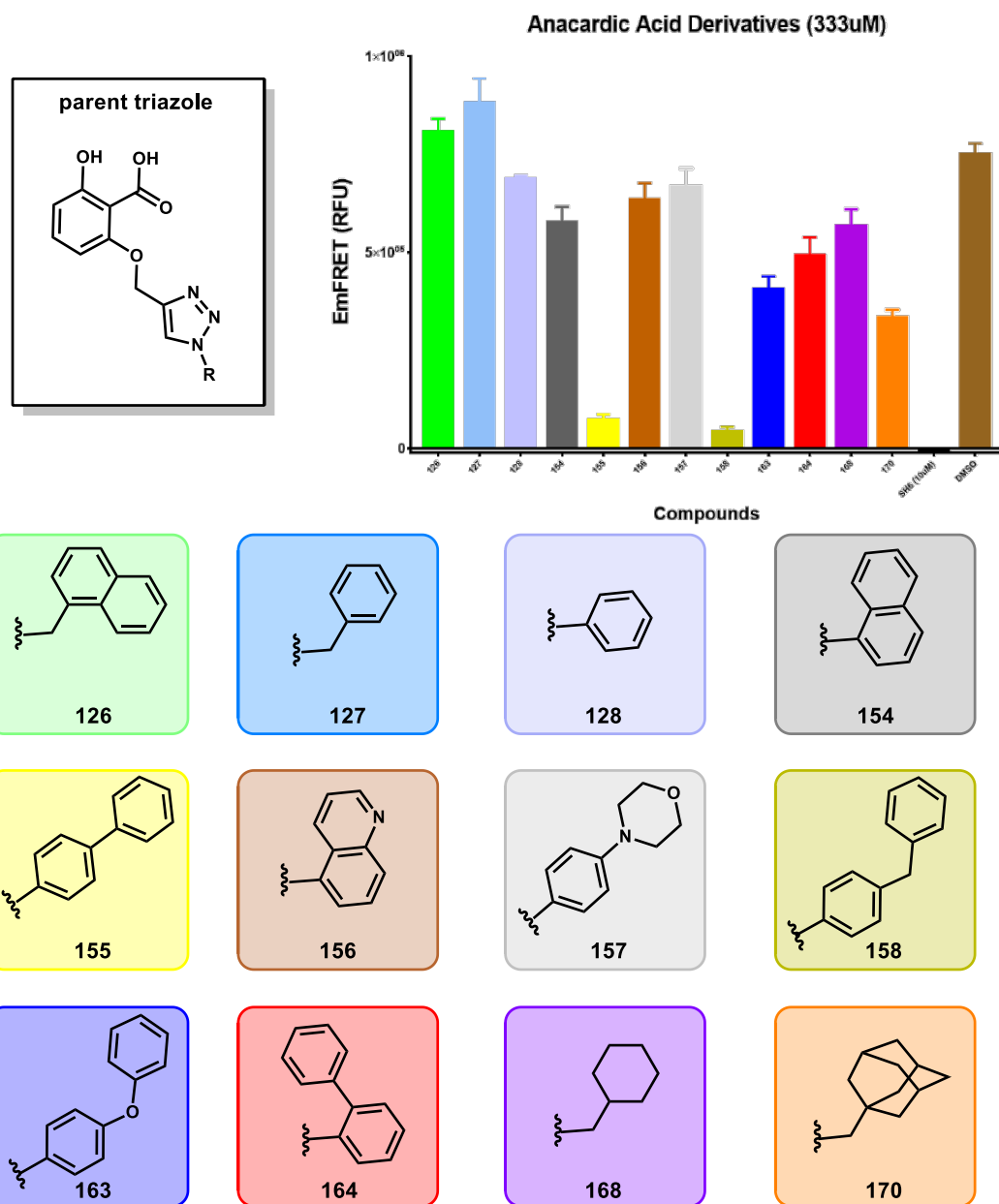


Figure 6.10 – FRET Analysis of Triazole-Linked Anacardic Acid Derivatives
SUMOylation assay performed by the Liao Lab, UCR Bioengineering at 333 μ M inhibitor. Cypet-SUMO1, E1(Aos1/Uba2), Ypet-Ubc9 were mixed in SUMOylation buffer. After 2mM ATP was added, the conjugation of Cypet-SUMO1 to Ypet-Ubc9 resulted in FRET signal increase over time. Lower fluorescence indicates more effective inhibition of the SUMO/E1 complex.

6.5 - Conclusions

Anacardic acid derivatives were designed with the assistance of molecular docking and virtual screening and then synthesized using a variety of methods. The salicylic core of anacardic acid was unmodified and linear butyne and butoxy based linker regions were examined along with cyclic piperazines and triazoles. These linkers were combined with a variety of terminal aryl and heteroaryl modifiers in an effort to mimic the space filled by the curled tail of anacardic acid and improve binding to the SUMO E1 enzyme. **Figure 6.11** summarizes three of the most effective SUMO E1 inhibitors that were synthesized and assayed during the course of this investigation.

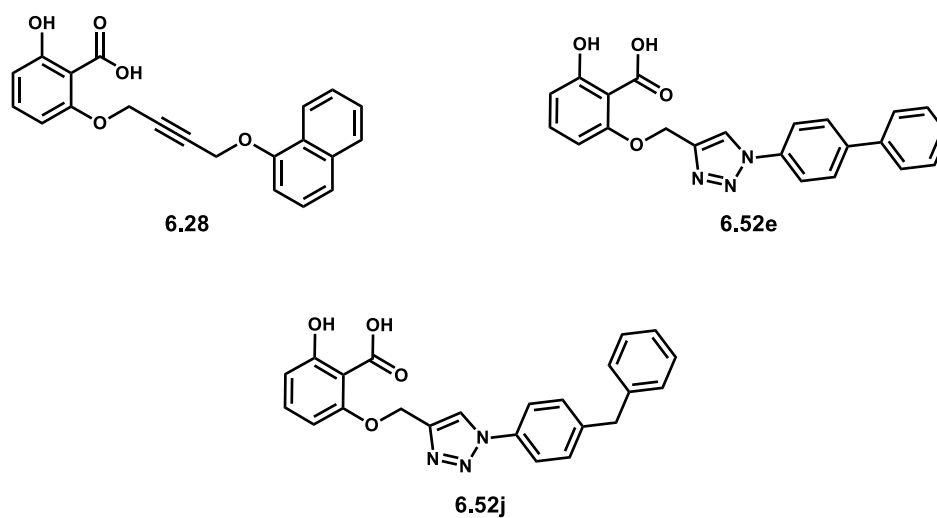


Figure 6.11 –Successful SUMO E1 Inhibitors Based on In-Situ FRET Assays

Further biochemical analysis should be undertaken to determine IC_{50} values and then compare those values to anacardic acid. These compounds represent good starting points for further SAR. The exact mode of binding for anacardic acid within the SUMO E1 active site is still unknown. The dynamic hinge-like structure of SUMO E1 means that the shape of the active site with bound ATP is not necessarily the shape of the active site

with when it most tightly bound to anacardic acid. While current assumptions about anacardic acid based on available data point to it acting as a competitive inhibitor for the ATP active site, a non-competitive mechanism of inhibition cannot be ruled out. For these reasons, a co-crystal structure with anacardic acid or one of its derivatives would significantly aid in the future design of SUMO E1 inhibitors based on anacardic acid.

6.6 - Experimental

6.6.1 - General Procedures:

6.6.1.1 - Procedure A: Copper Click Reactions

To a round bottom flask was added alkyne **6.50** (1 equiv), sodium ascorbate (4 mol%), $\text{CuSO}_4 \cdot 5\text{H}_2\text{O}$ (10 mol%), and 2:1 DCM: H_2O (0.1 M in DCM). The reaction mixture was then stirred and azide (1.6 equiv) was added. The reaction mixture was then stirred until deemed complete by a yellow color change. The reaction mixture was then diluted with more DCM and extracted with water and washed with brine. The organic layer was dried over MgSO_4 and the volatiles removed under reduced pressure. The residue was then purified with column chromatography.

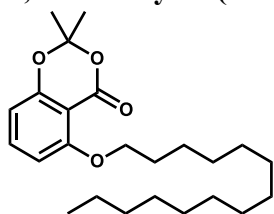
6.6.1.2 - Procedure B: KOTMS Acetonide Deprotection

To a vial containing a stir bar was added acetonide (1 equiv) and KOTMS (2.5 equiv) followed by THF (0.15 M). The reaction was then stirred until complete by TLC and was then acidified using dropwise addition of 3 M HCl until the formation of a persistent solid precipitate. The organic volatiles were then removed under vacuum leaving a residue and residual water. This was then extracted with DCM, washed with brine, and dried over MgSO_4 . The organic layers were reduced down to afford a residue that was then triturated in hexanes to afford a solid powder.

6.6.1.3 - Procedure C: KOH Acetonide Deprotection

To a round bottom flask containing a stir bar was added acetonide (1 equiv). followed by a 1:2 mixture of 5 M KOH:THF (0.2 M in THF) and then stirred at 60 °C until complete by TLC. The reaction mixture was then acidified with 3 M HCl and extracted with EtOAc. The organic layers were then washed with brine and dried over Na₂SO₄ and concentrated under reduced pressure. The crude residue was then purified with column chromatography.

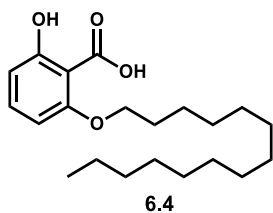
2,2-dimethyl-5-(tetradecyloxy)-4H-benzo[d][1,3]dioxin-4-one (6.3):



To a round bottom flask with stir bar was added aryl acetonide **6.1** (0.200 g, 1.03 mmol, 1 equiv), tetradecanol (0.265 g, 1.24 mmol, 1.2 equiv), and triphenylphosphine (0.294 g, 1.24 mmol, 1.2 equiv).

The reaction vessel was sealed with a septum and pumped and backfilled 3x times with nitrogen. Dry THF (6.5 mL) was then added via syringe and the contents were then stirred in an ice bath for 10 minutes. Diethyl azodicarboxylate (40% wt. in toluene, 0.56 mL, 1.24 mmol, 1.2 equiv) was then added dropwise and the reaction vessel was removed from the ice bath and allowed to warm to rt. The reaction was then allowed to stir overnight. The volatiles were removed under reduced pressure and the residue was taken up in a minimal amount of 1:1 ethyl acetate: hexanes. This solution was loaded on a column and purified using column chromatography to give a waxy white solid (0.380 g, 98%) ¹H NMR (400 MHz, Chloroform-*d*) δ 7.41 (t, *J* = 8.3 Hz, 1H), 6.61 (d, *J* = 8.3 Hz, 1H), 6.53 (dd, *J* = 8.2, 0.9 Hz, 1H), 4.08 (t, *J* = 6.8 Hz, 2H), 1.89 (p, *J* = 6.8 Hz, 2H), 1.71 (s, 6H), 1.50 (p, *J* = 7.0 Hz, 2H), 1.40 – 1.20 (m, 18H), 0.93 – 0.85 (m, 3H).

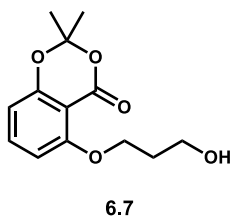
2-hydroxy-6-(tetradecyloxy)benzoic acid (6.4):



To a vial containing a stir bar was added 2,2-dimethyl-5-(tetradecyloxy)-4H-benzo[d][1,3]dioxin-4-one **6.3** (0.100 g, 0.124 mmol). The vial was placed under inert nitrogen atmosphere and dioxane (2 mL) and 5 M aq. KOH (1.2 mL) were added via syringe.

The reaction mixture was then stirred vigorously for 24 h at 60 °C. The reaction was then diluted with EtOAc (5 mL) and acidified using 3 M HCl (2.4 mL). The acidified mixture was then extracted with EtOAc (3x 10 mL), organic layers dried over Na₂SO₄, and the volatiles removed under vacuum. The resulting residue was passed through a short plug of silica with EtOAc then a 10% soln. of MeOH in EtOAc to give the product as a white residue (0.040 g, 91%). ¹H NMR (300 MHz, Chloroform-*d*) δ 12.18 (s, 1H), 11.61 (s, 1H), 7.40 (t, *J* = 8.4 Hz, 1H), 6.72 (dd, *J* = 8.4, 0.9 Hz, 1H), 6.48 (dd, *J* = 8.4, 0.8 Hz, 1H), 4.24 (t, *J* = 6.6 Hz, 2H), 1.92 (d, *J* = 6.6 Hz, 2H), 1.59 – 1.42 (m, 2H), 1.42 – 1.15 (m, 20H), 0.93 – 0.82 (m, 3H). ¹³C NMR (101 MHz, Chloroform-*d*) δ 171.1, 162.3, 160.1, 134.3, 108.2, 105.7, 103.8, 69.0, 31.7, 29.8, 29.7, 29.7, 29.6, 29.5, 29.4, 29.3, 26.3, 22.7, 14.1.

5-(3-hydroxypropoxy)-2,2-dimethyl-4H-benzo[d][1,3]dioxin-4-one (6.7):

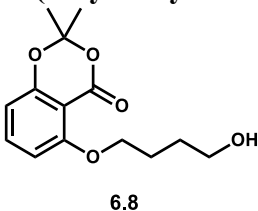


To a round bottom flask with stir bar was added aryl acetone **6.1** (1.00 g, 5.14 mmol, 1 equiv), propane diol **6.5** (1.10 mL, 15.44 mmol, 3.0 equiv), and triphenylphosphine (2.09 g, 7.71 mmol, 1.5 equiv). The

reaction vessel was sealed with a septum and pumped and backfilled 3x times with nitrogen. Dry THF (6.5 mL) was then added via syringe and the contents were then stirred in an ice bath for 10 minutes. Diethyl azodicarboxylate (40% wt. in toluene, 4.70 mL, 7.71 mmol, 1.5 equiv) was then added dropwise and the reaction vessel was

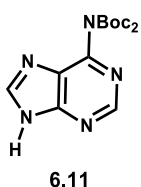
removed from the ice bath and allowed to warm to rt. The reaction was then allowed to stir overnight. The volatiles were removed under reduced pressure and the residue was taken up in a minimal amount of 1:1 ethyl acetate: hexanes. This solution was loaded on a column and purified using column chromatography (3:7 EtOAc : Hexanes) to give a white solid (0.944 g, 73%) **1H NMR** (300 MHz, Chloroform-d) δ 7.46 (t, J = 8.4 Hz, 1H), 6.62 (dd, J = 8.6, 0.9 Hz, 1H), 6.58 (dd, J = 8.3, 0.9 Hz, 1H), 4.24 (t, J = 5.6 Hz, 2H), 4.19 (t, J = 6.5 Hz, 1H), 3.97 – 3.88 (m, 2H), 2.15 (dt, J = 9.9, 5.5 Hz, 2H), 1.72 (s, 6H).

5-(3-hydroxybutoxy)-2,2-dimethyl-4H-benzo[d][1,3]dioxin-4-one (6.8):



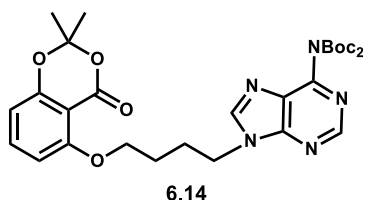
To a round bottom flask with stir bar was added benzyl protected acetonide **6.13** (0.400 g, 1.12 mmol, 1 equiv) and 10% palladium on carbon (0.12 g, 10 mol% Pd). The reaction vessel was sealed with a septum and pumped and backfilled 3x times with nitrogen. Dry EtOH (2.8 mL) was then added via syringe and the vessel contents were then sparged with nitrogen for 5 minutes. A balloon filled with hydrogen was then attached and the contents were stirred at rt for 5 hours until the reaction was complete by TLC. The reaction mixture was then filtered through a pad of celite and rinsed with DCM and the activated Pd was disposed of into a container of water. The filtrate was reduced under vacuum and the residue was purified using column chromatography to obtain a clear oil (0.288 g, 96%) **1H NMR** (300 MHz, Chloroform-d) δ 7.43 (td, J = 8.4, 0.9 Hz, 1H), 6.61 (dd, J = 8.6, 1.0 Hz, 1H), 6.54 (dd, J = 8.4, 1.0 Hz, 1H), 4.13 (t, J = 5.7 Hz, 2H), 3.75 (q, J = 5.3 Hz, 2H), 2.76 (s, 1H), 2.03 (p, J = 6.4 Hz, 2H), 1.81 (p, J = 6.5 Hz, 2H), 1.70 (s, 6H).

***N,N*-Bis Boc Adenine (6.11):**



To a round bottom flask with stir bar was added adenine **6.9** (0.500 g, 3.71 mmol, 1 equiv) and di-*tert*-butyl decarbonate (3.40 mL, 14.8 mmol, 4 equiv), and 4-dimethylaminopyridine (0.045 g, 0.37 mmol, 0.1 equiv). The reaction was placed under inert nitrogen atmosphere and 15 mL of dry THF was added via syringe. The reaction was then stirred at rt for 4 h until complete by TLC. The volatiles were removed under vacuum to afford a yellow oil. To this was added 40 mL MeOH and 10 mL sat'd. NaHCO₃ and the contents were stirred vigorously until the bis Boc product was observed by TLC (approx. 30 m). The volatiles were removed under vacuum and the remaining aq. solution was extracted with DCM. The crude residue was then purified using column chromatography to give a white solid (0.794 g, 68%) matching known literature spectra.^[31]

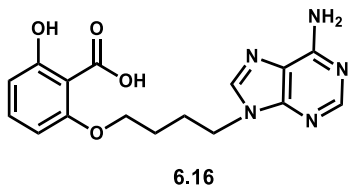
5-(3-(*N,N*-bisBoc-adenyl)butoxy)-2,2-dimethyl-4H-benzo[d][1,3]dioxin-4-one (6.14):



To a round bottom flask with stir bar was added arylbutoxy alcohol **6.8** (0.318 g, 1.19 mmol, 1 equiv), bis Boc adenine **6.11** (0.400 g, 1.19 mmol, 3.0 equiv), and triphenylphosphine (0.469 g, 1.79 mmol, 1.5 equiv). The reaction vessel was sealed with a septum and pumped and backfilled 3x times with nitrogen. Dry THF (20 mL) was then added via syringe and the contents were then stirred in an ice bath for 10 minutes. Diethyl azodicarboxylate (40% wt. in toluene, 3.51 mL, 1.79 mmol, 1.5 equiv) was then added dropwise and the reaction vessel was removed from the ice bath and allowed to warm to rt. The reaction was then allowed to stir overnight. The volatiles were removed under reduced pressure and the residue was taken up in a minimal amount of 1:1 ethyl acetate:

hexanes. This solution was loaded on a column and purified using column chromatography (7:3 EtOAc:Hexanes) to give a clear tacky residue (0.432 g, 92%) **1H NMR** (400 MHz, Chloroform-d) δ 8.86 (s, 1H), 8.30 (s, 1H), 7.44 (t, $J = 8.3$ Hz, 1H), 6.59 (dd, $J = 8.1, 6.8$ Hz, 2H), 4.55 (t, $J = 7.2$ Hz, 2H), 4.14 (t, $J = 7.0$ Hz, 2H), 2.29 (p, $J = 7.1$ Hz, 2H), 1.91 (p, $J = 6.2$ Hz, 2H), 1.73 (s, 6H), 1.46 (s, 18H). **HRMS** (ESI) m/z calcd for $C_{29}H_{38}N_5O_8$ (M+H)⁺ 583.2642, found 583.2644.

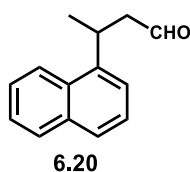
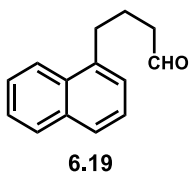
2-(4-(6-amino-9H-purin-9-yl)butoxy)-6-hydroxybenzoic acid (6.16):



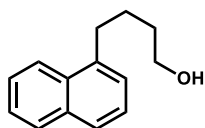
To a vial containing a stir bar was added **6.14** (0.432g, 1.09 mmol). The vial was placed under inert nitrogen atmosphere and dioxane (3 mL) and 5 M aq. KOH (1.6 mL) were added via syringe. The reaction mixture was then stirred vigorously for 24 h at 45 °C. The reaction was then diluted with EtOAc (8 mL) and acidified using 3 M HCl (5 mL). The acidified mixture was then extracted with EtOAc (3x 10 mL), organic layers dried over Na_2SO_4 , and the volatiles removed under vacuum. To the residue was added a 25% solution of TFA in DCM (5 mL) and the reaction was then stirred for 6 hours at rt. The reaction was then rotovapped down and the residue dissolved in 3 mL of DCM. 1 mL of sat'd Na_2CO_3 was added and the mixture was agitated. The pH of the aq. layer was adjusted to 7.00 using dropwise addition of 2 M HCl and extracted with 3x 10 mL portion of DCM and purified with column chromatography using 98:2:0.2 EtOAc:MeOH: NH_4OH to afford a tacky white foam (0.155 g, 42%). **1H NMR** (300 MHz, Deuterium Oxide) δ 12.11 (s, 1H), 8.75 (s, 1H), 7.99 (s, 1H), 7.38 (t, $J = 8.4$ Hz, 1H), 7.33 (m, 2H), 6.72 (d, $J = 8.5$ Hz, 1H), 6.44 (d, $J = 8.2$ Hz, 1H), 4.37 (t, $J = 7.0$ Hz, 2H), 4.28 (t, $J = 6.3$ Hz, 2H), 2.17 (d, $J = 7.1$ Hz,

2H), 2.04 – 1.89 (m, 2H). **¹³C NMR** (101 MHz, Deuterium Oxide) δ 171.0, 162.0, 160.3, 156.2, 152.5, 150.6, 141.0, 134.4, 119.1, 108.6, 105.6, 104.1, 68.8, 43.8, 27.0, 26.5. **HRMS** (ESI) m/z calcd for C₁₆H₁₈N₅O₄ (M+H)⁺ 343.1281, found 343.1278.

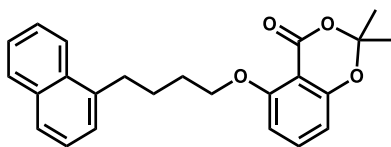
4-(naphthalen-1-yl)butanal (6.19):



1-iodonaphthylene (0.500 g, 1.96 mmol, 1 equiv), tetrabutylammonium chloride (1.09 g, 3.94 mmol, 2 equiv), lithium chloride (0.0834 g, 1.96 mmol, 1 equiv), lithium acetate (0.324 g, 4.92 mmol, 2.5 equiv), and palladium(II) acetate (0.022g, 0.98 mmol, 5 mol%) were weighed into a Schlenk vessel and capped with a septum. To the flask was added dimethylformamide (DMF) solvent (6 mL) then 2-propen-1-ol (0.136 mL, 1.96 mmol, 1.00 equiv) via syringe under a positive nitrogen pressure. The flask was then sealed and the reaction was stirred at 40 °C for 24 h. The resulting dark reaction mixture was quenched with DI water, extracted with diethyl ether (3x times), washed with brine and dried over Na₂SO₄ and concentrated *in-vacuo* to give the crude residue which was the purified using column chromatography (1:9 EtOAc:Hexanes) giving the product as a clear oil (0.270 g, 74%) as a mixture 9:1 mixture of linear and branched isomers. **¹H NMR** (300 MHz, Chloroform-*d*) Linear Isomer: δ 8.13 (d, J = 8.3 Hz, 1H); Branched Isomer: δ 1.47 (dd, J = 6.7, 1.0 Hz, 3H) Both Isomers: δ 9.83 – 9.76 (m, 1H), 8.07 (d, J = 8.3 Hz, 1H), 7.90 – 7.85 (m, 1H), 7.77 – 7.72 (m, 1H), 7.58 – 7.46 (m, 2H), 7.45 – 7.38 (m, 1H), 7.32 (d, J = 7.0 Hz, 1H), 3.14 (t, J = 7.6 Hz, 2H), 2.55 (t, J = 7.2 Hz, 2H), 2.12 (p, J = 7.3 Hz, 2H).

4-(naphthalen-1-yl)butanol (6.21):**6.21**

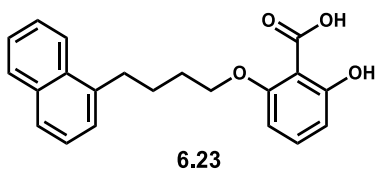
To a vial containing a stir bar was added 4-(naphthalen-1-yl)butanol **6.19** (0.321 g, 1.46 mmol, 1 equiv) and sodium borohydride (0.092 g, 2.19 mmol, 1.5 equiv). The vial was placed under nitrogen atmosphere and 5 mL MeOH was added via syringe. The reaction was stirred for 4 hours and then was quenched using 5 mL of water. Reaction mixture was then acidified using 1 mL of 2 M HCl and then the pH was adjusted to 3.00 by further dropwise addition. The mixture was then extracted using Et₂O (3x 15 mL), brine washed, and dried over Na₂SO₄. The resulting residue was then used in the following step without purification (0.312 g, 92%).

2,2-dimethyl-5-(4-(naphthalen-1-yl)butoxy)-4H-benzo[d][1,3]dioxin-4-one (6.22):**6.22**

To a round bottom flask with stir bar was added 4-(naphthalen-1-yl)butanol **6.21** (0.223 g, 1.11 mmol, 1 equiv), aryl acetonide **6.1** (0.281 g, 1.19 mmol, 1 equiv), and triphenylphosphine (0.438 g, 1.67 mmol, 1.5 equiv). The reaction vessel was sealed with a septum and pumped and backfilled 3x times with nitrogen. Dry THF (18 mL) was then added via syringe and the contents were then stirred in an ice bath for 10 minutes. Diethyl azodicarboxylate (40% wt. in toluene, 0.76 mL, 1.67 mmol, 1.5 equiv) was then added dropwise and the reaction vessel was removed from the ice bath and allowed to warm to rt. The reaction was then allowed to stir overnight. The volatiles were removed under reduced pressure and the residue was taken up in a minimal amount of 1:1 ethyl acetate: hexanes. This solution was loaded on a column and purified using column chromatography (1:9 EtOAc:Hexanes) to give a clear tacky residue (0.353 g, 85%). **¹H NMR** (300 MHz, Chloroform-d) δ 8.07 (d, *J* = 7.7 Hz, 1H), 7.86 (d, *J* = 7.4 Hz, 1H), 7.72

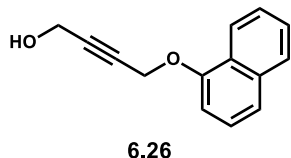
(d, $J = 7.7$ Hz, 1H), 7.58 – 7.33 (m, 5H), 6.58 (d, $J = 8.5$ Hz, 1H), 6.53 (d, $J = 8.2$ Hz, 1H), 4.19 – 4.04 (m, 2H), 3.18 (d, $J = 6.6$ Hz, 2H), 2.03 (p, $J = 3.6$ Hz, 4H), 1.71 (s, 6H). **¹³C NMR** (101 MHz, Chloroform-*d*) δ 162.7, 157.7, 157.1, 136.5, 134.6, 133.6, 132.7, 128.7, 127.2, 127.6, 126.4, 126.0, 124.3, 125.0, 108.8, 108.9, 105.7, 104.1, 69.1, 33.3, 29.3, 26.4, 25.6.

2-hydroxy-6-(4-(naphthalen-1-yl)butoxy)benzoic acid (6.23)



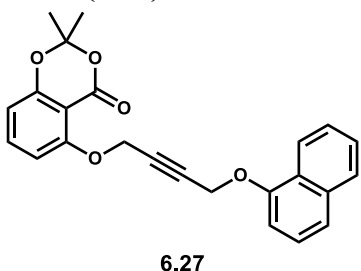
To a vial containing a stir bar was added 2,2-dimethyl-5-(4-(naphthalen-1-yl)butoxy)-4H-benzo[*d*][1,3]dioxin-4-one **6.22** (0.352 g, 0.942 mmol). The vial was placed under inert nitrogen atmosphere and dioxane (5 mL) and 5 M aq. KOH (2 mL) were added via syringe. The reaction mixture was then stirred vigorously for 24 h at 45 °C. The reaction was then diluted with EtOAc (5 mL) and acidified using 3 M HCl (2.4 mL) until a pH of 3.00. The acidified mixture was then extracted with Et₂O (3x 10 mL), organic layers dried over Na₂SO₄, and the volatiles removed under vacuum. The resulting residue was purified using column chromatography (3:7 EtOAc:Hexanes) to give the product as a white powder (0.267 g, 85%). **¹H NMR** (300 MHz, Chloroform-*d*) δ 12.17 (s, 1H), 11.56 (s, 1H), 8.01 (d, $J = 8.2$ Hz, 1H), 7.88 (dd, $J = 8.0, 1.6$ Hz, 1H), 7.75 (d, $J = 8.2$ Hz, 1H), 7.60 – 7.45 (m, 2H), 7.45 – 7.30 (m, 3H), 6.71 (dd, $J = 8.5, 1.0$ Hz, 1H), 6.44 (dd, $J = 8.5, 1.0$ Hz, 1H), 4.25 (t, $J = 6.0$ Hz, 2H), 3.19 (t, $J = 7.0$ Hz, 2H), 2.11 – 1.90 (m, 4H). **¹³C NMR** (101 MHz, Chloroform-*d*) δ 171.1, 162.0, 161.1, 135.4, 134.8, 134.4, 132.9, 127.9, 127.7, 127.7, 126.1, 126.1, 125.9, 124.8, 106.9, 105.9, 104.3, 64.9, 32.3, 29.7, 26.1. **HRMS** (ESI) m/z calcd for C₂₁H₂₁O₄ (M+H)⁺ 336.1362, found 336.1359.

4-(naphthalen-1-yloxy)but-2-yn-1-ol (6.26)



To a round bottom flask with stir bar was added 1-naphthol **6.25** (0.200 g, 1.38 mmol, 1 equiv), 1,4-butyne diol **6.24** (0.357 g, 4.14 mmol, 3 equiv), and triphenylphosphine (0.544 g, 2.07 mmol, 1.5 equiv). The reaction vessel was sealed with a septum and pumped and backfilled 3x times with nitrogen. Dry THF (20 mL) was then added via syringe and the contents were then stirred in an ice bath for 10 minutes. Diethyl azodicarboxylate (40% wt. in toluene, 0.94 mL, 2.07 mmol, 1.5 equiv) was then added dropwise and the reaction vessel was removed from the ice bath and allowed to warm to rt. The reaction was then allowed to stir overnight. The volatiles were removed under reduced pressure and the residue was taken up in a minimal amount of 1:1 ethyl acetate: hexanes. This solution was loaded on a column and purified using column chromatography (2:3 EtOAc:Hexanes) to give a white solid (0.194 g, 66%). **¹H NMR** (300 MHz, Chloroform-*d*) δ 8.34 – 8.24 (m, 1H), 7.84 – 7.78 (m, 1H), 7.53 – 7.47 (m, 3H), 7.39 (t, *J* = 7.9 Hz, 1H), 6.93 (d, *J* = 7.5 Hz, 1H), 4.95 (s, 2H), 4.38 – 4.29 (m, 2H).

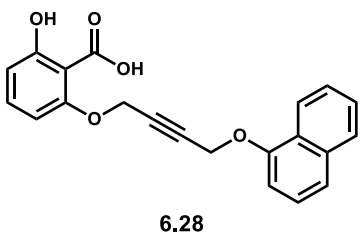
2,2-dimethyl-5-((4-(naphthalen-1-yloxy)but-2-yn-1-yl)oxy)-4H-benzo[d][1,3]dioxin-4-one (6.27):



To a round bottom flask with stir bar was added aryl acetonide **6.1** (0.165 g, 0.85 mmol, 1 equiv), 4-(naphthalen-1-yloxy)but-2-yn-1-ol **6.26** (0.180 g, 0.850 mmol, 1 equiv), and triphenylphosphine (0.333 g, 1.27 mmol, 1.5 equiv). The reaction vessel was sealed with a septum and pumped and backfilled 3x times with nitrogen. Dry THF (15 mL) was then added via syringe and the contents were then stirred

in an ice bath for 10 minutes. Diethyl azodicarboxylate (40% wt. in toluene, 0.55 mL, 1.27 mmol, 1.5 equiv) was then added dropwise and the reaction vessel was removed from the ice bath and allowed to warm to rt. The reaction was then allowed to stir overnight. The volatiles were removed under reduced pressure and the residue was taken up in a minimal amount of 1:1 ethyl acetate: hexanes. This solution was loaded on a column and purified using column chromatography (1:4 EtOAc:Hexanes). The resulting residue was triturated in hexanes to obtain to a white powder (0.231 g, 70%). **¹H NMR** (300 MHz, Chloroform-d) δ 8.29 – 8.19 (m, 1H), 7.84 – 7.75 (m, 1H), 7.55 – 7.42 (m, 3H), 7.31 (td, $J = 8.1, 4.7$ Hz, 2H), 6.87 (dd, $J = 7.7, 1.0$ Hz, 1H), 6.68 (dd, $J = 8.5, 0.9$ Hz, 1H), 6.57 (dd, $J = 8.3, 0.9$ Hz, 1H), 4.93 (t, $J = 1.7$ Hz, 2H), 4.90 (t, $J = 1.8$ Hz, 2H), 1.70 (s, 6H).

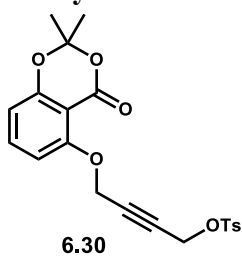
2-hydroxy-6-((4-(naphthalen-1-yloxy)but-2-yn-1-yl)oxy)benzoic acid (6.28):



To a vial containing a stir bar was added **6.27** (0.025 g, 0.060 mmol). The vial was placed under inert nitrogen atmosphere and dioxane (2 mL) and 5 M aq. KOH (1 mL) were added via syringe. The reaction mixture was then stirred vigorously for 24 h at 50 °C. The reaction was then diluted with EtOAc (5 mL) and acidified using 3 M HCl (2 mL) until a pH of 3.00. The acidified mixture was then extracted with Et₂O (3x 10 mL), organic layers dried over Na₂SO₄, and the volatiles removed under vacuum. The resulting residue was purified using column chromatography (2:3 EtOAc:Hexanes) to give the product as a sticky residue. Trituration in hexanes afforded a white powder (0.077 g, 41%). **¹H NMR** (300 MHz, Chloroform-d) δ 12.18 (s, 1H), 11.12 (s, 1H), 8.27 – 8.17 (m,

1H), 7.86 – 7.77 (m, 1H), 7.54 – 7.44 (m, 3H), 7.38 – 7.27 (m, 2H), 6.85 (dd, J = 7.7, 1.0 Hz, 1H), 6.74 (dd, J = 8.6, 0.9 Hz, 1H), 6.49 (dd, J = 8.4, 1.0 Hz, 1H), 4.97 (s, 4H).

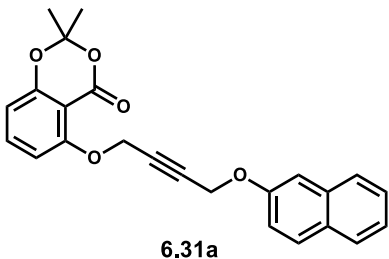
4-((2,2-dimethyl-4-oxo-4H-benzo[d][1,3]dioxin-5-yl)oxy)but-2-yn-1-yl 4-methylbenzenesulfonate (6.30):



To a round bottom flask with stir bar was added propargyl alcohol **6.29** (0.900 g, 3.43 mmol, 1 equiv), *p*-toluenesulfonate (1.31 g, 6.86 mmol, 2 equiv), and 4-dimethylaminopyridine (0.03 g, 0.27 mmol, 0.08 equiv). The reaction vessel was sealed with a septum and pumped

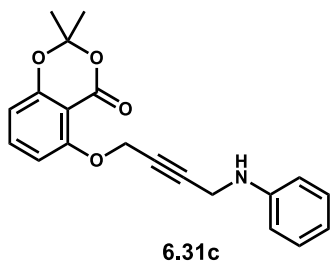
and backfilled 3x times with nitrogen. Dry DCM (25 mL) was added via syringe and the contents were then stirred in an ice bath for 10 minutes. Triethylamine (0.96 mL, 6.86 mmol, 2 equiv) was then added and the reaction was allowed to stir at 0 °C for 6 hours. The was then diluted using 5 mL of ether and 5 mL water. The aq. layer was acidified by dropwise addition of 3 M HCl and then extracted with ether (3x20 mL), brine washed, and dried over Na₂SO₄. The reaction was the purified using column chromatography (1:19 EtOAc:DCM) to obtain a white solid (1.12 g, 60%). **1H NMR** (400 MHz, Chloroform-d) δ 7.85 – 7.78 (m, 2H), 7.47 (t, J = 8.4 Hz, 1H), 7.40 – 7.33 (m, 2H), 6.65 (ddd, J = 8.3, 4.9, 0.9 Hz, 2H), 4.79 (t, J = 1.8 Hz, 2H), 4.75 (t, J = 1.8 Hz, 2H), 2.47 (s, 3H), 1.73 (s, 6H). **13C NMR** (126 MHz, Chloroform-d) δ 162.6, 157.3, 157.4, 143.2, 134.5, 133.6, 129.9, 127.3, 109.3, 109.2, 105.5, 104.4, 82.3, 77.7, 56.2, 55.6, 25.5, 21.5.

2,2-dimethyl-5-((4-(naphthalen-2-yloxy)but-2-yn-1-yl)oxy)-4H-benzo[d][1,3] dioxin-4-one (6.31a):



To a round bottom flask with stir bar was added propargyl tosylate **6.30** (0.250 g, 0.600 mmol, 1 equiv), 2-naphthol (0.104 g, 0.720 mmol, 1.2 equiv) and potassium carbonate (0.249 g, 1.80 mmol, 3 equiv). The reaction vessel was fitted with a reflux condenser and placed under nitrogen. Dry acetonitrile (15 mL) was added via syringe and the contents were then stirred at 80 °C for 24 hours. The volatiles were removed under vacuum and the residue taken in up in 10 mL of DCM and then extracted with water (3x5mL). The resulting solid was purified using column chromatography (3:7 EtOAc:Hex) to afford a white solid (0.210 g, 90%). **¹H NMR** (400 MHz, Chloroform-d) δ 7.76 (dd, $J = 11.6, 8.3$ Hz, 2H), 7.66 (d, $J = 8.2$ Hz, 1H), 7.44 (ddd, $J = 8.2, 6.8, 1.4$ Hz, 1H), 7.37 (ddd, $J = 8.1, 6.9, 1.3$ Hz, 1H), 7.23 – 7.12 (m, 3H), 6.66 (dd, $J = 8.5, 0.9$ Hz, 1H), 6.50 (dd, $J = 8.3, 0.9$ Hz, 1H), 4.90 (t, $J = 1.8$ Hz, 2H), 4.86 (t, $J = 1.8$ Hz, 2H), 1.70 (s, 6H). **¹³C NMR** (101 MHz, Chloroform-d) δ 159.2, 157.9, 155.4, 136.3, 134.4, 129.7, 129.4, 127.7, 127.1, 126.6, 124.1, 118.8, 110.2, 107.7, 107.4, 105.5, 103.9, 83.5, 81.9, 57.1, 56.0, 25.7. **HRMS** (ESI) m/z calcd for $C_{24}H_{21}O_5$ (M+H)⁺ 389.1384, found 389.1388.

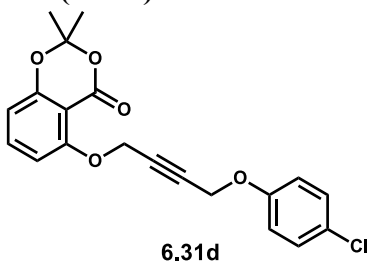
2,2-dimethyl-5-((4-(phenylamino)but-2-yn-1-yl)oxy)-4H-benzo[d][1,3] dioxin-4-one (6.31c):



To a round bottom flask with stir bar was added propargyl tosylate **6.30** (0.250 g, 0.600 mmol, 1 equiv), aniline (0.65 mL, 0.720 mmol, 1.2 equiv) and potassium carbonate (0.249 g, 1.80 mmol, 3 equiv). The reaction vessel was fitted with a reflux

condenser and placed under nitrogen. Dry acetonitrile (15 mL) was added via syringe and the contents were then stirred at 80 °C for 4 hours. The volatiles were removed under vacuum and the residue taken in up in 10 mL of DCM and then extracted with water (3x5mL). The resulting foamy solid was purified using column chromatography (gradient 1:4 to 1:1 EtOAc:Hex) to afford a clear foam (0.176 g, 65%). **¹H NMR** (400 MHz, Chloroform-d) δ 7.37 (td, $J = 8.4, 2.2$ Hz, 1H), 7.19 (dd, $J = 8.5, 7.3$ Hz, 2H), 6.78 (t, $J = 7.3$ Hz, 2H), 6.70 (d, $J = 8.6$ Hz, 1H), 6.65 (d, $J = 8.7$ Hz, 1H), 6.59 (d, $J = 8.3$ Hz, 1H), 4.83 (d, $J = 3.8$ Hz, 2H), 3.97 (t, $J = 1.9$ Hz, 2H), 1.71 (s, 6H). **¹³C NMR** (101 MHz, Chloroform-d) δ 159.4, 158.2, 157.9, 146.9, 136.3, 129.3, 118.7, 113.7, 110.1, 107.5, 105.4, 103.9, 85.9, 77.3, 57.3, 34.0, 25.7. **HRMS** (ESI) m/z calcd for C₂₀H₂₀NO₄ (M+H)⁺ 338.1387, found 338.1385.

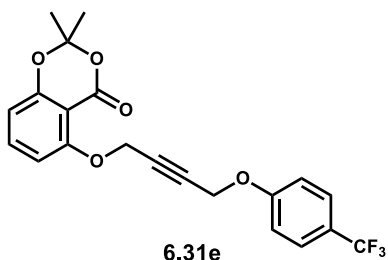
2,2-dimethyl-5-((4-(4-chlorophenoxy)but-2-yn-1-yl)oxy)-4H-benzo[d][1,3]dioxin-4-one (6.31d):



To a round bottom flask with stir bar was added propargyl tosylate **6.30** (0.250 g, 0.600 mmol, 1 equiv), *p*-chlorophenol (0.093 g, 0.720 mmol, 1.2 equiv) and potassium carbonate (0.199 g, 0.144 mmol, 3 equiv). The reaction vessel was fitted with a reflux condenser and placed under nitrogen. Dry acetonitrile (10 mL) was added via syringe and the contents were then stirred at 80 °C for 18 hours. The volatiles were removed under vacuum and the residue taken in up in 10 mL of DCM and then extracted with water (3x5mL). The resulting residue was purified using

column chromatography (3:7 EtOAc:Hex) to afford a white solid (0.220 g, 98%) **¹H NMR** (400 MHz, Chloroform-*d*) δ 7.36 (t, *J* = 8.4 Hz, 1H), 7.24 – 7.16 (m, 2H), 6.85 (d, *J* = 8.8 Hz, 2H), 6.66 (d, *J* = 8.5 Hz, 1H), 6.61 (d, *J* = 8.3 Hz, 1H), 4.89 (s, 2H), 4.71 (s, 2H), 1.72 (s, 6H). **¹³C NMR** (101 MHz, Chloroform-*d*) δ 159.1, 157.8, 156.0, 136.2, 129.3, 126.5, 116.3, 110.2, 107.3, 105.4, 83.0, 82.0, 56.9, 56.2, 25.6.

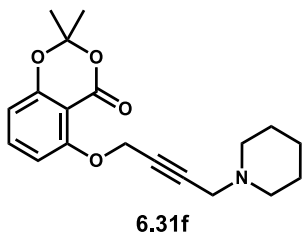
2,2-dimethyl-5-((4-(4-(trifluoromethyl)phenoxy)but-2-yn-1-yl)oxy)-4H-benzo[*d*][1,3]dioxin-4-one (6.31e):



To a round bottom flask with stir bar was added propargyl tosylate **6.30** (0.250 g, 0.600 mmol, 1 equiv), *p*-trifluoromethylphenol (0.116 g, 0.720 mmol, 1.2 equiv) and potassium carbonate (0.249 g, 1.80 mmol, 3 equiv).

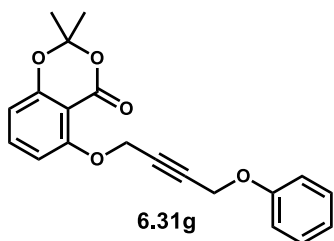
The reaction vessel was fitted with a reflux condenser and placed under nitrogen. Dry acetonitrile (15 mL) was added via syringe and the contents were then stirred at 80 °C for 6 hours. The volatiles were removed under vacuum and the residue taken in up in 10 mL of DCM and then extracted with water (3x5mL). The resulting residue was purified using column chromatography (3:7 EtOAc:Hex) to afford a white solid (0.230 g, 94%). **¹H NMR** (400 MHz, Chloroform-*d*) δ 7.51 (d, *J* = 8.7 Hz, 2H), 7.33 (t, *J* = 8.4 Hz, 1H), 6.98 (d, *J* = 8.7 Hz, 2H), 6.64 (dd, *J* = 8.5, 0.9 Hz, 1H), 6.59 (dd, *J* = 8.3, 0.9 Hz, 1H), 4.89 (t, *J* = 1.8 Hz, 2H), 4.78 (t, *J* = 1.8 Hz, 2H), 1.71 (s, 6H). **¹³C NMR** (101 MHz, Chloroform-*d*) δ 159.9, 159.2, 158.1, 158.0, 136.3, 127.0, 127.0, 124.1 (q, *J* = 268 Hz), 123.9 (q, *J* = 32 Hz), 115.1, 110.4, 107.4, 105.5, 82.7, 82.4, 57.0, 56.0, 25.7.

2,2-dimethyl-5-((4-(piperidin-1-yl)but-2-yn-1-yl)oxy)-4H-benzo[d][1,3]dioxin-4-one (6.31f):



To a round bottom flask with stir bar was added propargyl tosylate **6.30** (0.200 g, 0.480 mmol, 1 equiv) and potassium carbonate (0.199 g, 1.44 mmol, 3 equiv). The reaction vessel was fitted with a reflux condenser and placed under nitrogen. Dry acetonitrile (10 mL) was added via syringe followed by piperidine (0.56 mL, 0.58 mmol, 1.2 equiv) and the contents were then stirred at 80 °C for 3 hours. The volatiles were removed under vacuum and the residue taken in up in 10 mL of DCM and then extracted with water (3x5mL). The resulting foamy solid was purified using column chromatography (95:4:1 EtOAc:MeOH:NH₄OH) to afford a white foam (0.097 g, 61%) **1H NMR** (400 MHz, Chloroform-d) δ 7.46 (t, J = 8.4 Hz, 1H), 6.83 (dd, J = 8.6, 0.9 Hz, 1H), 6.60 (dd, J = 8.2, 0.9 Hz, 1H), 4.91 (t, J = 1.9 Hz, 2H), 3.29 (t, J = 1.9 Hz, 2H), 2.47 – 2.42 (m, 4H), 1.72 (s, 6H), 1.59 (p, J = 5.7 Hz, 4H), 1.44 – 1.38 (m, 2H). **13C NMR** (126 MHz, Chloroform-d) δ 161.9, 151.1, 149.7, 134.6, 108.8, 108.8, 105.9, 104.4, 83.2, 78.8, 56.1, 53.4, 43.9, 25.9, 25.6, 24.2. **HRMS** (ESI) *m/z* calcd for C₁₉H₂₄NO₄ (M+H)⁺ 330.1700, found 330.1704.

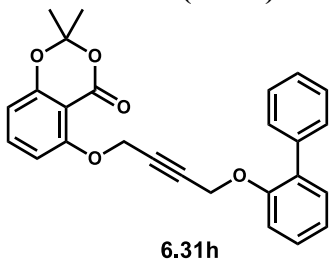
2,2-dimethyl-5-((4-phenoxybut-2-yn-1-yl)oxy)-4H-benzo[d][1,3]dioxin-4-one (6.31g):



To a round bottom flask with stir bar was added propargyl tosylate **6.30** (0.250 g, 0.600 mmol, 1 equiv), phenol (0.068 g, 0.720 mmol, 1.2 equiv) and potassium carbonate (0.199 g, 0.144 mmol, 3 equiv). The reaction vessel was fitted with a reflux condenser and placed under nitrogen. Dry acetonitrile (10 mL) was added via syringe and the contents were then stirred at 80 °C for 3 hours. The volatiles were removed

under vacuum and the residue taken in up in 10 mL of DCM and then extracted with water (3x5mL). The resulting solid was purified using column chromatography (3:7 EtOAc:Hex) to afford a white foam (0.097 g, 61%) **1H NMR** (400 MHz, Chloroform-d) δ 7.37 (t, J = 8.4 Hz, 1H), 7.27 (t, J = 7.8 Hz, 2H), 6.98 (d, J = 7.7 Hz, 1H), 6.93 (d, J = 8.9 Hz, 2H), 6.70 (d, J = 8.5 Hz, 1H), 6.60 (d, J = 8.5 Hz, 1H), 4.90 – 4.88 (m, 2H), 4.74 – 4.71 (m, 2H), 1.71 (s, 6H). **13C NMR** (126 MHz, Chloroform-d) δ 161.9, 157.7, 157.1, 157.1, 134.5, 129.6, 121.4, 115.2, 108.9, 108.8, 105.9, 104.4, 79.6, 79.6, 56.2, 54.9, 25.8. **HRMS** (ESI) m/z calcd for C₂₀H₁₉O₅ (M+H)⁺ 339.1227, found 330.1224.

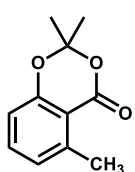
2,2-dimethyl-5-((4-([1,1'-biphenyl]-2-yloxy)but-2-yn-1-yl)oxy)-4H-benzo[d][1,3]dioxin-4-one (6.31h):



To a round bottom flask with stir bar was added propargyl tosylate **6.30** (0.250 g, 0.600 mmol, 1 equiv), [1,1'-biphenyl]-2-ol (0.122 g, 0.720 mmol, 1.2 equiv) and potassium carbonate (0.249 g, 1.80 mmol, 3 equiv). The reaction vessel was fitted with a reflux condenser and placed under nitrogen. Dry acetonitrile (10 mL) was added via syringe and the contents were then stirred at 80 °C for 4 hours. The volatiles were removed under vacuum and the residue taken in up in 10 mL of DCM and then extracted with water (3x5mL). The resulting solid was purified using column chromatography (3:7 EtOAc:Hex) to afford a clear residue (0.195 g, 95%) **1H NMR** (400 MHz, Chloroform-d) δ 7.51 (dd, J = 8.3, 1.3 Hz, 2H), 7.44 – 7.38 (m, 2H), 7.36 – 7.32 (m, 3H), 7.30 – 7.24 (m, 1H), 7.11 – 7.04 (m, 2H), 6.68 (dd, J = 8.6, 0.9 Hz, 1H), 6.59 (dd, J = 8.3, 0.9 Hz, 1H), 4.87 (t, J = 1.8 Hz, 2H), 4.70 (t, J = 1.8 Hz, 2H), 1.71 (s, 6H). **13C NMR** (101 MHz, Chloroform-d) δ 161.8, 157.0, 156.6, 154.7, 136.2, 134.5, 131.3, 129.6, 129.1, 129.0, 128.2, 127.8, 122.9,

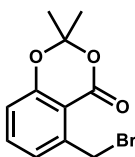
116.4, 109.3, 109.2, 107.7, 104.4, 79.6, 79.5, 56.5, 56.3, 25.6. **HRMS** (ESI) m/z calcd for $C_{26}H_{23}O_5$ (M+H)⁺ 415.1540, found 415.1541.

2,2,5-trimethyl-4H-benzo[d][1,3]dioxin-4-one (6.32):



6.32

To a round bottom flask containing 6-methyl-2-hydroxybenzoic acid, (6.00 g, 31 mmol, 1 equiv) and 4-dimethylaminopyridine (0.16 g, 1.24 mmol, 0.05 equiv) was added 30 mL of DME. The resulting solution was cooled to 0 °C before the addition of acetone (3.44 mL, 38 mmol, 1.2 equiv) followed by thionyl chloride (2.54 mL, 38.44, 1.2 equiv). The reaction mixture was stirred at 0°C for 1 hour and then at RT for 15 hours. The resulting red solution was neutralized using 25 mL aq. sodium bicarbonate and extracted using three 30 mL portions of diethyl ether. The combined organic layers were washed with brine, dried over $MgSO_4$, and volatiles removed under reduced pressure to afford a crude orange solid. Purification using silica gel chromatography with 1:4 ethyl acetate:hexanes resulted in an off-white solid (6.72 g, 82%) **¹H NMR** (500 MHz, Chloroform- d) δ 7.39 (t, J = 7.9 Hz, 1H), 6.93 (dt, J = 7.6, 0.9 Hz, 1H), 6.81 (d, J = 7.6 Hz, 1H), 2.69 (s, 3H), 1.71 (s, 6H).



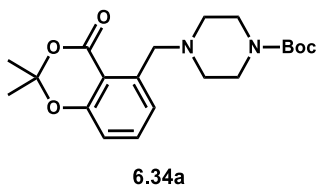
6.33

5-(bromomethyl)-2,2-dimethyl-4H-benzo[d][1,3]dioxin-4-one (6.33):

To a round bottom flask containing 6-methyl acetone 6.32, (0.500 g, 2.60 mmol, 1 equiv) and *N*-bromosuccinimide (0.532 g, 2.99 mmol, 1.15 equiv) was added 12 mL of DCM. The solution was stirred for 3 h inside a UV photoreactor. The reaction mixture was then cooled in an ice bath and the precipitated solids were collected via filtration. The filtrate was reduced under vacuum and purified using silica gel chromatography using a gradient from 2:98 to 10:90 ethyl acetate:hexanes

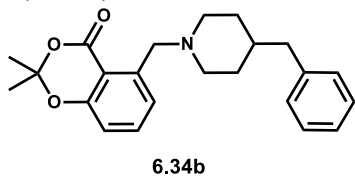
resulting in a white solid (0.46 g, 65%). **¹H NMR** (500 MHz, Chloroform-*d*) δ 7.49 (t, *J* = 8.0 Hz, 1H), 7.17 (dd, *J* = 7.6, 1.2 Hz, 1H), 6.95 (dd, *J* = 8.3, 1.1 Hz, 1H), 5.06 (s, 2H), 1.74 (s, 6H).

***tert*-butyl 4-((2,2-dimethyl-4-oxo-4H-benzo[d][1,3]dioxin-5-yl)methyl)piperazine-1-carboxylate (6.34a):**



To a round bottom flask with a stir bar was added benzylic bromide **6.33**, (0.557 g, 2.05 mmol, 1 equiv) and *N*-Boc piperazine (0.383 g, 2.05 mmol, 1 equiv). The flask was then sealed and placed under nitrogen. 16 mL of DCM was then added via syringe followed by triethylamine (0.63 mL, 4.52 mmol, 2.2 equiv). The reaction mixture was then stirred for 18 hours at rt. The volatiles were removed under vacuum and the resulting oil was purified using silica gel chromatography using a gradient from 15:85 to 40:60 ethyl acetate:hexanes resulting in a sticky residue. The residue was triturated in hexanes to afford a white powder (0.67 g, 87%). **¹H NMR** (400 MHz, Chloroform-*d*) δ 7.48 (t, *J* = 7.9 Hz, 1H), 7.35 (dd, *J* = 7.7, 1.1 Hz, 1H), 6.88 (dd, *J* = 8.1, 1.2 Hz, 1H), 4.01 (s, 2H), 3.46 – 3.42 (m, 4H), 2.52 – 2.45 (m, 4H), 1.71 (s, 6H), 1.47 (s, 9H). **HRMS** (ESI) *m/z* calcd for C₂₀H₂₉N₂O₅ (M+H)⁺ 377.2071, found 377.2067.

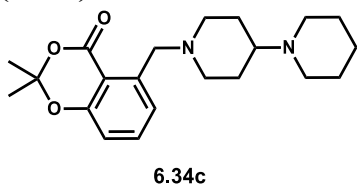
5-((4-benzylpiperidin-1-yl)methyl)-2,2-dimethyl-4H-benzo[d][1,3]dioxin-4-one (6.34b):



To a round bottom flask with a stir bar was added benzylic bromide **6.33**, (0.200 g, 0.737 mmol, 1 equiv) and 4-benzylpiperidine (0.129 g, 0.737 mmol, 1 equiv). The flask was then sealed and placed under nitrogen. 10 mL of DCM was then added via syringe

followed by triethylamine (0.26 mL, 1.62 mmol, 2.2 equiv). The reaction mixture was then stirred for 24 hours at rt. The volatiles were removed under vacuum and the resulting oil was purified using silica gel chromatography (95:4:1 EtOAc:MeOH:NH₄OH) resulting in a sticky residue. The residue was triturated in hexanes to afford a white powder (0.22 g, 77%). **¹H NMR** (500 MHz, Chloroform-d) δ 7.47 – 7.41 (m, 1H), 7.38 (d, J = 7.7 Hz, 1H), 7.26 – 7.23 (m, 2H), 7.18 – 7.09 (m, 3H), 6.82 (d, J = 8.1 Hz, 1H), 3.94 (s, 2H), 2.86 (d, J = 11.2 Hz, 4H), 2.53 (d, J = 7.0 Hz, 4H), 2.03 (d, J = 1.0 Hz, 6H), 1.64 – 1.56 (m, 2H), 1.56 – 1.49 (m, 1H). **HRMS** (ESI) *m/z* calcd for C₂₃H₂₈NO₃ (M+H)⁺ 366.2064, found 366.2061.

5-([1,4'-bipiperidin]-1'-ylmethyl)-2,2-dimethyl-4H-benzo[d][1,3]dioxin-4-one (6.34c):



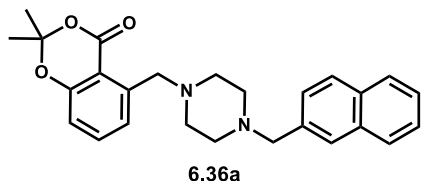
To a round bottom flask with a stir bar was added benzylic bromide **6.33**, (0.200 g, 0.737 mmol, 1 equiv) and 1,4'-bipiperidine (0.124 g, 0.737 mmol, 1 equiv). The flask was

then sealed and placed under nitrogen. 10 mL of DCM was then added via syringe followed by triethylamine (0.26 mL, 1.62 mmol, 2.2 equiv). The reaction mixture was then stirred for 24 hours at rt. The volatiles were removed under vacuum and the resulting oil was purified using silica gel chromatography (95:4:1 EtOAc:MeOH:NH₄OH) resulting in a sticky residue. The residue was triturated in hexanes to afford a white powder (0.21 g, 82%). **¹H NMR** (400 MHz, Chloroform-d) δ 7.49 (t, J = 7.9 Hz, 1H), 7.40 (d, J = 7.7 Hz, 1H), 6.86 (d, J = 8.1 Hz, 1H), 3.98 (s, 2H), 3.02 – 2.94 (m, 2H), 2.53 (t, J = 5.4 Hz, 4H), 2.26 (ddt, J = 11.6, 7.6, 3.8 Hz, 1H), 2.12 (td, J = 11.7, 2.2 Hz, 2H),

1.85 – 1.76 (m, 2H), 1.72 (d, J = 0.8 Hz, 6H), 1.64 – 1.56 (m, 6H), 1.50 – 1.41 (m, 2H).

HRMS (ESI) m/z calcd for $C_{21}H_{31}N_2O_3$ (M+H)⁺ 359.2329, found 359.2330.

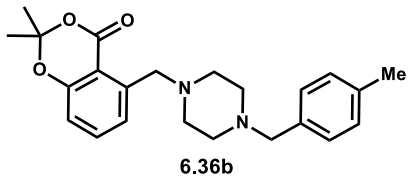
2,2-dimethyl-5-((4-(naphthalen-2-ylmethyl)piperazin-1-yl)methyl)-4H-benzo[d][1,3]dioxin-4-one (6.36a):



To a round bottom flask with a stir bar was added 2-naphthaldehyde (0.072 g, 0.45 mmol, 1 equiv) and then placed under nitrogen atmosphere. DCE (4 mL) and

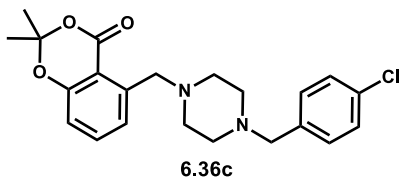
deprotected piperazine **6.35** (1 mL 0.45 M in DCE, 0.45 mmol, 1 equiv) were then added via syringe. The septa was quickly removed to allow the addition of sodium triacetoxyborohydride (0.153 g, 0.720 mmol, 1.6 equiv) and then was resealed. Acetic acid (0.025 mL, 0.45 mmol, 1 equiv) was then added via syringe and the reaction was stirred for 2.5 hours at rt. The volatiles were then removed under vacuum and the resulting residue was purified using silica gel chromatography (97:2:1 EtOAc:MeOH:NH₄OH) resulting in a sticky residue (0.096 g, 51%). **¹H NMR** (400 MHz, Chloroform-d) δ 7.86 – 7.77 (m, 3H), 7.75 (s, 1H), 7.54 – 7.42 (m, 4H), 7.37 (d, J = 7.7 Hz, 1H), 6.85 (d, J = 8.1 Hz, 1H), 4.02 (s, 2H), 3.69 (s, 2H), 2.62 – 2.53 (m, 8H), 1.71 (s, 6H). **¹³C NMR** (101 MHz, Chloroform-d) δ 160.4, 157.2, 144.5, 136.0, 135.2, 133.5, 132.9, 128.0, 127.8, 127.8, 127.7, 126.1, 125.7, 123.8, 115.9, 112.5, 105.4, 63.4, 59.7, 53.6, 53.5, 25.8. **HRMS** (ESI) m/z calcd for $C_{26}H_{29}N_2O_3$ (M+H)⁺ 417.2173, found 417.2179.

2,2-dimethyl-5-((4-(4-methylbenzyl)piperazin-1-yl)methyl)-4H-benzo[d][1,3]dioxin-4-one (6.36b):



To a round bottom flask with a stir bar was added *p*-tolualdehyde (0.080 g, 0.347 mmol, 1.2 equiv) and deprotected piperazine **6.35** (0.080g, 0.29 mmol, 1 equiv) and then placed under nitrogen atmosphere. DCE (4 mL) were then added via syringe. The septa was quickly removed to allow the addition of sodium triacetoxyborohydride (0.098 g, 0.463 mmol, 1.6 equiv) and then was resealed. Acetic acid (0.017 mL, 0.29 mmol, 1 equiv) was then added via syringe and the reaction was stirred for 3 hours at rt. The volatiles were then removed under vacuum and the resulting residue was purified using silica gel chromatography (90:10 EtOAc:MeOH) resulting in a sticky residue (0.084 g, 76%). **¹H NMR** (400 MHz, Chloroform-*d*) δ 7.46 (td, *J* = 8.1, 3.0 Hz, 1H), 7.34 (d, *J* = 7.8 Hz, 1H), 7.21 (dd, *J* = 7.8, 2.5 Hz, 2H), 7.13 (dd, *J* = 7.8, 2.5 Hz, 2H), 6.85 (dt, *J* = 8.9, 1.9 Hz, 1H), 4.01 (s, 2H), 3.52 (s, 2H), 2.61 – 2.57 (m, 4H), 2.55 – 2.50 (m, 4H), 2.34 (s, 3H), 1.70 (s, 6H). **¹³C NMR** (101 MHz, Chloroform-*d*) δ 160.2, 157.1, 143.8, 136.9, 135.1, 134.0, 129.5, 129.0, 123.8, 116.0, 112.4, 105.2, 62.4, 59.4, 52.8, 52.8, 25.6, 21.1. **HRMS** (ESI) *m/z* calcd for C₂₃H₂₉N₂O₃ (M+H)⁺ 381.2173, found 381.2172.

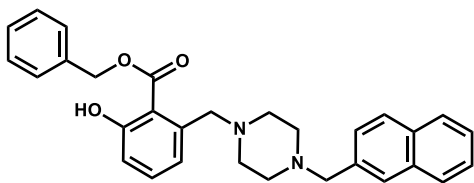
2,2-dimethyl-5-((4-(4-chlorobenzyl)piperazin-1-yl)methyl)-4H-benzo[d][1,3]dioxin-4-one (6.36c):



To a round bottom flask with a stir bar was added *p*-chlorobenzaldehyde (0.041 mL, 0.347 mmol, 1.2 equiv) and deprotected piperazine **6.35** (0.080 g, 0.29 mmol, 1 equiv) and then placed under nitrogen atmosphere. DCE (4 mL) were then added via syringe. The septa was quickly removed to allow the addition of sodium

triacetoxyborohydride (0.098 g, 0.463 mmol, 1.6 equiv) and then was resealed. Acetic acid (0.017 mL, 0.29 mmol, 1 equiv) was then added via syringe and the reaction was stirred for 16 hours at rt. The volatiles were then removed under vacuum and the resulting residue was purified using silica gel chromatography (90:10 EtOAc:MeOH) resulting in a sticky residue (0.099 g, 85%). **¹H NMR** (400 MHz, Chloroform-d) δ 7.48 (d, J = 7.9 Hz, 1H), 7.37 – 7.22 (m, 5H), 6.86 (dt, J = 8.1, 1.3 Hz, 1H), 4.02 (s, 2H), 3.50 (s, 2H), 2.61 – 2.56 (m, 4H), 2.54 – 2.46 (m, 4H), 1.70 (s, 6H). **¹³C NMR** (101 MHz, Chloroform-d) δ 160.3, 157.1, 143.5, 139.8, 135.9, 135.2, 133.0, 130.8, 128.6, 128.5, 128.3, 124.0, 116.1, 112.5, 105.3, 64.2, 61.9, 59.3, 52.8, 25.7. **HRMS** (ESI) m/z calcd for C₂₂H₂₆ClN₂O₃ (M+H)⁺ 401.1626, found 401.1621.

benzyl 2-hydroxy-6-((4-(naphthalen-2-ylmethyl)piperazin-1-yl)methyl)benzoate (6.37a):

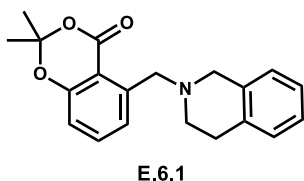


6.37a

To a round bottom flask with a stir bar was added hexane-washed sodium hydride (0.027 g, 1.55 mmol, 5 equiv) and then was sealed and placed under nitrogen and cooled with an ice bath. THF (3 mL), and benzyl alcohol (0.047 mL, 0.462 mmol, 2 equiv) were then added via syringe. This mixture was allowed to react for 30 min then naphthyl derivative **6.36a** (0.096 g, 0.231 mmol, 1 equiv) dissolved in THF (1 mL) was slowly added via syringe over 5 minutes. After 20 min., the reaction was quenched using sat'd ammonium chloride until the mixture was neutral by pH paper. The mixture was then extracted using ether, brine washed, and dried over sodium sulfate. The volatiles were then removed under vacuum and the resulting residue was purified using silica gel chromatography (70:30 EtOAc:Hex) resulting in a

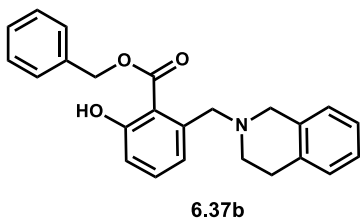
sticky residue (0.111 g, 64%). **¹H NMR** (500 MHz, Chloroform-d) δ 10.30 (s, 1H), 7.81 (q, $J = 7.8$ Hz, 2H), 7.72 (s, 1H), 7.50 – 7.41 (m, 5H), 7.37 (d, $J = 14.2$ Hz, 3H), 7.33 – 7.28 (m, 2H), 6.94 – 6.88 (m, 2H), 5.38 (s, 2H), 3.67 (s, 2H), 3.64 (s, 2H), 2.47 – 2.37 (m, 4H), 2.31 – 2.27 (m, 4H).

5-((3,4-dihydroisoquinolin-2(1H)-yl)methyl)-2,2-dimethyl-4H-benzo[d][1,3]dioxin-4-one (E.6.1):



To a round bottom flask with a stir bar was added benzylic bromide **6.33**, (0.250 g, 0.922 mmol, 1 equiv) and tetrahydroisoquinoline (0.141 mL, 1.11 mmol, 1.1 equiv). The flask was then sealed and placed under nitrogen. 8 mL of DCM was then added via syringe followed by triethylamine (0.28 mL, 2.02 mmol, 2.2 equiv). The reaction mixture was then stirred for 24 hours at rt. The volatiles were removed under vacuum and the resulting oil was purified using silica gel chromatography (95:4:1 EtOAc:MeOH:NH₄OH) resulting in a sticky residue. The residue was triturated in hexanes to afford a white powder (0.21 g, 82%). **¹H NMR** (400 MHz, Chloroform-d) δ 7.49 (d, $J = 4.8$ Hz, 2H), 7.14 (d, $J = 11.0$ Hz, 1H), 7.05 – 6.98 (m, 1H), 6.88 (t, $J = 4.7$ Hz, 1H), 4.20 (s, 2H), 3.76 (s, 2H), 2.94 (t, $J = 5.9$ Hz, 2H), 2.83 (t, $J = 5.9$ Hz, 2H), 1.72 (s, 6H).

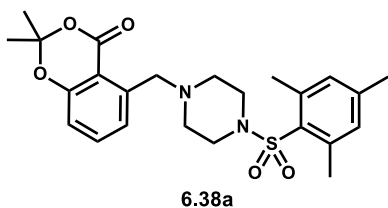
benzyl 2-((3,4-dihydroisoquinolin-2(1H)-yl)methyl)-6-hydroxybenzoate (6.37b):



To a round bottom flask with a stir bar was added hexane-washed sodium hydride (0.085 g, 3.55 mmol, 5 equiv) and then was sealed and placed under nitrogen and cooled with an ice bath. THF (15 mL), and benzyl alcohol (1.43 mL, 1.42 mmol, 2 equiv) were then added via syringe. This mixture was allowed to react for 30

min then tetrahydroisoquinoline derivative **E.6.1** (0.096 g, 0.231 mmol, 1 equiv) dissolved in THF (1 mL) was slowly added via syringe over 5 minutes. After 2 hours., the reaction was quenched using sat'd ammonium chloride until the mixture was neutral by pH paper. The mixture was then extracted using ether, brine washed, and dried over sodium sulfate. The volatiles were then removed under vacuum and the resulting residue was purified using silica gel chromatography (85:10:5 Hex:DCM:MeOH) resulting in a sticky residue (0.170 g, 64%). **¹H NMR** (400 MHz, Chloroform-d) δ 10.41 (s, 1H), 7.45 – 7.39 (m, 2H), 7.39 – 7.34 (m, 4H), 7.16 – 7.05 (m, 4H), 7.01 (d, J = 7.5 Hz, 1H), 6.95 (d, J = 8.3 Hz, 1H), 6.90 (d, J = 7.1 Hz, 1H), 5.34 (s, 2H), 3.84 (s, 2H), 3.45 (s, 2H), 2.77 (t, J = 5.9 Hz, 2H), 2.53 (t, J = 5.9 Hz, 2H).

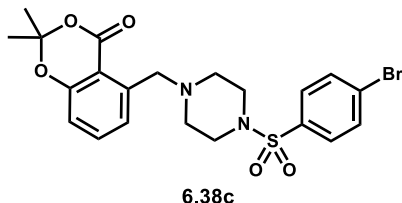
5-((4-(mesitylsulfonyl)piperazin-1-yl)methyl)-2,2-dimethyl-4H-benzo[d][1,3]dioxin-4-one (6.38a):



To a round bottom flask with a stir bar was added benzyl piperazine **6.35**, (0.050 g, 0.180 mmol, 1 equiv) and mesitylenesulfonyl chloride (0.047 g, 0.217 mmol, 1.2 equiv). The flask was then sealed and placed under nitrogen. 2 mL of DCM was then added via syringe followed by triethylamine (0.28 mL, 2.02 mmol, 2.2 equiv). The reaction mixture was then stirred for 7 hours at rt. The volatiles were removed under vacuum and the resulting residue was purified using silica gel chromatography (1:4 to 1:1 EtOAc:Hex) resulting in a sticky residue. The residue was triturated in hexanes to afford a white powder (0.054 g, 65%). **¹H NMR** (400 MHz, Chloroform-d) δ 7.47 (t, J = 7.9 Hz, 1H), 7.30 (d, J = 7.8 Hz, 1H), 6.96 (s, 2H), 6.88 (d, J

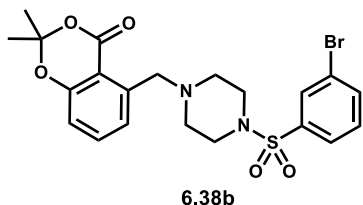
= 8.2 Hz, 1H), 4.00 (s, 2H), 3.19 (t, J = 5.0 Hz, 4H), 2.63 (s, 6H), 2.55 (t, J = 4.9 Hz, 4H), 2.31 (s, 3H), 1.70 (s, 6H).

5-((4-((4-bromophenyl)sulfonyl)piperazin-1-yl)methyl)-2,2-dimethyl-4H-benzo[d][1,3]dioxin-4-one (6.38c):



To a round bottom flask with a stir bar was added benzyl piperazine **6.35**, (0.050 g, 0.180 mmol, 1 equiv) and *p*-bromobenzenesulfonyl chloride (0.055 g, 0.217 mmol, 1.2 equiv). The flask was then sealed and placed under nitrogen. 2 mL of DCM was then added via syringe followed by triethylamine (0.28 mL, 2.02 mmol, 2.2 equiv). The reaction mixture was then stirred for 7 hours at rt. The volatiles were removed under vacuum and the resulting residue was purified using silica gel chromatography (1:4 to 1:1 EtOAc:Hex) resulting in a sticky residue. The residue was triturated in hexanes to afford a white powder (0.050 g, 56%). **¹H NMR** (400 MHz, Chloroform-*d*) δ 7.73 – 7.66 (m, 2H), 7.66 – 7.57 (m, 2H), 7.43 (t, J = 7.9 Hz, 1H), 7.18 (dd, J = 7.7, 1.1 Hz, 1H), 6.86 (dd, J = 8.2, 1.2 Hz, 1H), 3.99 (s, 2H), 3.07 – 3.02 (m, 4H), 2.63 (t, J = 4.9 Hz, 4H), 1.68 (s, 6H). **¹³C NMR** (101 MHz, Chloroform-*d*) δ 160.1, 157.3, 143.0, 135.1, 134.8, 132.4, 129.3, 127.9, 123.7, 116.4, 112.3, 105.3, 59.2, 52.2, 46.2, 25.6.

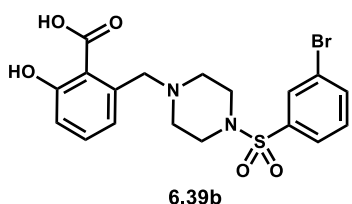
5-((4-((3-bromophenyl)sulfonyl)piperazin-1-yl)methyl)-2,2-dimethyl-4H-benzo[d][1,3]dioxin-4-one (6.38b):



To a round bottom flask with a stir bar was added benzyl piperazine **6.35**, (0.050 g, 0.180 mmol, 1 equiv) and *m*-bromobenzenesulfonyl chloride (0.031 mL, 0.217 mmol, 1.2 equiv). The flask was then sealed and placed under nitrogen.

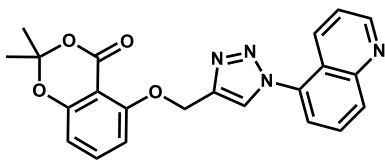
2 mL of DCM was then added via syringe followed by triethylamine (0.28 mL, 2.02 mmol, 2.2 equiv). The reaction mixture was then stirred for 7 hours at rt. The volatiles were removed under vacuum and the resulting residue was purified using silica gel chromatography (1:4 to 1:1 EtOAc:Hex) resulting in a sticky residue. The residue was triturated in hexanes to afford a white powder (0.043 g, 48%). **¹H NMR** (400 MHz, Chloroform-d) δ 7.90 (t, J = 1.8 Hz, 1H), 7.75 (dd, J = 8.0, 2.0 Hz, 1H), 7.69 (dd, J = 7.8, 1.7 Hz, 1H), 7.43 (t, J = 7.9 Hz, 2H), 7.21 – 7.14 (m, 1H), 6.86 (dd, J = 8.2, 1.2 Hz, 1H), 3.99 (s, 2H), 3.06 (t, J = 4.7 Hz, 4H), 2.63 (t, J = 4.9 Hz, 4H), 1.68 (s, 6H).

2-((4-((3-bromophenyl)sulfonyl)piperazin-1-yl)methyl)-6-hydroxybenzoic acid (6.39b):



To a stirring solution of KOTMS (0.076 g, 0.593 mmol, 7 equiv) in THF (2 mL) inside a round bottom flask was added **6.38b**, (0.042 g, 0.084 mmol, 1 equiv). The reaction mixture was then stirred for 30 minutes at 60 °C. 2 M acetic acid (0.29 mL) was then added drop wise to neutralize remaining KOTMS. The resulting precipitate was collected via vacuum filtration to give a white solid (0.027 g, 71%). **¹H NMR** (400 MHz, Chloroform-d) δ 7.88 (s, 1H), 7.81 (d, J = 8.0 Hz, 1H), 7.66 (d, J = 7.8 Hz, 1H), 7.47 (t, J = 7.8 Hz, 1H), 7.33 (t, J = 7.9 Hz, 1H), 7.18 (s, 2H), 7.06 (d, J = 8.4 Hz, 1H), 6.67 (d, J = 7.4 Hz, 1H), 3.86 (s, 4H), 3.14 (d, J = 11.7 Hz, 2H), 2.71 (s, 2H), 2.58 (t, J = 12.1 Hz, 2H). **¹³C NMR** (101 MHz, DMSO-d₆) δ 173.2, 163.6, 137.1, 137.0, 132.4, 132.1, 130.2, 127.2, 123.1, 122.3, 119.2, 119.0, 59.9, 49.4, 44.1.

2,2-dimethyl-5-((1-(quinolin-5-yl)-1H-1,2,3-triazol-4-yl)methoxy)-4H-benzo[d][1,3]dioxin-4-one (6.51a):

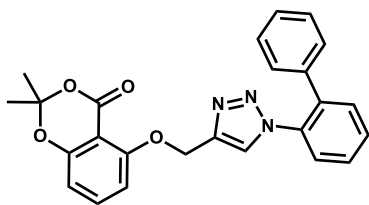


6.51a

According to general procedure A, alkyne **6.50** (0.180g, 0.775 mmol, 1 equiv), azide **6.42** (0.260 g, 1.16 mmol, 1.5 equiv), sodium ascorbate (0.016 g, 0.085 mmol, 0.1 equiv), and $\text{CuSO}_4 \cdot 5\text{H}_2\text{O}$ (0.007 g, 0.031 mmol, 0.04 equiv) were

reacted in a round bottom flask. Purification using column chromatography (96:4 DCM:MeOH) resulted in a yellow solid (0.290 g, 88%). **¹H NMR** (400 MHz, Chloroform-*d*) δ 9.03 (dd, *J* = 4.2, 1.7 Hz, 1H), 8.39 (s, 1H), 8.32 (dt, *J* = 8.5, 1.0 Hz, 1H), 8.17 (ddd, *J* = 8.6, 1.7, 0.9 Hz, 1H), 7.84 (dd, *J* = 8.6, 7.4 Hz, 1H), 7.70 (dd, *J* = 7.4, 1.2 Hz, 1H), 7.58 – 7.46 (m, 2H), 6.87 (dd, *J* = 8.5, 0.9 Hz, 1H), 6.65 (dd, *J* = 8.3, 0.9 Hz, 1H), 5.52 (s, 2H), 1.72 (s, 6H).

5-((1-([1,1'-biphenyl]-2-yl)-1H-1,2,3-triazol-4-yl)methoxy)-2,2-dimethyl-4H-benzo[d][1,3]dioxin-4-one (6.51b):



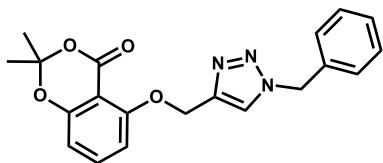
6.51b

According to general procedure A, alkyne **6.50** (0.180g, 0.775 mmol, 1 equiv), azide **6.44** (0.220 g, 1.16 mmol, 1.5 equiv), sodium ascorbate (0.016 g, 0.085 mmol, 0.1 equiv), and $\text{CuSO}_4 \cdot 5\text{H}_2\text{O}$ (0.007 g, 0.031 mmol, 0.04 equiv) were

reacted in a round bottom flask. Purification using column chromatography (3:7 EtOAc:Hexanes to 1:1 EtOAc:Hexanes) resulted in a white solid (0.089 g, 28%). **¹H NMR** (400 MHz, Chloroform-*d*) δ 7.64 – 7.58 (m, 1H), 7.61 – 7.47 (m, 4H), 7.42 (t, *J* = 8.4 Hz, 1H), 7.26 – 7.12 (m, 3H), 7.09 – 7.02 (m, 2H), 6.74 (dd, *J* = 8.6, 0.9 Hz, 1H), 6.58 (dd, *J* = 8.3, 0.9 Hz, 1H), 5.34 – 5.29 (m, 2H), 1.70 (s, 6H). **¹³C NMR** (101 MHz,

Chloroform-d) δ 159.9, 157.9, 143.8, 137.5, 137.3, 136.5, 135.1, 131.2, 130.1, 128.7, 128.6, 128.5, 127.9, 126.8, 125.7, 109.9, 107.4, 105.4, 63.4, 25.7.

5-((1-benzyl-1H-1,2,3-triazol-4-yl)methoxy)-2,2-dimethyl-4H-benzo[d][1,3]dioxin-4-one (6.51c):

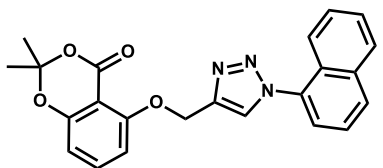


6.51c

According to general procedure A, alkyne **6.50** (0.050g, 0.214 mmol, 1 equiv), azide **6.47** (0.063 g, 0.247 mmol, 1.3 equiv), sodium ascorbate (0.046 g, 0.023 mmol, 0.04 equiv), and $\text{CuSO}_4 \cdot 5\text{H}_2\text{O}$ (0.002 g, 0.09 mmol, 0.1 equiv)

were reacted in a round bottom flask. Purification using column chromatography (1:1 EtOAc:Hexanes to 3:1 EtOAc:Hexanes) resulted in a tan solid (0.070 g, 70%). **¹H NMR** (400 MHz, Chloroform-d) δ 7.79 (d, J = 0.8 Hz, 1H), 7.37 (t, J = 8.4 Hz, 1H), 7.33 – 7.22 (m, 3H), 7.26 – 7.17 (m, 2H), 6.71 (dd, J = 8.5, 0.9 Hz, 1H), 6.51 (dd, J = 8.3, 0.9 Hz, 1H), 5.46 (s, 2H), 5.26 (d, J = 0.8 Hz, 2H), 1.62 (s, 6H).

2,2-dimethyl-5-((1-(naphthalen-1-yl)-1H-1,2,3-triazol-4-yl)methoxy)-4H-benzo[d][1,3]dioxin-4-one (6.51d):



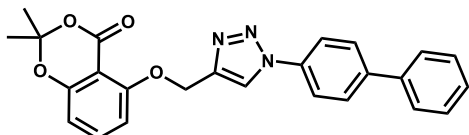
6.51d

According to general procedure A, alkyne **6.50** (0.180g, 0.775 mmol, 1 equiv), azide **6.41** (0.226 g, 1.16 mmol, 1.5 equiv), sodium ascorbate (0.016 g, 0.085 mmol, 0.1 equiv), and $\text{CuSO}_4 \cdot 5\text{H}_2\text{O}$ (0.007 g, 0.031 mmol, 0.04 equiv) were

reacted in a round bottom flask. Purification using column chromatography (96:4 DCM:MeOH) resulted in an orange solid after trituration in hexane (0.185 g, 62%). **¹H NMR** (400 MHz, Chloroform-d) δ 8.34 (s, 1H), 8.04 (d, J = 7.9 Hz, 1H), 8.01 – 7.94 (m,

1H), 7.69 – 7.48 (m, 6H), 6.90 (dd, J = 8.4, 0.9 Hz, 1H), 6.64 (dd, J = 8.3, 0.9 Hz, 1H), 5.54 (s, 2H), 1.72 (s, 6H).

5-((1-([1,1'-biphenyl]-4-yl)-1H-1,2,3-triazol-4-yl)methoxy)-2,2-dimethyl-4H-benzo[d][1,3]dioxin-4-one (6.51e):

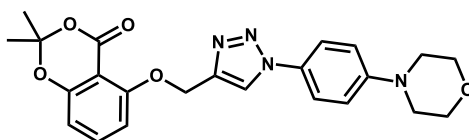


6.51e

According to general procedure A, alkyne **6.50** (0.180g, 0.775 mmol, 1 equiv), azide **6.45** (0.226 g, 1.16 mmol, 1.5 equiv), sodium ascorbate (0.016 g, 0.085 mmol, 0.1 equiv), and CuSO₄•5H₂O (0.007

g, 0.031 mmol, 0.04 equiv) were reacted in a round bottom flask. Purification using column chromatography (96:4 DCM:MeOH) resulted in an yellow solid (0.290 g, 88%). **1H NMR** (400 MHz, Chloroform-d) δ 8.48 (s, 1H), 7.91 – 7.83 (m, 2H), 7.78 – 7.71 (m, 2H), 7.67 – 7.60 (m, 2H), 7.55 – 7.45 (m, 3H), 7.44 – 7.38 (m, 1H), 6.84 (dd, J = 8.5, 0.9 Hz, 1H), 6.63 (dd, J = 8.2, 0.9 Hz, 1H), 5.46 (d, J = 0.9 Hz, 2H), 1.74 (s, 6H).

2,2-dimethyl-5-((1-(4-morpholinophenyl)-1H-1,2,3-triazol-4-yl)methoxy)-4H-benzo[d][1,3]dioxin-4-one (6.51f):



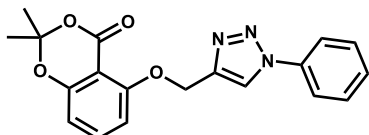
6.51f

According to general procedure A, alkyne **6.50** (0.150g, 0.645 mmol, 1 equiv), azide **6.40** (0.197 g, 0.968 mmol, 1.5 equiv), sodium ascorbate (0.014 g, 0.071 mmol, 0.1 equiv), and

CuSO₄•5H₂O (0.006 g, 0.025 mmol, 0.04 equiv) were reacted in a round bottom flask. Purification using column chromatography (95:5 DCM:MeOH) resulted in an yellow solid after trituration in hexane (0.244 g, 87%). **1H NMR** (400 MHz, Chloroform-d) δ 8.32 (s, 1H), 7.69 – 7.61 (m, 2H), 7.49 (t, J = 8.4 Hz, 1H), 7.00 (d, J = 9.0 Hz, 2H), 6.88 – 6.81 (m,

1H), 6.62 (dd, J = 8.3, 0.9 Hz, 1H), 5.44 (s, 2H), 3.93 – 3.86 (m, 4H), 3.27 – 3.20 (m, 4H), 1.73 (s, 6H).

2,2-dimethyl-5-((1-phenyl-1H-1,2,3-triazol-4-yl)methoxy)-4H-benzo[d][1,3]dioxin-4-one (6.51g):

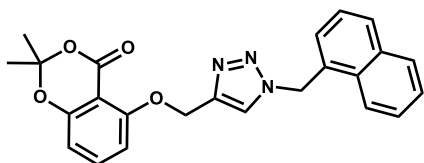


6.51g

According to general procedure A, alkyne **6.50** (0.050g, 0.214 mmol, 1 equiv), azide **6.46** (0.033 g, 0.274 mmol, 1.3 equiv), sodium ascorbate (0.046 g, 0.023 mmol, 0.04 equiv), and CuSO₄•5H₂O (0.002 g, 0.09 mmol, 0.1 equiv)

were reacted in a round bottom flask. Purification using column chromatography (1:1 EtOAc:Hexanes to 3:1 EtOAc:Hexanes) resulted in a tan solid (0.047 g, 64%). **1H NMR** (400 MHz, Chloroform-d) δ 8.46 – 8.41 (m, 1H), 7.83 – 7.75 (m, 2H), 7.57 – 7.40 (m, 4H), 6.83 (dd, J = 8.5, 0.9 Hz, 1H), 6.62 (dd, J = 8.3, 0.9 Hz, 1H), 5.44 (s, 2H), 1.73 (s, 6H).

2,2-dimethyl-5-((1-(naphthalenylmethyl)-1H-1,2,3-triazol-4-yl)methoxy)-4H-benzo[d][1,3]dioxin-4-one (6.51h):



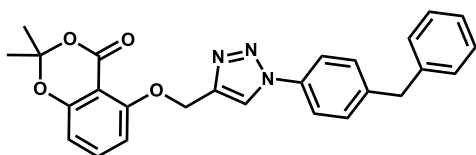
6.51h

According to general procedure A, alkyne **6.50** (0.050g, 0.214 mmol, 1 equiv), a mixture of isomers **6.48/6.48** (0.037 g, 0.279 mmol, 1.3 equiv), sodium ascorbate (0.046 g, 0.023 mmol, 0.04 equiv), and

CuSO₄•5H₂O (0.002 g, 0.09 mmol, 0.1 equiv) were reacted in a round bottom flask. Purification using column chromatography (3:7 EtOAc:Hexanes to 7:3 EtOAc:Hexanes) resulted in a tan solid (0.050 g, 64% %, as a mixture of 1- and 2- naphthyl isomers). **1H NMR** (400 MHz, Chloroform-d) δ 7.96 – 7.86 (m, 1H), 7.83 – 7.74 (m, 2H), 7.64 (d, J = 0.8 Hz, 1H), 7.47 – 7.28 (m, 5H), 6.66 (dd, J = 8.5, 0.9 Hz, 1H), 6.46 (dd, J = 8.3, 0.9 Hz,

1H), 5.90 (s, 2H), 5.19 (d, J = 0.8 Hz, 2H), 1.58 (s, 6H). **13C NMR** (101 MHz, Chloroform-d) δ 160.0, 157.9, 144.5, 136.6, 134.1, 131.3, 130.1, 130.0, 129.1, 128.0, 127.3, 126.5, 125.6, 123.3, 123.0, 110.0, 107.4, 105.5, 64.0, 52.6, 25.7.

5-((1-(4-benzylphenyl)-1H-1,2,3-triazol-4-yl)methoxy)-2,2-dimethyl-4H-benzo[d][1,3]dioxin-4-one (6.51j):

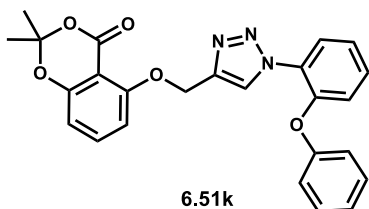


6.51j

According to general procedure A, alkyne **6.50** (0.150g, 0.645 mmol, 1 equiv), azide **6.43** (0.202 g, 0.968 mmol, 1.5 equiv), sodium ascorbate (0.046 g, 0.071 mmol, 0.01 equiv), and

CuSO₄•5H₂O (0.006 g, 0.025 mmol, 0.04 equiv) were reacted in a round bottom flask. Purification using column chromatography (98:2 DCM:MeOH to (94:6 DCM:MeOH) resulted in an off-white solid after trituration in hexane (0.264 g, 92%). **1H NMR** (400 MHz, Chloroform-d) δ 8.38 (d, J = 0.8 Hz, 1H), 7.69 (d, J = 8.5 Hz, 2H), 7.49 (t, J = 8.4 Hz, 1H), 7.37 – 7.28 (m, 4H), 7.32 – 7.17 (m, 3H), 6.83 (dd, J = 8.5, 0.9 Hz, 1H), 6.62 (dd, J = 8.3, 0.9 Hz, 1H), 5.44 (s, 2H), 4.06 (s, 2H), 1.73 (s, 6H).

2,2-dimethyl-5-((1-(2-phenoxyphenyl)-1H-1,2,3-triazol-4-yl)methoxy)-4H-benzo[d][1,3]dioxin-4-one (6.51k):



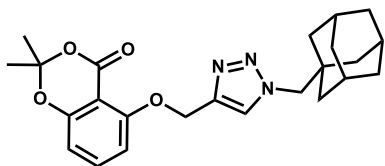
6.51k

According to general procedure A, alkyne **6.50** (0.180g, 0.775 mmol, 1 equiv), aryl azide (0.245 g, 1.16 mmol, 1.5 equiv), sodium ascorbate (0.016 g, 0.085 mmol, 0.1 equiv), and CuSO₄•5H₂O (0.007 g, 0.031 mmol, 0.04 equiv) were

reacted in a round bottom flask. Purification using column chromatography (3:7 EtOAc:Hexanes to 1:1 EtOAc:Hexanes) resulted in a white solid (0.31 g, 90%). **1H NMR**

(400 MHz, Chloroform-d) δ 8.47 (d, J = 0.8 Hz, 1H), 7.88 (dd, J = 8.0, 1.7 Hz, 1H), 7.48 – 7.21 (m, 5H), 7.12 (t, J = 7.4 Hz, 1H), 7.04 (dd, J = 8.3, 1.3 Hz, 1H), 7.03 – 6.95 (m, 2H), 6.84 (dd, J = 8.5, 0.9 Hz, 1H), 6.58 (dd, J = 8.3, 0.9 Hz, 1H), 5.42 (s, 2H), 1.70 (s, 6H).

5-((1-adamantylmethyl)-1H-1,2,3-triazol-4-yl)methoxy)-2,2-dimethyl-4H-benzo[d][1,3]dioxin-4-one (6.51m):

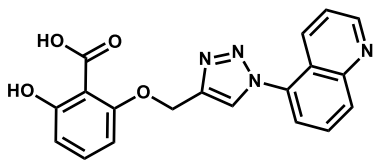


6.51m

According to general procedure A, alkyne **6.50** (0.180g, 0.775 mmol, 1 equiv), adamantyl azide (0.222 g, 1.16 mmol, 1.5 equiv), sodium ascorbate (0.016 g, 0.085 mmol, 0.1 equiv), and $\text{CuSO}_4 \cdot 5\text{H}_2\text{O}$ (0.007 g, 0.031 mmol, 0.04

equiv) were reacted in a round bottom flask. Purification using column chromatography (4:6 EtOAc:Hexanes to 7:3 EtOAc:Hexanes) resulted in a white solid (0.123 g, 37%). **¹H NMR** (400 MHz, Chloroform-d) δ 7.83 (d, J = 0.8 Hz, 1H), 7.45 (t, J = 8.4 Hz, 1H), 6.78 (dd, J = 8.5, 0.9 Hz, 1H), 6.58 (dd, J = 8.3, 0.9 Hz, 1H), 5.37 (s, 2H), 4.02 (s, 2H), 1.98 (p, J = 3.0 Hz, 3H), 1.71 (s, 6H), 1.69 – 1.65 (m, 2H), 1.62 – 1.54 (m, 3H), 1.51 (d, J = 2.9 Hz, 6H). **¹³C NMR** (101 MHz, Chloroform-d) δ 160.1, 158.4, 157.9, 143.7, 136.7, 124.6, 110.0, 107.4, 105.5, 64.2, 62.5, 40.3, 36.6, 34.3, 28.2, 25.7. **HRMS** (ESI) m/z calcd for $\text{C}_{24}\text{H}_{30}\text{N}_3\text{O}_4$ ($\text{M}+\text{H}$)⁺ 424.2231, found 424.2229.

2-hydroxy-6-((1-(quinolin-5-yl)-1H-1,2,3-triazol-4-yl)methoxy)benzoic acid (6.52a):

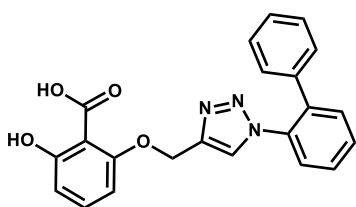


6.52a

According to general procedure B, acetonide **6.51a** (0.080 g, 0.198 mmol, 1 equiv), KOTMS (0.051 g, 0.397 mmol, 2 equiv), and THF (4 mL) to give the product as a tan solid (0.165 g, quant.). **¹H NMR** (400 MHz, Chloroform-d) δ

11.38 (s, 1H), 9.06 (dd, J = 4.2, 1.7 Hz, 1H), 8.36 (d, J = 8.5 Hz, 1H), 8.11 – 8.02 (m, 2H), 7.87 (dd, J = 8.6, 7.4 Hz, 1H), 7.68 (dd, J = 7.5, 1.0 Hz, 1H), 7.57 – 7.44 (m, 2H), 6.80 (t, J = 8.7 Hz, 2H), 5.61 (s, 2H). **HRMS** (ESI) m/z calcd for $C_{19}H_{15}N_4O_4$ (M+H)⁺ 363.1088, found 363.1087.

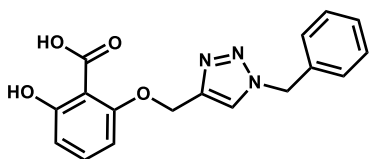
2-((1-([1,1'-biphenyl]-2-yl)-1H-1,2,3-triazol-4-yl)methoxy)-6-hydroxybenzoic acid (6.52b):



6.52b

According to general procedure B, acetone **6.51b** (0.089 g, 0.208 mmol, 1 equiv), KOTMS (0.066 g, 0.520 mmol, 2 equiv), and THF (5 mL) to give the product as an off-white solid (0.077 g, 97%). **HRMS** (ESI) m/z calcd for $C_{22}H_{18}N_3O_4$ (M+H)⁺ 388.1292, found 388.1291.

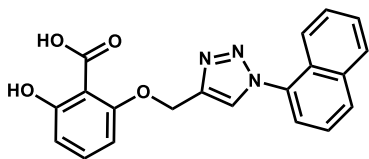
2-((1-benzyl-1H-1,2,3-triazol-4-yl)methoxy)-6-hydroxybenzoic acid (6.52c):



6.52c

According to general procedure C, acetone **6.51c** (0.050 g, 0.137 mmol, 1 equiv), 5 M KOH (1 mL), and THF (2 mL) were stirred in a round bottom flask for 18 hours and purified using column chromatography (97:3:0.1 DCM:MeOH:AcOH) to give the product as a light pink solid (0.018 g, 40%). **¹H NMR** (400 MHz, Chloroform-d) δ 11.28 (s, 1H), 7.58 (s, 1H), 7.46 – 7.35 (m, 4H), 7.35 – 7.26 (m, 2H), 6.74 (dd, J = 8.5, 0.9 Hz, 1H), 6.66 (dd, J = 8.3, 0.9 Hz, 1H), 5.58 (s, 2H), 5.40 (s, 2H).

2-hydroxy-6-((1-(naphthalen-1-yl)-1H-1,2,3-triazol-4-yl)methoxy)benzoic acid (6.52d):

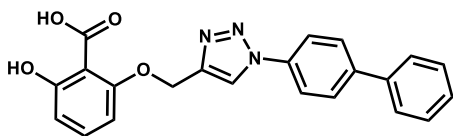


6.52d

According to general procedure B, acetonide **6.51d** (0.080 g, 0.187 mmol, 1 equiv), KOTMS (0.051 g, 0.397 mmol, 2 equiv), and THF (4 mL) to give the product as a white solid (0.086 g, 97%). **¹H NMR** (400 MHz, Chloroform-*d*) δ

11.42 (s, 1H), 8.12 – 8.04 (m, 2H), 8.00 (d, *J* = 8.1 Hz, 1H), 7.67 – 7.58 (m, 3H), 7.63 – 7.54 (m, 1H), 7.54 (d, *J* = 8.2 Hz, 1H), 7.48 (t, *J* = 8.4 Hz, 1H), 6.79 (dd, *J* = 8.3, 1.9 Hz, 2H), 5.61 (s, 2H). **HRMS** (ESI) *m/z* calcd for C₂₀H₁₆N₃O₄ (M+H)⁺ 362.1135, found 362.1135.

2-((1-([1,1'-biphenyl]-4-yl)-1H-1,2,3-triazol-4-yl)methoxy)-6-hydroxybenzoic acid (6.52e):

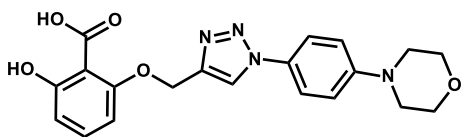


6.52e

According to general procedure B, acetonide **6.51e** (0.08 g, 0.187 mmol, 1 equiv), KOTMS (0.048 g, 0.374 mmol, 2 equiv), and THF (2 mL) to give the

product as a tan solid (0.091 g, 95%). **HRMS** (ESI) *m/z* calcd for C₂₂H₁₈N₃O₄ (M+H)⁺ 388.1292, found 388.1296.

2-hydroxy-6-((1-(4-morpholinophenyl)-1H-1,2,3-triazol-4-yl)methoxy)benzoic acid (6.52f):



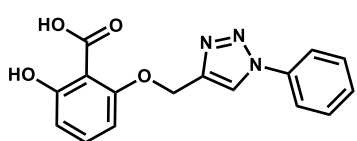
6.52f

According to general procedure B, acetonide **6.51f** (0.080 g, 0.183 mmol, 1 equiv), KOTMS (0.058 g, 0.458 mmol, 2.5 equiv), and THF (2 mL) to give the

product as a tan solid (0.079 g, 92%). **¹H NMR** (400 MHz, Chloroform-*d*) δ 8.02 (s, 1H), 7.61 (d, *J* = 8.5 Hz, 2H), 7.44 (t, *J* = 8.2 Hz, 1H), 7.01 (d, *J* = 8.4 Hz, 2H), 6.75 (dd, *J* =

13.8, 8.4 Hz, 2H), 5.51 (s, 2H), 3.93 – 3.86 (m, 4H), 3.25 (t, J = 4.9 Hz, 4H). **HRMS** (ESI) m/z calcd for $C_{20}H_{21}N_4O_5$ (M+H)⁺ 397.1506, found 397.1508.

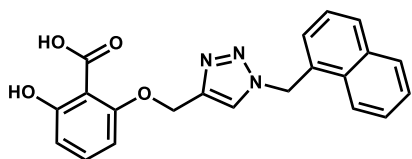
2-hydroxy-6-((1-phenyl-1H-1,2,3-triazol-4-yl)methoxy)benzoic acid (6.52g):



6.52g

According to general procedure C, acetone 6.51g (0.047 g, 0.133 mmol, 1 equiv), 5 M KOH (1 mL), and THF (2 mL) were stirred in an round bottom flask for 16 hours and purified using column chromatography (97:3:0.1 DCM:MeOH:AcOH) to give the product as a light pink solid (0.035 g, 86%). **¹H NMR** (400 MHz, Chloroform-d) δ 11.30 (s, 1H), 8.14 (s, 1H), 7.75 (d, J = 8.2 Hz, 1H), 7.57 (t, J = 7.6 Hz, 2H), 7.53 – 7.45 (m, 1H), 7.45 (t, J = 8.4 Hz, 1H), 6.77 (dd, J = 8.5, 0.9 Hz, 1H), 6.74 (dd, J = 8.3, 1.0 Hz, 1H), 5.53 (s, 2H).

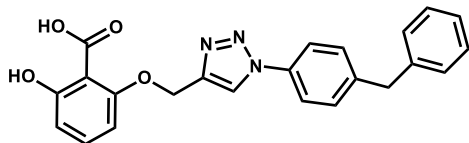
2-hydroxy-6-((1-(naphthalen-1-ylmethyl)-1H-1,2,3-triazol-4-yl)methoxy)benzoic acid (6.52h/i):



6.52h

According to general procedure C, acetone 6.51h/i (0.070 g, 0.166 mmol, 1 equiv), 5 M KOH (2 mL), and THF (4 mL) were stirred in an round bottom flask for 18 hours and purified using column chromatography (97:3:0.1 DCM:MeOH:AcOH) to give the product as a light pink solid (0.017 g, 28%). **¹H NMR** (400 MHz, Chloroform-d) δ 11.08 (s, 1H), 7.99 – 7.86 (m, 2H), 7.60 – 7.51 (m, 2H), 7.54 – 7.45 (m, 2H), 7.43 (s, 1H), 7.37 (t, J = 8.4 Hz, 1H), 6.71 (dd, J = 8.5, 0.9 Hz, 1H), 6.60 (dd, J = 8.4, 0.9 Hz, 1H), 6.03 (s, 2H), 5.31 (d, J = 1.9 Hz, 2H). **HRMS** (ESI) m/z calcd for $C_{21}H_{18}N_3O_4$ (M+H)⁺ 376.1292, found 376.1294.

2-((1-(4-benzylphenyl)-1H-1,2,3-triazol-4-yl)methoxy)-6-hydroxybenzoic acid (6.52j):



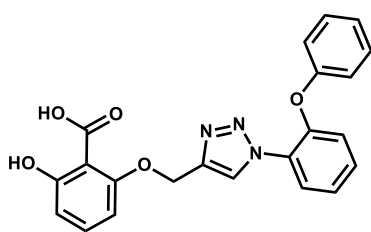
6.52j

According to general procedure B, acetonide **6.51j** (0.02 g, 0.045 mmol, 1 equiv), KOTMS (0.024 g, 0.09 mmol, 2 equiv), and THF (2 mL) to give the product as a white solid (0.017 g, 91%). **¹H NMR**

(400 MHz, Chloroform-d) δ 11.34 (s, 1H), 8.09 (s, 1H), 7.65 (d, $J = 8.5$ Hz, 2H), 7.43 (t, $J = 8.4$ Hz, 1H), 7.41 – 7.29 (m, 4H), 7.33 – 7.23 (m, 1H), 7.22 – 7.17 (m, 2H), 6.76 (dd, $J = 8.5, 0.9$ Hz, 1H), 6.72 (dd, $J = 8.3, 1.0$ Hz, 1H), 5.51 (s, 2H), 4.07 (s, 2H). **¹³C NMR** (101 MHz, Chloroform-d) δ 173.2, 164.1, 161.9, 149.8, 142.7, 140.9, 138.7, 136.7, 131.4, 131.1, 130.6, 130.5, 129.3, 128.9, 122.6, 121.0, 120.8, 111.0, 108.0, 106.4, 63.4, 43.5.

HRMS (ESI) m/z calcd for $C_{22}H_{20}N_3O_4$ (M+H)⁺ 402.1448, found 404.1443.

2-hydroxy-6-((1-(2-phenoxyphenyl)-1H-1,2,3-triazol-4-yl)methoxy)benzoic acid (6.52k):

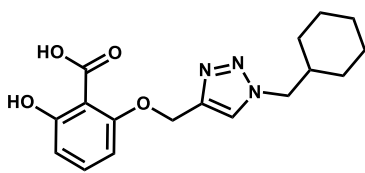


6.52k

According to general procedure B, acetonide **6.51k** (0.211 g, 0.475 mmol, 1 equiv), KOTMS (0.024 g, 0.09 mmol, 2 equiv), and THF (4 mL) to give the product as a clear oil (0.194 g, 99%). **¹H NMR** (400 MHz, Chloroform-d) δ

11.23 (s, 1H), 8.24 (s, 1H), 7.90 (dd, $J = 8.0, 1.7$ Hz, 1H), 7.39 – 7.19 (m, 5H), 7.13 – 7.05 (m, 1H), 6.99 (dd, $J = 8.3, 1.4$ Hz, 1H), 6.94 – 6.87 (m, 2H), 6.64 (ddd, $J = 19.4, 8.4, 0.9$ Hz, 2H), 5.40 (s, 2H). **HRMS** (ESI) m/z calcd for $C_{22}H_{18}N_3O_5$ (M+H)⁺ 404.1241, found 404.1237.

2-((1-(cyclohexylmethyl)-1H-1,2,3-triazol-4-yl)methoxy)-6-hydroxybenzoic acid (6.52l):

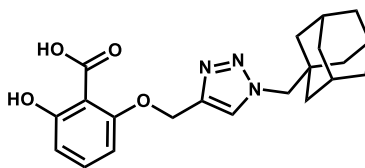


6.52l

According to general procedure B, acetonide **6.51l** (0.235 g, 0.619 mmol, 1 equiv), KOTMS (0.158 g, 1.23 mmol, 2 equiv), and THF (6 mL) to give the product as a white solid (0.153 g, 76%). **¹H NMR** (400 MHz, Chloroform-d) δ 7.62

(s, 1H), 7.43 (t, $J = 8.4$ Hz, 1H), 6.75 (dd, $J = 8.5, 0.9$ Hz, 1H), 6.69 (dd, $J = 8.3, 1.0$ Hz, 1H), 5.44 (s, 2H), 4.23 (d, $J = 7.2$ Hz, 2H), 1.91 (ttt, $J = 10.9, 7.1, 3.5$ Hz, 1H), 1.80 – 1.66 (m, 3H), 1.65 – 1.56 (m, 3H), 1.31 – 1.14 (m, 2H), 1.08 – 0.93 (m, 2H). **¹³C NMR** (101 MHz, Chloroform-d) δ 173.7, 162.4, 159.8, 144.3, 134.2, 126.1, 108.7, 105.7, 103.7, 61.7, 53.9, 37.3, 29.6, 26.5, 25.2.

2-((1-(adamantan-1-ylmethyl)-1H-1,2,3-triazol-4-yl)methoxy)-6-hydroxybenzoic acid (6.52m):



6.52m

According to general procedure B, acetonide **6.51m** (0.122 g, 0.283 mmol, 1 equiv), KOTMS (0.127 g, 0.991 mmol, 2 equiv), and THF (15 mL) to give the product as a white solid (0.079 g, 73%). **¹H NMR** (400 MHz, Chloroform-d)

δ 11.38 (s, 1H), 7.58 (s, 1H), 7.43 (t, $J = 8.4$ Hz, 1H), 6.75 (dd, $J = 8.5, 0.9$ Hz, 1H), 6.69 (dd, $J = 8.4, 1.0$ Hz, 1H), 5.45 (s, 2H), 4.06 (s, 2H), 2.02 (s, 3H), 1.76 – 1.69 (m, 3H), 1.61 (q, $J = 2.2$ Hz, 3H), 1.50 (d, $J = 2.9$ Hz, 6H). **HRMS** (ESI) m/z calcd for $C_{21}H_{26}N_3O_4$ (M+H)⁺ 384.1918, found 384.1922.

6.7 - References

- (1) Johnson, E. S. Protein Modification by SUMO. *Annu. Rev. Biochem.* **2004**, *73*, 355–382.
- (2) Bettermann, K.; Benesch, M.; Weis, S.; Haybaeck, J. SUMOylation in Carcinogenesis. *Cancer Lett.* **2012**, *316*, 113–125.
- (3) Du, L.; Li, Y.-J.; Fakih, M.; Wiatrek, R. L.; Duldulao, M.; Chen, Z.; Chu, P.; Garcia-Aguilar, J.; Chen, Y. Role of SUMO Activating Enzyme in Cancer Stem Cell Maintenance and Self-Renewal. *Nat. Commun.* **2016**, *7*, 12326.
- (4) Fukuda, I.; Ito, A.; Hirai, G.; Nishimura, S.; Kawasaki, H.; Saitoh, H.; Kimura, K.-I.; Sodeoka, M.; Yoshida, M. Ginkgolic Acid Inhibits Protein SUMOylation by Blocking Formation of the E1-SUMO Intermediate. *Chem. Biol.* **2009**, *16*, 133–140.
- (5) Bossis, G.; Sarry, J.-E.; Kifagi, C.; Ristic, M.; Saland, E.; Vergez, F.; Salem, T.; Boutzen, H.; Baik, H.; Brockly, F.; Pelegrin, M.; Kaoma, T.; Vallar, L.; Récher, C.; Manenti, S.; Piechaczyk, M. The ROS/SUMO Axis Contributes to the Response of Acute Myeloid Leukemia Cells to Chemotherapeutic Drugs. *Cell Rep.* **2014**, *7*, 1815–1823.
- (6) Lois, L. M.; Lima, C. D. Structures of the SUMO E1 Provide Mechanistic Insights into SUMO Activation and E2 Recruitment to E1. *EMBO J.* **2005**, *24*, 439–451.
- (7) Knighton, D. R.; Zheng, J. H.; Eyck, L. T.; Ashford, V. A.; Xuong, N. H.; Taylor, S. S.; Sowadski, J. M. Crystal Structure of the Catalytic Subunit of Cyclic Adenosine Monophosphate-Dependent Protein Kinase. *Science* **1991**, *253*, 407–414.
- (8) Desterro, J. M. P.; Rodriguez, M. S.; Kemp, G. D.; Hay, R. T. Identification of the Enzyme Required for Activation of the Small Ubiquitin-like Protein SUMO-1. *J. Biol. Chem.* **1999**, *274*, 10618–10624.
- (9) Desterro, J. M. P.; Thomson, J.; Hay, R. T. Ubc9 Conjugates SUMO but Not Ubiquitin. *FEBS Lett.* **1997**, *417*, 297–300.
- (10) Sampson, D. A.; Wang, M.; Matunis, M. J. The Small Ubiquitin-like Modifier-1 (SUMO-1) Consensus Sequence Mediates Ubc9 Binding and Is Essential for SUMO-1 Modification. *J. Biol. Chem.* **2001**, *276*, 21664–21669.

- (11) Li, S.-J.; Hochstrasser, M. A New Protease Required for Cell-Cycle Progression in Yeast. *Nature* **1999**, *398*, 246–251.
- (12) Malakhov, M. P.; Mattern, M. R.; Malakhova, O. A.; Drinker, M.; Weeks, S. D.; Butt, T. R. SUMO Fusions and SUMO-Specific Protease for Efficient Expression and Purification of Proteins. *J. Struct. Funct. Genomics* **2004**, *5*, 75–86.
- (13) Yeh, E. T. H.; Gong, L.; Kamitani, T. Ubiquitin-like Proteins: New Wines in New Bottles. *Gene* **2000**, *248*, 1–14.
- (14) Luo, J.; Solimini, N. L.; Elledge, S. J. Principles of Cancer Therapy: Oncogene and Non-Oncogene Addiction. *Cell* **2009**, *136*, 823–837.
- (15) Menssen, A.; Epanchintsev, A.; Lodygin, D.; Rezaei, N.; Jung, P.; Verdoodt, B.; Diebold, J.; Hermeking, H. C-MYC Delays Prometaphase by Direct Transactivation of MAD2 and BubR1: Identification of Mechanisms Underlying c-MYC-Induced DNA Damage and Chromosomal Instability. *Cell Cycle* **2007**, *6*, 339–352.
- (16) Restuccia, A.; Yang, F.; Chen, C.; Lu, L.; Dai, W. Mps1 Is SUMO-Modified during the Cell Cycle. *Oncotarget* **2015**, *7*, 3158–3170.
- (17) Kessler, J. D.; Kahle, K. T.; Sun, T.; Meerbrey, K. L.; Schlabach, M. R.; Schmitt, E. M.; Skinner, S. O.; Xu, Q.; Li, M. Z.; Hartman, Z. C.; Rao, M.; Yu, P.; Dominguez-Vidana, R.; Liang, A. C.; Solimini, N. L.; Bernardi, R. J.; Yu, B.; Hsu, T.; Golding, I.; Luo, J.; Osborne, C. K.; Creighton, C. J.; Hilsenbeck, S. G.; Schiff, R.; Shaw, C. A.; Elledge, S. J.; Westbrook, T. F. A SUMOylation-Dependent Transcriptional Subprogram Is Required for Myc-Driven Tumorigenesis. *Science* **2012**, *335*, 348–353.
- (18) Bharadwaj, R.; Yu, H. The Spindle Checkpoint, Aneuploidy, and Cancer. *Oncogene* **2004**, *23*, 2016–2027.
- (19) Swords, R. T.; Coutre, S.; Maris, M. B.; Zeidner, J. F.; Foran, J. M.; Cruz, J.; Erba, H. P.; Berdeja, J. G.; Tam, W.; Vardhanabhuti, S.; Pawlikowska-Dobler, I.; Faessel, H. M.; Dash, A. B.; Sedarati, F.; Dezube, B. J.; Faller, D. V.; Savona, M. R. Pevonedistat, a First-in-Class NEDD8-Activating Enzyme Inhibitor, Combined with Azacitidine in Patients with AML. *Blood* **2018**, *131*, 1415–1424.

- (20) Estey, E. H. Acute Myeloid Leukemia: 2012 Update on Diagnosis, Risk Stratification, and Management. *Am. J. Hematol.* **2012**, *87*, 89–99.
- (21) Trott, O.; Olson, A. J. AutoDock Vina: Improving the Speed and Accuracy of Docking with a New Scoring Function, Efficient Optimization, and Multithreading. *J. Comput. Chem.* **2010**, *31*, 455–461.
- (22) Kumar, A.; Ito, A.; Hirohama, M.; Yoshida, M.; Zhang, K. Y. J. Identification of New SUMO Activating Enzyme 1 Inhibitors Using Virtual Screening and Scaffold Hopping. *Bioorg. Med. Chem. Lett.* **2016**, *26*, 1218–1223.
- (23) Kumar, A.; Ito, A.; Hirohama, M.; Yoshida, M.; Zhang, K. Y. J. Identification of Sumoylation Activating Enzyme 1 Inhibitors by Structure-Based Virtual Screening. *J. Chem. Inf. Model.* **2013**, *53*, 809–820.
- (24) Jiang, L.; Saavedra, A. N.; Way, G.; Alanis, J.; Kung, R.; Li, J.; Xiang, W.; Liao, J. Specific Substrate Recognition and Thioester Intermediate Determinations in Ubiquitin and SUMO Conjugation Cascades Revealed by a High-Sensitive FRET Assay. *Mol. Biosyst.* **2014**, *10*, 778–786.
- (25) Song, Y.; Liao, J. Systematic Determinations of SUMOylation Activation Intermediates and Dynamics by a Sensitive and Quantitative FRET Assay. *Mol. Biosyst.* **2012**, *8*, 1723–1729.
- (26) Brito, A. F.; Moreira, L. K. S.; Menegatti, R.; Costa, E. A. Piperazine Derivatives with Central Pharmacological Activity Used as Therapeutic Tools. *Fundam. Clin. Pharmacol.* **2019**, *33*, 13–24.
- (27) Horton, D. A.; Bourne, G. T.; Smythe, M. L. The Combinatorial Synthesis of Bicyclic Privileged Structures or Privileged Substructures. *Chem. Rev.* **2003**, *103*, 893–930.
- (28) Barral, K.; Moorhouse, A. D.; Moses, J. E. Efficient Conversion of Aromatic Amines into Azides: A One-Pot Synthesis of Triazole Linkages. *Org. Lett.* **2007**, *9*, 1809–1811.

- (29) Kolb, H. C.; Sharpless, K. B. The Growing Impact of Click Chemistry on Drug Discovery. *Drug Discov. Today* **2003**, *8*, 1128–1137.
- (30) Tatum, P. R.; Sawada, H.; Ota, Y.; Itoh, Y.; Zhan, P.; Ieda, N.; Nakagawa, H.; Miyata, N.; Suzuki, T. Identification of Novel SIRT2-Selective Inhibitors Using a Click Chemistry Approach. *Bioorg. Med. Chem. Lett.* **2014**, *24*, 1871–1874.
- (31) Dey, S.; Garner, P. Synthesis of Tert-Butoxycarbonyl (Boc)-Protected Purines. *J. Org. Chem.* **2000**, *65*, 7697–7699.
-